The Identification of β-Catenin and Other RNAs in Developing Thalamic Axons

John William Davey

Doctor of Philosophy

Institute for Adaptive and Neural Computation
School of Informatics
University of Edinburgh

2009

Abstract

This thesis provides evidence for the presence of multiple RNAs in the axons and growth cones of developing thalamic cells, particularly the mRNA for the cell adhesion and Wnt-signalling-related molecule β-catenin.

After many decades of effort, mRNAs have been shown to be present in the axons of many different systems in recent years. Furthermore, these mRNAs have been shown to be locally translated at the growth cone, and this local translation is required for axons to turn in response to multiple guidance cues. As studies accumulate, it is becoming clear that different axonal systems contain different complements of mRNAs and have different requirements for local translation.

One axonal system which has not been investigated to date is the thalamocortical tract. The nuclei of the thalamus are connected to the areas of the cortex via bundles of axons which travel from the thalamus to the cortex via the ventral telencephalon during embyronic development. These axons make a number of turns and are guided by many cues and other axonal tracts before innervating their cortical target.

In this thesis, a quantitative real-time polymerase chain reaction (qRT-PCR) approach is developed to isolate multiple mRNAs from developing thalamic axons *in vitro*, including β-catenin mRNA, β-actin mRNA, 18S ribosomal RNA and ten other mRNAs. The method used should be suitable for use with other axonal systems and also for testing the effect of guidance cues on mRNA expression in axons.

The qRT-PCR results for β-catenin, β-actin and 18S have been validated using in situ hybridisation. Analysis of in situ hybridisation results indicates that β-catenin and 18S, but not β-actin, are upregulated in the growth cone compared to the axon.

As β-catenin has been shown to be involved in axon guidance via Slit and ephrin guidance cues in other axonal systems, and these guidance cues act upon thalamocortical axons, the identification of β-catenin mRNA in thalamic axons is an important step towards a full understanding of the thalamocortical system.

The results presented here indicate that local protein synthesis is likely to occur in thalamic axons as it does in other axonal systems, and that local translation is likely to be important for thalamic axonal responses to guidance cues and other axonal tracts.

Acknowledgements

While the work presented in this thesis may be directly my own, it is indirectly the product of at least three communities, each of which has provided me with rare opportunities and constant support.

Firstly, I have been fortunate to be one of many students in the Neuroinformatics Doctoral Training Centre in the School of Informatics, which has provided not only the resources required to complete this Ph.D. but also the freedom to explore many different aspects of computer and biological science. I thank Mark van Rossum, David Willshaw, Jim Bednar and Pat Ferguson for fiercely protecting that freedom and encouraging us to make the most of it. In particular I thank my Informatics supervisor, Douglas Armstrong, who introduced me to molecular biology, and helped me to avoid many potholes on the road to a completed thesis. I also thank my friends, Tim O'Leary, Judith Law, Andy Fugard, Finlay Stewart, Chris Palmer and many others, for many long and formative discussions, some of which may even have been related to our work.

Secondly, it has been a privilege to work in the Developmental Biology Laboratory in the School of Biological Sciences. My neuroscientific supervisor, David Price, has been a constant source of sound scientific advice and moral support, and I thank him for being foresighted, or foolish, enough to allow a software engineer to take up residence at one of his lab benches. I would especially like to thank my co-supervisor Thomas Pratt, who attended every weekly meeting and tolerated countless other questions, discussions and emergencies with endless patience and good humour.

I would also like to thank Mark Barnett, for much assistance with qRT-PCRs and several wise lessons about the art of science, Mike Molinek, for introducing me to laboratory work and in situ hybridisations, and to Martin Simmen, for assistance during the first year of this project. In addition, I thank Catherine Carr, Tammy Lannagan, Chris Conway, Lasani Wijetunge, Alison Murray, Katy Gillies, Vassiliki Fotaki, Sally Till and Aoife McMahon for all their help, friendship and support both in and out of the laboratory.

I also thank my mother, my father, my brother Richard and all of my family, for always encouraging me to take and meet my opportunities, and, in common with all of the people listed here, for keeping their faith in me when I lost my own. Finally, my deepest thanks and love go to Mary, who has lived through this thesis with me and who has been my inspiration throughout.

Declaration

I declare that this thesis was composed by myself, and that this work has not been submitted for any other degree or professional qualification. I would like to acknowledge the following people for their contributions to the experiments reported here: Katy Gillies, who prepared all the culture medium used for these experiments; Mike Molinek and Rowena Smith, who supplied the fetal calf serum used for the qRT-PCR experiments; Mark Barnett for qRT-PCR training, Mike Molinek for in situ hybridisation training, and Tom Nowakowski, who worked with me on the initial design of the in situ hybridisation dissociated cultures. David Price and Thomas Pratt discussed experimental design with me in detail throughout the project and read and made comments on drafts of the thesis. However, all experiments reported here were performed by myself alone, and all remaining mistakes in the thesis are my own.

John William Davey

To my mother, who took me as far as she could,
and to Mary, who got me through the rest.

Table of Contents

List of Figures

Chapter 1

Introduction

1.1 Introduction

This thesis provides evidence for the existence of many mRNAs in developing thalamic axons, in particular the mRNA for β-catenin, a molecule with key roles in cell adhesion behaviour and the Wnt signalling pathway. The majority of the results presented here derive from quantitative real time polymerase chain reaction (qRT-PCR) experiments and in situ hybridisation experiments intended to assess the presence or absence of mRNAs in developing thalamic axons. In this opening section, the context and motivation for this work is presented, beginning by placing the work in its overarching biological context and presenting an overview of the argument of the rest of the chapter.

While great variety can be seen in the body plans of bilateral animals, the genes which underlie the development of these body plans are highly conserved, with common genetic regulatory networks determining the overall structure of the embryo and the position of various body parts (Davidson and Erwin, 2006). For example, the design of the eye varies considerably across different species, but the position and initial development of the eye is driven by the same small number of genes in many species. The Drosophila eye does not develop in the absence of seven critical genes, the homologues of which are also involved in the development of the mouse and human eye (Fernald, 2006). The study of development has been greatly enriched by the ability to link observations from many different species to the same gene or gene network. For example, McGlinn and Tabin (2006) explore the morphogen Sonic hedgehog's role in limb development by discussing studies in human, mouse, chick and Drosophila; similarly, Olson (2006) describes a gene regulatory network underlying the development of the heart that is common to simple chordates, reptiles, birds and

mammals.

The development of the brain has also been linked to genes which are common throughout organisms with nervous systems. The gross divisions of the brain into forebrain, midbrain and hindbrain are determined by the expression of homeobox genes such as Otx, Hox and Pax-2/5/8 (Reichert, 2005) and the further differentiation of each of these divisions also depends on genetic mechanisms. For example, the rhombomeres of the hindbrain are subdivided by the differential expression of a series of Hox genes (Kiecker and Lumsden, 2005). Other homeobox genes are crucial for the development of the forebrain; for example, Emx1 is essential for the development of the corpus collosum, Lhx5 is required for hippocampal progenitors to differentiate and the ventral forebrain is not correctly established in the absence of Nkx2-1 (Wigle and Eisenstat, 2008).

The development of the neocortex (hereafter the cortex) is of particular interest in this context (see Northcutt and Kaas (1995); Molnár et al. (2006); Abdel-Mannan et al. (2008) for reviews). The cortex can be divided into areas according to the organisation and behaviour of neural networks in different parts of the cortex. The differentiation of these areas requires the patterned expression of developmental genes such as Pax6, Emx2 and Sp8 (O'Leary and Sahara, 2008; Rash and Grove, 2005). Areas of the cortex are intimately connected to other organs; for example, the cells of the retina are connected to the visual cortex via a series of axonal relays, and the visual cortex is mapped to reflect the topographical organisation of the retina. Therefore, it will be particularly interesting to compare the gene regulatory networks underlying the arealisation of the cortex with those underlying the development of related organs of the body, as it might be expected that their co-development will place constraints on the evolution of these systems.

For example, Pax6 is one of the critical genes required for the initiation of eye development (Fernald, 2006) but it is also expressed in a gradient across the cortex during early brain development, and this gradient is required for the visual areas of the brain (among other areas) to form correctly (Bishop et al., 2000; Bayatti et al., 2008). This suggests that the evolution of the eye and visual cortex and the connections between the two could be investigated by comparing the evolution of Pax6 with changes in the structure and function of these systems. Therefore the study of the molecules underlying the development of the cortex and the connections between the organs of the body and regions of the brain, in addition to its considerable intrinsic appeal, may have profound implications concerning the function of the brain

throughout evolution.

The study of the thalamus is significant to this project both due to the central role of the thalamus in the overall functioning of the brain and due to the internal patterning of the thalamus itself, which requires explanation from a developmental perspective. In particular, the bundles of axons which grow from the thalamus to the cortex, collectively known as the thalamocortical tract, are of critical importance to understanding the thalamus and brain development in general, because they connect the cortex to sensory and motor organs via the thalamus and their correct organisation is crucial to the function of these organs and the organism as a whole.

The particular focus of this thesis is on RNAs in thalamocortical axons. The existence and functional importance of many RNAs in various axonal systems, while a controversial subject for many years, is now well established (Alvarez et al., 2000; Piper and Holt, 2004), although the precise purpose of these locally translated RNAs is still an open question. It appears that one reason why RNAs were not discovered earlier in axons is that protein synthesis at the tip of the growth cone is a feature of developing, but not mature, axons. This makes the thalamocortical tract an ideal system for the investigation of axonal RNA, as its development has a number of striking features where the existence of local protein synthesis appears to provide an advantage.

Firstly, the axons of the thalamocortical tract must navigate long distances from the thalamus to the cortex, responding to the presence of many molecular guidance cues during their journey. These guidance cues elicit rapid turning responses from the growth cones of thalamocortical axons, which suggest that the growth cones have some internal ability to alter their behaviour, which the local translation of intermittently required RNAs might explain.

Secondly, while all thalamocortical axons follow the same gross path from thalamus to cortex, when the axons reach the cortex they innervate different cortical areas according to the thalamic nucleus from which they originated. This indicates that thalamocortical axons are not all uniform and that growth cones develop and maintain different identities which enables them to find their various targets. The presence of different complements of RNAs in these growth cones might explain this behaviour.

However, to date, there has been no investigation of RNAs in thalamocortical axons. Before the function of RNAs in thalamocortical axons can be investigated, their presence must be established. This is the core finding which is presented in this thesis.

The development of the thalamocortical tract will be described in detail in this

chapter, following the growth of the axons from the thalamus to the cortex, and presenting the environment which these axons must navigate to reach their targets. Once this is established, the internal mechanics of growth cones will be explored, in an attempt to explain their behaviour during brain development. However, before these core topics can be addressed, they must be put into context. In the next section, some principles of development are established which are repeatedly referred to in what follows, including the regulation of transcription and translation, the use of molecular gradients in development and axon guidance and the mechanisms of cell adhesion. Following this, the structure, function and development of the thalamus and cortex will be outlined. At the end of the chapter, the aims and structure of the thesis will be described in full.

1.2 Principles of development

The development of the thalamocortical tract depends upon some basic mechanisms common to many aspects of development. In this section, the mechanisms involved in the control of gene expression and the application of these mechanisms both to the specification of body parts and the guidance of axons will be introduced. These mechanisms will be explored in more depth during the later discussions of the development of the cortex, thalamus and thalamocortical tract and the function of axonal growth cones.

1.2.1 The control of differential gene expression

Each of the vast number of cells in a eukaryotic organism contains a set of DNA molecules in its nucleus which comprise the entire genome for that organism. However, each of the cells expresses only a specific subset of all the proteins which could be produced from this genome, a subset which differs from cell to cell and which changes over time as each cell's environment changes. The production of the right proteins at the right time is regulated at each stage of the process of transcribing DNA into RNA and translating RNA into protein.

The protein for a gene is translated from a messenger RNA (mRNA) molecule, which in turn is transcribed from genomic DNA. The genomic DNA sequence for a protein-coding gene contains not only the sequence which will be transcribed into RNA, but also a control region upstream of the mRNA sequence (see Figure 1.1a). This

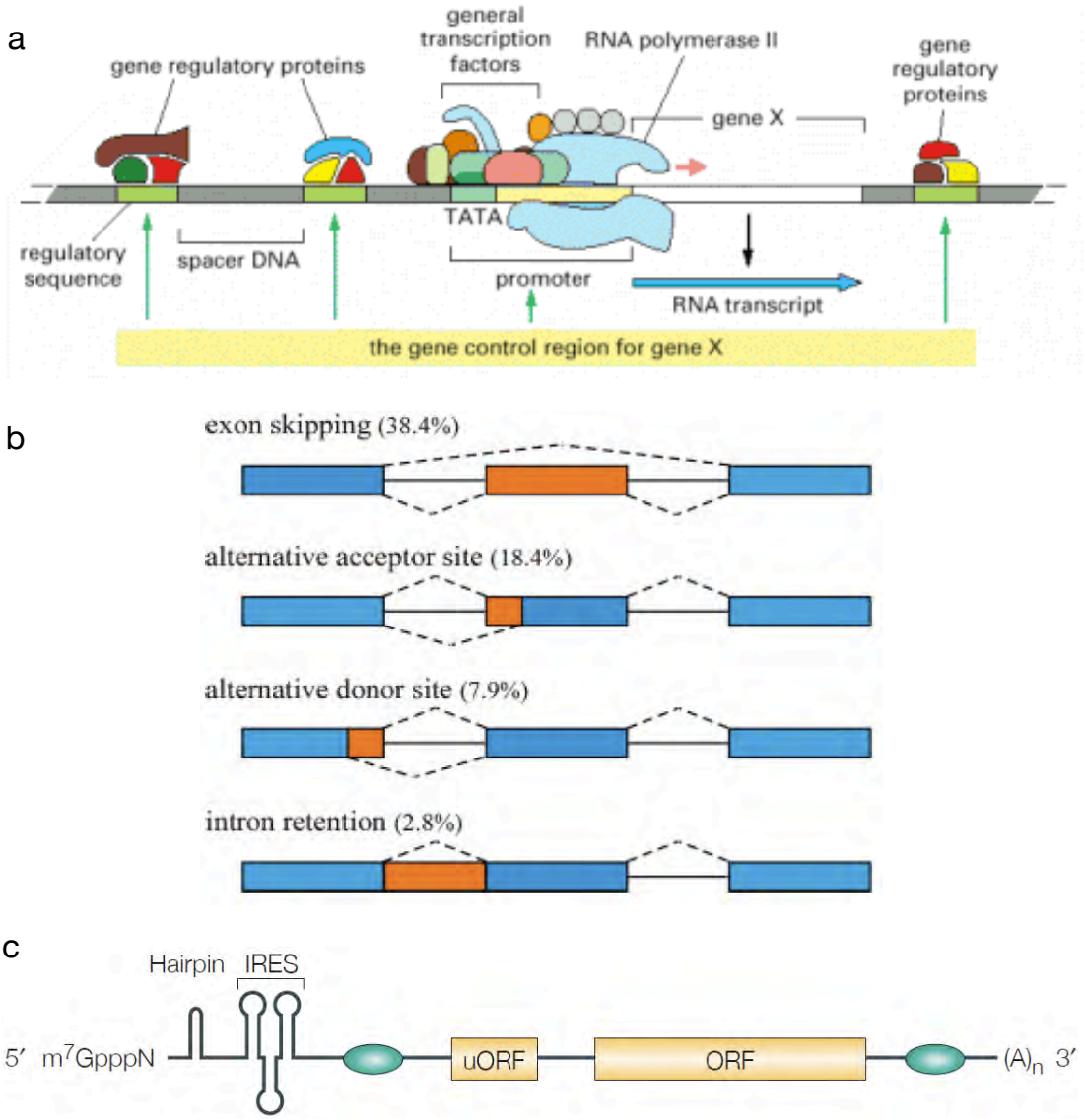

Figure 1.1: a) Genes contain many regulatory regions which must be bound by a number of proteins, including transcription factors and RNA polymerase II, in order for transcription to proceed. These gene control regions govern the spatial and temporal expression of the mRNA for the gene. b) Nuclear RNA can be spliced into mRNA via four main mechanisms: exons can be skipped entirely, individual exons can be spliced at alternative 5' (donor) or 3' (acceptor) sites, and introns can be retained. These mechanisms are responsible for roughly two thirds of alternative splicing events; the remaining third involve more complex mechanisms such as alternative transcription start sites and multiple polyadenylation sites. c) mRNAs contain 5' caps, 3' poly-A tails, open reading frames (ORF) which are translated into protein, upstream oRFs (uORFs) which normally repress translation, 5' and 3' UTRs around the ORF which can bind regulatory proteins and other RNAs such as microRNAs (green ovals), IRES sites which can be used to initiate cap-independent translation, and secondary structure elements such as hairpins which affect the mRNA's protein-binding capabilities. a) taken from Alberts et al. (2004); b) taken from Kim et al. (2008); c) taken from Gebauer and Hentze (2004).

control region contains several subregions known as promoter and enhancer regions. The core promoter region contains a TATA box, a site where several proteins known as basal transcription factors will bind, which enables the synthesis protein RNA polymerase II to bind to the DNA and begin transcription of mRNA (Kornberg, 2007). Other promoter and enhancer regions can be bound by other transcription factors, which act as switches to turn transcription of the mRNA on or off (Kadonaga, 2004).

This means that the transcription of the downstream sequence requires the binding of particular transcription factors to the promoter regions. For example, the Homeobox (or Hox) genes are a set of transcription factors which contain a homeodomain, an amino-acid motif which binds to DNA at specific promoter sites and can activate or repress transcription of the genes downstream of the promoter sites (Svingen and Tonissen, 2006). This mechanism enables the complex regulation of DNA transcription. Many genes can be regulated by a single transcription factor, providing all the genes contain the appropriate binding site for that transcription factor. Alternatively, a single gene can require binding by many transcription factors, which can enable very subtle spatial and temporal control of the expression of this gene. Examples of these methods of regulation will be seen in the rest of this chapter. Many transcription factors interact during development in complex gene regulatory networks which are involved in the determination of cell fate and therefore the specification of different tissues (de Leon and Davidson, 2007).

RNA is initially transcribed in the nucleus of the cell. This nuclear RNA (nRNA) is not the same as the mRNA which will be translated into protein in the cytoplasm of the cell. It contains long sequences which are spliced out of the RNA before it is transported out of the nucleus (see Figure 1.1b). These sequences are known as introns, because they remain in the nucleus, as opposed to the sequences that form part of the mRNA, which are known as exons. When the introns in the nRNA are spliced out to produce mRNA, it is also possible for some selection of exons to take place, which means many different proteins containing different groups of exons can be produced from the same genomic DNA (see Kim et al. (2008) for a recent review).

The initiation of most translation in the cell is dependent on the presence of a cap at the 5' end of the target mRNA, which is added in the nucleus. This cap is bound by eukaryotic initiation factor 4E (eIF4E), which is required for translation to begin (Goodfellow and Roberts, 2008). The 3' end of mRNA is also modified in the nucleus, with a poly(A) tail being added which must be bound by PABPC (Poly-A Binding Protein, Cytoplasm) for the initiation of translation to take place (Kühn and

Wahle, 2004). Translation initiation can be regulated by interfering with the binding of eukaryotic initiation factors and poly-A binding proteins.

Around 95-97% of mRNAs are translated via the cap-dependent pathway (Merrick, 2004), while the remainder are translated via sequences within the mRNA that can be translated directly, which are called internal ribosome entry sites (IRESs) (Komar and Hatzoglou, 2005). The translation of IRESs requires many of the same proteins required for cap-dependent translation, but not the cap itself, and so the absence of eIF4E does not affect this cap-independent translation (see Figure 1.2a).

After splicing and the addition of the cap and poly-A-tail, mRNA is transported into the cytoplasm where it can be translated by ribosomes, complexes of protein and RNA which assemble free amino acids into proteins according to the sequence of the mRNA (Kapp and Lorsch, 2004). An mRNA contains a protein-coding region as well as regions which are not translated at either end of the molecule, labelled the 5'UTR and 3'UTR (for Un-Translated Region; see Figure 1.1c). These UTRs contain regulatory sequences which can be bound by proteins and other RNAs such as the small regulatory RNAs known as microRNAs (Kuersten and Goodwin, 2003; Wu and Belasco, 2008). These sequences can act in a similar way to promoter regions in DNA, with multiple microRNAs regulating multiple mRNAs, enabling complex regulation of mRNA translation to occur.

In particular, the 3'UTR is involved in the localisation of an mRNA to particular places in a cell, contributing to cell polarity and functional compartmentalisation of the cell. mRNAs can be packaged in ribonucleoprotein complexes (RNPs) which can be transported along tracks in the cytoskeleton. The mRNAs are bound by translational repressors which usually bind to the 3'UTR of the mRNA. When the RNP reaches a source of protein which can remove the translational repressor, the mRNA can be translated at this location (see Besse and Ephrussi (2008); see Figure 1.2c/d).

Once an mRNA has been translated into protein, the protein can be modified in many ways which affect its behaviour and which can deactivate it completely. For example, proteins can be phosphorylated by protein kinases, which add phosphate groups to residues in the target protein, causing a conformational change in the protein which may alter its ability to bind to other proteins; this process can be reversed by protein phosphatases, which dephosphorylate the target protein (Hunter, 1995). Particular classes of kinases can phosphorylate particular residues; for example, tyrosine kinases add phosphate groups to tyrosine residues (Hunter, 1998).

Phosphorylation is involved in many cellular processes, and translation is no

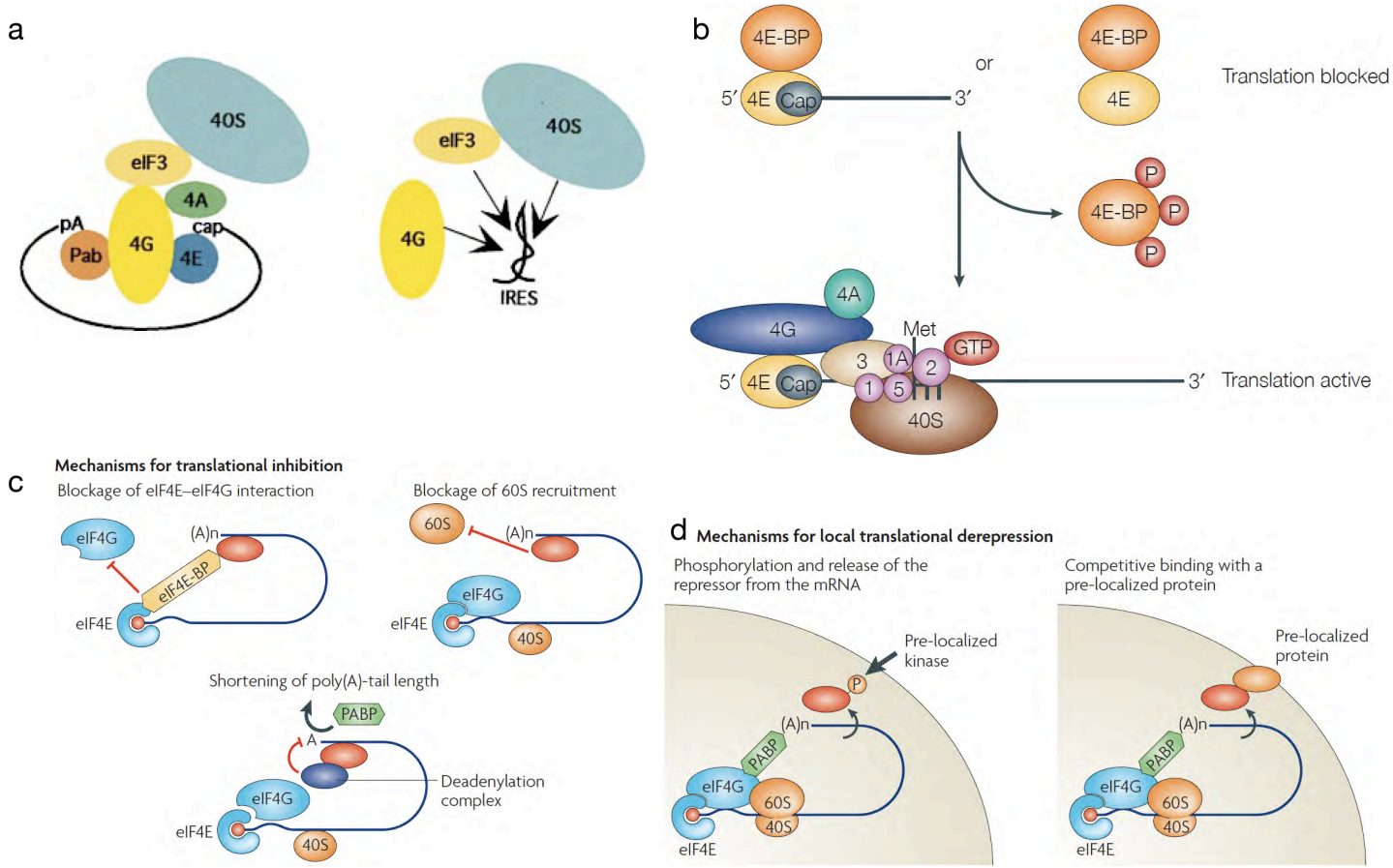

Figure 1.2: a) mRNAs can be translated via cap-dependent or cap-independent mechanisms. Cap-dependent translation (left) requires several eukaryotic initiation factors (eIFs) including eIF3, eIF4A, eIF4E and eIF4G, and the poly-A binding protein (Pab, or PABP), so that the ribosome (including the 40S rRNA subunit) can bind to the mRNA and begin translation. Cap-independent translation requires an IRES site in the mRNA and the initiation factors eIF3 and eIF4G, but not eIF4A, eIF4E or Pab. b) When the eIF4E binding protein 4EBP binds to eIF4E, whether bound to an mRNA or not, cap-dependent translation is blocked. Phosphorylation of 4EBP allows eIF4E to recruit the other members of the cap-dependent translation complex and translation can proceed. c) Translation can be inhibited by translational repressor proteins (red ovals), which can recruit 4EBP to inhibit eIF4E, block recruitment of the 60S rRNA subunit or recruit a deadenylation complex to shorten the poly-A tail and prevent PABP binding. d) mRNAs can be transported with repressors attached; the repressors can then be removed at the sites where mRNA translation is required. Repressors can be removed by phosphorylation by pre-localised kinases or competitive binding with a pre-localised protein. a) taken from Sachs (2000); b) taken from Gebauer and Hentze (2004); c,d) taken from Besse and Ephrussi (2008).

exception (see Figure 1.2b). For example, translation is usually repressed because eIF4E is bound by unphosphorylated 4EBP, the binding protein for eIF4E. When 4EBP is phosphorylated, it releases eIF4E, which can then initiate translation of capped mRNAs (Gingras et al., 1999). 4EBP is phosphorylated by a molecule called mTOR, or mammalian target of rapamycin. In turn, as its name suggests, the phosphorylation of mTOR is prevented by rapamycin (Hay and Sonenberg, 2004). Unphosphorylated mTOR cannot phosphorylate 4EBP, which in turn does not release eIF4E, and so cap-dependent translation is prevented by rapamycin treatment.

In summary, there are multiple mechanisms for controlling the differential expression of genes which can be used to explain the processes of development. In particular, the processing and localisation of RNA during transcription and translation is essential to the selective expression of genes and compartmentalisation of cell function which therefore makes RNA of particular relevance to the study of developmental problems.

1.2.2 Molecular gradients are involved in many aspects of development including axon guidance

A central problem in development is how cells acquire positional information in order to differentiate correctly. For example, the vertebrate hindbrain is divided into a series of eight rhombomeres, each with the same underlying structure but also with different features; for example, different sensory and motor cranial nerves emerge from different rhombomeres (Lumsden, 1990). What positional information is available to the neurons in these rhombomeres which causes them to develop the appropriate nerves?

One major mechanism for identifying positional information is the use of molecular gradients. For example, retinoic acid is expressed posterior to the hindbrain and diffuses anteriorly, creating a high concentration of retinoic acid in the posterior hindbrain and a low concentration in the anterior hindbrain (Glover et al., 2006). This gradient is required for the rhombomeres to differentiate appropriately. In the absence of retinoic acid, only the anterior rhombomeres (r1-4) develop, spreading out across the whole length of the hindbrain; as retinoic acid concentration gradually increases, the remaining posterior rhombomeres gradually differentiate (Gavalas, 2002).

This gradient of retinoic acid is at least in part responsible for the expression of a series of Hox transcription factors across the hindbrain in an overlapping pattern, which defines the positions of the rhombomeres (Wilkinson et al., 1989; Fraser et al.,

1990). For example, HOXB2 is expressed in rhombomeres 2-8, whereas HOXA1 is expressed in rhombomeres 4-6 and HOXB1 is expressed in rhombomere 4 alone (Kiecker and Lumsden, 2005); cumulatively the combinations of different Hox genes across the hindbrain confer unique identities on each rhombomere (see Figure 1.3b).

This is an example of a common process in development, shown in Figure 1.3c, whereby genes are expressed from organiser regions (often at boundaries between other regions), which creates a signalling gradient across a previously uniform sheet of cells. This gradient regulates expression of mutually repulsive transcription factors, causing the cells to take on different identities in different parts of the region. These regional identities are then sharpened by cell sorting activities. This enables formal boundary phenotypes to emerge, and these new boundaries can in turn act as organiser regions.

Genes which induce the formation of patterns, often through graded expression, are known as morphogens, examples of which include the Hedgehog and Wnt families, each of which have complex downstream signalling pathways (Kornberg and Guha, 2007). Many of the proteins in the functioning Hedgehog signalling pathway are phosphorylated, indicating a role for protein kinases in the regulation of this pathway (Aikin et al., 2008). In fact, there can be multiple pathways downstream of these molecules; Wnt proteins act through at least three major pathways, known as the canonical pathway, the planar cell polarity pathway and the calcium pathway (Huelsken and Behrens, 2002) and several variants of these pathways have been discovered (see, for example, Salinas (2007)).

Molecular gradients are also crucial for the guidance of axons to their destinations during development. As axons grow, they are attracted or repelled by molecular cues in their environment, which cause them to turn towards or away from the cue. Classically, there are four families of axon guidance cue molecules: ephrins (Flanagan and Vanderhaeghen, 1998), netrins (Barallobre et al., 2005), semaphorins (Roth et al., 2009) and Slits (Hohenester, 2008). While the details of their behaviours differ, the overall model of their function is the same. The guidance cue is distributed in a gradient across the growth cones of axons, which causes the axon to turn towards or away from the source of the cue, or causes the growth cone to collapse completely.

This behaviour is dependent on the presence in the membrane of the growth cone of an appropriate receptor for the guidance cue. Netrins bind to their receptors DCC or Unc-5, Slits bind to Robos, semaphorins bind to a range of different molecules including plexins and neuropilins, and ephrins bind to Ephs (Dickson, 2002). When a

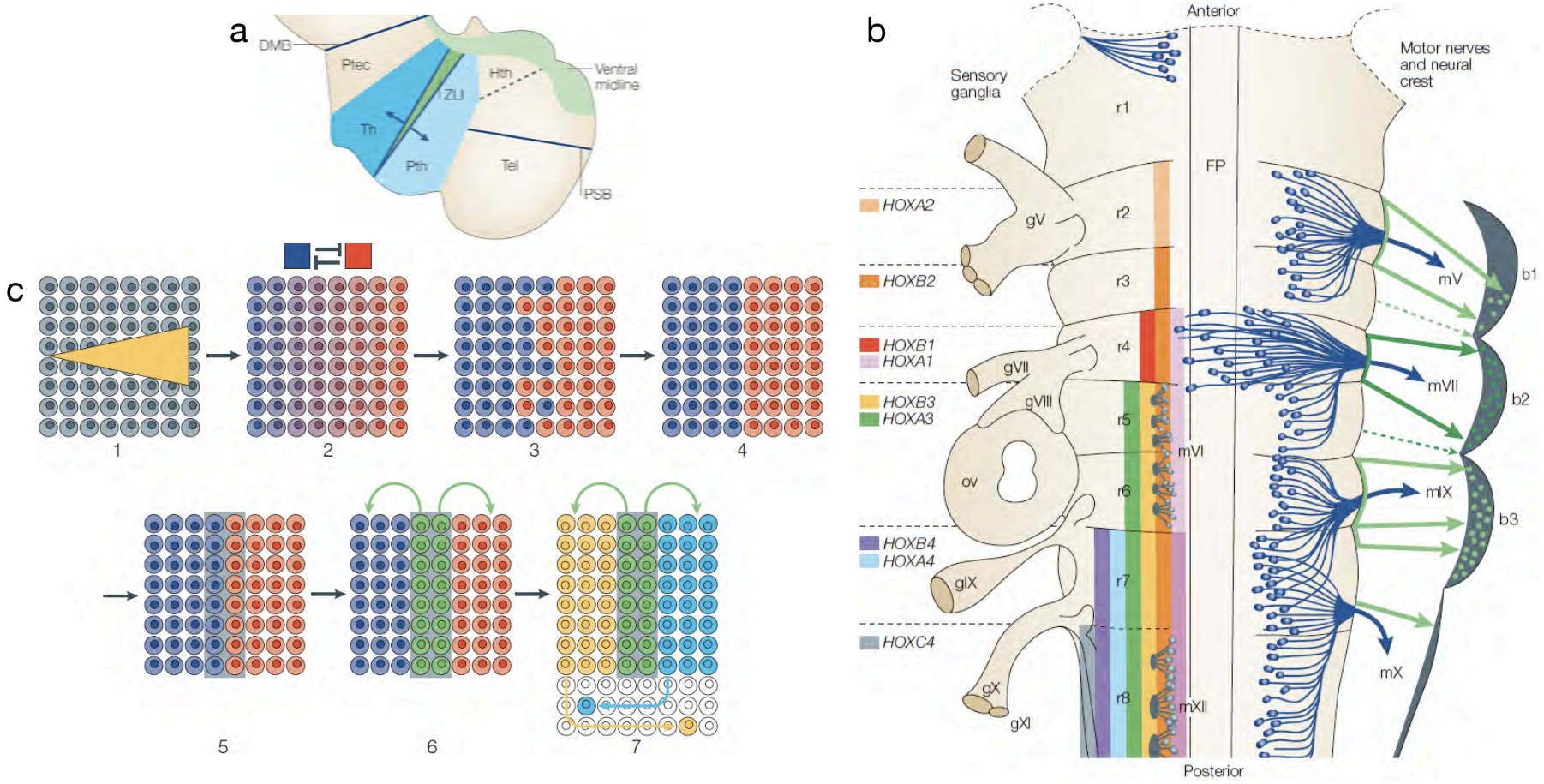

Figure 1.3: a) Early development of the forebrain. The thalamus (Th) and prethalamus (Pth) are separated by gene expression (blue arrows) from the zona limitans intrathalamica (ZLI). DMB, diencephalon-midbrain boundary; Ptec, pretectum; Hth, hypothalamus; PSB, pallial-subpallial boundary; Tel, telencephalon. b) The boundaries of rhombomeres r1-8 are established by overlapping, segmented expression of Hox genes, and give rise to rhombomere-specific cranial sensory ganglia (gV-XI) and cranial nerves (mV-mX) some of which project into branchial arches b1-b3. FP, floor plate; ov, otic vesicles. c) A model for the formation of boundaries in embryonic development. An initially uniform sheet of cells is polarized by an early signalling gradient (yellow; 1), which results in a coarse prepattern of transcription factor expression (red/blue; 2). Mutual repressive interactions between these factors establish two distinct populations of cells that are separated by a fuzzy interface (3). Cell-sorting processes result in a sharpening of this interface (4), and a specific boundary phenotype (loss of adhesion, expression of specific boundary markers) is generated (shaded area; 5). The boundary cells express signalling factors (green; 6) that induce prepattern-dependent cell fates (yellow/turquoise) in the adjacent territories. Postmitotic cells might be able to cross the boundary, as their fates are sealed (7). All pictures taken from Kiecker and Lumsden (2005).

guidance cue binds to one of its receptors, it triggers downstream activity within the growth cone, which causes the growth cone to turn or collapse.

The molecular gradient, rather than just the presence of a molecule, is crucial for these guidance behaviours. For example, axons of cortical explants grow towards increasing gradients of semaphorin-3C but not towards similar gradients of semaphorin-3A, and the semaphorin receptors neuropilin-1 and neuropilin-2 must be expressed in cortical axons for these turning responses to occur (Bagnard et al., 1998). However, in the presence of uniform distributions or decreasing gradients of semaphorins, as opposed to increasing gradients, these axons do not respond differently to the two guidance cues (Bagnard et al., 2000). The responses to increasing gradients of semaphorin-3C and semaphorin-3A are resilient to changes in both the absolute concentration of the semaphorins and in the slope of the gradient, indicating that the growth cones are detecting any increase in semaphorin concentration regardless of the actual quantity of semaphorin present (Bagnard et al., 2000).

Each guidance cue family contains many members which operate in many different systems. For example, the ephrins are divided into two subclasses, A and B, and their receptors, the Eph molecules, are divided into the same two subclasses, to represent their affinity with the ephrins (Flanagan and Vanderhaeghen, 1998). The Eph receptors are receptor tyrosine kinases which span the cell surface membrane and are activated when they are bound by ephrins (Schlessinger, 2000). For example, EphA2, a receptor for ephrinA signalling molecules, is known to have a role in the development of the tectal topographic map and in the guidance of spinal commissural axons (Wilkinson, 2001). EphrinA ligands are expressed in a caudal-to-rostral gradient in the tectum and repulse temporal retinal axons which express EphA receptors. The effects of ephrins can be widespread; Zhang et al. (2008) identify over 200 proteins in cell cultures whose expression is significantly changed after stimulation with ephrin-B1. Similarly, over 140 transcripts are differentially expressed in somatosensory cortex in wild-type and ephrin-A5-deficient mice (Peuckert et al., 2008).

In addition to the classical guidance cue families, many other molecules have been implicated in axon guidance, including several morphogens such as Hedgehogs and Wnts (Endo and Rubin, 2007; Sánchez-Camacho et al., 2005; Charron and Tessier-Lavigne, 2005) and cell adhesion molecules such as N-cadherin and NCAM (Kiryushko et al. (2004); see below). For example, Wnt4 mRNA is expressed in the floor plate of the mammalian spinal cord in a decreasing anterior-to-posterior gradient which attracts commissural axons (Lyuksyutova et al., 2003; Killeen and Sybingco,

2008), and retinal ganglion cells require Sonic hedgehog signalling both intrinsically and from the midline to navigate out of the retina in the correct topographical organisation (Sánchez-Camacho and Bovolenta, 2008).

As morphogens are implicated in axon guidance, so guidance cues are involved in patterning and compartment formation; for example, ephrins are involved in the sharpening of boundaries between rhombomeres in the hindbrain (Cooke and Moens, 2002) and in similar cell sorting behaviour in the intestinal epithelium, disruptions of which can lead to colorectal cancer (Clevers and Batlle, 2006). Therefore the morphogen and guidance cue labels should perhaps be considered as historical markers of the first discovered role of a molecule, rather than indicators of a molecule's entire range of behaviours. In what follows, many more examples of these behaviours will be seen to be involved in the development of thalamocortical axons, and the pathways which are downstream of these molecules will also be described.

1.2.3 Cell adhesion mechanisms are involved in the development of axons

Axons grow not only in response to molecular gradients but also by adhering to other cells and axons in their environment. This adhesion appears to operate using standard cell adhesion mechanisms, which will now be introduced. The involvement of various cell adhesion molecules in the development of the thalamocortical tract will be described in Section 1.4.1 and the details of how the cytoskeleton of the growth cone interacts with cell adhesion molecules will be considered in Section 1.6.2.

Broadly speaking, there are two different ways a cell can anchor itself. It can bind to another cell or it can attach itself to the extracellular matrix. Cell-cell adhesion is primarily mediated by molecules called cadherins, whereas cell-matrix adhesion is mediated by integrins (Shapiro et al., 2007). Cadherins have extracellular, transmembrane and intracellular domains. The extracellular domains of cadherins anchored in different cells bind together, forming adherens junctions which connect the cells. The intracellular domains bind to molecules called catenins, which in turn bind to the cytoskeletons of the cells. This means that intracellular changes in one cell can have effects on the cytoskeletons of other cells through their cadherin-based connections (Redies, 2000).

Cadherins are usually homophilic, which means that they will only bind to cadherins of the same type and not to different types (Stemmler, 2008). This has clear

significance for regional specification. If the cadherins being expressed in a group of cells are the same, they will bind together. If they are different, they will segregate, forming a divide between different groups. The quantity of cadherin expressed on the cell surface also has an adhesive effect. Cells expressing more of a certain cadherin on their surface bind together before cells expressing less of the same cadherin (Duguay et al., 2003).

These mechanisms are involved in the growth of neurites (Kiryushko et al., 2004). For example, if N-cadherin is inhibited *in vivo*, growth of retinal axons is severely impaired (Riehl et al., 1996); also, *in vitro* assays on cerebellar neurons show that neurite length increases with N-cadherin concentration (Doherty et al., 1991). As noted above, the specific functions of cell adhesion molecules in the development of thalamocortical axons will be returned to in later sections.

With these basic concepts established, it is now possible to turn to their application in the development of the cortex, the thalamus, and the thalamocortical tract.

1.3 The cortex and the thalamus

In this section, an interest in the development of the thalamocortical tract will be justified by considering the structure and function of the cortex and the thalamus, the relationships between them, and their importance to the overall function of vertebrate organisms (see Figure 1.4 for an overview). The development of both thalamus and cortex will also be reviewed, so that the development of the thalamocortical tract can be put into context.

1.3.1 The structure and function of the cortex

Much of the processing required for mammals to detect and respond to features of their environments is carried out by the cerebral cortex. The cortex can be divided into areas and layers on anatomical grounds by staining of patterns of cells and fibres (see, for example, Caviness Jr. (1975) for a description of the architectonic map of mouse cortex). These divisions correlate with differences in function, which can be identified by, for example, ablating particular cortical areas and observing functional defects (see Phillips et al. (1984) for a history) or by using imaging techniques to correlate behaviour with activity in cortical areas (see Op de Beeck et al. (2008) for review).

The cortex is segregated into frontal, temporal, parietal and occipital lobes, each of

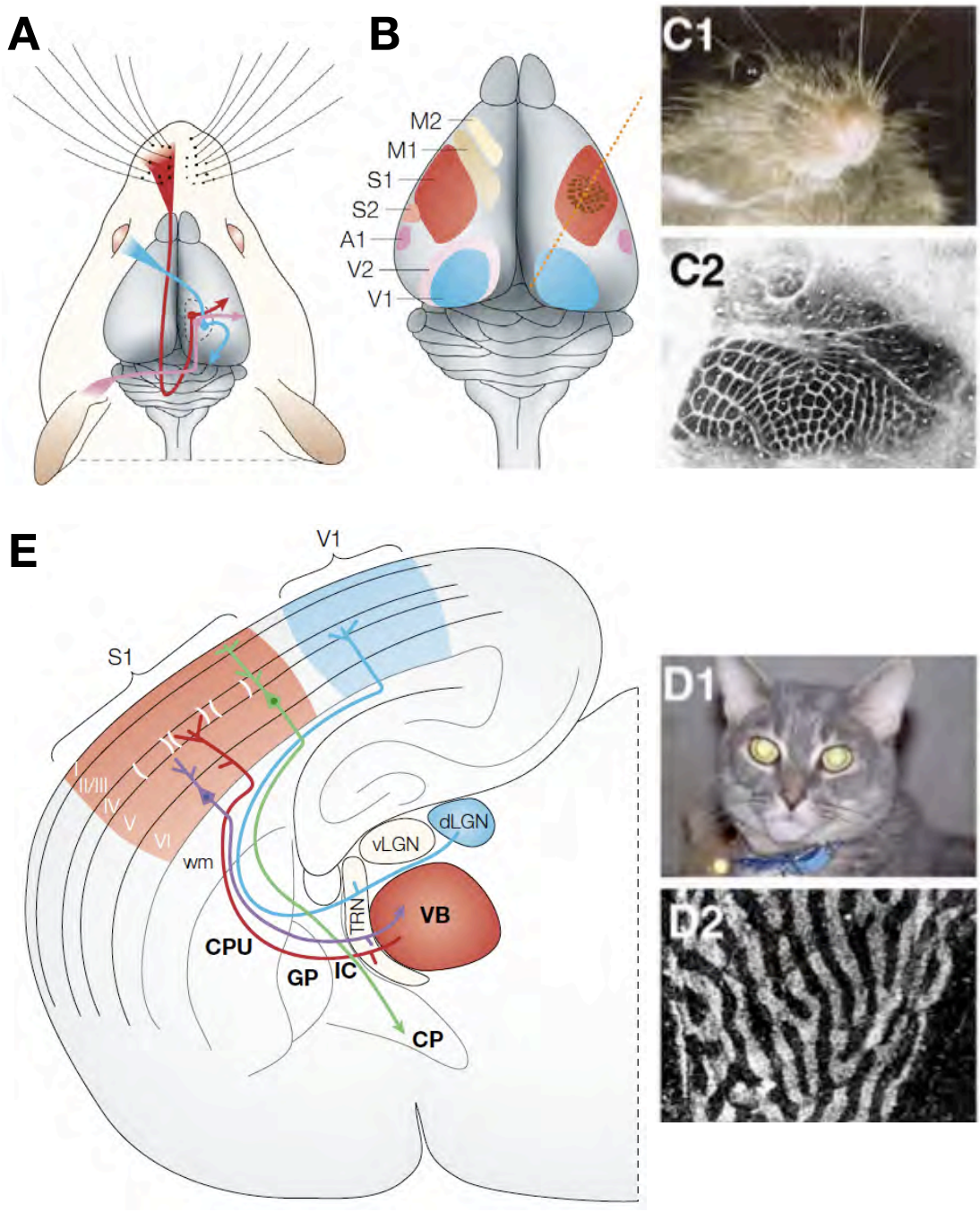

Figure 1.4: Sensory organs map their output to the cortex via the thalamus. A) The output of different modalities is transmitted to modality-specific nuclei of the thalamus and to areas of the cortex via axonal tracts. B) In the mouse, there are separate cortical areas for the initial processing of visual (V1, V2), auditory (A1), somatosensory (S1, S2) and motor (M1, M2) information. C, D) Cortical areas contain mappings of their input, which can vary greatly between modalities. Areas can be mapped topographically, as the whiskers of the mouse are topographically mapped in somatosensory cortex (C), or by feature, as the photoreceptors of the retina are mapped in ocular dominance columns in V1 (D), reflecting input from ipsilateral and contralateral eyes. E) The dorsal lateral geniculate nucleus (dLGN) projects axons to layer IV of V1 (blue), whereas the ventrobasal nuclei (VB) project axons to S1 (red). These axons also project branches into layer VI of the cortex and the thalamic reticular nucleus (TRN). Corticofugal axons project from layer VI to the thalamus (purple) and from layer V to the cerebral peduncle (CP, green). wm, white matter; CPU, caudate putamen; GP, globus pallidus; IC, internal capsule. a,b,e) taken from López-Bendito and Molnár (2003); c,d) taken from Lübke and Feldmeyer (2007).

which contains several functional areas. There are a number of primary areas which are functionally related to the processing of sensory and motor information (see Figure 1.4). For example, there is a topographic mapping of the pattern of the photoreceptors in the retina within an area of cortex in the occipital lobe which is labelled V1, and this area responds to changes in visual input (Huberman et al., 2008). Similarly, the whiskers on the face of a mouse are each connected to groups of neurons shaped into barrel-like structures, which are topographically organised to match the pattern of the whiskers. These barrels are required for the processing of somatosensory information from the whiskers (Lübke and Feldmeyer, 2007). These cortical areas have been conserved throughout mammalian evolution, although their topographic organisations are different depending on the particular sensory apparatus of each species (Krubitzer, 1995).

There are also a number of secondary areas which do not process sensory information directly but which primarily receive inputs from other cortical areas. Primates and, in particular, humans have much larger prefrontal and temporal lobes than other mammals, and these lobes are mostly involved in secondary processing (Kaas, 2005). These regions can be restricted to complex processing of one sensory modality; for example, the output of V1 is processed by many other areas of the brain which focus on particular features of visual information such as colour or direction of motion (see Wandell et al. (2007) for a review of human visual areas). However, there are also many association areas, particularly in the frontal cortex, which integrate information from many other cortical areas and have been linked to behaviours such as abstract thought and action selection (see Badre (2008) for review).

The cortex does not appear to be split into repeating segmented modules across its surface as the rhombomeres in the hindbrain are (Wilkinson et al., 1989; Fraser et al., 1990). The cortex is much more diverse, with areas of varying sizes, with much less well defined cell lineage restriction boundaries and many very different patterns within each cortical area, such as barrels in mouse somatosensory cortex and ocular dominance columns in visual cortex (Larsen et al., 2001; Chambers and Fishell, 2006). However, the same basic mechanisms appear to operate in the cortex as are found in other areas during development (see Figure 1.3 and Kiecker and Lumsden (2005)), with the expression of molecular gradients leading to the differentiation of cortical areas. Specific examples of gradients acting to form areas of thalamus and cortex will be discussed in Sections 1.3.3 and 1.3.4.

1.3.2 The structure and function of the thalamus

The thalamus is a region of the diencephalon which is central to the functioning of the brain as a whole system and as a series of specialised subsystems, and therefore the development of the thalamus itself and its connections with other areas of the brain is of great interest. The thalamus has been classically divided into three main parts; the dorsal thalamus, the ventral thalamus and the epithalamus (see Figure 3.2). The dorsal thalamus in turn is a collection of nuclei, each of which has structural and functional identifying marks (Jones (2007), Sections 3.1-3.4). Recently, it has been recommended that the dorsal thalamus is renamed the thalamus and the ventral thalamus is renamed the prethalamus (Puelles and Rubenstein, 2003). This convention will be followed from this point onward.

There is a simple model of thalamic function which runs as follows. Almost all input to the cortex first passes through the thalamus (Sherman and Guillery (2006), Chapter 1). Sensory and motor systems of the body send afferent connections to particular nuclei of the thalamus, which in turn sends connections to particular areas of the cortex (see Figure 1.4e). For example, the retina projects axons which form connections with the lateral geniculate nucleus, one of the nuclei of the thalamus, which in turn forms connections with V1 and other visual areas of the cortex (Huberman et al., 2008), whereas auditory information is passed to auditory cortex via the medial geniculate nucleus (Winer and Lee, 2007), and somatosensory information is passed to somatosensory cortex via the ventrobasal nuclei (Hand and Morrison, 1970; Inan and Crair, 2007). The thalamocortical tract is the collection of axons which project from the thalamus and innervate the cortex. There is a corresponding corticothalamic tract of axons which project from the cortex and innervate the thalamus.

This simple model has been elaborated over the years as it has become possible to investigate the anatomy of the thalamus, cortex and their connections in ever increasing detail (Percheron et al., 1996). For example, Jones (1998) proposes that in primates, many thalamic nuclei project diffuse connections to many different cortical areas, based on a group of thalamic cells which are immunoreactive to calbindin and which project to many areas of cortex, although this feature may be limited to primates as these calbindin-reactive cells could not be detected in rat thalami. Also, some single axons (but not all axons) from one nucleus can produce several branches which innervate different cortical areas (see, for example, Birnbacher and Albus (1987)).

Indeed, it increasingly appears that, although there are many connections between cortical areas, the thalamus also has a role to play in communication from cortical area to cortical area, with corticothalamic projections transmitting information to the thalamus which is then transmitted by the thalamus to other cortical areas (see Cudeiro and Sillito (2006) and Sherman and Guillery (2006) for full reviews).

These insights have led to a re-evaluation of the importance of the thalamus. In terms of sheer quantity of connections, it appears that the number of corticocortical connections dwarfs the number of thalamocortical connections (for example, Essen (2005) notes that in the primate visual system there is a 20-25-fold greater number of connections between visual areas V1 and V2 than between the lateral geniculate nucleus and V1). However, the fact that all sensory and motor systems project to the thalamus and that the thalamus communicates with all cortical areas in both directions has led to an increase in the study of the roles of thalamus in such general subjects as attention (McAlonan et al., 2008), memory (Mitchell and Gaffan, 2008) and even consciousness (Schiff, 2008).

Despite the complexity of the connections between thalamus and cortex, it remains the case that the thalamus has an internal organisation which is related to cortical organisation in a complex but reliable fashion. This raises a number of developmental questions. Firstly, how are the thalamic nuclei and cortical areas defined? Are the kind of genetic mechanisms which define cortical areas also the cause of thalamic segregation? Secondly, how do the thalamocortical axons traverse the long distance from the thalamus to the cortex, crossing several areas of the brain and requiring a number of changes of direction? Thirdly, how do the axons from particular nuclei make specific connections with related cortical areas? These questions will be addressed in the following sections.

1.3.3 The development of the thalamus

The thalamus, cortex and thalamocortical pathway develop during overlapping periods in mouse embryonic development; the neurons of the thalamus proliferate between E10 and E16 (Angevine, 1970); the cortex forms between E11 and E19 (Dehay and Kennedy, 2007) and the thalamocortical projection grows from the thalamus to the cortex between E11 and E18 (Deng and Elberger, 2003). How does this overlap in time bear on the developmental questions posed above? How interdependent are these systems?

The early brain is differentiated into the prosencephalon (forebrain), the mesencephalon (midbrain) and the rhombencephalon (hindbrain); the thalamus and cortex both develop from the prosencephalon (Kiecker and Lumsden, 2005). However, before this occurs the prosencephalon is further differentiated into the telencephalon and diencephalon (Puelles and Rubenstein, 2003). The cortex, basal ganglia and hippocampus develop from the telencephalon whereas the thalamus, epithalamus and pretectum develop from the diencephalon (Bertrand and Dahmane, 2006). Therefore the cortex and thalamus develop separately in the period before they are connected by the thalamocortical tract. These separate developmental processes are now described.

The developing diencephalon (reviewed by Lim and Golden (2007)) begins to segregate into three prosomeres (p1-3) at E10.5 in the embryonic mouse (Wolf et al., 2001); see Figure 1.3a). Prosomere p1 becomes the pretectum, p2 becomes the thalamus and the epithalamus and p3 becomes the prethalamus and eminentia thalami (Puelles and Rubenstein, 2003). Prosomeres p2 and p3 are separated by the appearance of the zona limitans intrathalamica (ZLI), a region whose position is determined by expression of Lrrn1 (Andreae et al., 2007), Otx1l and Otx2 (Scholpp et al., 2007) and which requires the secretion of the morphogen Sonic hedgehog (Shh) from the basal plate for its formation (Zeltser, 2005). The boundaries of the ZLI are defined both anteriorly by fezl, a protein containing a zinc finger DNA-binding domain which is expressed from the rostral diencephalon and is required for correct formation of the prethalamus (Hirata et al., 2006; Jeong et al., 2007), and posteriorly by Irx1b (Scholpp et al., 2007). Once formed, the ZLI expresses Shh independently of its basal plate expression, and it is this source of Shh which causes p2 and p3 to differentiate into thalamus and prethalamus (Vieira and Martinez, 2006). For Shh to induce the formation of thalamus and prethalamus the transcription factor Irx3 must be expressed in both of these regions (Kiecker and Lumsden, 2004).

The progenitor cells which give rise to the thalamus can be identified at E10.5-E11.5 by expression of Olig3, Ngn1 and Ngn2 (Vue et al., 2007). The homeodomain transcription factors Hoxa1, Hoxd2 and Pax6 are also expressed in p2 and p3 at this time (Wolf et al., 2001). Vue et al. (2007) show that there are opposing gradients of Dbx1 and Olig2 throughout the same cells at this time, which indicate that these cells are already heterogenous before the thalamus differentiates into nuclei. Angevine (1970) shows that thalamic cells are generated between E10.5 and E16.5 but that the cells of different nuclei proliferate at different times; for example, the cells of the lateral geniculate nucleus proliferate between E10.5 and E14.5. Postmitotic cells

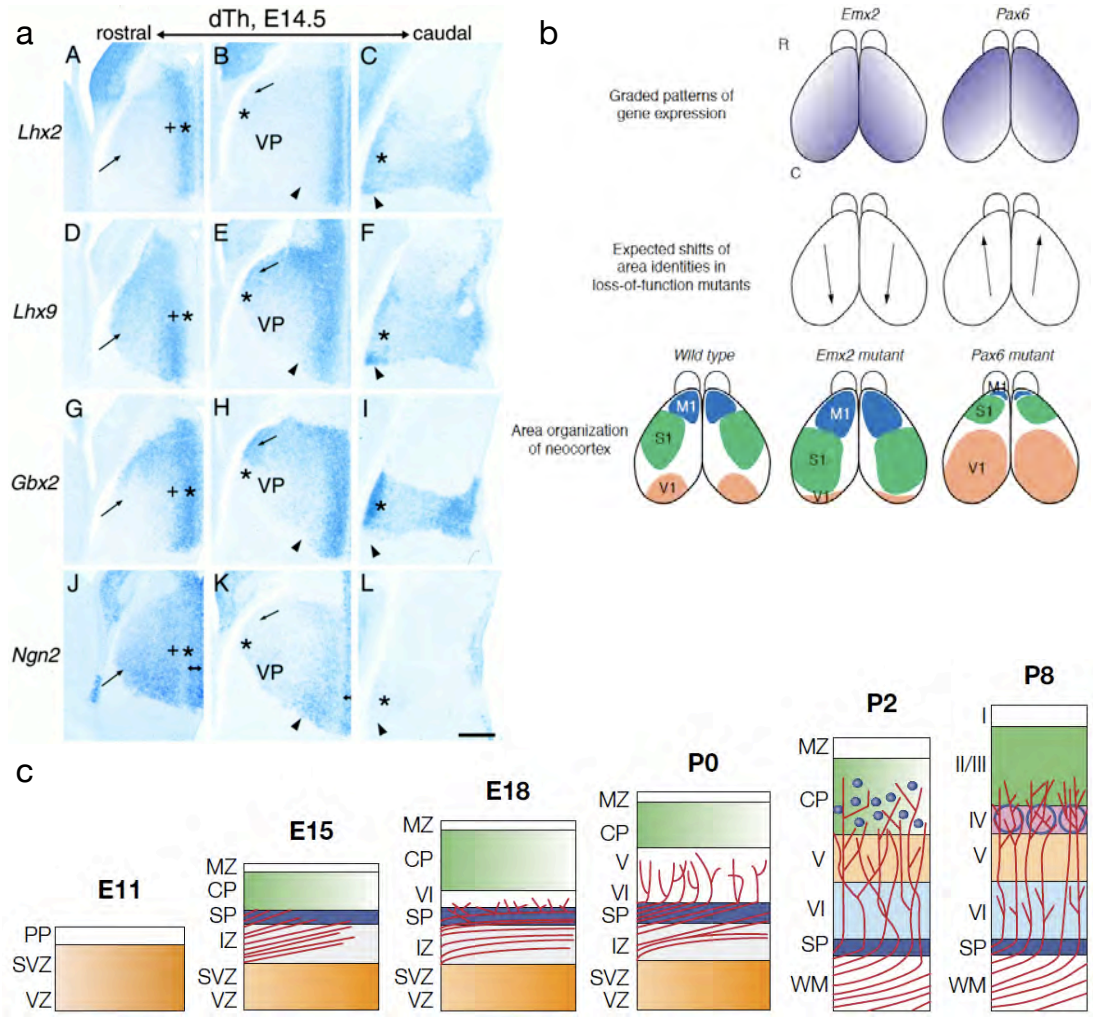

Figure 1.5: a) The mRNAs for Lhx2 (A-C), Lhx9 (D-F), Gbx2 (G-I) and Ngn2 (J-L) are differentially expressed in dorsal thalamus (dTh) at E14.5, along both medial to lateral and rostral to caudal axes. (A,D,G,J) The cross, asterisk and double-headed arrow in J indicate medial strips of differential expression. The arrows show expression of Lhx9 and Ngn2 but not Lhx2 and Gbx2 at the site of the laterodorsal nucleus. (B,E,H,K) Differential expression of the four mRNAs can be seen at the sites of the lateral posterior nucleus (arrows), dorsal lateral geniculate nucleus (asterisks) and ventroposterior nucleus (VP). (C,F,I,L) Differential expression can also be seen in the peripeduncular nucleus (arrowheads) and the ventral medial geniculate nucleus (asterisks). Scale bar, 200μm. b) Gradients of Emx2 and Pax6 are expressed across the cortex during development. In Emx2 and Pax6 loss-of-function mutants, the area organisation of the cortex is shifted caudally in the case of Emx2 and rostrally in the case of Pax6. c) Cortical layers develop from E11 to P8 in the mouse. Cortical neurons migrate from the ventricular zone (VZ) and subventricular zone (SVZ) into the preplate (PP) from E11. The preplate differentiates into the marginal zone (MZ), cortical plate (CP), subplate (SP) and intermediate zone (IZ). The layers of the cortical plate then form inside out, from layer VI to layers II/III. Thalamocortical axons innervate the cortex from E15 onwards, pausing in the subplate for several days and then forming synapses with neurons in layer IV postnatally. a) taken from Nakagawa and O'Leary (2001); b) taken from O'Leary and Nakagawa (2002); c) taken from López-Bendito and Molnár (2003).

initially form into clusters known as pronuclei; the final segregation of nuclei into fully functional units is not complete until the first few days after birth (Jones (2007), Section 6.4).

It may be that the differential expression of genes in the early thalamus is sufficient to determine all the thalamic nuclei. Nakagawa and O'Leary (2001) shows that Lhx2, Lhx9, Gbx2 and Ngn2 are expressed in distinct but overlapping patterns in the thalamus which match the locations of several thalamic nuclei (see Figure 1.5a), and that these genes are expressed from the time progenitor cells become post-mitotic until the nuclei are fully differentiated (although the role of Lhx2 has been questioned; see Section 1.4.2).

For example, the transcription factor Pax6 is involved in the development of the thalamus and the growth of the thalamocortical tract. In Small eye mice, in which Pax6 is non-functional, the thalamus forms but does not differentiate correctly, as expression of region-specific genes such as Nkx2.2 and Lim1/Lhx1 is disrupted (Pratt et al., 2000). There is also disruption of the expression of the cell adhesion molecule R-cadherin, which is usually co-expressed with Pax6 (Stoykova et al., 1997). R-cadherin can rescue the innervation of the thalamus by postoptic commissural axons (Nural and Mastick, 2004), a behaviour which is abnormal in $Pax6^{-/-}$ knockout mice (Andrews and Mastick, 2003).

Similarly, the neurotransmitter serotonin influences thalamic development, as its presence enhances neurite outgrowth in E15.5 thalamic explants (Lotto et al., 1999; Persico et al., 2006). There is differential expression of serotonin receptor variants across the thalamus at this stage, with 5-HT_{1A} and 5-HT_{1D} being expressed across the whole thalamus but 5-HT_{1A} being more strongly expressed dorsally and 5-HT_{1F} being more strongly expressed ventrally (Bonnin et al., 2006).

It is not only the presence, but also the quantity, of gene expression that determines the patterning of the thalamus. Gbx2, for example, is expressed throughout the thalamus during development but shows higher levels of expression in some regions than in others (Martinez-de-la-Torre et al., 2002). This effect can also be seen after the nuclei have differentiated; for example, the cadherins R-cadherin and N-cadherin are expressed across the thalamus at P1 but with varying levels of expression in different nuclei (Obst-Pernberg et al., 2001). As noted in Section 1.2.3, this causes the cadherins with similar quantities of expression to bind together, closely associating cells within nuclei while separating cells from different nuclei. In addition, there are areas where the mRNA for one of these cadherins is present but the protein is not; both R-cadherin

and N-cadherin mRNA can be found in the lateral geniculate nucleus but the translated proteins are not (Obst-Pernberg et al., 2001), indicating that the expression of protein is regulated post-transcriptionally in the postnatal thalamus.

Differential gene expression in the thalamus is required for thalamic afferents to form appropriate topographic mappings with thalamic nuclei. For example, there are gradients of ephrin-A2 and ephrin-A5 mRNA and protein across the lateral geniculate nucleus, which, if removed, cause retinal afferents to spread diffusely across the LGN rather than forming a tight topographic mapping of the cells of the retina (Feldham et al., 1998; Lyckman et al., 2001).

Other molecules including Fgf8 (Kataoka and Shimogori, 2008), Math4a, Dlx5 (González et al., 2002) and Frizzled5 (Liu et al., 2008) have been implicated in the differentiation of nuclei and many more studies are required before a full account of the formation of nuclei can be given. However, in principle there is no reason why patterning of transcription factors and secreted morphogens could not completely account for the segregation of thalamic nuclei. The patterning of the nuclei themselves is another matter; for example, the lateral geniculate nucleus is separated into layers, with retinal ganglion cells from each of the two eyes innervating alternate layers, and this segregation requires spontaneous firing of retinal neurons (Shatz and Stryker, 1988). Such activity-driven refinements of thalamic cells may well influence the behaviour thalamocortical axons; however, the innervation occurs late in embryonic development (in animals such as cat and monkey) or postnatally (in mouse and ferret) (Chalupa, 2007), by which time the thalamocortical axons have already reached the cortex, and so innervation of the thalamus is unlikely to play a role in the growth of thalamocortical axons to the cortex.

1.3.4 The development of the cortex

In the mouse, the cells of the cortex begin to proliferate from the ventricular zone which lines the cerebral ventricles at E10.5, the same time as thalamic cells begin to proliferate, and continue to proliferate from this region until E18.5 (Dehay and Kennedy, 2007). From E18.5 onward, progenitor cells begin to develop into glial cells rather than neurons (Levers et al., 2001). Between E11.5 and E13.5, the preplate and subventricular zone form above the ventricular zone and the preplate is then split into two regions, the marginal zone and the subplate, by cells which form the cortical plate. The cortical plate, which will contain the six layers of the mature cortex, develops

between E13.5 and the first week of birth (see Figure 1.5c).

The cortical layers develop outward from the ventricular zone and subventricular zone, with layer VI cells proliferating from E11.5 and populating the cortical plate until E16.5, layer V cells doing the same between E12.5 and E16.5, layer IV cells between E14.5 and E17.5 and layer II/III cells between E15.5 and E18.5 (Polleux et al., 1997; Kriegstein and Noctor, 2004). Cortical areas emerge as the cortical layers form. Early cortical neuroblasts begin to take on areal identities as early as between E10.5 and E12.5 and areas continue to be refined until at least E18.5 (Mallamaci and Stoykova, 2006).

Many genes have been implicated in the processes of cortical lamination and arealisation. Molyneaux et al. (2007) summarises evidence of the expression of 66 genes during cortical lamination, with genes showing expression in a single layer or multiple layers and expression changing over time. While far fewer genes have been linked to arealisation than lamination so far, it appears the processes involved are similar to those seen in the thalamus, where rather than one gene being expressed for each area, overlapping domains of expression of individual genes create a pattern of regions which express unique combinations of genes (Rash and Grove, 2005). As development progresses, the behaviour of different regions of the cortex can be related to graded and overlapping patterns of gene expression.

In the last decade, several secreted ligands, including several Fgfs, Bmps and Wnts (Cholfin and Rubenstein, 2008; Grove and Fukuchi-Shimogori, 2003), and transcription factors, including Emx1, Lhx2 and TBr1 (Donoghue and Rakic, 1999b), Emx2 (Hamasaki et al., 2004), Pax6 (Stoykova et al., 1997), Foxg1 (Pratt et al., 2002), COUP-TFI (Faedo et al., 2008) and Sp8 (Cholfin and Rubenstein, 2008) (see O'Leary et al. (2007) for review), have been identified which are required for the main cortical areas (V1, A1, S1 and M1) to form correctly (O'Leary and Sahara, 2008).

For example, the transcription factor Emx2 is expressed in a posterior-medial to anterior-lateral gradient across the telencephalon throughout corticogenesis (see Figure 1.5b); overexpression of Emx2 causes the posterior cortical area V1 to grow in size whereas the anterior area M1 shrinks. In heterozygous Emx2 knockout mice, where Emx2 is downregulated in the cortex, the reverse happens, with V1 shrinking in size and M1 expanding (Bishop et al., 2000; Hamasaki et al., 2004). In homozygous $Emx2^{-/-}$ knockout mice, a similar shift of areas is seen, with posterior-medial areas reduced and anterior-lateral areas increased in size (Mallamaci et al., 2000). This shows that the size of cortical areas can be regulated by the level of expression of

transcription factors.

Similarly, in Pax6 conditional knockouts, where the expression of Pax6 in the juvenile cortex is abolished but its expression elsewhere in the brain is normal, the cortex is substantially reduced in size and areal markers such as Id2 and EphA7 show that posterior areas of the brain are smaller but anterior areas are larger than in juvenile wild-type animals (Piñon et al., 2008). However, although areas differ in size, they form in their usual pattern. This indicates that Pax6 expression in the cortex does not intrinsically affect cortical boundary formation or thalamocortical connectivity.

The differential graded expression of Emx2 and Pax6 and the cell adhesion molecule Cadherin-6 (Cadh6) can be related to differences in cortical axon growth behaviour. Bellion and Métin (2005) dissected a dorsal area of E12.5 mouse cortex with strong Emx2 expression, weak Pax6 expression and no Cadh6 expression and compared it to a lateral area of the cortex with weak Emx2 expression, strong Pax6 expression and strong Cadh6 expression. The dorsal cortex projects long, fasciculated corticofugal axons, whereas the lateral cortex projects shorter, more diffuse corticofugal axons. This behaviour is not dependent on the position of the cortical areas, because the same behaviour is observed when both tissues are transplanted to the pallial-subpallial boundary, when the tissues are grown in culture, and when dissocated dorsal or lateral cells are grown in culture (Bellion and Métin, 2005). This behaviour is therefore likely to be dependent on the expression of different proteins in these tissues such as Emx2, Pax6 and Cadh6.

Genes are not only expressed in gradients across the cortex but also specifically within individual cortical areas and layers, as can be shown by the Eph receptor molecules, which are expressed selectively in cortical areas and layers in the macaque (Donoghue and Rakic, 1999b,a). For example, EphA6 is restricted to layer VI of the cortical plate in the visual system. This patterning appears to be tissue-autonomous, as expression of the EphA receptors is the same in wild-type cortex, cortical explants grown *in vitro* and in Mash-1 knockout mice, where no thalamocortical connections are made (Yun et al., 2003). However, the expression of the Eph ligand ephrin-A5 did change in cultured cells and Mash-1 knockout mice, suggesting that this ligand may regulated by factors extrinsic to the cortex (Yun et al., 2003).

As with the development of the thalamus, although the precise mechanisms and genes are so far poorly understood, there is no a priori reason why cortical areas could not entirely be specified by genetic regulatory networks intrinsic to the cortex. However, it will become clear in what follows that extrinsic factors, such as

thalamocortical innervation, are involved in some aspects of cortical development.

1.4 The development of the thalamocortical tract

The thalamocortical tract is the fundamental pathway for the transmission of sensory and motor information to the cortex. The axons within the tract form connections between the nuclei of the thalamus and the areas of the cortex in complex patterns which are not fully understood. In this section, the formation of this tract and its relevance to brain development in general will be explored, demonstrating the variety and complexity of the behaviour of thalamocortical axons during their development. In what follows, the growth of thalamocortical axons from thalamus to cortex, the topographical organisation of these axons as they grow, and the innervation of the cortex by these axons will be discussed in detail.

1.4.1 The growth of the thalamocortical tract to the cortex

While the cells of the thalamus are proliferating and differentiating to form nuclei, they begin to project axons which will grow towards and innervate the cortex. These axons (which are projected from 80-85% of lateral geniculate nucleus cells and 99% of the cells in the rest of the thalamus in rat and mouse (Arcelli et al., 1997)) have to make several changes of direction and navigate a number of obstacles and intermediate targets in order to reach their final destination in the cortex (see López-Bendito and Molnár (2003) and Price et al. (2006) for reviews). The axons grow towards the hypothalamus, turn laterally, cross the boundary between the diencephalon and telencephalon, travel across the ventral telencephalon, and cross the boundary between the subpallium and pallium, after which they innervate the cortex, forming synaptic connections with neurons in layer IV of the cortex. This journey will now be described in detail.

1.4.1.1 Growth of the thalamocortical tract from the thalamus to the diencephalic-telencephalic boundary

At E12.5, thalamic cells begin to project axons out of the thalamus (see Figure 1.6). These axons grow to cross the thalamic reticular nucleus (TRN), which lies ventral to the thalamus, projecting branches into the TRN as they cross (Pinault, 2004). The axons then proceed ventrally but turn laterally before reaching the

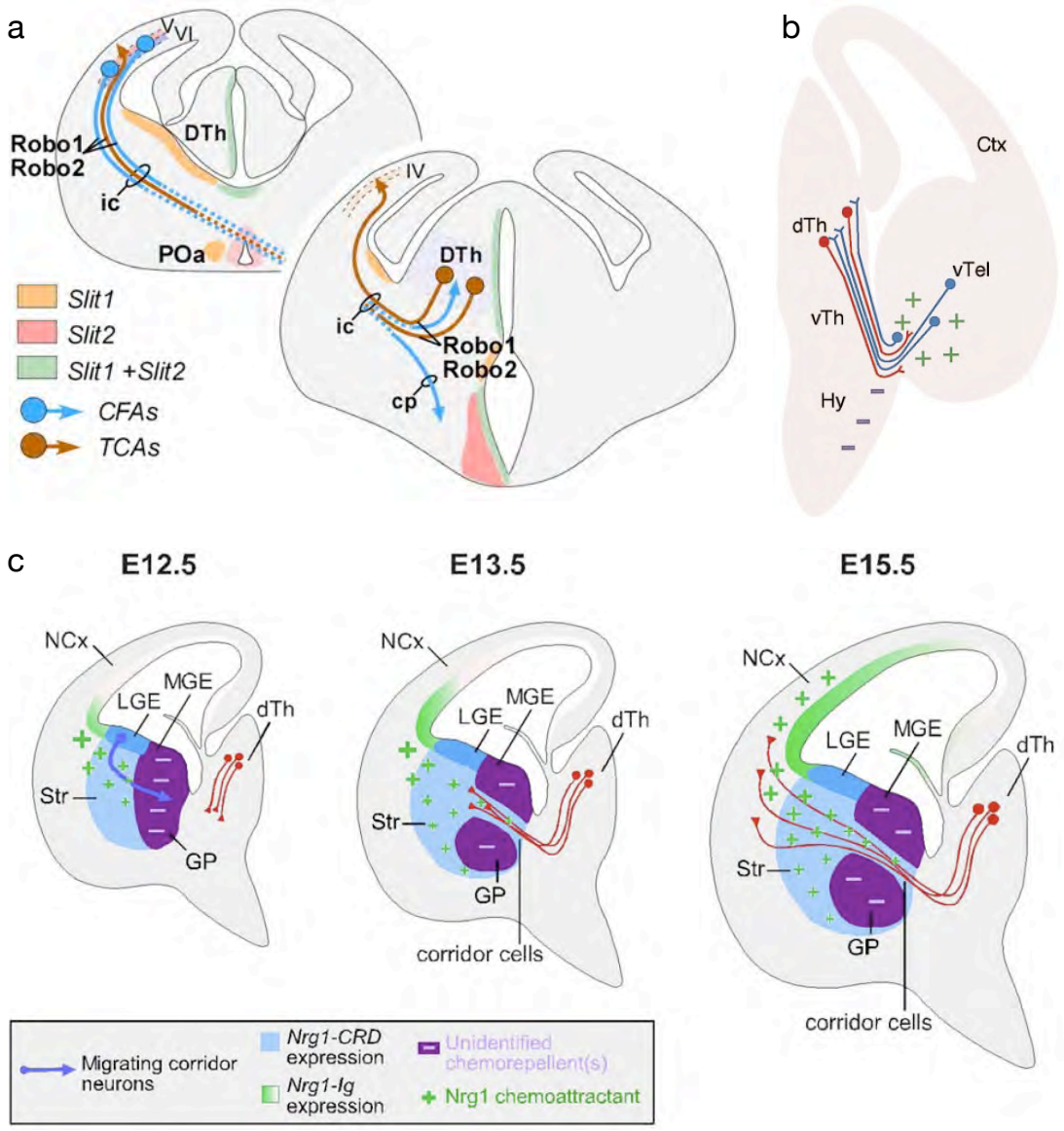

Figure 1.6: a) Thalamocortical axons are guided away from the hypothalamus and towards the internal capsule by expression of Slit1 and Slit2 in the hypothalamus and anterior preoptic area (POa), which requires the axons to express Robo1 and Robo2 in their growth cones. Corticofugal axons grow to the thalamus and the cerebral peduncle (cp). b) In addition to repulsive guidance cues in the hypothalamus and attractive guidance cues in the ventral telencephalon, ventral telencephalon neurons project axons to the thalamus which provide a scaffold for thalamocortical axons. c) At E12.5, the medial ganglionic eminence (MGE) is not permissive to thalamocortical axons (purple shading); neurons from the lateral ganglionic eminence (LGE) migrate to the MGE and provide a corridor for thalamocortical axons to grow through from E13.5 onwards. This requires Nrg1-CRD expression (blue shading) and Nrg1-Ig expression (green shading). NCx, neocortex; Str, striatum; dTh, dorsal thalamus; GP, globus pallidus. a) taken from López-Bendito et al. (2007); b) taken from Braisted et al. (1999); c) taken from López-Bendito et al. (2006).

hypothalamus. At E13.5, the axons cross the boundary between the diencephalon and telencephalon (diencephalic-telencephalic boundary, or DTB) and begin to cross the ventral telencephalon through a region called the internal capsule (Molnár et al., 2003). Why do thalamic axons destined for cortex turn and cross the DTB rather than innervate the hypothalamus?

As indicated in Section 1.2.2, thalamocortical axons are attracted to and repelled by molecular guidance cues, which are produced by nearby regions of the brain and are usually expressed in gradients. The presence of these molecular signals can be inferred because, for example, thalamocortical axons cultured *in vitro* fail to grow towards explants of hypothalamus but do grow towards explants of ventral telencephalon, indicating that some secreted molecule is influencing axon growth by repelling axons away from the hypothalamus (Braisted et al., 1999).

It was subsequently shown that two molecules from the Slit guidance cue family, Slit1 and Slit2, are expressed in the hypothalamus as the thalamocortical axons grow and that in both Slit2$^{-/-}$ single knockout and Slit1/Slit2$^{-/-}$ double knockout mice some thalamocortical axons are able to grow into the hypothalamus (Bagri et al., 2002). This indicates that Slit1 and Slit2 are repulsive guidance cues, influencing the thalamocortical axons to turn towards the ganglionic eminences. In addition, the receptors for Slits, Robo1 and Robo2, have also been implicated in thalamocortical axon guidance. Both Robo1 and Robo2 are expressed in thalamocortical axons, and the thalamocortical axons in a Robo1/Robo2$^{-/-}$ double knockout exhibit the same abnormal behaviour as the Slit1/Slit2$^{-/-}$ double knockout described above (López-Bendito et al. (2007); see Figure 1.6a).

This indicates that both the expression of Slit from the hypothalamus and the expression of Robo receptors in the thalamocortical axons is required for the axons to grow correctly. In fact, it appears that Robo2 rather than Robo1 is essential for correct growth, as axons in a Robo2$^{-/-}$ single knockout mouse behave the same as the axons in both the Slit and the Robo double knockouts, whereas in two different Robo1$^{-/-}$ knockouts (Andrews et al., 2006; López-Bendito et al., 2007) thalamocortical axons appear to follow their normal route, although is appears that the thalamocortical projection is further advanced into the cortex at E14.5 than in wild-type mice (Andrews et al., 2006).

Thalamocortical axons therefore require a molecular guidance cue to turn away from the hypothalamus, but it appears that they require the guidance of other axons to cross the DTB. Developing axonal projections can be traced by injecting crystals

of fluorescent carbocyanine dyes such as DiI, DiA and DiO. Crystals can be injected at the point of axonal termination, where the dye will spread towards the projecting cell (retrograde tracing) or at the projecting cell, where dye will spread along the axon towards the growth cone (anterograde tracing) (Godement et al., 1987). When DiI was injected into axon terminals in the thalamus of E14, E15 and E16 rat brains, the dye retrogradely traced projections back to cells in the thalamic reticular nucleus and the internal capsule (Molnár and Cordery, 1999), showing that these areas project axons into the thalamus (see Figure 1.6b).

The region of the internal capsule which projects axons into the thalamus is missing in Mash1$^{-/-}$ knockout mice, and thalamocortical axons are unable to cross the DTB (Tuttle et al., 1999). Similarly, in Emx2$^{-/-}$ knockout mice, internal capsule cells disperse and fail to project axons into the thalamus, causing thalamocortical axons to project disparately into the ventral telencephalon (López-Bendito et al., 2002). This indicates that internal capsule cells must project axons to the thalamus for thalamocortical axons to enter the internal capsule. Also, netrin-1 is expressed in the ventral telencephalon in wild-type animals, and in netrin-1$^{-/-}$ knockout mice the internal capsule is abnormally narrow and the thalamocortical axon projection is reduced (Braisted et al., 2000). Therefore it appears that molecular cues are required for thalamocortical axons to cross the DTB correctly, at least in part because these cues regulate cells of the internal capsule, which are required to project axons for thalamocortical axons to fasciculate onto and grow along.

Wnt signalling factors (see Section 1.2.2) have been indirectly implicated in this stage of thalamocortical development. Wnt ligands bind to the members of the Frizzled receptor family (Bhanot et al., 1996), and Frizzled-3$^{-/-}$ knockout mice show a complete loss of the thalamocortical and corticothalamic tracts (Wang et al., 2002). In these mice, axons growing out of the thalamus are unable to enter the internal capsule and instead grow posterior to the optic tract and enter the contralateral side of the thalamus (Wang et al., 2006).

The complete lack of thalamocortical and corticothalamic connections is also seen in mice without Celsr3, a molecule which is co-expressed with Frizzled-3 in the cortex, thalamus and striatum during brain development (Tissir et al., 2005). In Celsr3$^{-/-}$ knockout mice, thalamocortical connections cannot cross the DTB, and when Celsr3 is inactivated in Dlx5/6-expressing cells alone, which are found in the ganglionic eminences, thalamocortical axons are unable to enter the internal capsule and instead grow aberrantly into the basal telencephalon (Zhou et al., 2008).

This is significant because Frizzled-3 and Celsr3 are the homologues of the Drosophila genes frizzled and flamingo respectively, both of which are involved in the planar cell polarity pathway (Goodrich, 2008), one of at least three pathways through which Wnt signalling operates (Huelsken and Behrens, 2002). It may be that this indicates the planar cell polarity pathway operates during thalamocortical development, although other planar cell polarity genes such as members of the dishevelled (Dvl), van gogh-like (Vangl) and prickle-like families are not co-expressed closely with Frizzled-3 and Celsr3, with Vangl1 and Prickle1 having different expression patterns, Dvl1 having broad expression across the brain, and Dvl3 and Prickle2 having the closest pattern of expression to Frizzled-3 and Celsr3 (Tissir and Goffinet, 2006).

1.4.1.2 Growth of the thalamocortical tract through the ventral telencephalon

Once the thalamocortical projection has entered the internal capsule in the ventral telencephalon, the axons travel through the medial ganglionic eminence (MGE) via a transitory permissive corridor of neurons which is derived from cells from the lateral ganglionic eminence (LGE) (López-Bendito et al., 2006) and pause at E14.5 when they reach the boundary between the subpallium and pallium (Molnár and Cordery, 1999). The ganglionic eminences act as an intermediate target for thalamocortical axons, with cells in the MGE projecting axons to the thalamus which provide a scaffold for thalamocortical axons as they grow into the internal capsule (Métin and Godement, 1996).

A number of genes have been implicated in the formation of the permissive corridor of LGE cells (see Figure 1.6c). Two products of neuregulin-1, Nrg1-CRD and Nrg1-Ig, are expressed in the LGE and cause the LGE and the corridor of LGE cells in the MGE to be permissive to thalamocortical axons. When these neuregulin-1 isoforms are absent from these LGE cells, most thalamocortical axons do not cross the MGE and instead turn caudally towards the hypothalamus (López-Bendito et al., 2006). In addition, the corridor does not form in the absence of the protocadherin OL-pc, which is usually expressed in the striatum. The axons of wild-type striatal cells project through the globus pallidus and cross the DTB, growing adjacent to thalamocortical axons in the internal capsule. In OL-pc-deficient mice, striatal axons fail to grow through the globus pallidus and across the diencephalic-telencephalic boundary, the caudal globus pallidus fails to form and thalamocortical axons are unable to enter the internal capsule (Uemura et al., 2007). Therefore, similar to the role of axons from internal capsule cells described in the previous section, the growth of thalamocortical

axons across the ventral telencephalon appears to require the presence of co-located striatal axons.

Other molecules have been implicated in this stage of thalamocortical development. Part of the thalamocortical projection in Sema6A$^{-/-}$ knockout mice does not reach the cortex and instead grows aberrantly into the amygdala (Leighton et al., 2001). Sema6A is usually expressed throughout the thalamus during the development of the thalamocortical projection and so this may be a cell-autonomous effect, although Sema6A is also expressed in the amygdala during the same period in wild-type animals and so it may be that the lack of Sema6A in this region disrupts non-cell-autonomous signalling in the internal capsule (Leighton et al., 2001).

In Pax6$^{-/-}$ knockout mice, many thalamocortical axons do not cross the diencephalic-telencephalic boundary and others are unable to reach the pallial-subpallial boundary (Jones et al., 2002; Pratt et al., 2002); cells in the prethalamus and internal capsule which are thought to project axons into the thalamus and guide thalamocortical axons (see Section 1.4.1.1) disperse throughout the hypothalamus and ventral pallium, and cells in the LGE which usually express Pax6 are greatly reduced in number. This lack of Pax6-expressing cells and aberrant thalamocortical growth can also be seen in Small eye mice, which have non-functional Pax6 (Kawano et al., 1999; Hevner et al., 2002).

The transient thalamic afferents which grow from the MGE are disrupted in Pax6$^{-/-}$ knockout mice (Pratt et al., 2002), but this appears to be due to defects in the thalamus rather than the ventral telencephalon, because the expression of ventral telencephalic markers such as Mash1, Tbr1, Emx1 and Dlx1 is not affected in Pax6$^{-/-}$ or Small eye mutants (Pratt et al., 2002; Stoykova et al., 2000), and Pax6 is not expressed in this region while the transient afferents form (Stoykova et al., 1996). Also, there are other thalamic afferents, such as the tract of the postoptic commissure, which grow at the same time as the afferents from the ventral telencephalon and which do not innervate the thalamus in Pax6 mutants (Nural and Mastick, 2004). This perhaps indicates that although thalamocortical axons require these transient thalamic afferents as a scaffold to grow along as they enter the internal capsule, these afferents in turn require signals from the thalamus to form the appropriate scaffold.

1.4.1.3 Crossing the pallial-subpallial boundary: interaction with corticothalamic axons from the subplate

From E13.5 onwards (Auladell et al., 2000), thalamocortical axons reach the pallial-subpallial boundary (PSPB), a region which is distinctively marked by the expression

of several genes, Tbr1 and Emx1 expressed in the pallium and Dlx2 and Nkx2.1 expressed in the subpallium, patterns which are conserved in mouse and chick (Puelles et al., 2000). When thalamocortical axons reach this target, their behaviour changes. As the axons grow through the internal capsule, their growth cones are small and simple, their growth is rapid and they spend approximately 80% of their time advancing, 12% pausing and 8% retracting (Skaliora et al., 2000). In contrast, when the axons reach the pallial-subpallial boundary, growth cones become large and complex, the axons begin to project many exploratory side branches, the net growth rate is half of what it was during internal capsule growth and the axons spend approximately 37.5% of their time advancing, 37.5% pausing and 25% retracting (Skaliora et al., 2000).

This change in behaviour is most likely due to interactions with corticofugal axons on the subpallial side of the PSPB (Molnár et al., 1998a). As thalamocortical axons project to the cortex, so cortical axons are projected to the thalamus, with the corticothalamic pathway pioneered by axons projected from the subplate (Allendoerfer and Shatz, 1994). The cortex projects two major axonal tracts; the corticothalamic projection, which originates in layer 6 and project exclusively to the thalamus, and the pyramidal tract, which originates in layer 5 and innervates multiple targets including the pons, superior colliculus and spinal cord (Martin, 2005). These two projections grow concurrently through the ventral telencephalon and away from the basal telencephalon (Canty and Murphy, 2008). However, their growth is differentially regulated; in Nkx2-1$^{-/-}$ knockout mice, corticothalamic axons innervate the thalamus as normal, but pyramidal axons grow aberrantly into the basal telencephalon, where Nkx2-1 is normally expressed (Marín et al., 2002).

As the medial ganglionic eminence provides a scaffold for thalamocortical axons, so the lateral ganglionic eminence sends axons towards the cortex and provides a scaffold for corticofugal axons (Métin and Godement, 1996). This requires the expression of netrin-1 at the PSPB, without which corticofugal axons are unable to reach the LGE (Métin et al., 1997).

The development of thalamocortical axons and corticothalamic axons is closely related, with both groups of axons pausing and intermingling at the PSPB before progressing to the cortex and thalamus respectively (Molnár and Butler, 2002); see Figure 1.7b). In the adult, the axons from the two systems form tight bundles which are spatially ordered across the cortex (Molnár et al., 1998a). When subplate neurons are ablated in fetal cats, thalamocortical axons from the lateral geniculate nucleus do not innervate layer IV of the cortex, despite the presence of their target cells, but instead

grow through the entire cortical plate and into white matter at the surface of the brain (Ghosh et al., 1990).

Several studies of gene expression also indicate the importance of the relationship between subplate neurons and thalamocortical axons. For example, axons which express the neural cell adhesion molecule L1 innervate areas of the cortex which express neurocan, which binds L1 *in vitro* (Fukuda et al., 1997). At E16.5, neurocan expression is limited to the subplate, and L1-expressing axons will only innervate the subplate at this age without progressing to the cortical plate (Li et al., 2005). This behaviour is also observed in the reeler mutant mouse, where the subplate becomes a 'superplate' which grows above the cortical plate. L1-expressing axons innervate the superplate, which they preferentially innervate by growing through strips within the cortical plate which also express neurocan in these mutants (Li et al., 2005).

Tbr1 is a transcription factor which is expressed in the developing subplate and cortical layer 6, but not in the thalamus. In Tbr1$^{-/-}$ knockout mice, the development of the subplate is disrupted and the corticothalamic axonal projection stalls in the internal capsule and does not progress to the diencephalon (Hevner et al., 2001, 2002). The thalamocortical projection in these mice enters the internal capsule but does not cross the PSPB. The thalamocortical and corticothalamic projections intermingle as in control mice, but they are unable to progress towards their targets (Hevner et al., 2002). It may be that this misrouting is due to changes in molecular signalling from the cortex but, as the thalamocortical projection begins to be diverted at the place where it would usually interact with axons from the subplate, this further indicates that the thalamocortical axons depend on cortical axonal projections to navigate to their destinations correctly.

Similarly, in COUP-TFI$^{-/-}$ knockout mice, subplate neurons fail to differentiate properly and die prematurely, and the majority of thalamocortical axons fail to cross the PSPB (Zhou et al., 1999). Cortical layer IV is absent in these mice, which may indicate that cell survival in these regions is dependent on the presence of thalamocortical axon terminals (Windrem and Finlay, 1991). Axons from ventrobasal nuclei appear to grow normally through the internal capsule, which suggests that the failure of these axons to cross the PSPB is due to the lack of subplate neurons and not due to a cell-autonomous effect in the thalamus. However, such an effect cannot be ruled out because COUP-TFI is expressed in the developing thalamus as well as the subplate in wild-type animals.

Indeed, it appears that normal growth of the thalamocortical tract is required for the corticothalamic tract to grow correctly. Gbx2 is a transcription factor which is

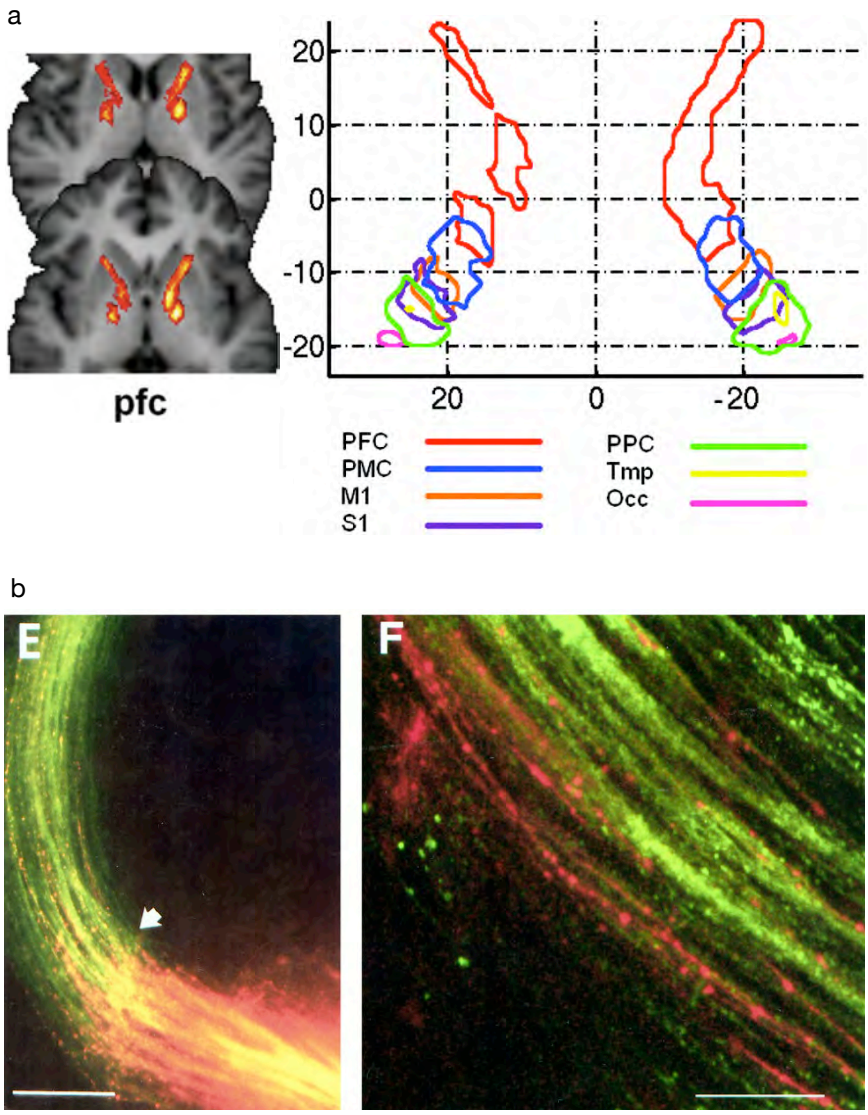

Figure 1.7: a) Left, example of diffusion tractography images taken of human internal capsules at two different points in the horizontal plane, in this case tracing fibres from the prefrontal cortex (PFC). Right, segmentation map of images of cortical fibres in the internal capsule, averaged over 11 human individuals. Fibres found in cortical regions were traced back to the internal capsule, where topographical organisation was evident. The majority of the connections were from the prefrontal cortex (PFC), and there was considerable overlap between regions. PMC, premotor cortex; ppc, posterior parietal cortex; Tmp, temporal lobe; Occ, occipital lobe. b) Thalamocortical axons labelled with a DiI crystal (red) and corticothalamic axons labelled with a DiO crystal (green) in an E15.5 rat. F is a higher magnification of the region in E marked with an arrow (Scale bars: E, 100μm; F, 10μm). Groups of axons from each tract bundle together and grow alongside each other. a) taken from Zarei et al. (2007); b) taken from Molnár et al. (1998a).

expressed in the developing thalamus but not in the cortex (see Section 1.3.3). In Gbx2$^{-/-}$ knockout mice, thalamocortical projections enter the internal capsule but fail to cross the pallial-subpallial boundary; corticothalamic projections also stall in the internal capsule (Hevner et al., 2002). This indicates that the thalamocortical projection must form correctly for the corticothalamic projection to reach the thalamus.

1.4.2 Establishing the topography of thalamocortical axons

As discussed in Section 1.3.2, the thalamus is organised into nuclei and the cortex into areas according to their function, and related thalamic nuclei and cortical areas are connected via thalamocortical axons. The internal topographic mappings of thalamic nucleus to cortical area are not simple, with some area mappings being mirror reversals of their nuclear mappings and others being simple rotations (Adams et al., 1997). This means that, in the mature brain, the bundle of thalamocortical axons is topographically organised according to the origin and destination of different groups of axons. Where and how does this organisation of axons occur? It has emerged over the last decade that thalamocortical axons are organised when they leave the thalamus, but that they require further organisation in the ventral telencephalon and by corticofugal axons to innervate the correct cortical area. In this section, the organisation of axons as they leave the thalamus and the influence of guidance cues, other axons and the cortex on thalamocortical organisation will be considered.

1.4.2.1 Thalamocortical axons are topographically organised throughout their journey

The thalamus must develop normally for thalamocortical projections to reach their targets. For example, the Wnt coreceptor Lrp6 is essential for the formation of the thalamus. In Lrp6$^{-/-}$ knockout mice, the zona limitans intrathalamica is disrupted and thalamic cells do not proliferate correctly, leading to a significant reduction in the size of the thalamus and a failure of thalamic nuclei to form, although prethalamus development is normal (Zhou et al., 2004a). Very few thalamocortical axons project out of the thalamus, as might be expected given the lack of thalamic cells; however, those that do leave the thalamus terminate in the striatum, indicating that these axons are able to turn at the diencephalic-telencephalic boundary but are unable to progress to the pallial-subpallial boundary.

The cortex alone is not sufficient to organise thalamic axons. When dorsal lateral

geniculate nucleus explants are cocultured with postnatal explants of either visual cortex or motor cortex, they do not preferentially innervate the visual cortex as they do *in vivo* but instead innervate both types of cortical explant (Molnár and Blakemore, 1991). This suggests that the cortex does not guide thalamocortical axons via area-specific cues, but it may be that prenatal cortex does express such cues but postnatal cortex does not. However, it may also be that cortical cues are present but that thalamocortical axons require exposure to intermediate cues in order for them to respond to cortical cues appropriately.

Indeed, in humans, the topography of thalamocortical axons is broadly preserved from the time when the axons cross the ventral telencephalon to when they reach the cortex. By using diffusion tractography to trace thalamocortical (and corticothalamic) connections from the cortex to the internal capsule in human brains it can be shown that the topographic organisation of connections in the internal capsule was the same as that across the cortex, and that this organisation is remarkably consistent across different individuals, strongly indicating genetic regulation of this organisation long before the axons reach the cortex (Zarei et al., 2007); see Figure 1.7a). In the following sections, evidence will be provided showing that there is also topographical organisation of axons in the internal capsules of mice.

1.4.2.2 Topographical organisation of thalamocortical axons requires molecular gradients

The topographical organisation of thalamocortical axons which can be observed in the ventral telencephalon is established by molecular gradients in the thalamus and the ventral telencephalon. Rostral, medial and caudal regions of thalamus project axons which preferentially innervate respectively rostral, medial and caudal regions of the ventral telencephalon both *in vivo* (observed by DiI tracing) and *in vitro*, in explant co-cultures (Seibt et al., 2003). Several proteins have been shown to be required for this preferential innervation to take place.

Some studies have indicated that the topography of thalamocortical axons is determined by gene expression in the ventral telencephalon. For example, in Ebf1$^{-/-}$ and Dlx1/2$^{-/-}$ knockout mice, which appear to have normally regionalised thalami and cortices but which have abnormal ganglionic eminences, thalamocortical projections are shifted medially in the cortex, which suggests that regionalisation of the thalamus itself is not the only influence on the topographical organisation of the thalamus and intermediate decision points such as the ganglionic eminences have a role to play in

this organisation (Garel et al., 2002).

Conversely, other studies have claimed a cell-autonomous role for genes expressed in the thalamus in organising the topography of thalamocortical axons. For example, neurogenin-2 (Ngn2) is expressed in a high rostral to low caudal gradient in the thalamus from E13.5 to E15.5, as thalamic axons are emerging and growing through the ventral telencephalon (Seibt et al., 2003). When rostral thalamic slices from Ngn2-deficient mice are cocultured with wild-type ventral telencephalon, their axons innervate a more caudal region of ventral telencephalon than wild-type rostral thalamic axons (Seibt et al., 2003). This indicates that Ngn2 regulates the topography of thalamocortical axons in a cell-autonomous way by modulating the responsiveness of these axons to existing intermediate cues in the ventral telencephalon.

In addition, the neural cell adhesion molecule Close Homolog of L1 (CHL1) is expressed in a high rostral to low caudal gradient in the developing thalamus and is also expressed in thalamocortical axons but not in the ganglionic eminences (Wright et al., 2007). In $CHL1^{-/-}$ knockout mice, the projection of axons from the ventrobasal nuclei is caudally shifted in the ventral telencephalon and in the cortex, where these axons innervate visual rather than somatosensory cortex; DiI tracings show that axons innervating V1 all originate in the lateral geniculate nucleus in wild type animals but, in $CHL1^{-/-}$ knockouts, V1 is also innervated by axons from the ventroposterior lateral and ventroposterior medial nuclei, which are among the ventrobasal nuclei (Wright et al., 2007). Therefore it appears that expression of different genes in both the thalamus, such as CHL1 and Ngn2, and the ventral telencephalon, such as Ebf1 and Dlx1/2, is required for correct topographical organisation of thalamocortical axons to take place.

CHL1 forms a stable complex with neuropilin-1, a receptor for Semaphorin-3A. Both CHL1 and neuropilin-1 are expressed in thalamic axons and Semaphorin-3A is expressed in a low caudal to high rostral gradient across the ventral telencephalon. Wright et al. (2007) show that thalamic axons grow abnormally across ventral telencephalon in mice where neuropilin-1 cannot bind semaphorin-3A, and that CHL1 is required for semaphorin-3A to cause thalamic axons to collapse in culture. This is further evidence that correct topographic organisation of thalamocortical axons requires both cell-autonomous gene expression in thalamic axons and intermediate cue expression in ventral telencephalon (see Garel and Rubenstein (2004) for review).

1.4.2.3 Topographical organisation of thalamocortical axons requires classical guidance cues

Corresponding gradients of guidance cues in ventral telencephalon and guidance cue receptors in thalamus have been seen for members of the classical guidance cue families the netrins and the ephrins. A high rostral to low caudal gradient of netrin-1 mRNA (de la Torre et al., 1997) has been demonstrated in E14.5 and E15.5 mouse ganglionic eminences and the lack of this gradient causes those thalamocortical axons which normally grow to rostral cortex in the wild-type to grow to all regions of the cortex in netrin-$1^{-/-}$ knockout mice (Powell et al., 2008). This netrin-1 gradient in the ventral telencephalon is matched by a high rostro-medial to low caudo-lateral gradient of the netrin-1 receptor DCC in the thalamus, which indicates that thalamocortical growth cones also express graded quantities of DCC receptors in their membranes.

These results are supported by demonstrations that different parts of the thalamus have different responses to exposure to netrin-1 (see Figure 1.8). Axons from rostral regions of the thalamus, with high levels of DCC expression, are repelled by netrin-1, whereas axons from caudal thalamus, with low levels of DCC expression, are attracted by netrin-1 (Bonnin et al., 2007). This behaviour is modulated by serotonin receptors 5-HT_{1B} and 5-HT_{1D} (see Section 1.3.3), which have patterns of expression which overlap with DCC and another netrin-1 receptor, Unc5c. When treated with serotonin, axons from caudal thalamus are repulsed by netrin-1, rather than attracted, but this change in behaviour fails to occur when receptor 5-HT_{1D} is blocked by an antagonist (Bonnin et al., 2007). This study demonstrates not only that axonal responses are in part determined by the gene expression of their originating cells but also that these responses can be reversed via expression of other genes.

Dufour et al. (2003) show that at E13.5-E14.5, before the thalamic nuclei can be identified, a high rostral to low caudal gradient of the RNA for the guidance cue ephrin-A5 can be found in the ventral telencephalon and a high rostro-medial to low caudo-lateral gradient of the RNA of the ephrin-A5 receptor EphA4, as well as RNAs for EphA3 and EphA7 (see Figure 1.8f). In ephrin-A5/EphA4 double knockout mice, thalamocortical axons grow in a considerably more caudal direction when compared to wild-type mice, which indicates that the gradients of ephrin-A5 in the ventral telencephalon and EphA4 in the thalamus influence the topographic organisation of thalamocortical axons.

Furthermore, thalamocortical axons bind to soluble ephrin-A5 protein (introduced

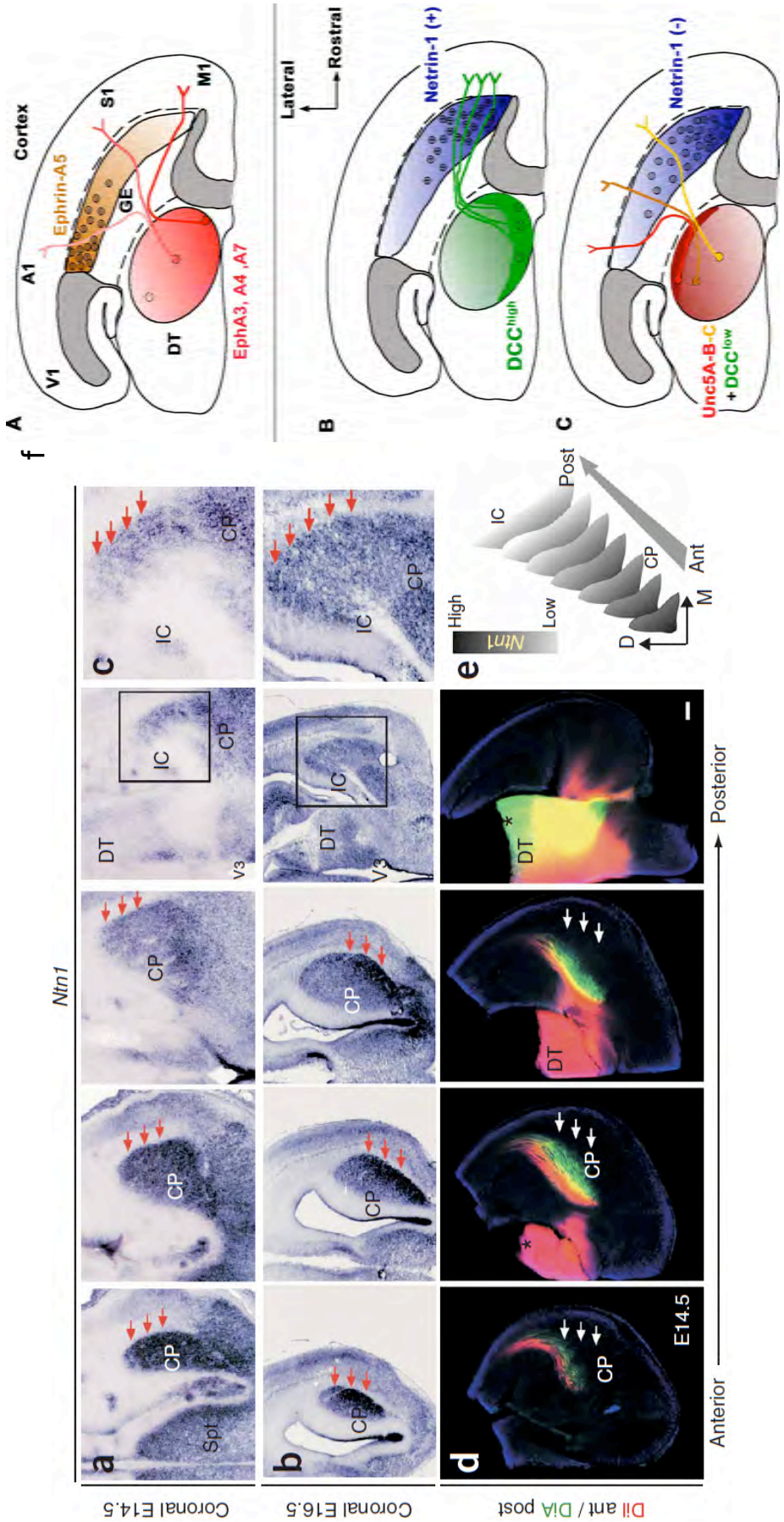

Figure 1.8: a-e) Graded expression of netrin-1 mirrors topographic organisation of thalamocortical axons. Staining for netrin-1 mRNA at a) E14.5 and b) E16.5 shows gradients from high anterior expression to low posterior expression and high ventrolateral to low dorsomedial expression. c) Magnification of boxed regions in a) and b) showing the internal capsule. d) Injecting DiI (red) in anterior thalamus and DiA (green) in posterior thalamus (asterisks show sites of injection) shows that thalamocortical axons retain topographic organisation in the internal capsule (IC), with posterior axons growing along a path with high netrin-1 mRNA expression and anterior axons following low netrin-1 expression. e) Schematic of netrin-1 expression. CP, caudate putamen; Spt, septum; DT, dorsal thalamus. Arrows in a-d indicate the edge of the internal capsule; scale bar, 100μm. f) Gradients of ephrins and netrins in ventral telencephalon and their receptors in the thalamus (DT) mediate growth of thalamocortical axons. A) High rostromedial to low caudolateral gradient of EphA receptors in thalamus causes thalamocortical axons to respond differently to gradient of ephrin-A5 signal in the ganglionic eminences (GE). B) Thalamic axons with high DCC expression are attracted to high netrin-1 expression and innervate rostral cortex, whereas C) axons with low DCC expression but high Unc5 expression innervate more caudal cortical regions. a-e) taken from Bonnin et al. (2007); f) taken from Powell et al. (2008).

in situ), with highest binding activity in rostral regions of the ventral telencephalon, indicating that not only do the thalamocortical axons contain ephrin-A5 binding receptors but also that these receptors are differentially expressed in a pattern which corresponds with gradients of receptors found in the thalamus (Dufour et al., 2003). This suggests that the organisation of thalamocortical axons is influenced not only by gradients of guidance cues in the ventral telencephalon but also by the complements of receptors present in the growth cones of the axons, because different groups of axons show different binding responses to ephrin-A5 protein and so will have varying sensitivities to gradients of the protein.

Eph receptors do not simply operate due to their binding of ephrin ligands, causing activation of kinase signalling, but also because the receptors cluster together, and that these two behaviours have different functions. Normally, EphA4 kinase receptor is activated by the binding of ephrin ligands. Egea et al. (2005) show that mouse mutants which have EphA4 receptors that are kinase active without the presence of ephrin ligands have defects in thalamocortical axon growth but not in other EphA4-related behaviours such as midline axon pathfinding across the spinal cord. Also, when cortical axons from these mice are grown *in vitro*, their growth cones collapse in response to ephrin-B3, as do the growth cones of wild-type animals. However, when the EphA4 receptors in these mutant axons are prevented from clustering together by blocking the globular domains of the receptors, the mutant growth cones no longer collapse in response to ephrin-B3 (Egea et al., 2005).

These results demonstrate two separate processes in which EphA4 receptors mediate axon guidance behaviours, although the thalamocortical role of EphA4 receptors appears to be due to the binding of ephrinA ligands and not to receptor clustering. Further evidence for the role of ligand binding is provided by Dufour et al. (2006), who demonstrated that EphA4's influence on topographic mapping of thalamocortical axons is dependent on the presence of a tyrosine kinase domain in EphA4, but not PDZ-binding motif or Sterile-α motif domains, two other non-catalytic domains with poorly understood functions. Selective mutations of EphA4 with any one of these domains removed can still be expressed in a gradient across the thalamus, but only the tyrosine kinase domain mutant mouse has disrupted thalamocortical axon topography.

1.4.2.4 Topographical organisation of thalamocortical axons involves interactions with other axonal tracts

All of the above results indicate that gradients in the ventral telencephalon must be matched by gradients in the thalamus for thalamocortical axons to be correctly topographically organised. It appears that many of the molecules expressed in these gradients operate directly by binding to the growth cones of thalamocortical axons (eg netrin-1, semaphorin-3A). However, it may be that they also act indirectly by influencing the development of pioneer axon tracts, which thalamocortical axons fasciculate onto and grow along.

One prominent explanation for the topographical organisation of thalamocortical axons is the 'handshake' hypothesis: as thalamocortical axons fasciculate onto corticothalamic axons from the subplate and grow along these axons until they reach the cortex (see Section 1.4.1.3), and as corticothalamic axons originate from different cortical areas, perhaps thalamocortical axons from each thalamic nucleus fasciculate onto the corticothalamic axons from the appropriate cortical area for this nucleus (Molnár and Blakemore, 1995).

Indeed, DiI and DiA labelling of thalamocortical and corticothalamic axon tracts demonstrates that when the projections meet at the lateral edge of the internal capsule thalamocortical axons destined for a particular area bundle together with corticothalamic axons from that area, rather than travel to the area independently (Molnár et al., 1998a). This is the case even in reeler mice, where the entire cortical plate forms below the subplate (now a 'superplate') and thalamocortical axons still innervate the correct cortical areas. It appears that thalamocortical axons grow through the developing cortical plate by following fascicles of 'superplate' axons which project through the cortical plate, remain at the 'superplate' for several days and then grow downward to innervate the cortical plate below the 'superplate' (Molnár et al., 1998b). This supports the case that the corticothalamic projections from each cortical area are required for thalamocortical axons to grow to their appropriate target area.

Further support for the handshake hypothesis comes from knockouts of the zinc finger gene fez-like (fezl). In $fezl^{-/-}$ knockout mice, the number of mature subplate neurons, and therefore the size of the corticofugal projection, is reduced (Hirata et al., 2004). In addition, the corticofugal projections from the subplate neurons which do develop are delayed, being unable to cross the pallial-subpallial boundary until E15.5 rather than crossing at E14.5 as they do in the wild-type (Komuta et al., 2007), and so

failing to provide a scaffold for thalamocortical axons to grow upon.

The number of thalamocortical axons in these mice is reduced and those that do grow connect with the cortex aberrantly. The aberrant growth of thalamocortical axons appears to be due to the lack of the corticofugal projection rather than disruption of gene expression, because the expression of many genes which are related to thalamocortical axon growth such as Pax6, netrin-1, neuregulin-1, Emx1, Tbr1 and Gsh2 is unchanged in fezl$^{-/-}$ knockouts (Komuta et al., 2007; Chen et al., 2005). However, it cannot be ruled out that some other untested gene has been misexpressed in these knockouts, or that the reduced number of thalamocortical axons has caused the axon bundle to be disorganised from the time the axons begin to grow out of the thalamus.

It may be that pioneer axons from internal capsule cells are also involved in the topographical organisation of thalamocortical axons. The transcription factor Lhx2 is expressed in the thalamus and cortex during development and influences the parcellation of these regions into nuclei and areas, but it is also expressed in the ventral telencephalon (Rétaux et al., 1999; Bulchand et al., 2001). Mice which do not express Lhx2 have a substantial reduction in the number of internal capsule cells in the ventral telencephalon near the diencephalic-telencephalic boundary (Lakhina et al., 2007). As discussed in Section 1.4.1.1, these internal capsule cells project axons which guide thalamocortical axons across the diencephalic-telencephalic boundary, and the reduction in internal capsule cells therefore reduces the number of axons available to guide thalamocortical axons.

The thalamus segregates normally in Lhx2$^{-/-}$ knockout mice according to a wide range of markers, but the thalamic axons are unable to enter the ventral telencephalon. *in vitro*, Lhx2$^{-/-}$ thalamus projects axons into wild-type ventral telencephalon and the topography of these axons is normal. However, when wild-type thalamus projects axons into Lhx2$^{-/-}$ ventral telencephalon, the axonal topography is aberrant, with axons from caudal thalamus, which usually innervate caudal ventral telencephalon, being shifted rostrally (Lakhina et al., 2007). This may indicate that internal capsule axons influence the topography of thalamocortical axons and the reduction in number of these axons in Lhx2$^{-/-}$ mice causes the thalamocortical axon topography to be disrupted. However, it may be that Lhx2-expressing cells express some other guidance cue which attracts thalamocortical axons, and that it is a reduction in guidance cue expression which disrupts the growth of the axons. More studies are required to determine if it is internal capsule axons, or simply internal capsule cells, which are

required for correct topographical organisation of thalamocortical axons.

Given the many examples of gene expression in the thalamus and ventral telencephalon influencing the topography of thalamocortical axons, it is consistent with the evidence to claim that, while the corticofugal projection does appear to be necessary for thalamocortical axons to innervate the cortex correctly, it is not sufficient for the organisation of thalamocortical axons, and that the axons are already organised to some extent when they reach the lateral edge of the internal capsule and interact with the corticofugal projection.

1.4.3 Innervation of the cortex by thalamocortical axons

Thalamocortical axons innervate the cortex in a controlled fashion, with some groups of axons spreading out across the whole cortex but others innervating a single cortical area (Jones, 1998). As described in Sections 1.3.4 and 1.4.2, by the time thalamocortical axons reach the cortex, the axons are topographically organised and the cortex is arealised to some extent by the expression of guidance cues and transcription factors (Sur and Rubenstein, 2005). In this section, the innervation of the cortex by the thalamocortical projection will be discussed, considering the influence of the thalamocortical projection on lamination, inter-areal patterning and intra-areal patterning of the cortex and also the role of activity in these processes.

1.4.3.1 Lamination

Thalamocortical axons mostly innervate layer IV of the cortex, and it is in this layer where topographic mappings such as barrels in somatosensory area S1 can be seen (see Inan and Crair (2007) for review). This layer-specific innervation only occurs when thalamocortical axons are presented with postnatal cortex. In explant cultures of rat tissue, thalamic axons do not innervate cortical slices taken prior to E19. In slices taken after E19 but before P2, axons will enter the cortex and project radially throughout the slice. In slices taken after P2, the axons arborise and terminate in layer 4 of the cortex (Molnár and Blakemore, 1999). When presented with a choice between E18-19 cortical tissue and P0-1 cortical tissue, thalamic axons prefer to grow on the postnatal tissue, a choice which is mediated in part by higher levels of expression of the neural cell adhesion molecules L1 and N-CAM in the postnatal cortical tissue (Tuttle et al., 1995).

When cortical slices are taken at earlier ages and cultured for over 7 days, the

innervation of these slices by thalamic axons is closer to that seen for the chronological age of the slice, rather than the age at which it was dissected (Molnár and Blakemore, 1999). This indicates that not only do changes in the cortex regulate the behaviour of thalamic axons as they innervate the cortex but also that these changes are at least partly intrinsic to the cortex, because they persist in the absence of the rest of the brain.

Several genes have been identified which restrict thalamocortical axons to layer IV of the cortex. For example, semaphorin-7A, ephrin-A5 and kit ligand are expressed in the upper layers of the cortex and inhibit the growth of thalamocortical axons (Mann et al., 2002; Maruyama et al., 2008). Similarly, N-cadherin is expressed in layer IV of the cortex and if N-cadherin is blocked by inhibitory peptides, thalamocortical axons grow to layer IV at the same rate as normal but then continue to extend to the outer edge of the cortex (Poskanzer et al., 2003).

The neurotrophins, a family of chemoattractants which operate through two receptor systems, Trk, which is upstream of PI-3 kinase, and p75, which is upstream of RhoA (Chao, 2003), are also involved in thalamocortical innervation of the cortex. Multiple neurotrophins are expressed in the cortex during development and stimulate dendritic growth. Different neurotrophins regulate each other's effects, with, for example, neurotrophin-3 (NT-3) being expressed in layer 4 and inhibiting BDNF-stimulated dendritic growth, and BDNF being expressed in layer 6 and inhibiting NT-3-stimulated dendritic growth (McAllister et al., 1997). When expression of NT-3, which operates through TrkC, is ablated in the cortex, thalamocortical axons which would normally terminate in layer 4 in visual cortex fail to innervate the cortical plate, instead accumulating in the subplate and eventually retracting (Ma et al., 2002). Also, the tyrosine receptor kinase TrkB, which is bound by neurotrophin and BDNF, is required for thalamocortical axons to be restricted to layer IV, because in its absence in $TrkB^{-/-}$ knockout mice, thalamocortical axons also invade layer III of the cortex (Vitalis et al., 2002).

1.4.3.2 Inter-areal patterning

As discussed in Section 1.3.4, the cortex is already divided into areas by the time it is innervated by thalamocortical axons and it is not thought that the thalamocortical projection has a significant influence on the arealisation of the cortex. For example, in $Gbx2^{-/-}$ knockout mice, the thalamocortical projection does not cross the pallial-subpallial boundary, but the cortex develops normally, with many area-specific genes maintaining the patterns of expression seen in wild-type animals (Miyashita-Lin et al.,

1999).

This area-specific gene expression is required for thalamocortical axons to innervate the appropriate cortical areas. For example, Fgf8 is a signalling molecule which is secreted in the developing forebrain and influences the arealisation of the cortex (Grove and Fukuchi-Shimogori, 2003); see Figure 1.9a). Electroporating constructs expressing excess Fgf8 into the anterior forebrain at E10.5/E11.5 causes cortical somatosensory area S1 to develop posterior to its normal position, whereas blocking Fgf8 causes S1 to develop anterior to its normal position (Fukuchi-Shimogori and Grove, 2001). Fukuchi-Shimogori and Grove (2001) also show that electroporating Fgf8-expressing constructs posteriorly causes a second S1 area to develop in the posterior forebrain. Thalamocortical axons from the ventrobasal (VB) nucleus, which innervates S1 in wild-type animals, also innverates S1 in these modified cortices, with VB axons even branching when they reach the cortex to innervate both the anterior and posterior S1 areas in the latter case (Shimogori and Grove, 2005).

Similarly, the membrane protein and neural cell adhesion molecule LAMP is expressed in limbic regions such as the perirhinal cortex and attracts thalamocortical axons from the lateral dorsal nucleus (Barbe and Levitt, 1992; Mann et al., 1998). If LAMP-expressing cells are transplanted into developing somatosensory cortex, the lateral dorsal thalamocortical axons innervate somatosensory cortex instead of perirhinal cortex (Barbe and Levitt, 1992). These lateral dorsal axons are also influenced by the expression of ephrin-A5, which is expressed in somatosensory cortex; in ephrin-A5 knockouts, they innervate both perirhinal cortex and somatosensory cortex, rather than perirhinal cortex alone (although ventrobasal axonal connections to somatosensory cortex are unaffected in these mutants) (Uziel et al., 2002). Therefore, as ephrin-A5 appears to inhibit growth of lateral dorsal axons and LAMP encourages growth, both chemoattractive and chemorepulsive signals appear to be necessary for laterodorsal axons to navigate to their destinations correctly.

These area-specific innervations require the expression of appropriate receptors in thalamocortical axons. For example, as ephrin-A5 is expressed in somatosensory cortex but not in perirhinal cortex or other limbic regions, so the ephrin-A5 receptor Eph-A5 is expressed in limbic thalamic nuclei but not in somatosensory thalamic nuclei (Gao et al., 1998). Axons which express Eph-A5, from the limbic nuclei, will not innervate somatosensory cortex, indicating that the interaction between ephrin-A5 and Eph-A5 has a repulsive effect (Gao et al., 1998).

These gene-specific effects may be due to changes in corticofugal axon behaviour.

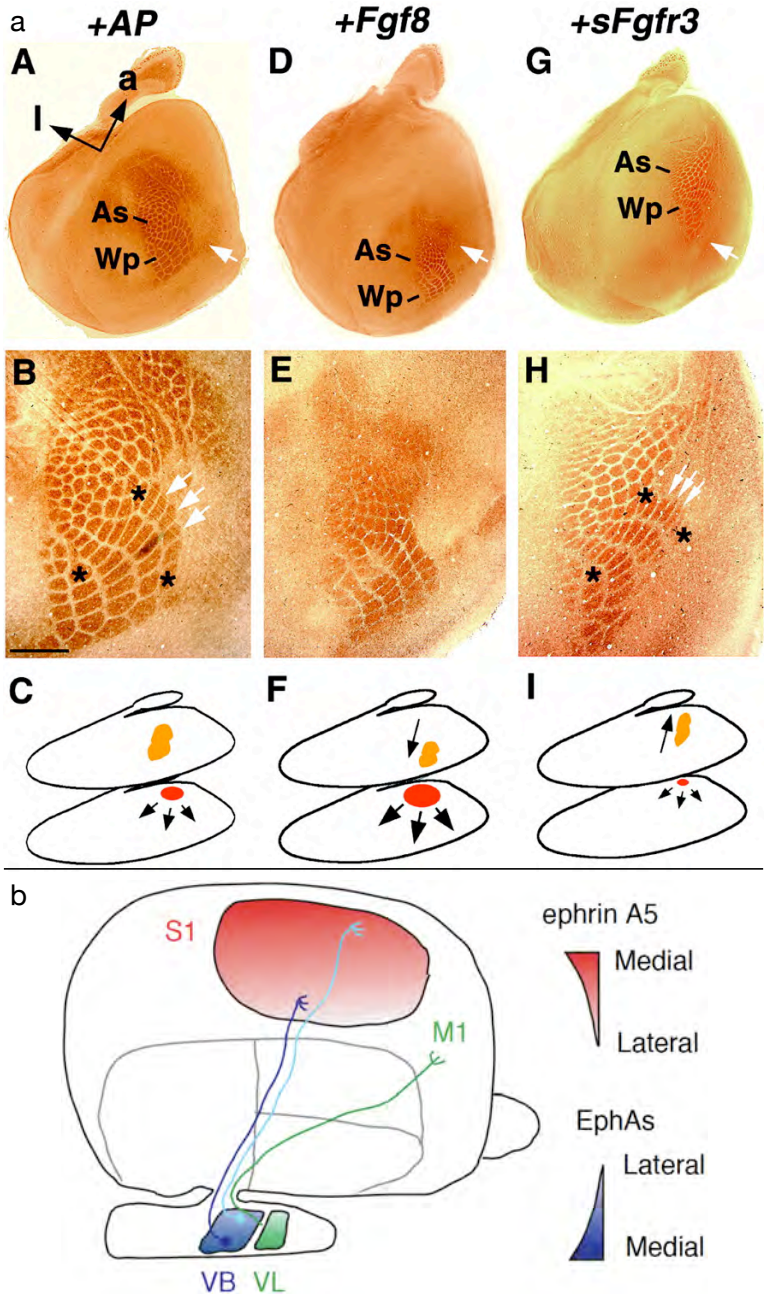

Figure 1.9: a) Electroporation of Fgf8 causes barrel cortex to shift position. A,D,G) Layer IV of flattened P6 mouse cortices stained with cytochrome oxidase to mark barrels. B,E,H) Magnifications of A,D,G respectively. C,F,I) Schematics of experimental conditions in A,D,G respectively, with red dots marking size and location of Fgf8 source and orange dots marking barrels. Electroporation with alkaline phosphatase control (A,B,C; +AP) showed the whisker pad (Wp) and anterior snout (As) at a central position at the midpoint between the anterior and posterior poles of the neocortex (white arrows in A,D,G). Anterior electroporation of Fgf8 (D,E,F; +Fgf8) shifted the barrel cortex posteriorly, compressing individual barrels; blocking Fgf8 with overexpression of a soluble FGF receptor sFgfr3 (G,H,I; +sFgfr3) shifted the barrel cortex anteriorly, elongated individual barrels (see white arrows in B and H) and skewed and elongated the Wp subfield (compare asterisks in B and H). a, anterior; l, lateral. Scale bar in B is 2.0mm for A,D,G and 0.7mm for B,D,H. b) Axons exposed to high EphA expression in the ventrobasal nucleus (VB) innervate regions of S1 with low lateral ephrin-A5 expression, and vice versa. VL, ventrolateral nucleus. a) taken from Fukuchi-Shimogori and Grove (2001); b) taken from Vanderhaeghen and Polleux (2004).

Subplate neurons express p75 neurotrophin receptors during the period where thalamocortical axons innervate the cortex, in a high-caudal to low-rostral gradient (McQuillen et al., 2002). In the absence of p75 receptors, subplate axons from visual cortex (where p75 expression is usually high) grow ectopically and thalamocortical innervation of visual cortex is reduced, but innervation of auditory and somatosensory cortex (where p75 expression is usually low) is normal (McQuillen et al., 2002). This appears to be due to a defect in subplate growth cone morphology; subplate neuron generation and cell death are similar throughout development in wild-type and $p75^{-/-}$ knockout mice, but the number of cytoskeletal actin filaments in subplate growth cones is substantially reduced (McQuillen et al., 2002).

1.4.3.3 Intra-areal patterning

Once each group of thalamocortical axons has made its way to the correct area and grown into layer IV, the axons within the group must organise themselves appropriately to match the function of their originating nucleus and destination cortical area. While thalamocortical innervation does not appear to be required for cortical areas to form, it does have a role to play in the patterning of individual cortical areas. For example, thalamocortical axons appear to cause various cadherins to be expressed in cortical areas. N-cadherin is co-expressed with thalamocortical arbors in barrel cortex during the first postnatal week, and this expression is due to the positioning of the axons rather than intrinsic signalling because if the pattern of axonal innervation is disrupted by lesioning the infraorbital nerve which connects the whiskers to the thalamus, the pattern of N-cadherin expression is disrupted in the same way as the axons (Huntley and Benson, 1999).

Cadherin-6, -8 and -10 are also expressed in barrel cortex, in partially overlapping but distinct patterns throughout the cortical layers (Gil et al., 2002). Just as N-cadherin is co-expressed with terminating ventrobasal axons in barrel cortex, so cadherin-8 protein and mRNA are co-expressed with terminating axons from the posterior nucleus in barrel septa, and are not enriched in barrel cell somata. Cadherin-8 mRNA is enriched in the posterior thalamic nucleus, which suggests that cadherin-8 may be transported along the axons and expressed at the axon terminals in the cortex. However, the ability of thalamocortical axons to affect cadherin expression appears to be limited to intra-areal patterning. When expression of cadherins 6, 8 and 11 was tested in wild-type mice and $Mash1^{-/-}$ knockout mice (in which the internal capsule does not form and thalamocortical axons are unable to cross the diencephalic-telencephalic boundary

and reach the cortex), the laminar, graded and inter-areal patterning of the cadherins in the cortex was unaffected (Nakagawa et al., 1999); intra-areal patterning was not examined in this study).

Molecular gradients have a role to play in intra-areal patterning. For example, just as a gradient of ephrin-A5 across the whole cortex matches a complementary gradient of EphA5 receptor in the thalamus during embyronic development (see Section 1.4.3.2), postnatally a gradient of ephrin-A5 can be found across somatosensory cortical area S1 which complements a gradient of EphA receptors in the ventrobasal thalamic nucleus (Bolz et al., 2004); see Figure 1.9b), and absence of this gradient disrupted the topographic mapping of innervating ventrobasal axons (Vanderhaeghen et al., 2000; Prakash et al., 2000). In addition, one of the ephrin-A5 receptors, EphA7, has been shown to be required for the somatosensory cortex to form correctly, with S1 being reduced in size in EphA7$^{-/-}$ knockout mice compared to wild-type control mice, and with the lateral region of S1 being significantly more reduced than the medial region, an effect which was even more pronounced in ephrin-A5/EphA7$^{-/-}$ double knockouts (Miller et al., 2006).

This indicates that ephrin-A5 and EphA7 are required for correct topographical formation of somatosensory cortex, but EphA7 is expressed in gradients across the thalamus and the cortex. Are both gradients required for correct formation of the thalamocortical projection or only one? In fact, misexpressing EphA7 in the cortex alone (using electroporation) disrupts the intra-areal, but not inter-areal, patterning of corticothalamic axons at their thalamic nuclei targets (Torii and Levitt, 2005). However, misexpressing EphA7 in the cortex does not interfere with the inter- or intra-areal connectivity of the thalamocortical axons with the cortex (Torii and Levitt, 2005). This suggests that the two gradients of EphA7 are independent of each other, with the cortical EphA7 influencing corticothalamic axon innervation of the thalamus and the thalamic EphA7 influencing thalamocortical axon innervation of the cortex.

Once thalamocortical axons reach the cortex, they are able to form synapses with cortical cells and activity begins to play a role in development. Artificial stimulation of thalamic cells in rats can cause propagation of excitation through thalamocortical axons and into the cortex from E17, and by E19 there is fully functional thalamocortical synaptic transmission to the subplate (Higashi et al., 2002), which means it is quite possible for activity to operate during the time that intra-areal patterns are forming. Activity may even be involved in inter-areal patterning, as there is evidence to suggest that activity is required for thalamocortical axons to innervate

the appropriate cortical areas correctly. Preventing action potentials in the cat brain by blocking sodium channels with tetradotoxin during the time when lateral geniculate nucleus axons innervate the cortex causes these axons to innervate not only the visual cortex (their usual target) but also auditory cortex, and those axons which do innervate visual cortex are not correctly topographically organised (Catalano and Shatz, 1998).

However, in the SNAP-25$^{-/-}$ knockout mouse, in which action potentials do not evoke neurotransmitter release, although spontaneous neurotransmitter release can still occur, the major features of prenatal thalamocortical development are unchanged, with thalamocortical axons growing to and innervating the cortex with their normal topography and also being able to send action potentials to cortex (Molnár et al., 2002). This indicates that the role of activity is limited to postnatal, intra-areal patterning behaviours such as the branching of axons after innervation of layer IV (Hayano and Yamamoto, 2008). For example, the transcription factor NeuroD2 is expressed in the early postnatal cortex and is required for thalamocortical synapses to form correctly. In NeuroD2 null mice, synaptic transmission at thalamocortical synapses is defective and total excitatory synaptic currents are reduced in layer IV. These mice also exhibit defects in barrel cortex formation, with thalamocortical axon terminals failing to segregate into barrel hollows, presumably because they are unable to form synapses correctly (Ince-Dunn et al., 2006).

In summary, therefore, the growth cones of thalamocortical axons exhibit many complex and closely regulated behaviours in order for these axons to make their way to the cortex, become topographically organised, innervate the correct cortical areas and form the appropriate patterns within each cortical area. Whether by regulation by gene expression or by activity, the differentiation of these growth cones must be reflected by the proteins that can be found within the growth cones themselves. With this in mind, it is now possible to turn to the growth cone, its contents and its regulation.

1.5 A role for RNA in axonal growth cones

How do developing axons (including thalamocortical axons, as shown in the previous section) navigate through their environment, extending themselves while responding to the directional cues around them? Attempts to explain these behaviours focus on the growth cone, the complex structure at the tip of each axon which detects and responds to the axon's environment (see Gordon-Weeks (2000) for comprehensive review). In this section, the structure and function of the growth cone is explored, with a focus on

the recently discovered role of locally translated mRNAs in axon guidance behaviour (see Willis et al. (2007); Hengst and Jaffrey (2007); Lin and Holt (2008) for reviews). There is a range of evidence indicating that locally translated mRNAs are required for growth cones to respond to their environment, and therefore, as thalamocortical axons exhibit the same behaviours as axons from other systems, there is good reason to believe that thalamocortical axons contain mRNAs which are locally translated.

1.5.1 The structure and function of the growth cone

The axon cytoskeleton, which is composed of bundles of microtubules, microfilaments and (in some systems) neurofilaments, is extended at the growth cone (Dent and Gertler, 2003). The growth cone itself is also composed of microtubules and microfilaments, although they are not bundled in the same way as in the trunk of the axon. The microtubules, which are dimers of α-tubulin and β-tubulin isoforms, diverge and extend singly into the growth cone, where they form the bulk of the central (C)-domain of the growth cone (Gordon-Weeks, 1993). The microfilaments, which are composed of β-actin and γ-actin isoforms, dominate the peripheral (P)-domain of the growth cone, which extends and contracts in response to its environment (Gallo and Letourneau, 2004). Neurofilaments do extend into the growth cones of peripheral nervous system axons but instead of being incorporated into the growth cone cytoskeleton, they return to the main body of the axon and form part of the axon cytoskeleton (Uchida and Brown, 2004); they have not been found in vertebrate central nervous system growth cones (Dent and Gertler, 2003) and will not be considered further here.

The microfilaments of the P-domain are largely incorporated into two types of processes, lamellipodia, which form a sheet-like mesh extending distally from the C-domain, and filopodia, which are long, thin processes which are spaced among the lamellipodia and protrode outward in all directions (Faix and Rottner, 2006). The growth of the axon involves a standard, three-step procedure of protrusion, engorgement and consolidation (see Figure 1.10a): filopodia protrude outward beyond the existing perimeter of the growth cone and are supported by lamellipodia which follow behind; microtubules engorge the extended P-domain using the lamellipodia as a substrate; and the microtubules consolidate into bundles while the microfilaments around them are depolymerised, leaving a cylindrical form which becomes the distal part of the axon (Goldberg and Burmeister, 1986; Schaefer et al., 2008).

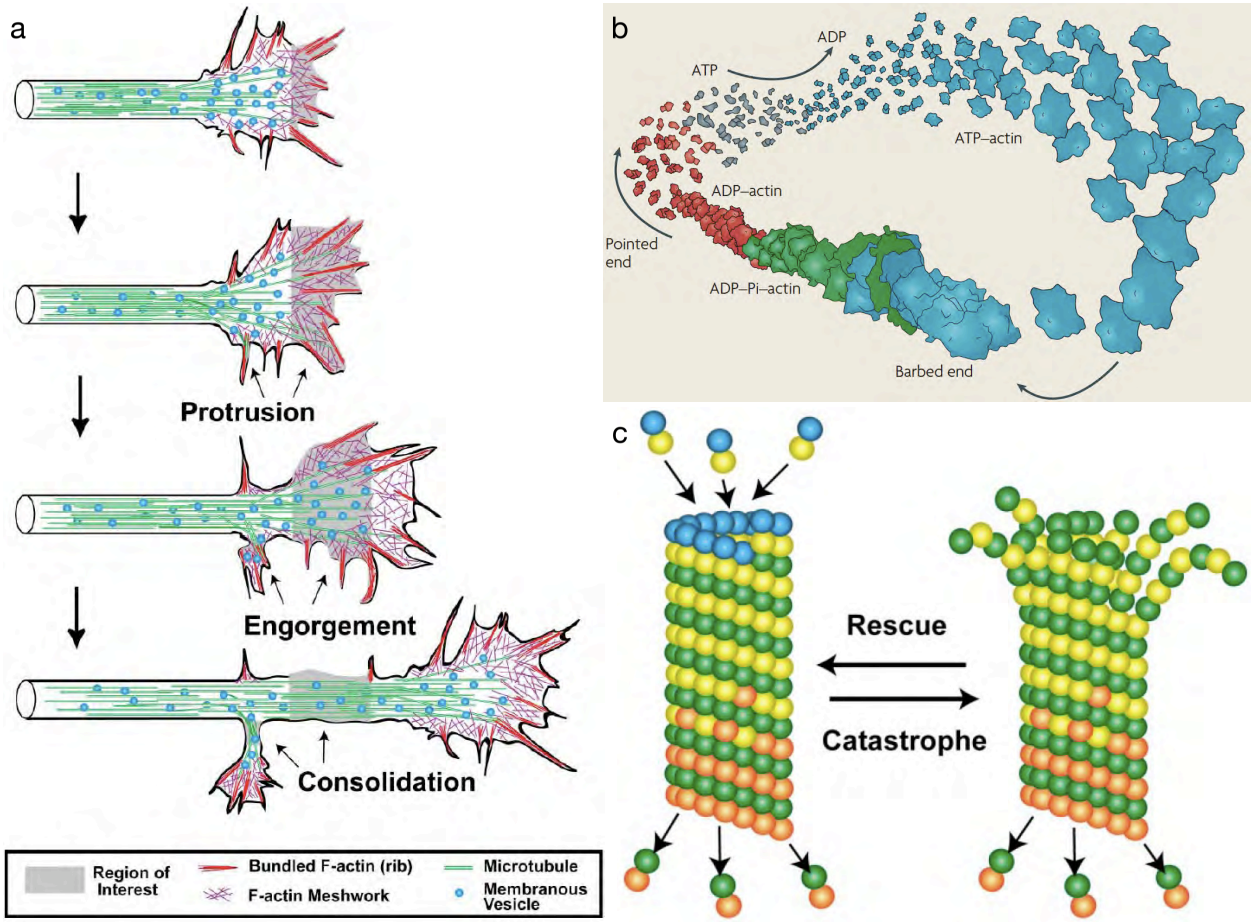

Figure 1.10: a) The growth cone extends the axon by a three-stage process of protrusion, where actin filaments explore the environment, engorgement, where microtubules, vesicles and organelles invade the area staked out by actin filaments, and consolidation, where actin filaments are depolymerised and microtubules form stable bundles. b) The polymerisation of actin filaments involves recycling of actin monomers. Actin bound to ATP (blue) is incorporated into the barbed end of the filament. ATP is hydrolysed, leaving actin bound to ADP and an inorganic phosphate ion P_i (green). P_i is then released, leaving ADP-actin (red) at the pointed end of the filament, which is removed. ADP is exchanged for ATP and the resulting ATP-actin monomer can be reincorporated at the barbed end. c) Polymerisation at the plus end (top) and minus end (bottom) of a microtubule. β-tubulin bound to GTP (blue) and tyrosinated α-tubulin (yellow) is incorporated into the plus end of the microtubule, while GDP-β-tubulin (green) and detyrosinated α-tubulin (orange) is removed from the minus end. The plus end can collapse, with the tubulin polymers separating and depolymerising (catastrophe), followed by reorganisation and repolymerisation (rescue), in a process known as dynamic instability. a,c) taken from Dent and Gertler (2003); b) taken from Pak et al. (2008).

The growth cone also contains a wide variety of organelles in its C-domain including mitochondria, smooth endoplasmic reticulum and vesicles (Tennyson, 1970; Yamada et al., 1971; Chada and Hollenbeck, 2003). In addition, microtubules and microfilaments are regulated by many associated proteins. For example, microfilaments are polymerised by proteins such as Ena/VASP and N-WASP, with Arp2/3 being required for lamellipodia to be formed and fascin being required for filopodia to be formed (Ishikawa and Kohama, 2007; Pak et al., 2008), whereas microtubules are stabilised by microtubule-associated proteins including MAP1, MAP2 and MAP Tau (Gordon-Weeks, 1993; Dehmelt and Halpain, 2004). Also, many receptors, channels and cell adhesion molecules can be found in the membrane of the growth cone, enabling it to integrate signals from its environment and turn appropriately (Wen and Zheng, 2006).

Actin filaments grow outward by a process known as actin treadmilling (see Figure 1.10b; see Le Clainche and Carlier (2008) for review). Actin filaments are polarised, with a barbed end and a pointed end, and grow in the direction of the barbed end. A single filament is not translocated intact, as a whole; rather, new actin monomers are incorporated onto the barbed end of the filament and removed from the pointed end. Actin monomers form a complex with ATP which preferentially binds to the barbed ends of actin filaments. 1-2 seconds after incorporation of the monomer into the filament, ATP is hydrolysed into ADP and an inorganic phosphate ion P_i; several minutes later P_i is released, leaving actin associated with ADP at the pointed end of the filament. These actin-ADP complexes are depolymerised from the filament at the pointed end, after which an ATP-ADP exchange enables the now actin-ATP complex to be reincorporated at the barbed end of the filament.

Therefore actin monomers are continually recycled as the filaments move, and the actin filament is polarised due to the position of the three different actin complexes along its length. These different complexes are preferentially bound by different proteins (see Figure 1.11a); for example, Ena/VASP proteins, which promote the elongation of actin filaments and prevent the branching of filaments, bind preferentially to ATP-actin and so associate with the barbed end of filaments (Drees and Gertler, 2008), whereas cofilin, which depolymerises actin filaments, preferentially binds ADP-actin and so is found at the pointed end where actin monomers are removed from the filament (Fass et al., 2004). Therefore the growth of actin filaments and the formation of superstructures such as filopodia and lamellipodia can be regulated not only by supplying or removing a source of actin monomers but also by interfering with the

action of many actin-binding proteins at different stages of filament formation (Pak et al., 2008).

Microtubules are polarised like actin filaments, but their kinetics are different (see Figure 1.10c). They have a fast-growing 'plus' end and a slow-growing 'minus' end. The plus end is capped by β-tubulin, whereas the minus end is capped by α-tubulin, with both forms of tubulin being bound to GTP (Morrison, 2007). When capped by GTP-bound β-tubulin, stable β-tubulin heterodimers can bind together at the plus end of the microtubule, causing the microtubule to extend rapidly. When GTP is hydrolysed to GDP, GDP-β-tubulin heterodimers separate, causing the microtubules to retract. This frequent, repeated extension and retraction process is known as dynamic instability (Gardner et al., 2008). In growth cones, the minus ends of microtubules are anchored in the C-domain, whereas the plus ends probe the actin filament network in the P-domain for signals from guidance cues via dynamic instability, until they are stabilised with actin filaments once a direction of growth has been established (Gordon-Weeks, 2004).

Actin filaments and microtubules can each be targeted directly by guidance cues; for example, when mouse retinal growth cones are exposed to a gradient of Slit2, there is an increase of the actin-depolymerising protein cofilin and a decrease in actin filaments, causing the growth cones to collapse (Piper et al., 2006). Similarly, exposing mouse dorsal root ganglion (DRG) cells to neurotrophin triggers an actin-independent pathway involving phosphoinositide 3 kinase (PI-3 kinase) and glycogen synthase kinase (GSK)-3β which causes the adenomatous polyposis coli (APC) protein to bind to microtubule plus ends and promote microtubule assembly (Zhou and Cohan, 2004). These pathways will be examined in more detail in the sections that follow.

Over the last decade, several lines of evidence have indicated that growth cone behaviour requires the translation of mRNAs in the growth cone itself. In order to turn and grow in response to their environment, growth cones synthesise protein from a complement of local mRNAs, and this complement of mRNAs varies with changes in the environment (Willis et al., 2005). In the remainder of this section, the behaviour of growth cones will be further explored in the context of local protein regulation.

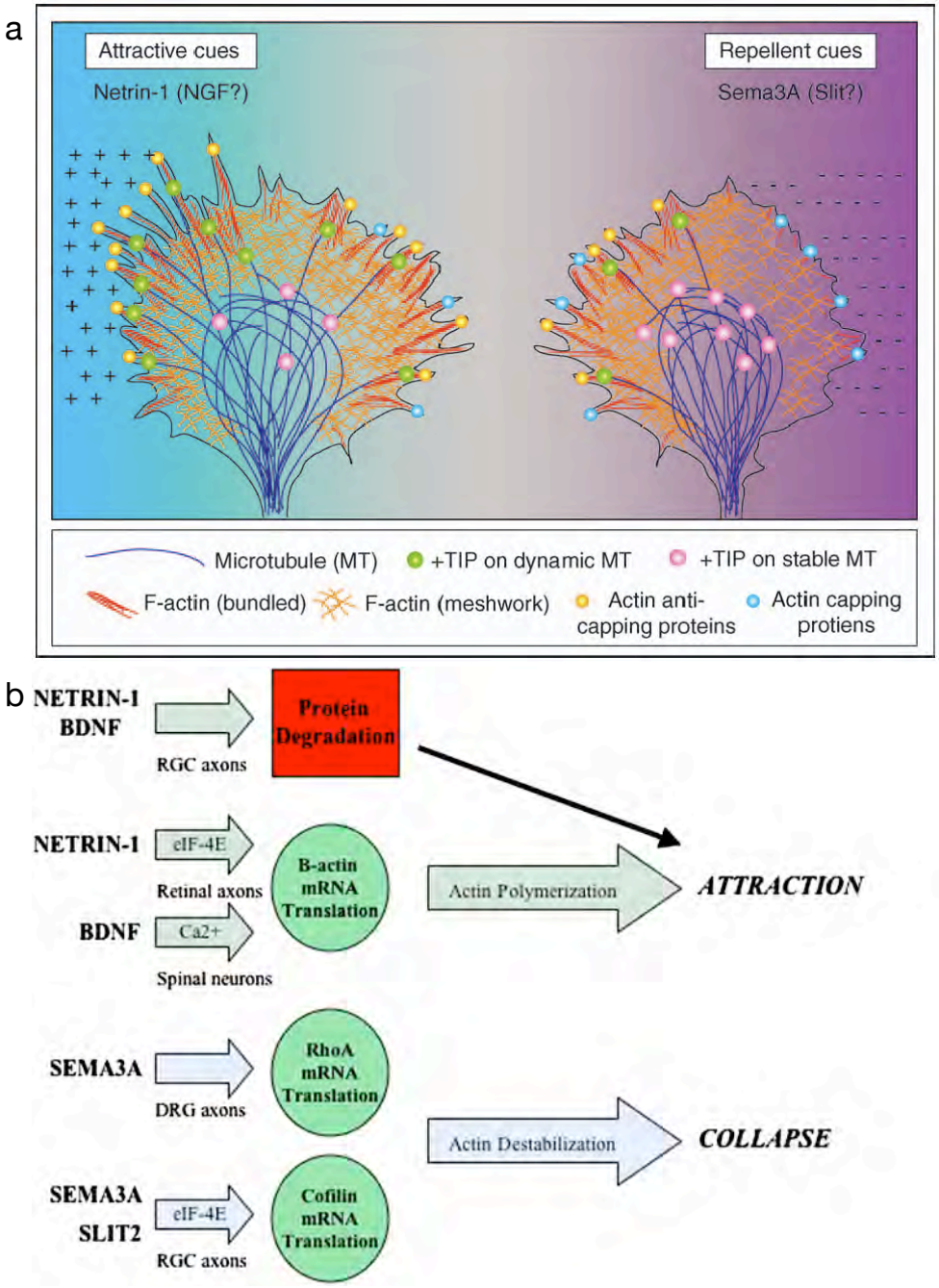

Figure 1.11: a) Guidance cues modify actin filaments and microtubules by regulating growth cone proteins. Attractive guidance cues such as netrin-1 (left) activate actin anti-capping proteins such as Ena/VASP (yellow dots) and proteins such as APC on the plus end of dynamic microtubules (+TIP proteins, green dots) which enable the elongation of actin filaments and microtubules in the direction of the cue. Other actin capping proteins enable repulsive guidance cues such as Sema3A to cause growth cones to collapse. b) A recent summary of currently known guidance cue pathways involving local protein regulation. The red box indicates protein degradation; green circles indicate protein synthesis. a) taken from Kalil and Dent (2005); b) taken from Farrar and Spencer (2008).

1.5.2 Axonal responses to netrin-1 require local protein synthesis and degradation

For each of the four classical guidance cue families, the netrins, ephrins, semaphorins and Slits, in at least one species and axonal system, it has now been shown that regulation of protein synthesis and degradation is required in the growth cone for the guidance cues to cause growth cones to turn or collapse (Campbell and Holt, 2001; Brittis et al., 2002; Wu et al., 2005; Piper et al., 2006); see Figure 1.11b for overview). However, it is not yet certain whether this is the case for all species and all systems, with at least one paper finding no requirement for protein synthesis in growth cone turning behaviour (Roche et al., 2009). Evidence for and against a link between protein regulation and guidance cues will now be described by example, beginning with netrin-1.

Netrin-1 was among the first guidance cues to be identified and is involved in the development of many neuronal and non-neuronal tissues (Barallobre et al., 2005). It was discovered as a chemoattractant for spinal cord commissural axons and, as discussed in Section 1.4.2, it is present in a gradient across the ventral telencephalon and is involved in the topographical organisation of thalamocortical axons. In culture, Xenopus retinal axons are attracted to, and turn towards, point sources of netrin-1 and this attraction requires the presence of the netrin receptor DCC (de la Torre et al., 1997).

Netrin-1 was also the first guidance cue to be linked to local protein synthesis, via treatments of netrin-1-induced turning behaviour in developing Xenopus retinal growth cones (Campbell and Holt, 2001). Growth cones were exposed to a gradient of netrin-1, which was generated by focal application of netrin-1 by micropipette. The protein synthesis inhibitors anisomycin and cycloheximide and the transcription inhibitor α-amanitin were individually added to the culture medium. The turning effects induced by netrin-1 were inhibited by anisomycin and cycloheximide but not by α-amanitin, indicating that protein synthesis, but not transcription, is required for these axons to turn in response to netrin-1. Most importantly, these effects were not only seen in axons with cell bodies, but also in severed axons where cell bodies had been removed. A similar study, exposing severed axons from cultured Xenopus spinal neurons to a gradient of netrin-1, also found that anisomycin and cycloheximide, but not the transcriptional inhibitor DRB, abolished the attractive reponse of the growth cone (Ming et al., 2002). This indicates that protein synthesis is required for growth

cone turning in at least two Xenopus axonal systems, and that the protein synthesis required for axons to turn in response to netrin-1 occurs within the axon, rather than in the cell bodies.

These results suggest that translation machinery must be present at the growth cone and must be triggered by netrin-1, presumably by the cap-dependent translation initiation pathway described in Section 1.2.1. To investigate this translation pathway, Campbell and Holt (2001) applied antibodies for phosphorylated eIF-4E and 4EBP to the same netrin-1 turning assays, because both of these proteins are required for cap-dependent translation to take place. A rapid increase in eIF-4E and 4EBP phosphorylation was seen shortly after netrin-1 treatment. This increase was abolished, however, when growth cones were treated with rapamycin, which inhibits the 4EBP phosphorylation molecule mTOR (Campbell and Holt, 2001); see Section 1.2.1.

A growth factor that has been linked to netrin-1-induced growth cone turning (Guo-li Ming et al., 1999) and is upstream of mTOR (Hay and Sonenberg, 2004) is PI-3 kinase. Treatment with the PI-3 kinase inhibitor wortmannin abolished netrin-1-induced turning behaviour in axons with both cell bodies intact and with cell bodies removed (Campbell and Holt, 2001). In summary, therefore, netrin-1, via its receptor DCC, upregulates PI-3 kinase, which in turn upregulates mTOR. mTOR phosphorylates 4EBP, which releases eIF4E and enables cap-dependent translation of growth cone mRNAs to begin.

It has also been shown that degradation of proteins in Xenopus retinal growth cones is required for netrin-1 to induce growth cone turning. Most proteins are degraded by the 26S proteasome, a complex composed of a 20S core complex, a 19S regulatory complex and an 11S regulatory complex, and are targeted to the proteasome when they are tagged with ubiquitin via 4 regulatory enzymes, E1-E4 (see Tai and Schuman (2008) for recent review). Campbell and Holt (2001) shown that the 20S core complex, ubiquitin and E1 are all present in Xenopus retinal growth cones, and that when proteasome inhibitors are added to the culture medium, retinal axons are no longer attracted to gradients of netrin-1, thus demonstrating that axon guidance in this system requires the regulation of protein synthesis and protein degradation.

1.5.3 The localisation of EphA2 and tau mRNAs to the growth cone requires an intact 3'UTR

Local protein synthesis has also been implicated in the function of Eph receptors. The axons of spinal commissural neurons cross the midline via the floor plate and then grow longitudinally on the contralateral side of the spinal cord to the neuron's soma. EphA2 is synthesised locally in these axons, suggesting a regulatory role in this axon guidance behaviour (Brittis et al., 2002); see Figure 1.12C). A reporter containing GFP and the 3'UTR of EphA2 was electroporated into commissural neurons and was shown to be expressed in the soma and in the section of the axon which had crossed the midline, both on emerging from the floor plate and after turning and growing longitudinally. There was a section of axon between the soma and the growth cone where no GFP was expressed, strongly suggesting local upregulation at the distal portion of the axon. This upregulation was not seen in ipsilateral axons. This indicates that the 3'UTR of the EphA2 mRNA is sufficient for the mRNA to be translated in axons and growth cones, as the remainder of the mRNA was not present in the reporter.

Local translation in oocytes and dendrites is mediated by cytoplasmic polyadenylation elements (CPEs) in the 3'UTR of relevant mRNAs. These CPEs are required to activate poly(A)-tail lengthening of mRNAs, which can be required for translation to take place (Wilkie et al., 2003). The CPE-binding protein CPEB, which must be phosphorylated for poly(A)-tail lengthening to occur, is present in isolated axons (Brittis et al., 2002). The upregulation of EphA2 in contralateral axon segments is also dependent on a CPE sequence which is part of the EphA2 3'UTR. Electroporation of a GFP-3'UTR EphA2 mutation which did not include the CPE sequence abolished contralateral GFP expression but made no difference to expression in the soma, indicating that expression of EphA2 mRNA in the cell body and in the axon is regulated in different ways. Further mutations of the polyadenylation sequence abolished the specific localisation of GFP to the distal portion of the axon and instead caused either no or very low level expression along the entire axon. These results suggest that a 3'UTR which contains both the CPE and the polyadenylation sequence are essential for EphA2 to be localised to contralateral axon segments.

Similarly, tau mRNA is transported to the axons of PC12 cells, where it can be found to be colocalised with tau protein (Aronov et al., 2001). This localisation is dependent on the tau 3'UTR; if the 3'UTR is removed, both tau mRNA and tau protein are found only in the cell body. In addition, if the tau 3'UTR is replaced with the

3'UTR for MAP2, a dendritic protein, then tau is localised to dendrites; if the MAP2 3'UTR is replaced with the tau 3'UTR, then MAP2 is localised to axons (Aronov et al., 2001). This demonstrates that not only is the 3'UTR essential for localisation of mRNAs, but also that specific 3'UTRs direct mRNAs to different parts of the neuron and its neurites.

1.5.4 Sema3A causes translation of RhoA, which is required for growth cone collapse

Sema3A is a member of the classical guidance cue family the semaphorins, which causes Xenopus retinal axons to collapse, although many axons later recover from this collapse and extend new branches, suggesting that Sema3A has a role as a branching factor (Campbell et al., 2001). Sema3A-related growth cone collapse is not limited to Xenopus but can also be seen in rat DRG neurons (Wu et al., 2005) and chick retinal and DRG neurons (Roche et al., 2009).

Sema3A-induced behaviour in Xenopus retinal axons under the influence of various inhibitors was examined (Campbell and Holt, 2001). Similarly to the results acquired for netrin-1, collapse and turning behaviour of these axons were both abolished by the translation inhibitors anisomycin and cycloheximide but not by the transcription inhibitor α-amanitin. Both the collapse behaviour and the turning behaviour triggered a rapid rise in phosphorylated eIF4E and 4EBP. Treatment with the mTOR inhibitor rapamycin also abolished collapse behaviour, although, in contrast to netrin-1 results, treatment with the PI-3 kinase inhibitor wortmannin did not. Also in contrast to netrin-1 results, the inhibition of the proteasome had no effect on Sema3A-induced collapse, indicating that protein degradation is not required for this behaviour.

These results demonstrate that Sema3A-induced growth cone behaviour in Xenopus axons requires local protein synthesis, and that Sema3A triggers protein synthesis through the mTOR - 4EBP - eIF4E pathway. However, Sema3A-induced growth cone behaviour does not require PI-3 kinase, as netrin-1-induced effects do. Sema3A signals through a complex of neuropilin and class A plexin receptors (Kruger et al., 2005). To date, no link has been found between plexinAs or neuropilin and mTOR. However, a recent study has identified a target of this protein synthesis pathway.

The small GTPase RhoA is a potential candidate for Sema3A regulation because it has already been linked to growth cone collapse. Ephrin-A1 signalling via EphA4 receptors (which are involved in thalamocortical development; see Section 1.4.2)

tyrosine phosphorylates the guanine exchange factor ephexin1, which activates RhoA (Sahin et al., 2005). Ephexin1 activation via ephrin signalling causes the growth cones of rat DRG cell axons to collapse (Shamah et al., 2001). This collapse is mediated by the phosphorylation of RhoA by RhoA kinase (ROCK), which causes actin filaments to bundle together and prevents further actin polymerisation (Gallo, 2006). Conversely, netrin-1, via its receptor DCC, inactivates RhoA in E13 rat dorsal spinal cord axons, which causes growth cones to turn towards the netrin-1 source (Moore et al., 2008), presumably due to the prevention of actin regulation by RhoA.

Using fluorescent in situ hybridisations, RhoA mRNA can be found in E15-16 rat DRG axons (see Figure 1.12A). Wu et al. (2005) demonstrated that this RhoA mRNA was translated in the axon and that this axonal translation was triggered by Sema3A. A GFP-expressing vector containing the RhoA 3'UTR was seen to be expressed in axons and growth cones, an effect which was not due to diffusion because a separate vector with a minimal 3'UTR was only expressed in the soma. The mRNA was seen in puncta along the axons which increased in intensity with Sema3A treatment.

Wu et al. (2005) also demonstrated that this Sema3A-related translation of RhoA mRNA was both necessary and sufficient for Sema3A-induced growth cone collapse. All endogenous cap-dependent translation was abolished by treating axons with rapamycin; following this, a vector containing an IRES, EGFP and RhoA was transfected into these axons. This vector, expressed via cap-independent translation, rescued growth cone collapse caused by treatment with Sema3A, indicating that axonal RhoA translation is sufficient for Sema3A-induced growth cone collapse to occur.

However, this does not appear to be the case in all systems and in all conditions. Roche et al. (2009) examined the role of local protein synthesis in E7 chick DRG axons and could find no difference in Sema3A-induced growth cone collapse when axons were treated with cycloheximide or anisomycin. While both phosphorylated 4EBP and protein synthesis could be detected in axons when they were treated with Sema3A, and protein synthesis was no longer detected in the presence of cycloheximide, the collapse response was robustly maintained in the presence and absence of cycloheximide or anisomycin. In addition, no significant variation in RhoA expression in the presence of Sema3A, cycloheximide, or Sema3A plus cycloheximide.

It may be that E7 chick DRG axons simply do not require protein synthesis for axon guidance behaviour, whereas DRG axons at later developmental stages or in other systems behave differently. However, Roche et al. (2009) also failed to abolish the Sema3A-induced collapse response in the presence of cycloheximide or anisomycin in

E13 chick DRG axons and E15 mouse DRG axons (although they did not test E15-16 rat DRG axons, as Wu et al. (2005) did, or stage 35/36 Xenopus retinal axons, as Campbell and Holt (2001) did). The differences may also be due to variations in protocol, as Roche et al. (2009) used different culture medium, substrates and exposure times to both protein synthesis inhibitors and guidance cues than Wu et al. (2005) and Campbell and Holt (2001). Therefore, while the differences in the studies may reflect genuine differences in the behaviour of axonal systems, more consistent studies are required before general conclusions can be reached.

In summary, it is now known that netrin-1 and Sema3A contact causes Xenopus axons to phosphorylate mTOR, which triggers axonal protein translation via 4EBP and eIF4E. In rat DRG axon cultures, RhoA is translated in axons on contact with Sema3A, and this RhoA translation is necessary and sufficient for growth cone collapse. However, this pathway may not operate in all axonal systems, in all species, at all points in development, and more studies are required to fully discover what exactly is the requirement for local protein synthesis in axon guidance.

1.5.5 β-actin mRNA is asymmetrically upregulated in growth cones exposed to guidance cue gradients

The results described above indicate that local protein regulation is required for axons to be guided in some species and axonal systems. But why should an axon turn in response to an expression gradient of a guidance cue? This requires the cytoskeleton to grow in one direction but not another, which implies that the guidance cue causes the contents of the growth cone to differ from one side of the growth cone to the other. How does this differentiation occur?

Microfilaments are composed of many β-actin and γ-actin molecules, and so in order for the growth cone to be extended new actin molecules must be available in the growth cone. These molecules could be transported or synthesised locally. Bassell et al. (1998) showed that, while γ-actin protein is uniformly distributed across the neuron and neurites, β-actin protein is enriched in growth cones and filopodia. Bassell et al. (1998) also showed that γ-actin mRNA is absent from E19 rat cortical axons and growth cones but that β-actin mRNA is present at the growth cone and is associated with microtubules and polyribosomes.

Application of neurotrophin-3 to chick hippocampal and cortical cultured neurons stimulated the localisation of both β-actin mRNA and β-actin protein to the growth

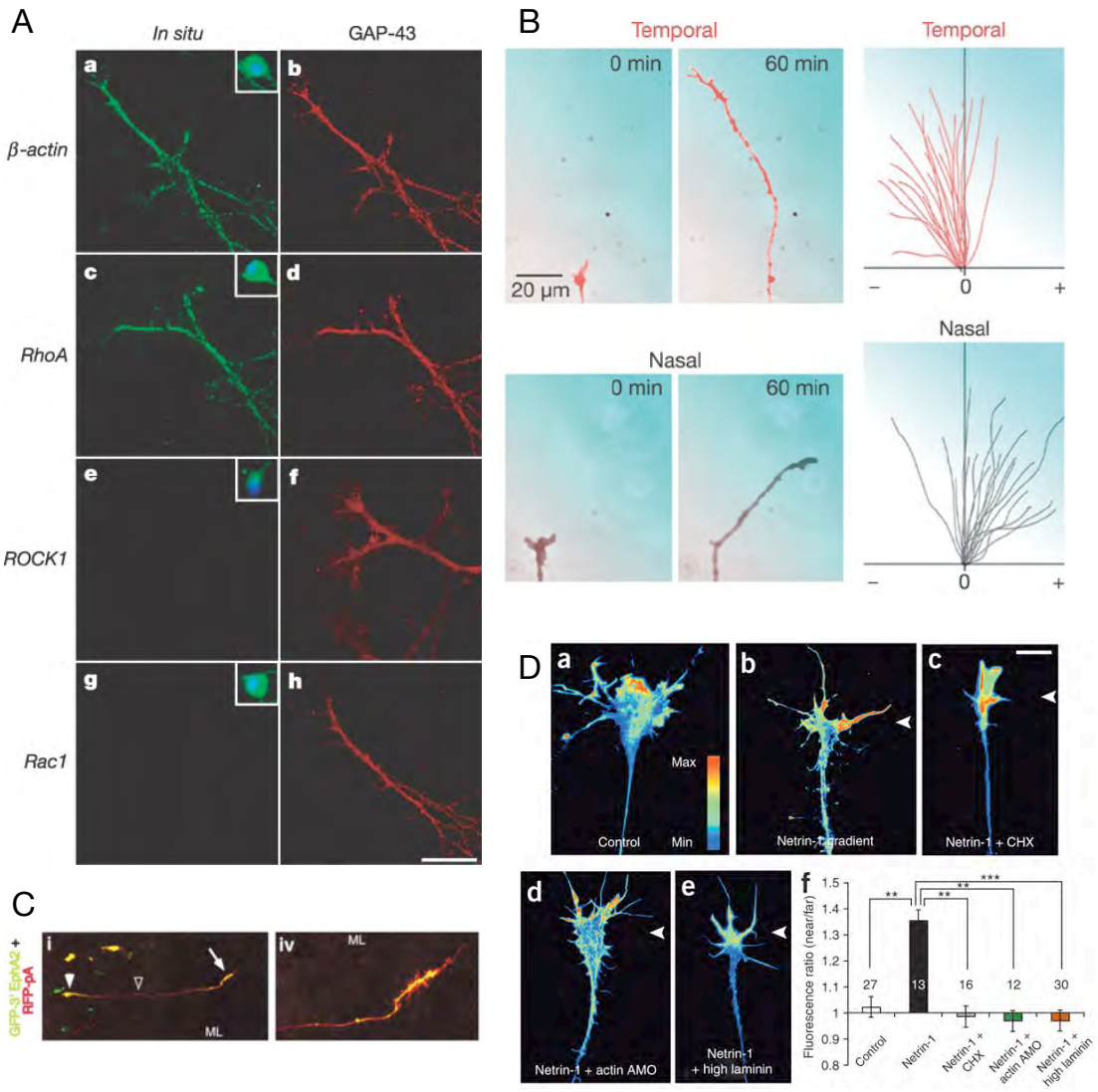

Figure 1.12: A) Rat DRG axons stained with riboprobes for a) β-actin, c) RhoA, e) ROCK1 and g) Rac1 mRNAs in situ (green); axons also immunostained for GAP-43 protein (b,d,f,h; red). All four riboprobes were present in cell bodies (insets, also stained blue with cell marker DAPI) but only β-actin and RhoA were detected in axons. Scale bar, 10μm. B) When exposed to a gradient of engrailed-2 (shown in blue), temporal retinal axons turn away from the gradient, but nasal retinal axons turn towards the gradient (left). Results for many axons shown on the right, with most axons tested turning in the same manner. C) A commissural axon crossing a flattened spinal cord at the midline (ML) and treated with an axonal marker (RFP-pA in red) and a GFP reporter attached to the 3'UTR of EphA2 (green). GFP staining can be seen in the cell body (filled arrowhead) and the growth cone (arrow, and magnification on the right) but not in the axon shaft (hollow arrowhead). D) Xenopus retinal growth cones immunostained for β-actin and pseudocoloured according to fluorescent intensity (see scale in a)). a) Control growth cone; b-e) growth cones treated with netrin-1 gradient (source shown by white arrowheads). b) There is upregulation of β-actin where netrin-1 expression is highest. This asymmetric response is abolished when the growth cone is treated with c) protein synthesis inhibitor cycloheximide (CHX) or d) β-actin antisense morpholino oligonucleotide (AMO), and when axons are grown on a laminin substrate (e). Scale bar, 10μm. f) Fluorescence ratios of the growth cone side near to the netrin-1 source compared to the side far from the netrin-1 source are close to 1, except for netrin-1 treatment alone. **P=0.003, ***P<0.001, Kruskal-Wallis test. Error bars are standard error of the mean. A) taken from Wu et al. (2005); B) taken from Brunet et al. (2005); C) taken from Brittis et al. (2002); D) taken from Leung et al. (2006).

cone (Zhang et al., 1999). This localisation has been linked to a region of the β-actin mRNA 3'UTR known as the zipcode, which is bound by a protein called Zipcode Binding Protein-1 (ZBP1) (Ross et al., 1997). ZBP1 is associated with β-actin mRNA shortly after transcription via a second zipcode binding protein, ZBP2, whose absence prevents ZBP1-associated β-actin transport and inhibits neurite outgrowth (Pan et al., 2007). Once transported to the growth cone, the translation of β-actin is controlled by Src, a protein kinase which phosphorylates a tyrosine residue of ZBP1 that is required for ZBP1 to bind to mRNA, and so releases β-actin mRNA from ZBP1 which enables it to be translated (Hüttelmaier et al., 2005).

If antisense oligonucleotides for the zipcode sequence are introduced into the axon, intended to prevent binding of the zipcode by ZBP1, β-actin mRNA is not localised to growth cones in the presence of neurotrophin-3, but it is localised to growth cones in the presence of neurotrophin-3 when the axons are treated with control reverse antisense oligonucleotides (Zhang et al., 2001). Expression of the mRNA in cells is the same in all conditions, indicating that the antisense oligonucleotides specifically affect localisation via the zipcode. Zhang et al. (2001) also show that an EGFP construct containing the β-actin 3'UTR is upregulated in neurotrophin-3-treated cultured growth cones, indicating that, as appeared to be the case with EphA2 (Brittis et al., 2002), MAP2 and tau (Aronov et al., 2001), the β-actin 3'UTR is both necessary and sufficient for β-actin mRNA and protein to be transported to the growth cone.

The same increase in transport of β-actin mRNA and synthesis of β-actin protein at the growth cone can be seen in Xenopus retinal growth cones in response to netrin-1 signalling (Leung et al., 2006); see Figure 1.12D), and Xenopus spinal growth cones in response to neurotrophin-3 and calcium signalling (Yao et al., 2006). These studies show an asymmetric growth cone response to molecular gradients. Leung et al. (2006) show that, when Xenopus retinal axons are exposed to a gradient of netrin-1, β-actin protein, the eIF4E-binding protein 4EBP and the Xenopus ZBP1 homologue Vg1RBP are all upregulated on the side of the growth cone with high netrin-1 expression. This asymmetric response does not occur in the presence of the protein synthesis inhibitor cycloheximide or a morpholino designed to bind to the start codon of β-actin mRNA, indicating that the asymmetry depends on the presence and translation of β-actin mRNA.

The neurotrophin BDNF causes Xenopus spinal axons to turn, a response which is dependent on the presence of calcium in the growth cone (Song et al., 1997). Yao et al. (2006) show that this response is blocked by the protein synthesis inhibitors

cycloheximide and anisomycin and by antisense oligos which block the zipcode of β-actin mRNA. They also show that, when growth cones are exposed to a gradient of BDNF, both ZBP1 and β-actin mRNA particles are more dense on the side of the growth cone with high BDNF expression. This indicates that growth cone turning behaviour in Xenopus requires not only local protein translation but also the targeting of β-actin mRNA to the region of growth cone expansion.

However, the involvement of β-actin in guidance cue responses may not hold for all systems and species. Roche et al. (2009) found no difference in β-actin protein expression in E7 chick DRG axons after treatment with a different neurotrophin, NGF, and could also find no difference in expression in the presence of the protein synthesis inhibitor cycloheximide, with NGF treatment or without. As discussed in Section 1.5.4, this may be because local protein synthesis is not required at early developmental stages, but it may also be because NGF, unlike BDNF and neurotrophin-3, does not upregulate β-actin mRNA or protein. This appears to be the case in chick forebrain axons, where stimulation with NT-3 and BDNF causes β-actin to localise to growth cones, whereas NGF does not (Zhang et al., 1999); also, NGF, BDNF and neurotrophin-3 have been shown to have differing effects on rat embryonic DRG axons (Paves and Saarma, 1997). More systematic studies of the effects of the various neurotrophins on a single system are required before the issue can be resolved.

1.5.6 Nasal and temporal retinal axons respond differently when exposed to the transcription factor Engrailed-2

As discussed in Section 1.2.2, molecules which were first identified as classical morphogens and transcription factors have been implicated in axon guidance. The transcription factor Engrailed-2 is among this group of molecules, and its involvement relies on the presence of locally translated RNA.

Using similar retinal axon turning assays to the previously described experiments with netrin-1 and Sema3A (Campbell and Holt, 2001), it can be shown that a gradient of Engrailed-2 molecule repels temporal retinal axons and attracts nasal retinal axons (Brunet et al., 2005); see Figure 1.12B). This provides evidence that axons from different sources can differ in their reaction to their environment, and therefore must contain different proteins which cause these differences in behaviour. Both intact and isolated growth cones produce the same turning effects, which are also not affected by the presence of the transcription inhibitor α-amanitin. However, they are abolished

by the protein synthesis inhibitor anisomycin, indicating that, as with netrin-1 and Sema3A, local protein synthesis is required for Engrailed-2-induced turning to occur. A mutation of Engrailed-2 which can not be internalised has no effect on treated growth cones, suggesting that the internalisation is essential to the turning behaviour and that Engrailed-2 does not operate by cell surface interactions.

Once internalised, Engrailed-2 binds directly to eIF4E, in common with many other homeodomain proteins. When Engrailed-2 with a mutated eIF4E binding region is presented to axons, it is internalised but no turning occurs. The internalisation of Engrailed-2 also causes upregulation of the phosphorylated forms of both eIF4E and 4EBP, suggesting that it is involved in the same protein synthesis pathway in which netrin-1 and Sema3A are involved (Brunet et al., 2005).

1.5.7 The RNA complement of growth cones

The above studies show that β-actin, RhoA, EphA2 and tau mRNAs are all present in the growth cone and also suggest that their translation at the growth cone is required for axons of some systems to be guided by external cues. However, many other RNAs have been discovered in developing vertebrate axons (see Piper and Holt (2004) for list), such as EphB2 (Brittis et al., 2002), neurofilament (Sotelo-Silveira et al., 2000) and β-tubulin (Eng et al., 1999) and including more which have been implicated in axon guidance such as CREB (Cox et al., 2008) and cofilin (Leung et al., 2006). It is unclear how many more RNAs are present in growth cones, how many of them will be involved in guidance behaviour and how consistent this behaviour will be across different species and systems.

Two recent papers indicate that, in fact, hundreds of RNAs appear to be present in growth cones. Hengst and Jaffrey (2007) refers to the generation of a cDNA library from developing rat DRG axons, as yet unpublished, which contained around 100 RNAs. Willis et al. (2007) have published a similar survey showing the presence of over 200 different mRNAs in regenerating rat DRG axons. This survey was performed by treating cDNA arrays containing over 4,000 rat cDNAs with amplified cDNAs prepared from isolated axonal rat DRG RNA. This confirms that the growth cone contains a fraction of all RNAs that are expressed in cells, although this fraction is much larger than had previously been shown.

Willis et al. (2007) go on to show that the expression of many of these RNAs is modified in response to guidance cues such as BDNF, NT3 and Sema3A by quantifying

RNA expression using qRT-PCR in the presence or absence of guidance cues. They show that the response of RNAs differs to guidance cues in a complex fashion. For example, the chemoattractants BDNF and NT-3 increase β-actin mRNA and ribosomal protein RP-L22 mRNA expression but Sema3A, which causes axons to collapse, decreases their expression. However, other RNAs such as Hsp90 were downregulated in response to NT-3 and upregulated in response to Sema3A, and other RNAs such as Vimentin were upregulated by both guidance cues.

This complexity may result from differential regulation of mRNAs via their 3'UTRs. The zipcode sequence found in the 3'UTR of β-actin mRNA, which is required for β-actin mRNA to be transported to growth cones and locally translated, is not present in any of the mRNAs found by Willis et al. (2007), nor is it present in another axonal mRNA, cofilin (Leung et al., 2006). This suggests other regulatory elements are present in the 3'UTRs of other axonal mRNAs which are yet to be discovered.

The RNAs discovered by Willis et al. (2007) include many ribosomal proteins, a translation elongation factor, ATP synthases and RNA polymerase II. Combined with the known presence of mRNAs for cytoskeletal proteins such as β-actin and β-tubulin and guidance cue receptor or pathway proteins such as EphA2 and RhoA, it is clear that axonal RNA has a role to play in many different aspects of growth cone behaviour and is important for axon guidance in many different axonal systems.

1.6 RNAs in thalamic axons

The above sections clearly show that locally translated mRNAs have many important roles in axon guidance and that, as thalamocortical axons exhibit the same guidance behaviours as axons from other systems, it is reasonable to investigate which mRNAs, if any, are present in thalamocortical axons. In this section, the construction and contents of a library of thalamocortical growth cone mRNAs is discussed, focussing on one particular mRNA which was identified in this library, β-catenin. Finally, the rationale for the work presented in the following chapters and the structure of the thesis is given.

1.6.1 A library of thalamic axonal mRNAs

A library of thalamic axonal growth cone mRNAs was constructed (T.Pratt, unpublished). Thalamic axons were cultured and severed from cell bodies following Brittis et al. (2002) and the mRNA from these axons was then cloned and sequenced with the differential display technique (Liang and Pardee, 1992) with modifications for increased efficiency and improved validation of results (Miele et al., 1998, 1999). In this method, random 10mers and oligo-dT primers are used to reverse transcribe and amplify as many mRNAs (which have poly-A tails) as possible using polymerase chain reaction (Saiki et al., 1988). Because a limited set of random 10mers were used, this library will not provide an exhaustive catalogue of axonal mRNAs. However, a number of mRNAs were retrieved using this method. The mRNAs retrieved and the number of times they were cloned are shown in Figure 1.13.

While this table shows that a wide variety of mRNAs was present in these thalamic axon samples, it is striking that the only axonal mRNA identified in the literature which appears in the library is β-actin, and that none of the other mRNAs in the library have previously been found in axons. This could reflect differences in sensitivity of methods used, or differences in axons from different parts of the nervous system. It should be noted that Willis et al. (2007) also failed to find several known growth cone mRNAs such as RhoA and EphA2 in their cDNA microarray study. In the case of EphA2 mRNA, this may be because, as it was shown to be present in spinal cord axons, it is not present in the DRG axons that Willis et al. (2007) surveyed, but this explanation does not hold for RhoA, which was previously discovered in DRG axons via in situ hybridisation (Wu et al., 2005). Therefore it appears that there is variability in the axonal complements of different systems and that some difficulty remains in accurately and consistently identifying axonal mRNAs.

The library contains several mRNAs which are already linked to axonal function. RPS3 (Lee et al., 2006) is a ribosomal protein, similar to the many ribosomal proteins identified by Willis et al. (2007), further indicating that ribosomes are present in axons and are apparently also constructed there via local protein synthesis. Reticulon-1 is one of a family of reticulon proteins which are associated with the endoplasmic reticulum, which is present in axons (Droz et al., 1975; Alvarez et al., 2000). Reticulon-1 has been identified in hippocampal axons (Steiner et al., 2004) and interacts with spastin, a protein which is mutated in hereditary spastic paraplegias, disorders which are believed to be due to disruptions in axonal transport (Mannan et al., 2006).

RNA	Positions of clones	Number of clones
RPS3	5'UTR	6
β-catenin	3'UTR	5
β-actin	5'UTR	4
SRP9	Intron	3
Small EDRK-rich factor 1	Coding and 3'UTR	3
Neurexin-1α	Intron	2
Phosphogluconate dehydrogenase	5'UTR	2
RalA	Coding	2
Replication Protein A1 (RPA1)	5'UTR	2
Reticulon-1	Intron	2
BPGM	3'UTR	1
Ascc3l1	3'UTR	1
Bat2d1	Coding	1
Ccdc11	Intron	1
DNA polymerase β	Intron	1
EnTpD 1	3'UTR	1
Gluthathione S-transferase Mu 5	3'UTR	1
Muskelin-1	Intron	1
Reep5	5'UTR	1
Synaptotagmin-13	3'UTR	1
SRrp130	3'UTR	1
tripartite motif-containing 59	Coding	1
Ubiquilin-1	5'UTR	1
Ubiquitin associated protein 2-like	Intron	1
Nucleolar complex protein 14	Coding	1

Figure 1.13: A library of mRNAs isolated from samples of thalamic axons and identified by reverse transcribing the mRNAs into cDNAs, then cloning and sequencing the cDNAs. The table shows the names of the mRNAs identified with the number of times they were cloned.

Synaptotagmin-1 is enriched in growth cones and is involved in calcium signalling via vesicle trafficking (Kabayama et al., 1999); Synaptotagmin-13, which was found in the thalamic axonal mRNA library, has a different structure to synaptotagmin-1 and does not appear to be involved in calcium signalling but is still believed to have a role in vesicle trafficking (Fukuda and Mikoshiba, 2001). The synaptotagmins also interact with neurexin 1α, which was also found in the thalamic axonal mRNA library (Fukuda and Mikoshiba, 2001). RalA, which is a small GTPase like RhoA (Lundquist (2006), see Section 1.5.4), promotes neurite branching in cortical neurons (Lalli and Hall, 2005) by acting via GAP-43, another protein whose mRNA is present in growth cones (Smith et al., 2004).

One mRNA in the library, β-catenin, is of particular interest and has been chosen as a focus for study in this thesis. The reasons for considering this a good candidate for investigation are now discussed.

1.6.2 Potential roles for β-catenin in thalamic axonal development

β-catenin protein is expressed in the growth cones of DRG axons (Zhou et al., 2004b), hippocampal axons and PC12 cell axons (Votin et al., 2005) as well as thalamic axons (T. Pratt, unpublished data). It was the second most-cloned mRNA in the growth cone library, with the ribosomal protein S3 being the most cloned and β-actin being the third most-cloned (see Figure 1.13). This suggests that β-catenin has an important role, or roles, to play in the growth of axons, which is beginning to be borne out by various lines of evidence. β-catenin has critical roles in cell adhesion and Wnt signalling. Indeed, there is considerable debate at present regarding the interactions between these two processes, and it appears that β-catenin is one of the key protagonists in these interactions (Nelson and Nusse, 2004; Bienz, 2005; Brembeck et al., 2006).

β-catenin is a member of the armadillo protein family, each of which contains a central domain containing twelve 'arm repeats', which are 42-amino-acid motifs which cluster together to form a positively-charged groove that binds to many different negatively-charged ligands (Huber and Weis, 2001). The N-terminal and C-terminal domains of the protein are less stable, with the exception of a highly conserved α-helix at the N-terminal region of the C-terminal domain (Xing et al., 2008). These ends are important for the recruitment of binding partners to the central domain, and phosphorylation and dephosphorylation of these ends changes the protein-binding capabilities of β-catenin (Daugherty and Gottardi, 2007).

Figure 1.14a shows β-catenin (green circles) playing a critical role in cell adhesion, forming a bridge between E-cadherin (grey bars) and α-catenin (black dots), which connects to actin filaments in the cytoskeleton (black lines). The figure also shows how Wnts, a class of morphogens which regulate many aspects of the embryonic body plan, initiate transcription of target genes. In the absence of Wnts, a complex containing Axin, CK1, APC and GSK3β phosphorylate β-catenin, causing it to be recognised by the ubiquitin ligase subunit β-Trep, which targets β-catenin for ubiquitination and degradation (Huang and He, 2008). Wnts bind to the cell surface receptors Frizzled and Lrp6 and cytoplasmic protein Dishevelled, causing the phosphorylation of several PPPSPxS (P, proline, S, serine, x, any residue) motifs in Lrp6. This phosphorylated Lrp6 recruits a complex of Axin and GSK3β which inhibits GSK3β (Piao et al., 2008). This prevents GSK3β from phosphorylating β-catenin and targeting it for degradation. In the absence of phosphorylation, β-catenin is targeted to the nucleus by Pygopus (Pygo) and Legless/BCL9-2 (Lgs). Here it binds to TCF transcription factors, which stimulate the transcription of target genes.

The potential roles of cadherin-based adhesion and Wnt signalling in growth cones will now be considered, with a focus on the involvement of β-catenin in these processes.

1.6.2.1 Cadherin-based adhesion is involved in thalamocortical development

Growth cones must adhere both to the extracellular matrix via the class of adhesion molecules known as integrins and sometimes to other cells or axons via the cadherins in order to grow (see Section 1.2.3). These behaviours require a pool of β-catenin which can be incorporated into adherens junctions, which suggests a role for local translation of β-catenin mRNA.

β-catenin has been linked to axon guidance molecules via the adhesion pathway. Rhee et al. (2002) demonstrate that Slit, via its receptor Robo, inactivates N-cadherin-mediated adhesion in chick retinal axons by activating the tyrosine kinase Abl, which phosphorylates β-catenin, causing it to dissociate from N-cadherins (see Figure 1.14b). This causes the local retraction of parts of the growth cone while still allowing other parts to continue to grow. The phosphorylated β-catenin is transported to the nucleus and triggers transcription via TCF/Lef, although it is unclear which genes are transcribed (Rhee et al., 2007). This strongly suggests that β-catenin is required at thalamocortical growth cones, as thalamocortical axons are repelled by Slit expression in the hippocampus (see Section 1.4.1.1).

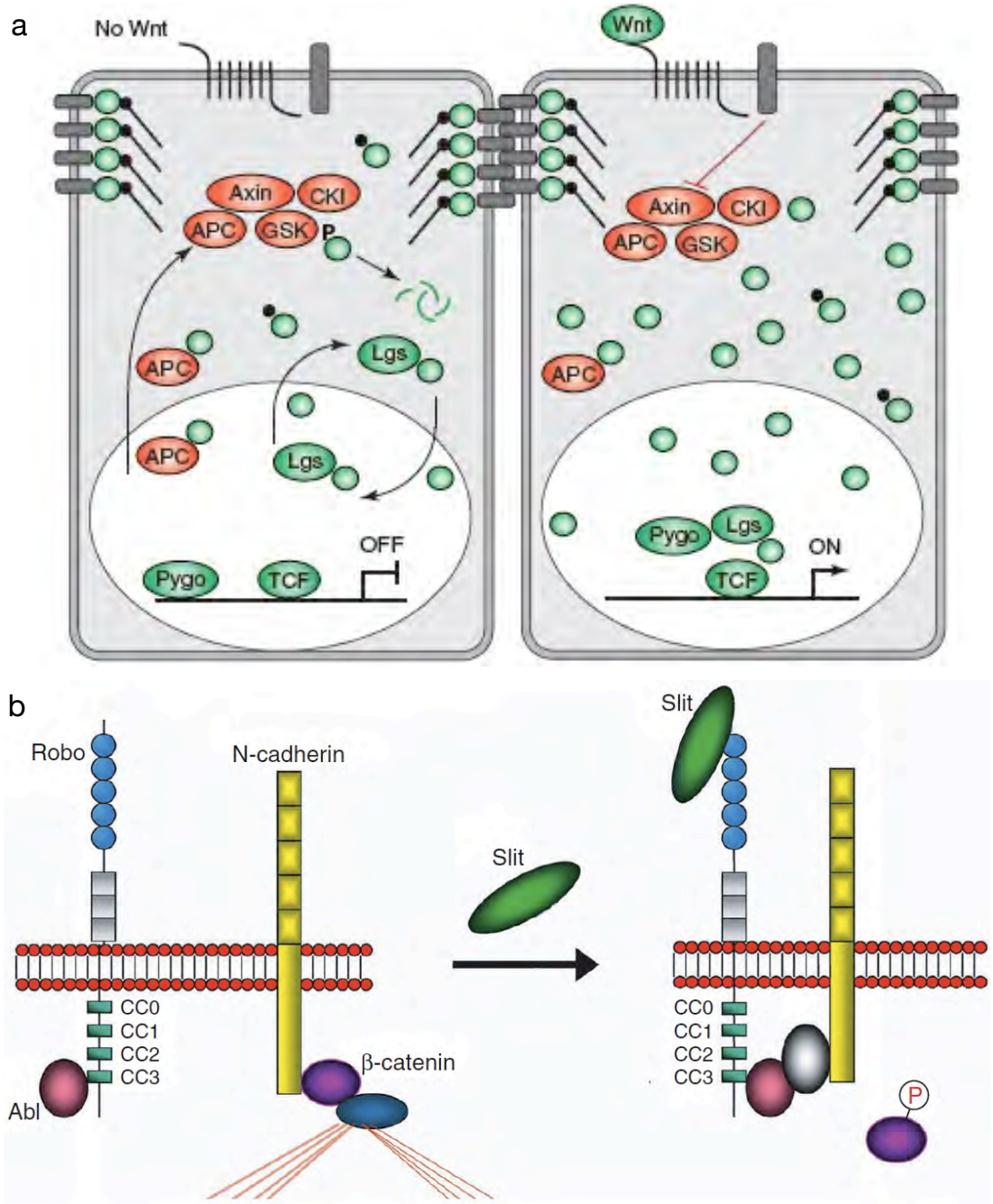

Figure 1.14: a) β-catenin (green circles) connects E-cadherin (grey bars) to actin filaments (black lines) via α-catenin (black circles). In the absence of Wnt (left), β-catenin is phosphorylated by a complex of Axin, CKI, APC and GSK (orange ovals). In the presence of Wnt (right), the complex is inhibited, allowing β-catenin to be targeted to the nucleus by Legless (Lgs) and Pygopus (Pygo), where it binds to TCF transcription factors and stimulates the transcription of target genes. b) Slit causes N-cadherin and β-catenin to disassociate. On the left, Robo receptors bind to Abl, while N-cadherin connects to actin filaments (red lines) via β-catenin and α-catenin (blue circle). On the right, Slit binding to Robo causes Abl to bind to Cables (grey circle), which tyrosine phosphorylates β-catenin at Y489, causing β-catenin to disassociate from N-cadherin. a) taken from Bienz (2005); b) taken from Rhee et al. (2002).

In addition to this direct link between cell adhesion, β-catenin and axon guidance molecules, there are a number of other links between β-catenin and molecules known either to be present in, or to interact with, the growth cone, which have been discovered in other cell-cell interactions.

As seen in earlier sections, the guidance cue ephrin-A5 is involved in many stages of thalamic development; it is expressed in the thalamus, where it regulates the topography of innervating retinal axons (see Section 1.3.3), it is expressed in the ventral telencephalon, where it regulates the topography of growing thalamocortical axons (see Section 1.4.2) and it is expressed in the cortex, where it is involved in inter- and intra-areal patterning, lamination and thalamocortical innervation (see Section 1.4.3). Ephrin-A5 has also recently been shown to regulate the formation of adherens junctions in the lens of the eye (Cooper et al., 2008). In ephrin-A5$^{-/-}$ knockout mice, the shapes of lens cells are highly irregular, neighbouring lens cells are often separated from each other by extracellular vacuoles (suggesting the lack of adherens junctions) and N-cadherin, which is normally localised to lens cell membranes, is instead distributed across the cytoplasm of lens cells.

The ephrin-A5 receptor EphA2 is co-expressed with β-catenin at lens cell membranes in wild type and ephrin-A5$^{-/-}$ knockout mice, indicating that ephrin-A5 is not required for β-catenin to associate with the EphA2 receptor. However, stimulation with ephrin-A5 and EphA2 both independently increased N-cadherin and β-catenin association (shown by immunoprecipitation for N-cadherin followed by Western blot for β-catenin; Cooper et al. (2008)). This suggests that ephrin-A5 stimulation causes cadherin-catenin complexes to form via EphA2. EphA2 appears to operate through both the Src kinase and RhoA, phosphorylated by its kinase ROCK (Fang et al., 2008).

To date, expression of EphA2 protein in thalamocortical axons has not been investigated, and EphA2 was not found in embryonic or postnatal cortex in a study of EphA family expression (Yun et al., 2003). As seen in the earlier sections noted above, ephrin-A5 in the brain appears to operate through EphA4, EphA5 and EphA7, and so it may not regulate cadherin-catenin complexes in the brain as it does in the retina via EphA2. However, as EphA4 has been shown to regulate both the formation of adherens junctions and the level of actin filaments in Xenopus blastomeres (Winning et al., 2001), and is also known to operate through ROCK to cause the collapse of rat DRG axons (see Section 1.5.4), a link between EphA4 and β-catenin in thalamocortical axons is certainly worthy of investigation.

In addition, ephrin-A5 has been shown to cause both the collapse of retinal growth

cones via ROCK and also the initial withdrawal of lamellipodia before collapse, which is mediated through Abl (Harbott and Nobes, 2005). As Abl mediates Slit function by phosphorylating β-catenin, it seems likely that ephrin-A5 also phosphorylates β-catenin via Abl, thus preventing it from binding to cadherins and perhaps therefore preventing the anchoring of lamellipodia, enabling their withdrawal. Similarly, Src has been shown to phosphorylate β-catenin at tyrosine residue 654, which decreases β-catenin binding to E-cadherin (Piedra et al., 2003); Src also phosphorylates N-cadherin, which reduces its binding to β-catenin (Qi et al., 2006). Given Src's known role in EphA2 signalling (see above) and in initiating β-actin mRNA translation in growth cones (see Section 1.5.5), it may be that Src is also linked to β-catenin function in growth cones.

Finally, PI-3 kinase, which is required in growth cones for netrin-1 to induce turning behaviour (see Section 1.5.2), has been shown to interact with β-catenin in epidermal cells (Espada et al., 1999). β-catenin can be bound to PI-3 kinase, preventing β-catenin from being phosphorylated. This increases the amount of β-catenin in the cytoplasm and nucleus and therefore makes more β-catenin available for incorporation into cadherin-catenin complexes. As with Abl and ephrin-A5, PI-3 kinase appears to mediate lamellipodial extension specifically, and is not involved in the formation of adherens junctions; this coincides with a strong co-expression of β-catenin with actin filaments in lamellipodia (Gavard et al., 2004).

In summary, there is direct evidence that β-catenin is involved in axonal responses to Slit and several reasons to believe that ephrin-A5 signalling involves β-catenin, and both Slit and ephrin-A5 operate in thalamocortical axon guidance. In addition, several proteins including Src, Abl and PI-3 kinase, which have been implicated in growth cone function, are known to directly interact with β-catenin, increasing the likelihood that the involvement of β-catenin in cell adhesion has a role to play in thalamocortical development.

1.6.2.2 An alternative canonical Wnt signalling pathway is involved in axon guidance

Given the strong evidence for β-catenin's involvement in adhesion-related behaviours in thalamocortical growth cones, does Wnt signalling involving β-catenin also have a role in the development of thalamocortical axons? As has been discussed in Section 1.4.1.1, Wnts have been indirectly linked to thalamocortical axon guidance. Wnts can act as guidance cues for axons, because vertebrate commissural axons have been

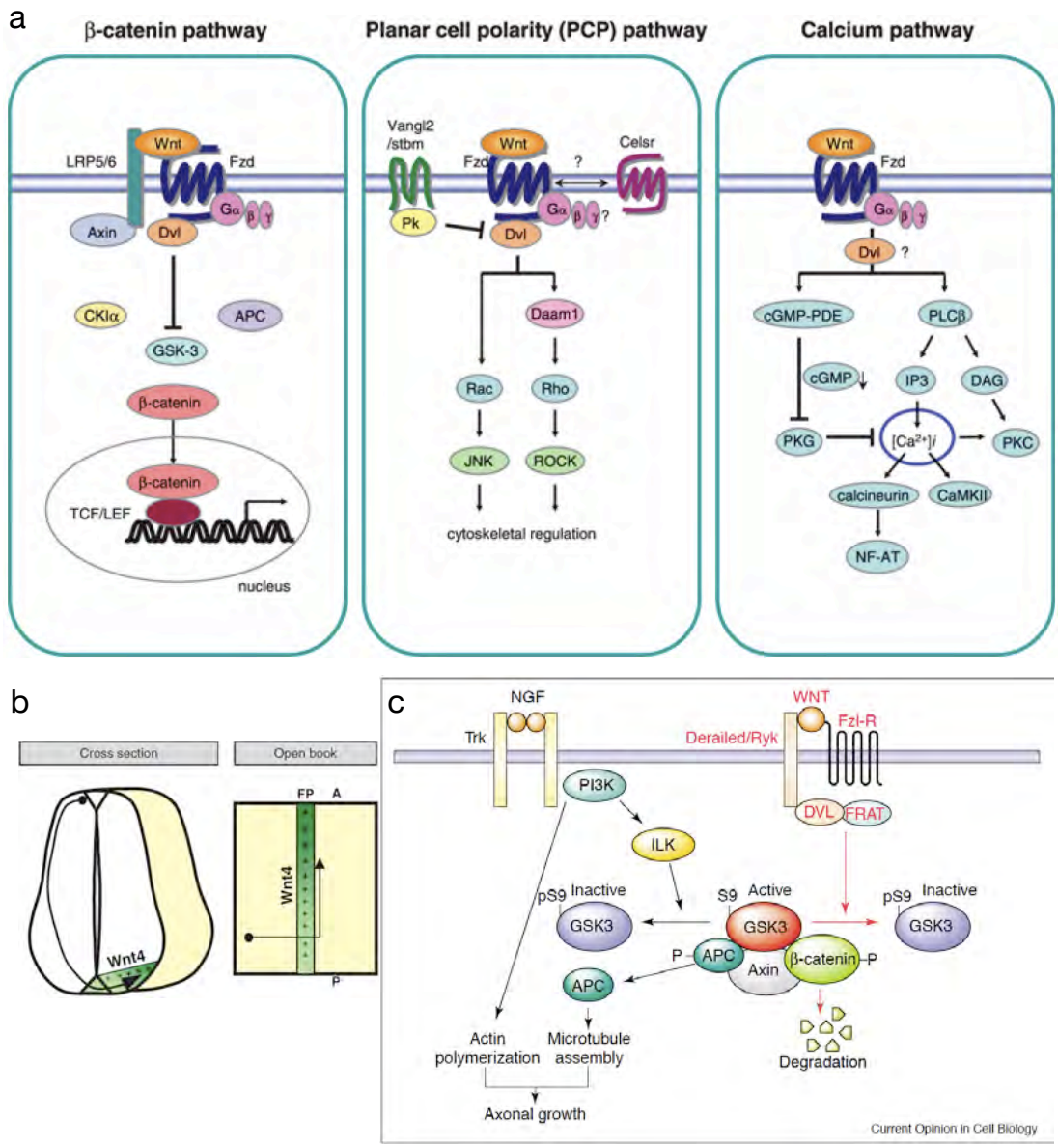

Figure 1.15: a) A recent summary of the major Wnt signalling pathways: the canonical, β-catenin pathway, the planar cell polarity (PCP) pathway and the calcium pathway. b) Wnt4 is expressed at the midline of the spinal cord and influences the growth of commissural axons. FP, floor plate; A, anterior; P, posterior. c) In addition to their roles in Wnt signalling, GSK3 and APC are also involved in microtubule assembly via a neurotrophin (NGF)-PI3K pathway. PI3K also directly regulates actin polymerisation. a) taken from Endo and Rubin (2007); b) taken from Charron and Tessier-Lavigne (2005); c) taken from Arévalo and Chao (2005).

shown to ignore Wnt4 as they approach the midline and become attracted to them after midline crossing, causing them to turn anteriorly (see Figure 1.15b), whereas Drosophila ventral nerve cord axons are repelled by DWnt5 (Zou, 2004). In addition, Wnts are known to be expressed in the cortex during embryonic development and are involved in cortical arealisation (Grove and Fukuchi-Shimogori, 2003), which may mean they are involved in thalamocortical innervation of the cortex. There are also several Wnt-related proteins including Lrp6, Frizzled-3 and Celsr-3 that have been linked to thalamocortical development (see Sections 1.4.1.1 and 1.4.2).

However, to date Wnts have not been shown to directly influence thalamocortical development and, in the cases noted above, it is unlikely that β-catenin is involved. Wnt activity is mediated through several different pathways, the most well-understood of which are canonical Wnt signalling, planar cell polarity (PCP) and Wnt/Calcium signalling (see Figure 1.15a). β-catenin is only involved in canonical Wnt signalling, which stabilises cell-cell adherens junctions and also causes transcription of many target genes.

So far there is little evidence that the full canonical pathway is involved in axon guidance. For example, Lrp6, which is required for the canonical pathway to function, does not appear to be involved in the development of commissural axons, which grow normally in Lrp6's absence (Lyuksyutova et al., 2003); in addition, the lack of thalamocortical axons in Lrp6 mutants appears to be due to severe defects in the thalamus rather than changes in growth cone behaviour (Zhou et al., 2004a). It is most likely that the PCP pathway (or a PCP-like pathway) is responsible for Wnt signalling behaviour in axons (Zou, 2004; Price et al., 2006), as the lack of the PCP protein Celsr-3 prevents thalamocortical axons from entering the internal capsule (see Section 1.4.1.1). The PCP pathway is also a more likely candidate for growth cone regulation because it interacts with the cytoskeleton rather than initiates transcription (Goodrich, 2008) and is known to interact with Rho GTPases such as RhoA (see Section 1.5.4 and Figure 1.15a).

However, in recent years it has been shown that a variant of the canonical Wnt signalling pathway is involved in the regulation of microtubules (Salinas (2007); see Figure 1.15c). As discussed in Section 1.5.1, both GSK-3β and APC, core components of the β-catenin degradation complex in the canonical Wnt signalling pathway, are involved in the regulation of microtubule growth and stabilisation. This pathway has been shown to act in mouse DRG axons, not through Wnt, but through the neurotrophin NGF (Zhou et al., 2004a). In these axons, NGF causes GSK-3β to be

phosphorylated via PI-3 kinase. This phosphorylation prevents GSK-3β from binding to APC, allowing APC to bind to the plus end of microtubules and stabilise them, resulting in growth of the axon.

In canonical Wnt signalling, inactivating GSK-3β and APC in this way should prevent the phosphorylation of β-catenin and enable the accumulation of β-catenin in the cytoplasm, and indeed inhibiting either NGF or PI-3 kinase caused a decrease in β-catenin levels in growth cones (Zhou et al., 2004b). However, it is unclear whether this regulation of β-catenin by GSK-3β and APC has an effect on axon growth. Ciani et al. (2004) show that Dishevelled, which is downstream of Wnt and Frizzled, is found associated with axonal microtubules in the axons of cultured NB2a neurons, and also inhibits GSK-3β via Axin, another member of the complex which targets β-catenin for degradation in the canonical Wnt signalling pathway. This inhibition of GSK-3β leads to an increase in β-catenin, but this increase is not required for Dishevelled to stablise microtubules, and neither is β-catenin-driven, TCF-related transcriptional activity (Ciani et al., 2004). Similarly, Orme et al. (2003) show that Axin and GSK-3β are required for neurite outgrowth in neuroblastoma cells, but β-catenin/TCF-related transcription and stablised β-catenin are not. However, in contrast, Votin et al. (2005) show that not only are APC and β-catenin co-localised in the neurites of PC12 cells, but also that there is a dose-dependent relationship between the quantity of stabilised β-catenin in the neurites and neurite length, with higher levels of stabilised β-catenin causing correspondingly greater inhibition of neurite growth.

It is not clear how these studies can be reconciled; it is possible that PC12 cells act differently to COS-7 and neuroblastoma cells. It may also be due to different methods of stabilisation of β-catenin; Orme et al. (2003) stabilise β-catenin by treatment with Wnt3 or by expressing β-catenin attached to the phospholipid-binding domain of AKAP79, and both approaches may prevent β-catenin from interacting with its usual partners because of interference by Wnt3 or the AKAP79 domain. In contrast, Votin et al. (2005) stabilised β-catenin by specifically removing its GSK-3β binding sites and transcriptional transactivation domain, which may have more successfully preserved β-catenin's other binding abilities and enabled it to interact with neurite outgrowth-regulating proteins.

Even if it proves that β-catenin is not required for neurite outgrowth, one coherent interpretation of these results would be that β-catenin is upregulated in tandem with the stablisation of microtubules, and this upregulation increases the formation of cadherin-catenin complexes and therefore the stablisation of the actin cytoskeleton. The lack of

β-catenin may not impede neurite outgrowth, but it does appear to affect axon guidance via regulation of the actin cytoskeleton (see Section 1.6.2.1), and so it may be that β-catenin is a crucial bridge between the action of microtubules and actin filaments.

In summary, the case for β-catenin's involvement in variants of the Wnt signalling pathway in thalamocortical axons is less clear than its role in adhesive behaviours in these axons, and further studies are required to fully determine its behaviour in this context. However, it is clear that β-catenin is present in growth cones, that a constant supply of β-catenin is required to form cadherin-catenin complexes as the axon grows, and that β-catenin accumulates when GSK-3β is inhibited. This suggests that β-catenin is a strong candidate as a locally translated growth cone mRNA, and therefore the presence of β-catenin mRNA in thalamocortical growth cones has been investigated in detail in what follows.

1.6.3 Thesis rationale and structure

The library presented in Section 1.6.1 indicates that many mRNAs are present in thalamic axons. However, the library requires validation from other sources of evidence in order to be confident that the mRNAs in question really are present in thalamic axons. Firstly, controls were not performed to test for the presence of cells in the axonal samples. Secondly, the mRNAs were cloned using random primers rather than gene-specific primers, and it is desirable to show that each mRNA is present using specific probes or primers in order to be confident that the mRNA has been identified correctly.

Therefore, this thesis describes the design and implementation of several methods intended to validate this mRNA library by confirming the presence of these mRNAs in thalamic axons. There are two major strands to this work: a series of quantitative real time PCR (qRT-PCR) experiments on many mRNAs, and a number of in situ hybridisation experiments primarily intended to identify β-catenin mRNA in thalamic axons.

qRT-PCR, where gene-specific primers are used to exponentially amplify a particular cDNA sequence and measurements taken during amplification can be used to quantify the amount of cDNA, has been chosen for use here due to its high sensitivity and specificity. While qRT-PCR does not have the breadth of microarrays or SAGE (serial analysis of gene expression), which can test for the expressions of thousands of genes at a time, it is more specific and sensitive than either of these methods. Low

abundance transcripts are often not detected using microarrays (Evans et al., 2003) and SAGE does not detect specific genes but relies on amplification at restriction enzyme sites and alignment of amplified sequences to reference sequences for gene identification (Ding and Cantor, 2004); in this respect it is similar to the method used to generate the library of thalamic mRNAs). qRT-PCR is capable of detecting single-copy numbers of RNA molecules (Rameckers et al., 1997) and can be used with gene-specific primers. Therefore it has been used to validate the library of thalamic axons presented above.

The experiments carried out to identify mRNAs in samples of thalamic axons using qRT-PCR are presented in Chapters 3 and 4 of the thesis, following the description of a number of standard materials and methods in Chapter 2. Chapter 3 describes the approach taken to harvest samples of uncontaminated axonal RNA from thalamic axons for use in qRT-PCR experiments. Chapter 4 reports and analyses the results of two sets of qRT-PCR experiments, testing for the presence of a subset of mRNAs from the library described above in samples of thalamic axons harvested according to the method described in Chapter 3.

While qRT-PCR is a very good method for confirming the presence of mRNAs in a sample of tissue, it does not specify the location of mRNAs within the tissue. This is of great interest with axonal mRNAs, because mRNAs are located in granules along the axon and are also located in different parts of the growth cone (see Sections 1.5.4 and 1.5.5 for discussion). As it has not yet been possible to isolate growth cones away from axons for quantification, it is necessary to use a method which can visualise mRNA in intact growth cones and axons to observe axonal mRNA distribution. Therefore, in situ hybridisation, where a probe which is specific for the mRNA of interest is bound to mRNA in a tissue sample and detected using fluorescent antibodies or colorimetric stains, has been used here to detect several mRNAs, in particular β-catenin.

The in situ hybridisation experiments carried out for this thesis are presented in Chapters 5 and 6. Chapter 5 presents a number of in situ hybridisations on cultured thalamic axons, primarily for β-catenin but also for β-actin and the ribosomal RNA 18S. Chapter 6 presents a series of in situ hybridisations on coronal sections of embyronic mouse brains, showing the thalamus and internal capsule during thalamocortical development, in an attempt to identify β-catenin, β-actin, 18S and RPS3 in these areas.

Finally, Chapter 7 summarises the results of the thesis and explores their implications.

Chapter 2

Materials and Methods

2.1 Introduction

This chapter contains the protocols for all of the standard materials and methods used to carry out the work described in this thesis. This includes tissue culture, molecular biology, immunohistochemistry, reverse transcription polymerase chain reaction (RT-PCR) and data analysis methods. Non-standard methods or methods which are discussed within the following chapters are presented in the chapters where they are relevant.

2.2 Tissue Culture

This section contains information about the animals and media used for the primary thalamic cell cultures described in Chapters 3, 4 and 5.

2.2.1 Animals

All mice were housed and cared for under Home Office regulations.

2.2.2 Culture medium

Serum-free culture medium was prepared by mixing the following reagents together under sterile conditions and stored for not more than two weeks at 4 °C until use. Medium was warmed and equilibriated in a 37 °C humidified incubator containing 5% CO_2 for at least one hour prior to use.

- 100ml F12, Hams (Sigma, Catalogue Number N4888)
- 100ml Dulbecco's modified Eagles' medium (DMEM) (Sigma, Catalogue Number D5671)
- 1mg insulin (Sigma, Catalogue Number I6634), final concentration 5μg/ml
- 2mg apo-transferrin (Sigma, Catalogue Number T1147), final concentration 10μg/ml
- 3ml HEPES buffer (Sigma, Catalogue Number H0887)
- 0.24g Na_2HCO_3 (Sigma, Catalogue Number S5761), final concentration 0.12mg/ml
- 3ml antibiotics stock: 100mg gentamycin (Sigma, Catalogue Number G1264) and 200mg kanamycin (Sigma, Catalogue Number K1377) added to 20ml sterile double deionised water, filter-sterilised and stored at $-20\,^{\circ}$C .
- 2ml putrescene stock: 100μM stock, 161.1mg/100ml in sterile double deionised water, filter-sterilised and stored at $-70\,^{\circ}$C (Sigma, Catalogue Number P5780), final concentration 16.11μg/ml
- 20ul progesterone stock: 20μM stock, 6.29mg/100ml ethanol stored at $-70\,^{\circ}$C (Sigma, Catalogue Number P8783), final concentration 6.29ng/ml
- 20ul Na_2SeO_3 stock: 30μM stock, 5.2mg/100ml in sterile double deionised water, filter-sterilised and stored at $-70\,^{\circ}$C (Sigma, Catalogue Number S5261), final concentration 5.2ng/ml
- 2ml L-glutamine stock: 0.2M stock, 6.344g/100ml in sterile double deionised water, filter-sterilised and stored at $-70\,^{\circ}$C (Sigma, Catalogue Number G2128), final concentration 25μg/ml

2.2.3 EBSS

Earle's Balanced Salt Solution (EBSS) was prepared by mixing the following reagents together under sterile conditions and stored for not more than two weeks at $4\,^{\circ}$C until use.

- 100ml Earle's balanced salt solution 10X (Sigma, Catalogue Number E-7510)

- 0.22g Na_2HCO_3 (Sigma, Catalogue Number S5761), final concentration 22mg/ml
- 0.065g glucose (Sigma, Catalogue Number G-7021), final concentration 6.5mg/ml
- 900ml double deionised water

EBSS was oxygenated by bubbling with 95% O_2 and chilled on ice prior to use.

2.3 Molecular biology

This section contains details of the standard molecular biology techniques used to test for the presence and quality of RNA in Figures 3.8, 4.7b and4.12b and used to generate in situ hybridisation probes for the experiments presented in Chapters 5 and 6.

2.3.1 Gel electrophoresis

DNA and RNA samples were tested for size and purity using the following method.

1. Prepare an agarose (Sigma) solution of 1% agarose: 0.5g agarose in 50ml 1xTBE.
2. Microwave on medium power for 2 minutes, replacing evaporation losses with ddH_2O.
3. Add 1ul SYBRSafe (Invitrogen) and mix gently.
4. Pour into a gel casting tray and immediately insert comb.
5. Allow to set for 30 minutes.
6. Prepare sample DNA/RNA by adding 1μl 6X loading buffer per 5μl sample.
7. Load 6μl sample per well.
8. Run gels at 80V for 30 minutes or until bands have resolved.
9. Visualise by exposure to UV light.

1xTBE was diluted from a 10xTBE solution (108g Tris Base, 55g Boric Acid, 20mL 0.5M EDTA, with Water up to 1L).

2.3.2 Templates

As described in Chapter 5, two long β-catenin probes were constructed and used for in situ hybridisation experiments. The β-catenin clones used to make these probes were inserted into a vector and amplified. The clones were then cut out of the vectors to produce cDNA templates for each probe. The cDNA templates were then transcribed into RNA probes. These methods used to produce the RNA probes are now described. For details of vectors, restriction enzymes, promoters and RNA polymerases used, see Section 5.2.1.

2.3.2.1 Insertion of clone into vector

Clones were inserted into new vectors by cutting the clones from their existing vectors with the appropriate restriction enzymes. The strands were separated on a gel. To confirm that the DNA had been cut successfully and to identify the required strands of DNA, a 1Kb DNA ladder was run alongside three controls for each vector; a vector cut with the first restriction enzyme only, a vector cut with the second restriction enzyme only and an uncut vector. The clone sequence and the vector were cut out of the gel and the DNA extracted from the agarose gel using a QIAquick Gel Extraction Kit (Qiagen, Catalogue Number 28704) following manufacturer's instructions. The elutions from the kit were run on a gel to confirm the presence of both DNA strands. The strands were then ligated overnight at 4 °C using T4 ligase (Roche, Catalogue Number 481220). The successful incorporation of the template into the vector was confirmed by sequencing.

2.3.2.2 Transformation of vectors into bacteria

The ligated vector produced above, containing a clone within a vector, was transformed into bacteria for amplification as follows.

1. Add 2μL of ligation reaction and 50μL of JM109 Competent Cells (Stratagene, Catalogue Number 200235) to a 10 mL sterile tube.
2. Mix gently and leave tubes on ice for 20 minutes.
3. Heat shock cells in waterbath for 45-50s at 42 °C.
4. Put tubes on ice for 2 minutes.
5. Add 950μL of room temperature SOC medium (Sigma, Catalogue Number S1797).

6. Incubate for 1-1.5 hours at 37 °C, shaking at 200rpm.

7. Plate cells on agar plates (see below for protocol) and leave to dry for half an hour.

8. Incubate plates at 37 °C overnight.

A single bacterial colony was taken from an incubated plate and incubated overnight in LB broth (see below for protocol). The DNA from these liquid cultures was purified using a QIAprep Spin Miniprep Kit (Qiagen, Catalogue Number 27104). The DNA was then tested by cutting with the appropriate restriction enzymes and running on a gel to confirm that both the clone sequence and vector were present. The DNA was then sent for sequencing by MWG Biotech to confirm the presence of the expected clone sequence.

Agar plates for this protocol were prepared as follows:

1. Stir 17.5g of LB Agar powder (Sigma, Catalogue Number L2897) in 500mL ddH_2O in 1L conical flask.

2. Autoclave flask and keep at 50 °C in water bath until ready to pour.

3. Add 500 μL of 100mg/mL ampicillin (Sigma, Catalogue Number A5354) and mix gently.

4. Pour molten solution into petri dishes in flow hood.

5. Leave to set for 1 hour and store upside down at 4 °C until ready to use.

LB Broth for this protocol was prepared as follows:

1. Add 1 LB tablet (Sigma, Catalogue Number L7275) for each 50mL of water.

2. Autoclave to dissolve tablet and cool to room temperature.

3. Add ampicillin at 100μg/mL.

2.3.2.3 Amplification and isolation of cDNA templates

Having created and tested a vector containing the required clone, this vector could be amplified and cut to create Antisense and Sense templates. The amplification was carried out as follows.

1. Prepare a starter culture by incubating a single bacterium in 3mL LB Broth containing 3μL ampicillin for 8 hours.
2. Make 150mL LB Broth and add 150μL ampicillin and 300μL of the above starter culture.
3. Incubate overnight at 37 °C, shaking at 200rpm.
4. Purify DNA from liquid culture using a Qiagen Plasmid Maxi Kit (Qiagen, Catalogue Number 12162).
5. Quantify purified DNA using a mass spectrometer.

Antisense and Sense cDNA templates were cut from the vector prepared above by incubating the vector overnight at 37 °C in ddH_2O with the appropriate restriction enzymes for each strand, in both cases adding Buffer H (provided with restriction enzymes).

2.3.3 *In vitro* transcription of labelled probes from cDNA templates

The cDNA templates produced above were used to transcribe Antisense and Sense RNA probes, labelled with digoxigenin, as follows:

1. Mix 1μg of linearised cDNA template with 2μL DIG RNA Labeling Mix (Roche, Catalogue Number 11277073910), 2μL of the appropriate RNA Polymerase, 2μL 10xTranscription buffer (provided with RNA Polymerases) and sterile RNase free ddH_2O, to 20μL.
2. Centrifuge briefly and incubate for 2 hours at 37 °C.
3. Add 2μL DNase I, RNase free (Roche, Catalogue Number 10776785001) and incubate for 15 minutes at 37 °C.
4. Stop the reaction by adding 2μL 0.2M EDTA (pH 8.0).
5. Add 2.5μL 4M LiCl and 75μL prechilled ethanol and mix well.
6. Leave for 2 hours at −20 °C and centrifuge for 5 minutes at 13000xg.
7. Decant the ethanol and dry the pellet.
8. Dissolve pellet in 50μL sterile RNase free ddH_2O.

2.4 Immunohistochemistry and In Situ Hybridisation

Standard protocols and solutions for immunohistochemistry and in situ hybridisation follow. Specific in situ hybridisation protocols are presented in Chapters 5 and 6.

2.4.1 Immunohistochemistry

Immunohistochemical staining of thalamic explants with axonal growth, presented in Chapter 3, was carried out as follows. All treatments were performed at room temperature unless otherwise stated.

1. Fix explants in 4% PFA for 30 minutes.
2. Permeabilise for 15 minutes in 1% Triton-X/1xPBS.
3. Pre-treat with blocking solution for 30 minutes.
4. Treat with primary antibody (neurofilament (Biomol, Catalogue Number NA1297-0100), 1:150 in antibody blocking solution) overnight at 4 °C.
5. Rinse with 1xPBS for 5 minutes.
6. Treat with secondary antibody (Alexa Fluor 488 anti-rabbit (Invitrogen (Molecular Probes), Catalogue Number A11008), 1:200 in antibody blocking solution) for 2 hours.
7. Apply nuclear counterstain (propidium iodide) for 10 minutes.
8. Wash three times with 1xPBS for five minutes each.
9. Mount using Mowiol and store in the dark at 4 °C until ready to view.

2.4.2 Solutions

In this section, protocols and recipes are presented for the solutions required for the immunohistochemical and in situ hybridisation protocols described in Chapters 3, 5 and 6.

2.4.2.1 DEPC Water

All solutions used prior to and including hybridisation of in situ probes were made with DEPC water, which was prepared as follows. Bottles and stirrers were baked at 150°C for 4 hours before use. Bottle tops were autoclaved. 2mL DEPC (Diethyl pyrocarbonate, Sigma, Catalogue number D5758) was added for every 1L of ddH_2O and stirred overnight. After stirring, bottles were heated at 60°C for 1 hour and autoclaved.

2.4.2.2 4% PFA

4g of paraformaldehyde was added for every 100mL of 1xPBS. 50μL 10M NaOH was added and the solution was heated to 55°C and shaken in a waterbath. After the paraformaldehyde had completely dissolved, the solution was cooled to room temperature. Finally, the solution was adjusted to the appropriate pH (7.5 unless otherwise stated), tested using pH indicator sticks (Fisher, Catalogue Number FB33003).

2.4.2.3 Immunohistochemistry

The following solutions were used for the immunohistochemistry protocol described in Section 2.4.1.

- **10xPBS buffer**
  - 20.5g NaCl
  - 1.075g $NaH_2PO_4.2H_2O$
  - 4.35g Na_2HPO_4
  - DEPC-treated water up to 250mL
- **Antibody blocking solution**
  - 0.06g BSA
  - 0.2mL Goat Serum
  - 0.2mL Tween-20
  - 1xPBS up to 20mL

2.4.2.4 Fluorescent axonal in situ hybridisation

The following solutions were used for the fluorescent axonal in situ hybridisation protocol described in Section 5.2.3.2. See previous section for other solutions.

- **10xTBS buffer**
  - 87.66g NaCl
  - 24.228g Tris Base
  - pH to 7.5
- **20xSSC**
  - 87.66g NaCl
  - 44.12g Trisodium citrate
  - ddH_2O to 500mL
  - pH to 7.5
- **Acetylation solution**
  - 10mL 100mM HEPES (Sigma, Catalogue Number H4034), pH 8.0
  - 25μL Acetic anhydride
- **Hybridisation buffer**
  - 40% Formamide
  - 10% Dextran sulphate
  - 4xSSC
  - 20mM Ribonucleoside vanadyl complex (New England Biolabs, Catalogue Number S1402S)
  - 10mM DL-Dithiothreitol (Sigma, Catalogue Number 43819)
  - 1mg/ml yeast tRNA (Roche, Catalogue Number 10109495001)
  - 1mg/ml salmon sperm DNA (Sigma, D7656)
- **Antibody blocking solution**
  - 100mM Tris Base, pH 7.5

- 150mM NaCl
- 8% Formamide
- 5% BSA
- 2.5% Goat Serum
- 2.5% Horse Serum

2.4.2.5 Colorimetric axonal in situ hybridisation

The following solutions were used for the colorimetric axonal in situ hybridisation protocol described in Section 5.2.3.2. See previous sections for other solutions.

- **1xPBT**
  - 0.1% Tween-20 in 1xPBS
- **Buffer 3**
  - 12.1g Tris Base
  - 5.8g NaCl
  - ddH_2O to 1L
  - pH to 9.5
  - Add 10.15g Mg_2Cl_2
- **Hybridisation buffer**
  - 5mL Formamide
  - 2.5mL 20xSSC pH 4.5
  - 100mg B-Block
  - 2mL DEPC Water
  - Dissolve in water bath at 65°C
  - 100μL 0.5M EDTA
  - 100μL Tween-20
  - 100μL CHAPS, 10% in H_2O
  - 4μL 50mg/mL Heparin
  - 200μL 50mg/mL yeast tRNA, pre-denatured at 95°C for 5 minutes

2.4.2.6 Wax section in situ hybridisation

The following solution was used for the wax section in situ hybridisation protocol described in Section 5.2.3.1. See previous sections for other solutions.

- **10xTEA**
  - 133mL Triethanolamine, pH 8
  - Add ddH_2O to 1L

2.4.2.7 Vibratome section in situ hybridisation

The following solutions were used for the vibratome section in situ hybridisation protocol described in Section 6.2.1. See previous sections for other solutions.

- **PBT**
  - 50mL 10xPBS
  - 0.5mL Tween-20
  - Add DEPC Water to 500mL
- **10xTBS**
  - 20g NaCl
  - 0.5g KCl
  - 62.5ml 1M Tris-HCl, pH 7.5
  - ddH_2O to 250mL
- **TBST**
  - 50ml 10xTBS
  - 5ml Tween-20
  - ddH_2O to 500mL
- **NTMT**
  - 10mL 5M NaCl
  - 50mL 1M Tris-HCl, pH 9.5
  - 25 mL 1M $MgCl_2$

- 5 mL Tween-20
- ddH_2O to 500mL

- **Solution 1**
  - 500mL Formamide
  - 250mL 20xSSC, pH 4.5
  - 10g SDS
  - ddH_2O to 1L

- **Solution 3**
  - 500mL Formamide
  - 100mL 20xSSC, pH 4.5
  - ddH_2O to 1L

- **Hybridisation buffer**
  - 25mL Formamide
  - 12.5 mL 20xSSC, pH 4.5
  - 0.25mL tRNA (10mg/mL)
  - 0.5g SDS
  - 0.25mL 10mg/mL Heparin
  - DEPC Water to 50mL

2.4.2.8 Mowiol mounting medium

Mowiol mounting medium solidifies once used and allows direct mounting of the coverslips onto glass slides. Once mounted, the coverslips can be viewed with immersion lenses as the coverslips will not move. The coverslips are also removeable by gently sliding off the side of the slide, using tweezers. The Mowiol can be removed by immersing the coverslips in ddH_2O for a few minutes.

1. Add 2.4g Mowiol (Calbiochem Catalogue Number 475904) to 6g of Glycerol (Glycerol density = 1.26g/ml - for 6g = 6/1.26 = 4.76 mls) in a 50ml conical flask.

2. Stir with a pipette to mix.

3. Add 12ml dH_2O and leave stirring for several hours or overnight at room temperature.

4. Add 12ml 0.2M Tris (pH8.5) and heat to 50°C for 1-2hr or until Mowiol is completely dissolved. Vortex occasionally. (1M Tris = 121.14 g/l, 100nM = 12.114g/l, 200nM = 24.228g/l or 2.423g/100ml)

5. Centrifuge at 2000rpm for 15 minutes.

6. Add 1,4-diazobicyclooctane (DABCO) Sigma (Antifade) to 2.5% (=0.72g) Aliquot and store at −20°C.

7. Centrifuge before use to pull down any bubbles.

2.5 Extraction and amplification of RNA for RT-PCR and qRT-PCR

In this section, the protocols and programs used for cDNA synthesis, RT-PCR and qRT-PCR are described.

2.5.1 cDNA synthesis

cDNA synthesis was carried out using SuperScript III First-Strand Synthesis SuperMix kits (Invitrogen, Catalogue Number 18080400) on a PTC-225 thermal cycler (MJ Research).

1. Mix RNA with 1μL random hexamers, 1μL annealing buffer and RNase/DNase-free water to 8μL. For the qRT-PCR experiments described in Chapter 4, 1μL of Cells RNA was used to 5μL of water, whereas 4μL of Axons, Blank Near and Blank Far RNA was used to 2μL of water, to improve the amplification of these samples.

2. Incubate in a thermal cycler at 65°C for 5 minutes.

3. Place tubes on ice for at least 1 minute and centrifuge briefly.

4. Add 10μL of 2xFirst-Strand Reaction Mix and 2μL of SuperScript III/RNase-OUT Enzyme Mix, mix by pipetting and centrifuge briefly.

5. Incubate in a thermal cycler at 25 °C for 10 minutes, 50 °C for 50 minutes and 85 °C for 5 minutes.

6. Chill tubes on ice and store at −20 °C.

2.5.2 Standard RT-PCR

The standard RT-PCR program used to produce the results for Figure 3.8 ran as follows on a DNA Engine Dyad thermal cycler (MJ Research):

1. 94 °C for 5 minutes

2. Cycle 30 times:

   (a) 94 °C for 1 minute (strand denaturation)

   (b) 55 °C for 1 minute (primer annealing)

   (c) 72 °C for 1 minute (strand elongation)

3. 70 °C for 10 minutes

2.5.3 Quantitative RT-PCR

Quantitative RT-PCR experiments were carried out using Quantitect Sybr Green PCR Kits (Qiagen, 204143). All tubes were prepared and kept on ice throughout. Primer mixes containing left and right primers were prepared with 12.5μL left primer, 12.5μL right primer and 75μL sterile RNase-free water. Master mixes were prepared containing 12.5μL SYBR Green, 1μL primer mix and 10.5μL RNase-free water for every tube required in the reaction. Each tube was prepared with 1μL cDNA and 24μL master mix. Tubes were mixed by pipetting and centrifuged briefly. 24μL from each tube was added to 8-tube strips with clear caps (Biorad, Strips Catalogue Number TLS-0851, Caps Catalogue Number TCS-0803). Tube strips were spun briefly. Reactions were performed on a DNA Engine Opticon System (MJ Research) with initial data analysis performed using Opticon Monitor v1.08. The following program was used for all qRT-PCR experiments:

1. 95 °C for 5 minutes

2. Cycle 50 times:

(a) 94 °C for 15 seconds

(b) 55 °C for 30 seconds

(c) 72 °C for 30 seconds

3. Run melting curve: from $60-95$ °C, read plate, hold for 1 second and increment temperature by 1 °C.

r^2 values and melting curve peaks were provided by the Opticon Monitor software. The cycle threshold for each RNA was chosen at the point in the region of exponential amplification where r^2 was highest. Following standard practice, percentage efficiencies was calculated as $E = (10^{-1/Slope} - 1) * 100$, where Slope is the slope of the standard curve regression line, provided by the Opticon Monitor software.

2.5.4 Primers

Primers were designed using PerlPrimer (Marshall, 2004) using the Ensembl sequences listed in Table 4.5 as input. The primers were checked for other matching sequences against the mouse genome using BLAST (Altschul et al., 1990). PerlPrimer produces a list of likely primer-dimers and primers with low probability of forming primer-dimers were selected based on this list. The primers were all designed to be intron spanning except for 18S, which only has one exon. Primers were supplied by MWG Biotech.

2.6 Equipment and software

In this section, the tools used to analyse data and prepare this thesis are listed.

2.6.1 Microscopy

2.6.1.1 Light microscopy

Slides were photographed using a Leica DMLB upright compound microscope connected to a Leica DSC480 digital camera, using Leica IM50 image management software.

2.6.1.2 Confocal microscopy

Fluorescent staining was viewed using a Leica DMRE compound microscope, part of a Leica TCS NT confocal system using 'Leica Lite' software.

2.6.2 Software

Figures and tables were prepared using Numbers, the spreadsheet program in Apple's iWork'08 office suite (`www.apple.com/iwork/`). Numerical and statistical analysis was performed using iWork and NeoOffice (`www.neooffice.org`). Figures 4.1, 4.2 and 4.9 were produced using the Opticon Monitor software which controlled the qRT-PCR machine. Figure 4.11 was produced using R (R Development Core Team, 2008), using the errbar function in the package Hmisc (Harrell, 2005). The image editor Pixelmator (www.pixelmator.com) was used to carry out minor edits on the figures in Chapter 1, draw the diagram in Figure 3.2 and to remove air bubbles and other debris from the images in Chapter 6. The thesis, including all mathematical formulae, was typeset in LaTeX using the editor TeXShop (`www.uoregon.edu/~koch/texshop/`) and a template by Mary Ellen Foster (available from `www.inf.ed.ac.uk/systems/tex/local-packages.html`).

Chapter 3

Harvesting Axonal RNA for Amplification by qRT-PCR

3.1 Introduction

The identification of multiple RNAs in an axonal system poses a number of technical challenges. Firstly, the detection of the very small amounts of RNA present in axons requires an extremely sensitive identification method. Secondly, the method should be high throughput, so that many RNAs can be tested with a relatively small amount of time and effort. To meet these challenges, a method using quantitative reverse transcription polymerase chain reaction (qRT-PCR) technology has been developed. This chapter explains and justifies the novel development of a method for harvesting axonal RNA in such a way that the amounts of RNA in axons can be quantified by qRT-PCR. Chapter 4 describes the quantification of thalamic RNA harvested using this method.

3.2 Materials and methods

3.2.1 Harvesting of RNA

A method for isolating axonal RNA from embryonic thalamic axons is now described, which should be applicable to any axonal system which will grow in culture. A flow diagram of the entire method can be seen in Figure 3.1. For detailed protocols and recipes, see Section 2.2. The qRT-PCR design will be more fully explained in Chapter 4.

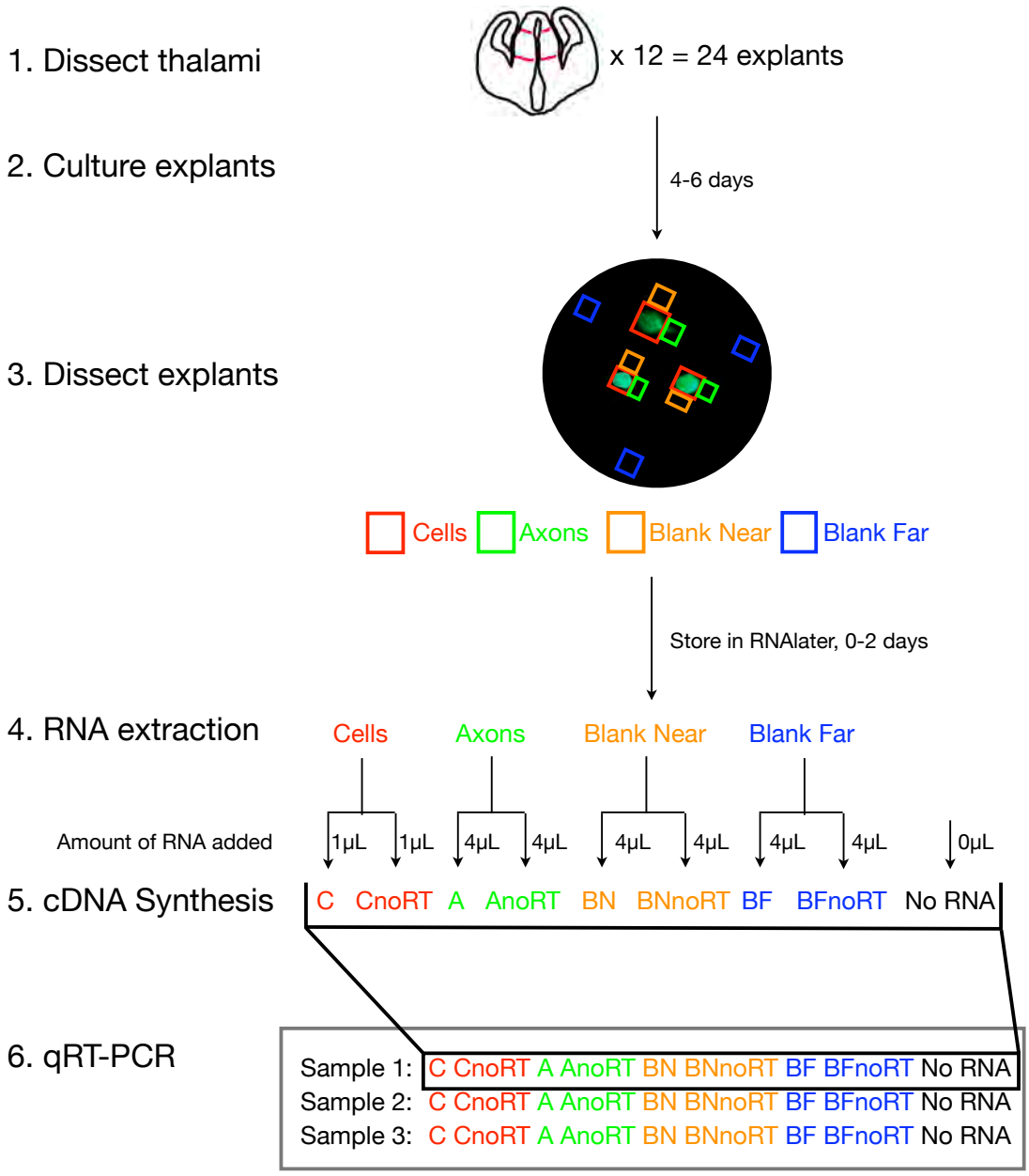

Figure 3.1: Flow diagram of a method for harvesting and quantifying thalamic axonal RNA. 1. Both thalami from up to 12 coronal sections of E14.5 mouse brains were dissected along the lines shown in red, producing up to 24 thalami. 2. Explants were cultured in serum-fed medium on collagen-coated Teflon inserts for 4-6 days to produce axonal carpets. 3. Inserts were dissected into four sets of pieces: axonal carpets, labelled Axons, explants, labelled Cells, blank pieces of insert next to the explants, perpendicular to the direction of fibre growth, labelled Blank Near, and blank pieces of insert from the edges of the insert, labelled Blank Far. Pieces of insert were stored in the RNA stablisation buffer RNAlater at 4 °C for 0-2 days. 4. RNA was extracted at most two days after dissection. 5. cDNA was synthesised from extracted RNA using reverse transcription. One cDNA synthesis reaction was performed for each sample of RNA (C, A, BN, BF) and the No RNA control. In addition, a tube containing no reverse transcriptase was processed using the cDNA synthesis protocol for each of the four RNA samples (C, A, BN, BF) to control for the presence of contaminating DNA. 1μL of Cells RNA was used for each of the C and CnoRT reactions, whereas 4μL of Axons, Blank Near or Blank Far RNA was used for each of the A, AnoRT, BN, BNnoRT, BF and BFnoRT reactions respectively to improve the amplification of small signals. A tube containing no RNA, labelled No RNA, was processed using the cDNA synthesis protocol to control for the presence of contaminating RNA during processing. 6. qRT-PCR was performed on three samples at a time (for full details, see Chapter 4). Abbreviations: C, Cells; A, Axons; BN, Blank Near; BF, Blank Far; noRT, No Reverse Transcriptase.

3.2.1.1 Culture

Embryonic mouse brains (CBA strain, E14.5) were dissected in ice-cold oxygenated EBSS. Each brain was sliced coronally into 200μm sections using a MacIlwain Tissue Chopper (Mickle, UK). Thalamic sections were dissected from these brain sections using sterile technique. The epithalamus and prethalamus were removed, leaving the thalamus (see Figure 3.2). These thalamus explants were placed on Costar collagen-coated Teflon inserts, 24mm membrane diameter, 3μm pore size (Fisher Scientific, UK) in 6-well dishes containing 75% basal culture medium (see Section 2.2 for recipe), 25% fetal calf serum, pre-incubated at 37°C in 95% oxygen, 5% carbon dioxide. Twenty-four explants were prepared for each culture, with three explants in each of eight inserts.

3.2.1.2 Dissection

The explants were cultured for 4-6 days, during which time the explants adhered to the insert and axons grew along the fibres of the membrane. The inserts were then dissected and the pieces placed into sterile 1.5ml Eppendorf tubes each containing 350μl of RNAlater (Qiagen), an RNA stabilisation agent which neutralises RNAses. A schematic of the dissection for one well is shown in Figure 3.3.

Four sets of pieces of insert were dissected: Cells, Axons, Blank Near and Blank Far. Cells was the explants, Axons was the axonal carpet and Blank Near and Blank Far were pieces of insert which appeared to be free of tissue and uncontaminated. Blank Near pieces were taken from blank regions roughly as far from each explant as the pieces of insert containing the axonal carpets, in the direction perpendicular to the direction of fibre growth. Blank Far pieces were taken from the edges of the insert away from all explants. The Blank Near pieces were dissected first, followed by Axons, Cells and Blank Far (the reason for dissecting pieces in this order is explained in Section 3.4.1).

For each well containing three explants, all three Blank Near pieces of insert were dissected, followed by all three Axon pieces and so on, in order to minimise cross-contamination. A different sterile scalpel blade and different sterile pair of forceps were used to dissect and transfer each type of insert piece. Before dissection, inserts were inspected for contamination under the microscope by eye and only included if no cells or other contaminating matter could be seen (see Section 3.3.2 for further discussion).

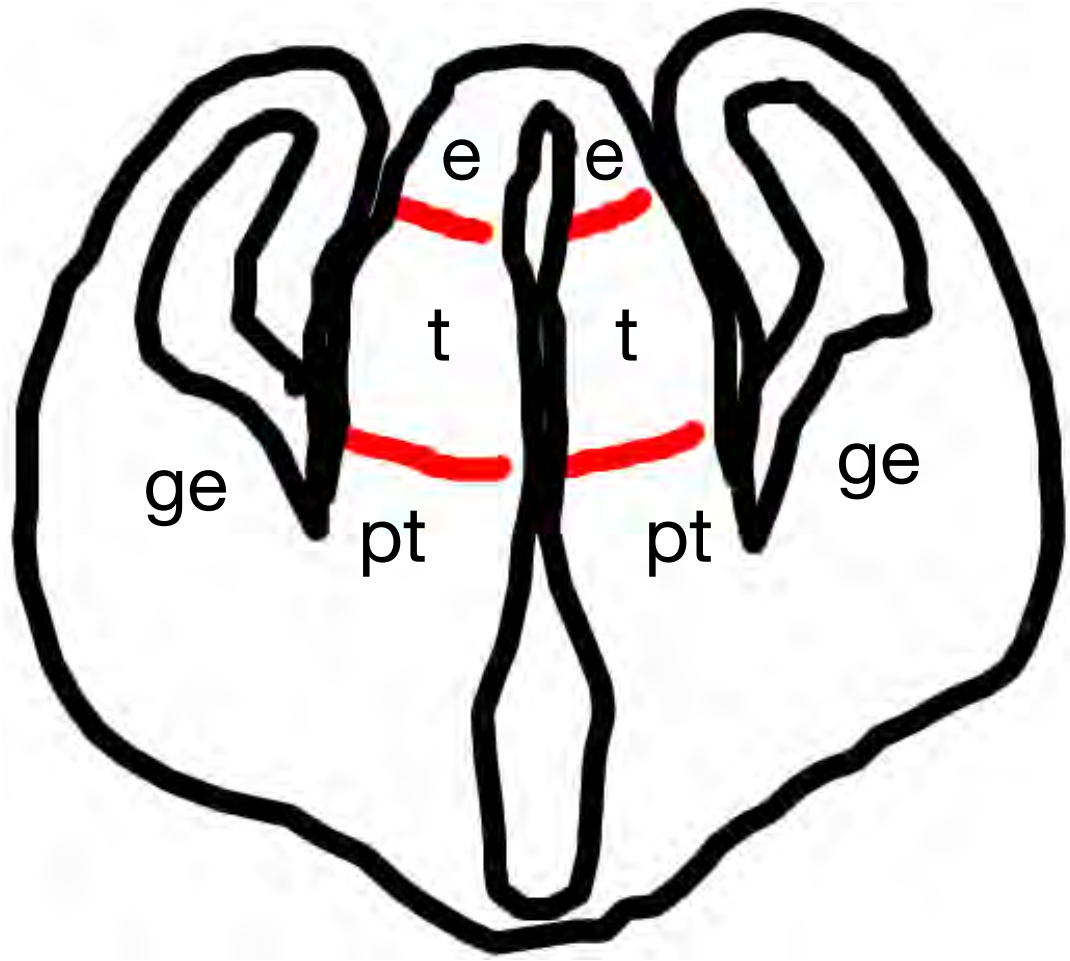

Figure 3.2: A diagram of a coronal section of an E14.5 mouse brain. Cuts were made along the red lines to isolate the thalamus. Key: t, thalamus, pt, prethalamus, e, epithalamus, ge, ganglionic eminences.

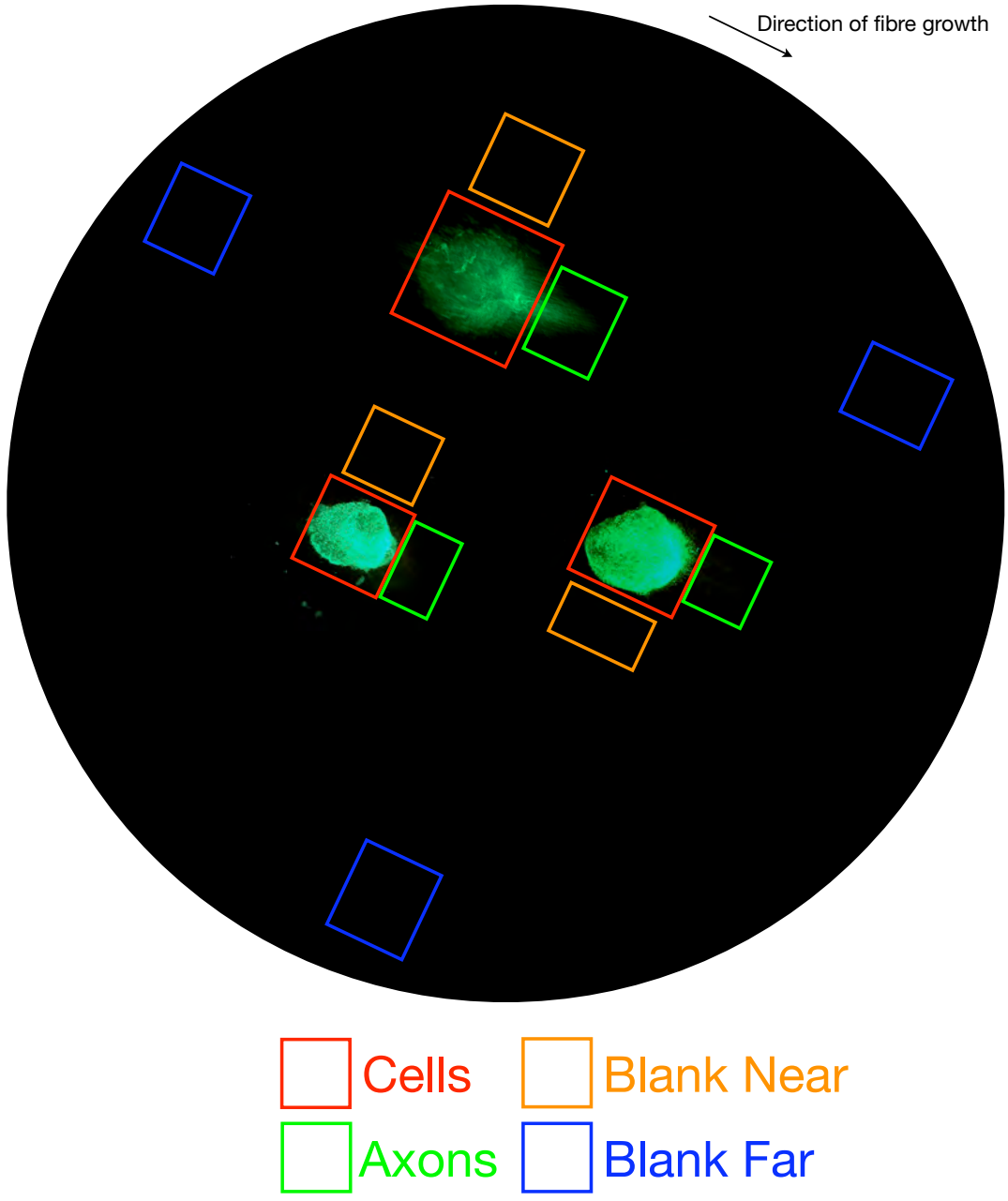

Figure 3.3: A schematic representation of the dissection of a single insert into four sets of pieces: Cells (shown in red), Axons (green), Blank Near (orange) and Blank Far (blue). Blank Near sections taken perpendicular to the direction of growth (see arrow). Images of explants taken from immunohistochemical stains for neurofilament.

3.2.1.3 RNA extraction and cDNA synthesis

The pieces of insert containing cellular and axonal tissue, as well as blank pieces of insert, were kept at 4°C in RNAlater and homogenised using a rotor-stator homogeniser. The RNA was extracted from the homogenised tissue 0-2 days after dissection using a QIAGEN RNeasy Micro Kit, following manufacturer's instructions and including DNAse treatment. 20μL cDNA was synthesised from this RNA for use in qRT-PCRs (see Section 2.5 for detailed methods). 1μL of RNA was used for each Cell condition, as this was sufficient to detect a signal from the Cells, whereas 4μL of RNA was used for each of the Axon, Blank Near and Blank Far conditions. Several control conditions were generated in addition to the four Cells, Axons, Blank Near and Blank Far conditions. Samples of each of the four cultured conditions containing no reverse transcriptase were run through the cDNA synthesis procedure, to control for the detection of any remaining DNA in these samples apart from any newly synthesised cDNA. These No Reverse Transcriptase (noRT) tubes were labelled CnoRT, AnoRT, BNnoRT and BFnoRT, for Cells (C), Axons (A), Blank Near (BN) and Blank Far (BF) respectively. In addition, a tube containing water alone, labelled No RNA, was processed using the cDNA synthesis kit, to detect any contaminating RNA.

3.2.2 Other methods

Explants for all figures in Section 3.3 were cultured and dissected according to the method in Sections 3.2.1.1 and 3.2.1.2, except for those in Figure 3.4, where fetal calf serum was added to or omitted from the culture medium as noted, and those in Figure 3.7 (see Section 3.2.2.2 below). Methods for standard RT-PCR and gel electrophoresis for Figures 3.8, immunohistochemistry for Figures 3.3, 3.4 and 3.6 and microscopy and image analysis for all figures are described in Chapter 2.

3.2.2.1 Use of GFP embryos

Figure 3.5 shows an explant cultured from embryos collected from a transgenic mouse which ubiquitously expresses green fluorescent protein (GFP) (strain $TP6.3[tauGFP^{+}]$, Pratt et al. (2000)). Embryos from this mouse were cultured in the same way as wild-type embryos. The embryos were confirmed to be expressing GFP before dissection by inspecting them under fluorescent light.

3.2.2.2 Optimisation of RNA extraction method

Explants for the RNA extraction tests shown in Figure 3.7 were dissected according to the method in Section 3.2.1.1 but were not cultured. Explant pieces were taken from a single explant which was cut in half and then in half again. Two quarters of equivalent size (established by eye under the microscope) were selected and used for RNA extraction. RNAlater samples were homogenised just before RNA extraction. QIAGEN Micro and Mini Kits were used according to manufacturer's instructions. qRT-PCRs were run according to the method in Section 2.5.3 using primers for β-actin (see Figure 4.5). A standard curve dilution series for units 1000, 500, 250 and 125 was used for quantification, prepared from cDNA synthesised from RNA from thalamic explants prepared as above.

3.3 Results

In the course of designing the method described in the previous section, several experiments were carried out to optimise the isolation of axonal RNA. The results of these experiments are presented here and will be discussed in the following section.

3.3.1 Effect of serum

To maximise the amount of axonal growth, 25% fetal calf serum was added to basal culture medium at the beginning of the axonal culture. Figure 3.4 shows that, whereas explants in serum-free medium produced short axons which require high magnification to be seen clearly (see Figure 3.4e), explants in medium with serum added grew many long axons which in some cases were as long as the explant itself (see Figure 3.4a). The figure shows three serum-fed explants and three serum-free explants which were selected from four serum-free explants and six serum-fed explants; the same difference in growth was seen across all serum-free and serum-fed explants. As a result of these tests, serum was used in all subsequent cultures.

In the pictures in Figure 3.4, cells can be seen to be spread out around the explant and on the axons. This is due to cells being dislodged during the immunohistochemistry procedure and not because the cells were present at time of dissection. For evidence of this, see Section 3.3.3.

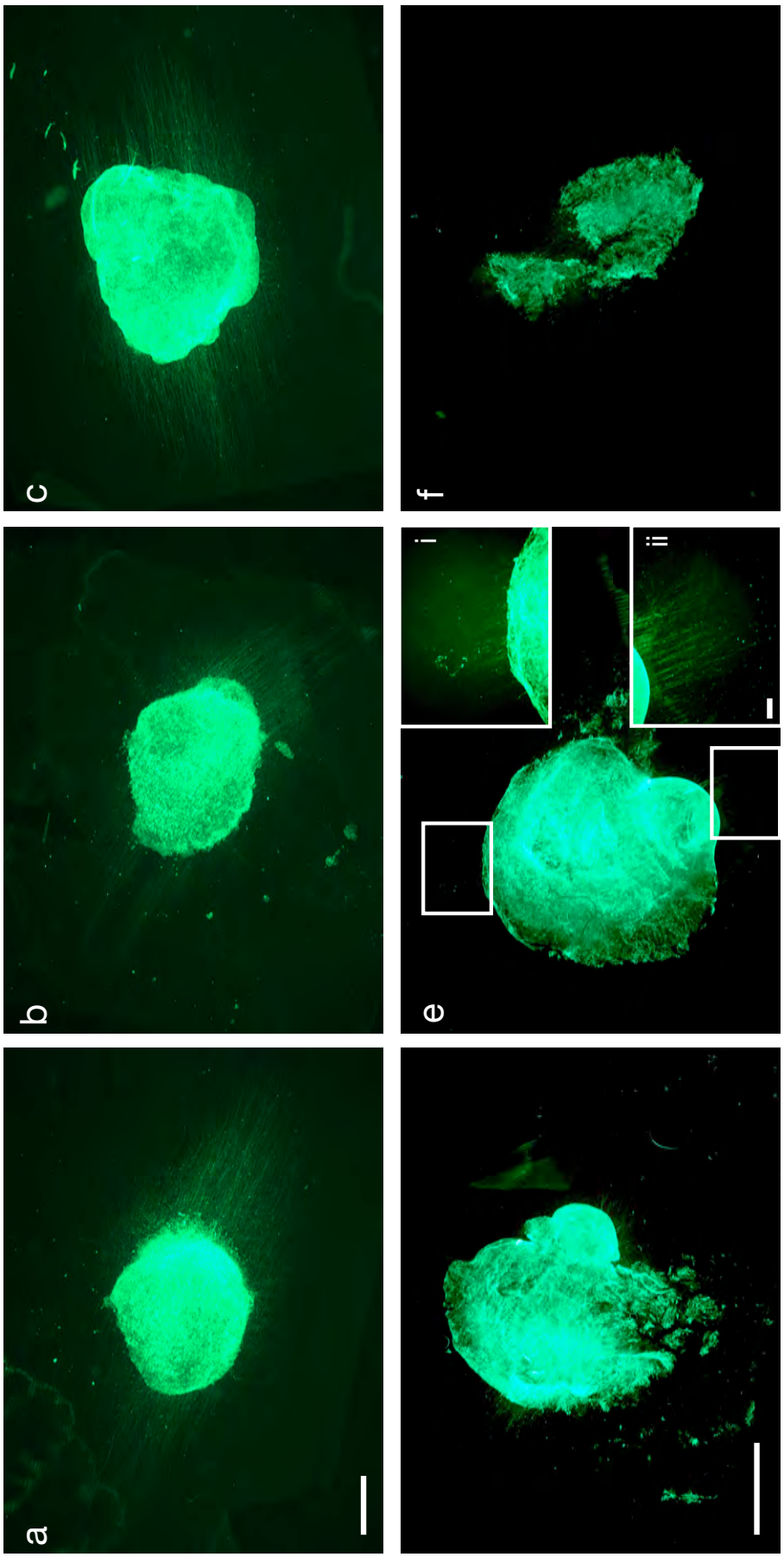

Figure 3.4: Thalamic explants cultured for axon growth, stained with neurofilament. (a-c) Explants cultured with 25% fetal calf serum. (d-f) Explants cultured in basal medium only. (e) i. Magnification of upper box. ii. Magnification of lower box. Scale bars in a) for a-c) and d) for d-f), 1mm; scale bar in e) i. for e) i. and ii., 100μm).

3.3.2 Test using GFP mouse embryos

Not all explants would grow axons and some axonal carpets would become contaminated with cells. Usable pieces of insert were identified by eye under the microscope using white light. As it was thought possible that cells would not be visible under this light, embryos from a transgenic GFP mouse, which express green fluorescent protein (GFP) throughout, were cultured and examined under fluorescent light. Figure 3.5 shows one of these GFP explants under white light and fluorescent light. As cells are clearly visible in a number of different places on this explant, it would not have been included for use in an RNA sample. It can be seen that there is no substantial difference in clarity between the two pictures; in fact, it is perhaps easier to see cells under white light than under GFP. Therefore all samples were collected from wild-type embryos dissected under white light.

3.3.3 Test for cellular contamination

To increase confidence that the RNA extracted from axonal samples was indeed axonal rather than cellular, some dissected axonal inserts which were believed to be free of cells during dissection were stained for the axonal marker neurofilament by immunohistochemistry and by the fluorescent dye and cell marker propidium iodide. Figure 3.6 shows that, if whole explants with intact axons are stained, cells are found to be present around the explant and on the axons. However, if the axons are dissected away from the explants before staining commences, no cells can be detected on the axonal carpets. Therefore, although the axons which were actually used for the qRT-PCR experiments in Chapter 4 could not be tested in this way because the tissue was homogenised in order to extract the RNA, it is believed that no cells are present in these samples based on these tests.

3.3.4 Storage of RNA

Once the explants have been dissected, there are a number of different ways to store and extract RNA from each set of explants. Figure 3.7 shows that storing explants in RNAlater and using a QIAGEN RNAeasy Micro Kit to extract the RNA produced the highest RNA yield.

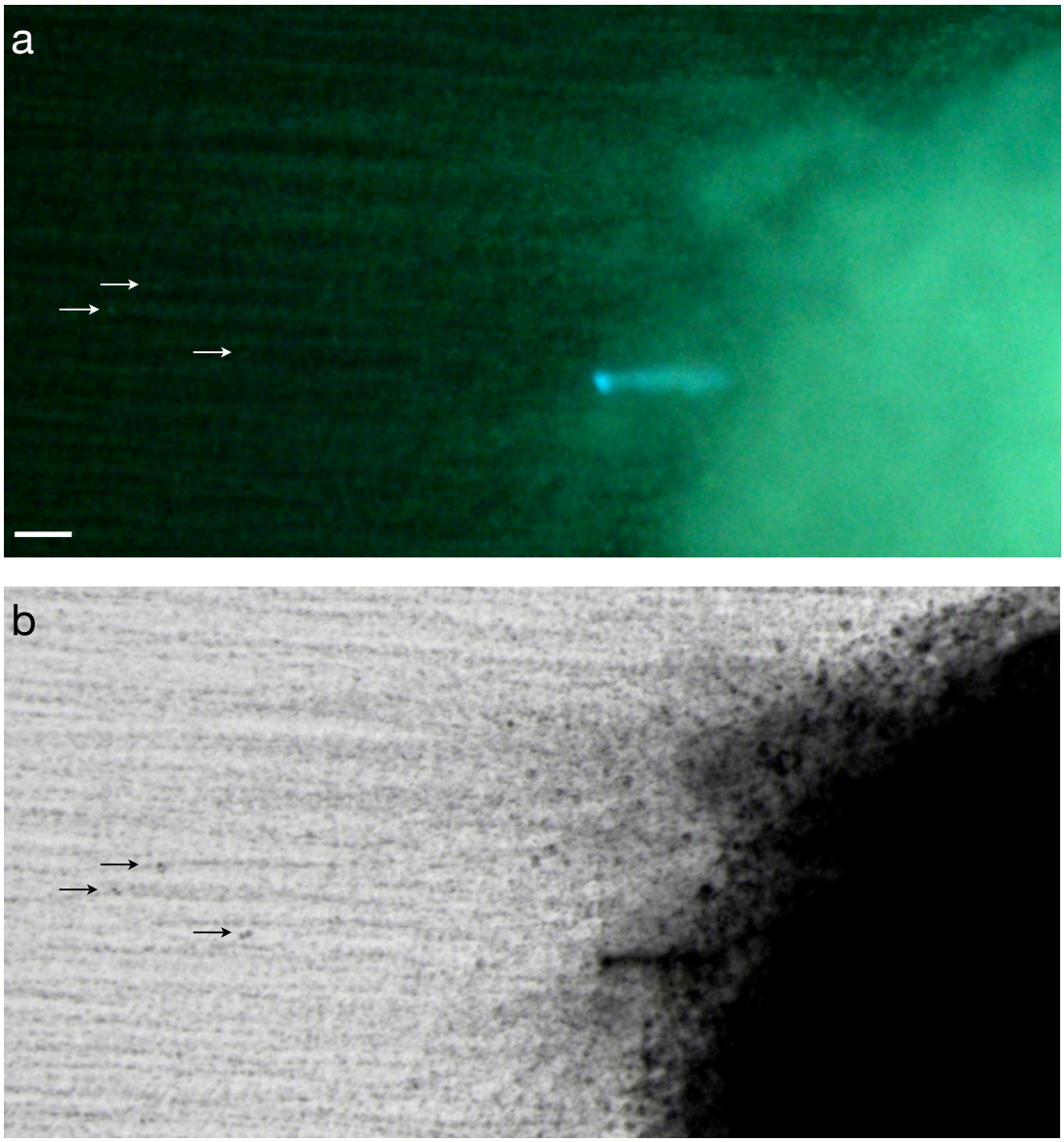

Figure 3.5: Cultured explant from a GFP mouse photographed using (a) fluorescence and (b) white light. Arrows point to cells on the axonal carpet, showing that cells are easier to identify under white light than under fluorescence. Scale bar, 20μm.

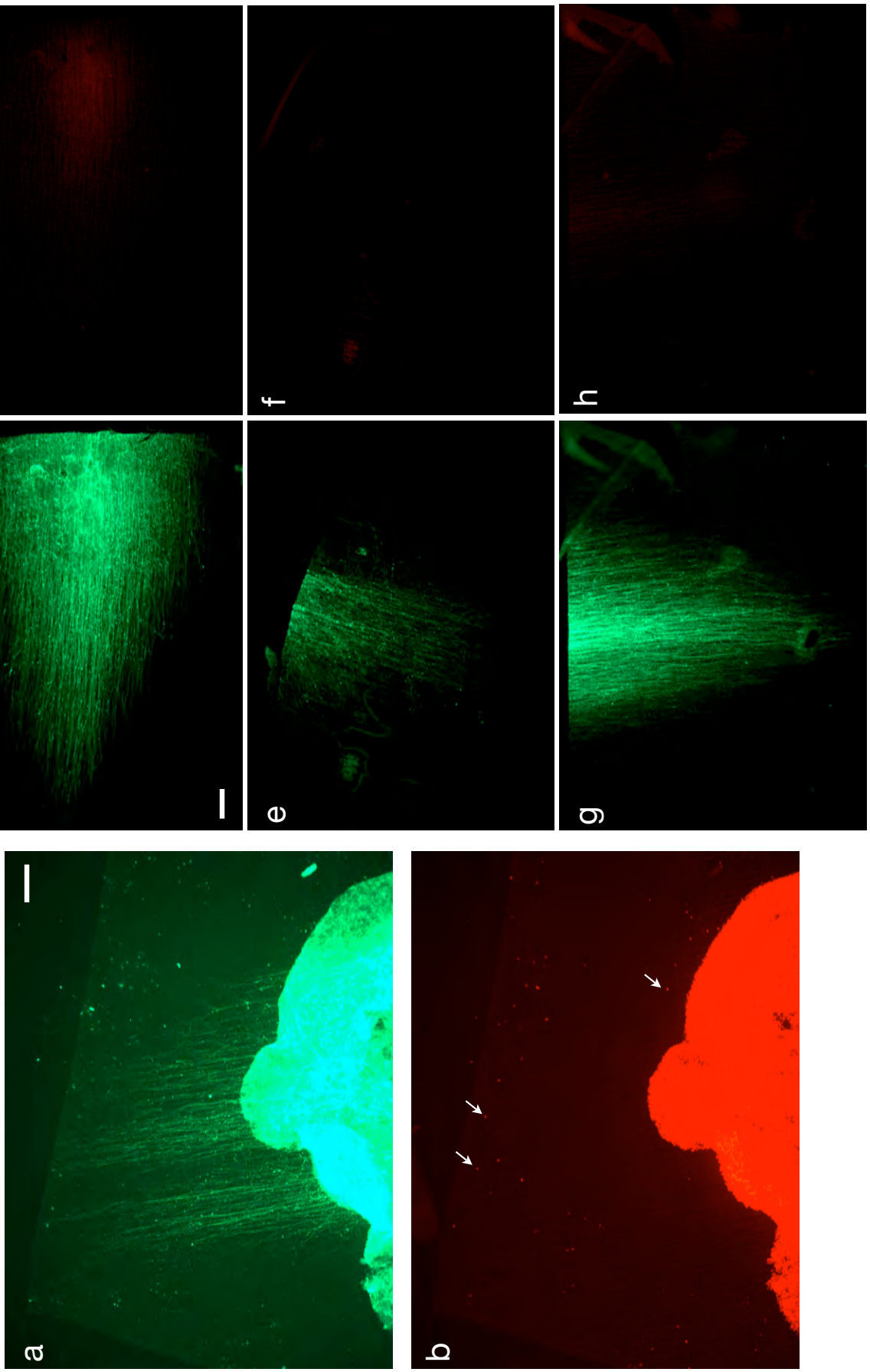

Figure 3.6: Axons are not contaminated with cells when dissected away from explants. (a,b) Stains for (a) neurofilament (axonal marker) and (b) propidium iodide (cellular marker) show that cells are present on axons when they are not dissected from the explant (arrows point to examples of stained cells). (c-h) When axons are dissected away from explants before staining, cells are not found on axons. (c,e,g) Neurofilament. (d,f,h) Propidium iodide. Scale bars in a) for a-b) and c) for c-g), 200μm.

RNA extraction (arbitrary units)	Micro Kit RNAlater 4°C	Micro Kit Lysis buffer -20°C	Mini Kit RNAlater 4°C	**Kit** **Storage buffer** **Temperature**
10 explants	3,088.593	1,562.411	1,025.280	
Explant piece	103.015	18.062	N/A	
Blank	0.001	0.007	N/A	

Figure 3.7: Comparison of RNAlater and lysis buffer storage and QIAGEN RNeasy Micro and Mini kits. The kit, storage buffer and temperature for each test are listed. Yield of RNA shown in units based on qRT-PCR using arbitrary 1000-unit scale. Tests not performed are labelled N/A.

3.3.5 Number of explants

The limit of detection of RNA was investigated by reducing the number of explants in each sample. Figure 3.8 shows the result of attempts to detect axonal RNA with small numbers of explants. 18S ribosomal RNA and β-actin and β-catenin mRNA were tested as representative RNAs of interest; 18S because ribosomes are known to be present in axons and rRNA is expected to be more abundant than mRNAs, and the mRNAs because β-actin mRNA has been found in several other axonal systems and β-catenin was identified in Thomas Pratt's library of thalamic mRNAs (see Sections 1.5.5 and 1.6.2 for discussion). While it was possible to detect 18S ribosomal RNA in axonal samples from 1, 7 or 12 explants, it was not possible to detect β-actin or β-catenin from 12 explants, indicating that more than 12 explants are required to ensure the possibility of detecting small quantities of mRNAs in axons, including at least two of the mRNAs of interest identified in Thomas Pratt's library of thalamic axonal mRNAs (see Section 1.6.1). However, it was possible to detect 18S, β-actin and β-catenin in a 16 explant sample. Therefore 16 explants or more should be sufficient to detect at least these three RNAs in axons.

Because of this result, each RNA sample contained at least 15 explants (see Section 4.4.2 for details of the collected usable samples).

3.4 Discussion

In this section, the decisions made during the design of the above method are discussed and justified. The criteria for considering an RNA to be present in axons and the choices made in the design of the culture system and RNA extraction process are explained.

3.4.1 Is the RNA axonal?

If an RNA is found to be present in a sample of axonal tissue, does this mean the RNA was present in the axons? In fact, there are a number of sources of contamination which must be controlled for before it is valid to claim that the RNA is indeed axonal.

Contamination may come from one of three sources. Firstly, as the axons are grown from thalamic explants, cells from the explants may be found to have floated onto or migrated with the axons (as axon growth and neuronal migration are closely linked; see, for example, Guan et al. (2007)), or dying cells may have burst and released

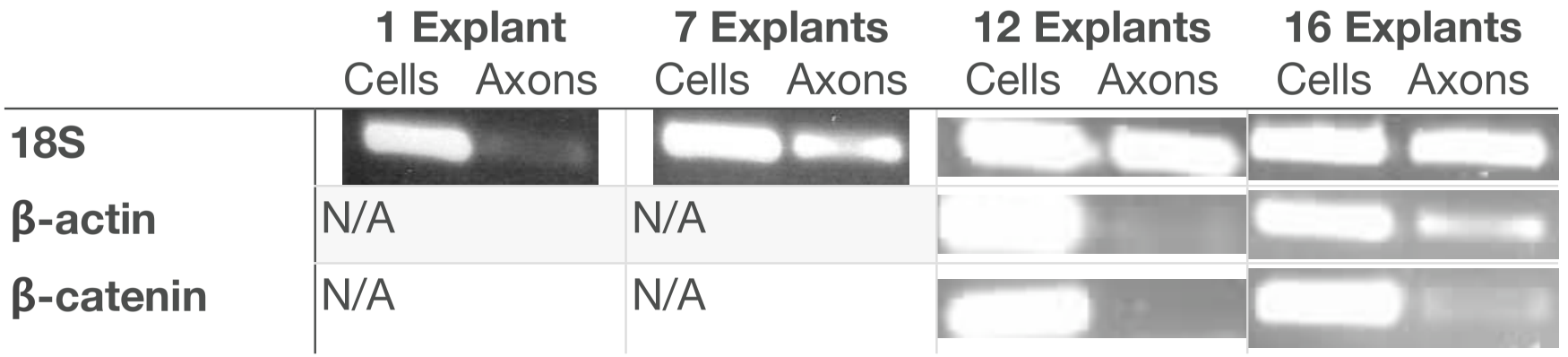

Figure 3.8: Signal acquired for 18S, β-actin and β-catenin from 1, 7 and 12 cellular or axonal samples after standard RT-PCR and 16 explant samples after qRT-PCR. N/A indicates test not performed.

mRNA into the culture medium. Secondly, despite being prepared in sterile conditions, contaminants may be introduced into the culture system during the culturing or incubation of the explants. Thirdly, contaminants might be introduced during the extraction and quantification of RNA.

Contamination from floating cells or other sources in the culture system is controlled for with the two blank conditions, Blank Near and Blank Far. The Blank Near pieces, from next to the explant, are dissected first, followed by the axonal tissue, as the dissection of the axonal tissue, which involves severing the axonal tissue from the explant, might cause many cells to float onto what was a blank piece of insert. However, performing the dissection in this order might cause cells to float onto the axonal tissue. To control for this possibility, the Blank Far pieces are dissected at a distance from the explant after the explants are removed. This piece of insert is considered to control for floating cells and any other contaminants which may have entered the culture system.

The explants, labelled Cells, are quantified for two reasons. Firstly, this sample can be used to demonstrate that the primers used for qRT-PCR are valid. This is important in the case where an RNA is below the level of detection in axons. If a negative result is found in the axonal and blank conditions, it may be that the RNA is not present in axons or that the qRT-PCR has failed. By also testing a sample of cells and finding a positive signal in this sample, the latter possibility can be ruled out and the RNA can be considered to be absent from the axons. Secondly, the cells can be used as a standard of comparison for the axonal RNA and allow different RNAs to be compared to each other. This will be discussed further in Section 4.5.3.

To check for the absence of migrating and floating cells on axonal carpets, transmitted light and fluorescence microscopy was used to look for cells after treatment with the cell nucleus stain propidium iodide. Figures 3.5 and 3.6 show that firstly, it was possible to see cellular matter on the axonal carpet and omit cultures containing contaminated axons and secondly, no cells could be detected on dissected axonal carpets.

Finally, contamination during the RNA extraction and cDNA synthesis procedures is controlled for with the No RNA and No RT controls. RNA contaminating the water or plasticware or introduced during the cDNA synthesis procedure is detected with the No RNA control, as any contaminating RNA should be reverse transcribed and detected by subsequent qRT-PCR. DNA contaminating the samples or introduced during the RNA extraction and cDNA synthesis procedures is controlled for by the

No RT controls, which contain RNA from the collected samples but no reverse transcriptase. Any signal from these controls detected by qRT-PCR must therefore represent a signal from contaminating DNA.

Therefore, comparison between the Cells and Axons samples, Blank Near and Blank Far samples, and No RNA and No RT controls, allow conclusions to be drawn as to whether an RNA can be considered axonal.

3.4.2 Culture and extraction of RNA samples

The culture system for these experiments was optimised to harvest the maximum amount of uncontaminated axonal tissue. An *in vivo* system is not suitable for this purpose because although axons are plentiful, it is not possible to isolate them from other brain tissue. Similarly, in a system where explants are dissociated or dissected and cultured on glass (similar to those described in Chapter 5), many axons may grow but it will not be possible to separate them from cellular matter which will adhere to all parts of the coverslip.

The basic explant culture system described here was used by Thomas Pratt to generate axonal matter for the library of mRNAs described in Section 1.6.1 and is similar to the method used by Olink-Coux and Hollenbeck (1996).

Olink-Coux and Hollenbeck (1996) used 20-50 chick sympathetic ganglion explants in their experiments. However, for this particular application of the present system using thalamic explants, it proved difficult to produce more than twenty-four good quality explants for one culture. Four to six explants could be acquired from one E14.5 brain in roughly forty-five minutes. This means that twenty-four explants could be acquired from four to six brains in three to four and a half hours. It was found that brains dissected after this time tended to become more brittle and more likely to shed cells than at earlier times, which increased the chance of cellular contamination when the explants were placed on the insert.

Cross-contamination of cells, axons and blanks was minimised by dissecting all of the pieces of insert for each condition in each well at the same time, rather than dissecting each explant sequentially. Cross-contamination was also minimised by the use of four separate sterile scalpel blades to dissect the insert and four different sterile pairs of forceps to pick up the inserts once they have been dissected, for each of the four conditions.

The QIAGEN RNeasy Micro Kit, which is optimised for small quantities of RNA,

was used to extract the RNA from these tissue samples (see Figure 3.7). The use of the Micro Kit means that only 14μL of RNA in solution can be obtained. Diluting this solution further made the axonal signal impossible to detect. This meant that only one cDNA synthesis was possible from each RNA extraction, producing a maximum of 20μL of cDNA. In practise, it proved that roughly 15 qRT-PCRs could be performed on one set of cDNA samples.

Figure 3.4 shows the substantial increase in axonal growth when fetal calf serum was added to basal culture medium. Because of this increase in growth, which enables a much larger amount of axonal tissue to be dissected, serum has been used in all cultures. However, this may have an effect on the expression of RNAs in axons as it is not known which molecules are present in the serum and the content of the serum in different batches may vary (Even et al., 2006; Lutz and Rössner, 2007). This was not considered to be a serious problem given the advantage of using serum but it may be something that should be investigated in the future.

In conclusion, the method described in this chapter is proposed as a general system for harvesting axonal RNA. The next chapter describes an implementation of this method for quantifying RNA in thalamic axons.

Chapter 4

Characterising RNA in Developing Thalamic Axons Using qRT-PCR

4.1 Introduction

This chapter provides evidence for the presence of many RNAs and the absence of several others in thalamic axons. The evidence is based on quantitative reverse transcription polymerase chain reactions (qRT-PCRs) for the RNAs of interest on axonal samples collected according to the method described in Chapter 3. qRT-PCRs will be introduced and the relevant technical terms defined. The methods used to select RNAs for investigation, to run and analyse the qRT-PCRs, and to generate a dilution series used to create a standard curve are explained. The results for two sets of qRT-PCRs testing for the presence of RNAs in thalamic axons are given. The quality of these results and the value of the method are then discussed, explaining the type and validity of the conclusions that can be drawn from this application of the method.

4.2 qRT-PCR methodology

In this section the basic qRT-PCR methodology will be explained, and technical terms which will be used in the rest of the chapter are defined.

4.2.1 Polymerase chain reaction

Polymerase chain reaction (PCR) (Saiki et al., 1988) is a method for amplifying DNA by exploiting the fact that DNA is composed of two complementary strands. A double

stranded DNA molecule can be separated into two strands. Enzymes called DNA polymerases (Hübscher et al., 2002) can then synthesise the complements of each of these single strands, producing two identical copies of the original DNA molecule. If the reaction is repeated, these two copies will both be duplicated, producing four copies of the original molecule. This exponential growth in DNA copy number means that millions of copies of a very small number of DNA molecules can be produced with just tens of these reactions (or cycles).

DNA polymerases can not bind to a single strand of DNA and begin to synthesise its complement, but must extend a region of the DNA which is already double stranded. Therefore, for PCR to work, small single strands of DNA, roughly 20-24 base pairs in length, must be bound to a single DNA strand of interest, to form a double stranded region to which DNA polymerase can bind and extend. These starter strands are called primers, and two different primers are required for any PCR, a forward and a reverse primer. These primers complement the start and end of the DNA sequence of interest, with the forward primer binding to the start of the DNA sequence, and the reverse primer binding to the end of the complement of the DNA sequence. This means when double stranded DNA is separated into two strands, the forward primer will bind to and enable the extension of one strand of the DNA, and the reverse primer will bind to and enable the extension of the other strand.

PCR therefore requires many copies of both forward and reverse primers and a supply of nucleotides which can be incorporated into new DNA strands. A PCR of many cycles can be split into four phases, initial, exponential, linear and plateau (see Figure 4.1). In the initial phase, there are very few DNA molecules and so the amplification is stochastic. In the exponential phase, there are less DNA molecules than primer pairs, and so the number of DNA molecules can be doubled with every cycle, causing an exponential growth in total DNA copy number. In the linear phase, the number of DNA molecules grows to exceed the number of primer pairs, which means that the maximum number of new DNA molecules that can be synthesised in one cycle is limited by the number of primer pairs, and so there can only be linear growth in DNA copy number. Finally, when all of the nucleotides have been incorporated into DNA copies, no further DNA synthesis can take place, causing the reaction to plateau.

The requirement for primers for the initiation of DNA synthesis means that it is possible to amplify a particular sequence of interest by synthesising primers which match that sequence. The sequence which is amplified by a PCR using a particular pair of primers is known as an amplicon.

To amplify RNA using PCR, complementary DNA (cDNA) must be synthesised from the RNA, using enzymes called reverse transcriptase to reverse transcribe the RNA. This cDNA can then be amplified using DNA polymerases in a PCR. The combination of cDNA synthesis and PCR is known as reverse transcription PCR or RT-PCR. Reverse transcriptase reactions must also be primed; it is common to use either random hexamers, which as a set bind to many different parts of the RNA molecules, or oligo dT primers, which bind only to the 3'UTR of mRNAs which contain a poly-A tail.

The final quantity of DNA amplified by PCR will not accurately reflect the initial quantity of DNA prior to PCR amplification, because the reaction is limited by the amount of nucleotides and primers. This means the number of cycles in each of the initial, exponential, linear and plateau phases is not known and the amount of amplification during each phase cannot be estimated. Therefore, quantification of initial DNA cannot be done by analysing the end products of a PCR. However, it is possible to quantify initial DNA by examining the reaction as it progresses, which is the approach of quantitative RT-PCR, or qRT-PCR, which will now be explained.

4.2.2 Quantitative Reverse Transcription PCR

qRT-PCR (Bustin, 2006) is a method for quantifying the amount of RNA in a sample prior to PCR by reverse transcribing the RNA into DNA and quantifying the amount of amplified DNA present after each cycle of PCR. Molecules which fluoresce when bound to double stranded DNA (SYBR Green for the qRT-PCR experiments presented in this thesis (Zipper et al., 2004)) are introduced into the PCR solution. After each cycle of the PCR, the amount of fluorescence is quantified. This means the reaction curve of the PCR through the initial, exponential, linear and plateau phases can be plotted from the readings of fluorescent emissions for all cycles (see Figure 4.1).

Using a plot like that shown in Figure 4.1, the exponential phase of each reaction can be identified. The cycles at which this phase occurs during the reaction are determined by the amount of initial DNA present. For example, consider a sample A which contains sixteen times as much initial DNA as another sample B. Sample A will reach the exponential phase of the reaction earlier than Sample B because initially the primers and DNA polymerase will be sixteen times more likely to amplify DNA in Sample A than in Sample B. In turn, this means that Sample A will contain a particular number of DNA molecules, and produce the level of fluorescence generated

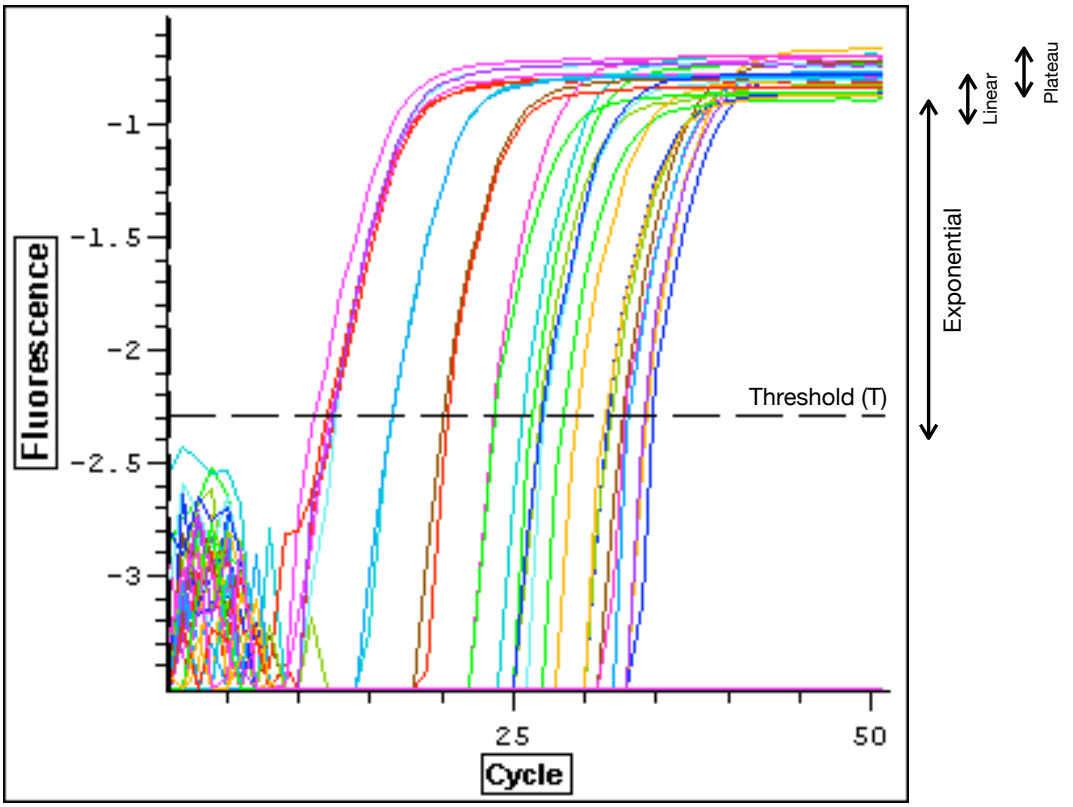

Figure 4.1: An example of the reaction curve for one qRT-PCR from the experiments presented in this chapter, for α-tubulin. The x-axis shows the cycle number of the qRT-PCR (from a 50 cycle qRT-PCR). The y-axis shows fluorescence detected, measured in logarithmic units. The graph shows, in the bottom left, background fluorescence noise levels before DNA is amplified, followed by the exponential phase which, because the graph is on a log scale, appears linear. The linear phase is shown where the lines begin to curve and the plateau phase begins when the lines are horizontal. The phase labels on the right show some overlap because there are multiple samples in the figure which progress to different phases at different points. The dashed line shows the threshold, T, chosen for this reaction, which is at a point in the early exponential phase. During the exponential phase, it can be seen that all samples in this sample were amplified with roughly the same efficiency, as the lines remain parallel until the linear phase begins (see Section 4.2.3.2 for discussion.)

by that number of DNA molecules bound to SYBR Green, earlier than will Sample B. Therefore, by comparing the cycle at which Sample A reaches a chosen threshold level of fluorescence with the cycle at which Sample B reaches that same level, it is possible to measure the relative quantities of DNA in these samples. In this case, provided the amount of DNA is reliably doubling in the exponential phase, it would be expected that Sample B would cross the threshold 4 cycles later than Sample A, because a sixteen-fold increase is equivalent to 4 doublings.

The threshold level of fluorescence chosen for comparison, hereafter T, can be anywhere in the exponential phase of the reaction, although it is preferable to choose a point early in this phase because there will be small variations in the amount of DNA amplified at each cycle and this variation will also be exponentially amplified, causing error to be introduced into the quantifications, with more error introduced the more cycles are carried out. In theory, these errors could be accounted for by measuring the slope of the line between each pair of cycle points and taking variations of amplification into account when estimating unit values, but in practise it is simpler and more accurate to choose a threshold early in the exponential phase and avoid having to correct for this variation. Once a threshold is chosen, the cycle at which a sample reaches this threshold can be determined and labelled C(T) for "Cycle at threshold T". These C(T) values are calculated for all samples in the reaction and are used to quantify the amounts of DNA in each sample relative to the other samples.

Quantification of a DNA sample using qRT-PCR is always relative to some other DNA sample which was amplified in the same reaction. Two types of quantification are commonly used; comparative quantification and standard curve quantification. In comparative quantification, C(T) values for two samples are converted into a fold difference of expression; so, for example, for Samples A and B above, a difference of 4 between the C(T) values for these cycles could be reported as a sixteen-fold difference in starting amount. In standard curve quantification, a dilution series of DNA samples is prepared where the fold differences between the samples in the series is known, and arbitrary units can be assigned to the samples in the series. For example, a large quantity of starting DNA could be labelled 1000 units and diluted two-fold three times, producing 500 unit, 250 unit and 125 unit samples.

When the samples in the dilution series are amplified, it should be possible to draw an exponential curve through the C(T) values for these samples, because the C(T) values should reflect the two-fold dilutions of the samples. This curve is known as the standard curve, and can be used to infer quantifications in arbitrary units for other

samples amplified in the same reaction by inferring the unit value for the point in the curve representing the C(T) value of the sample of interest. Standard curves are usually represented on logarithmic graphs as straight regression lines (see Figure 4.2).

A different standard curve must be generated for each RNA of interest, although the same pool of source cDNAs can be used to generate the standard curve. Different standard curves are necessary because amplifications of different amplicons will be affected by the length and structure of the amplicons and so the amplifications will usually not be equally efficient; in fact, even if the amplifications were equally efficient, it could not be guaranteed that original copy number was related to C(T) value in the same way for both amplicons. For example, variations in length may mean different copy numbers produce the same amount of fluorescence, and variations in structure may affect the ability of the fluorescent molecule to bind to the cDNAs. While in theory the C(T) values could be adjusted to take account of amplicon length and structure, as it is possible to adjust the C(T) values to account for efficiency, in practise the effects of these factors are not well understood and so have not been modelled accurately. Therefore direct comparison of C(T) values has not been attempted here.

This in turn means that, although standard curve unit values for different samples of one RNA can be compared, unit values for different RNAs are not compared directly because the units for one RNA do not relate to the units for another RNA. 100,000 units of β-actin are not the same as 100,000 units of 18S, even if the C(T) values are exactly the same for both samples and the amplicons are amplified with exactly the same efficiencies (or, indeed, if the unit values were adjusted to account for variation in efficiency; see Section 4.2.3.2). The two identical unit values may refer to different copy numbers of the two cDNAs because the two cDNA molecules may each produce a different amount of fluorescence. Therefore, if comparison of RNAs is required, it is necessary to cancel out the standard curve units by comparing ratios of expression of each RNA in different tissues.

If different qRT-PCRs are to be compared, whether they are for the same RNAs or for different RNAs, it is imperative that cDNA samples from the same tissue source are used to generate standard curves for all qRT-PCRs, because samples from different sources will have different complements of cDNA and so will produce different scales of measurement.

A comparison of expression in different tissue samples is only meaningful if the amount of biological material is controlled for. For example, measurements of the differential expression of genes in brain and heart tissue are only meaningful if the

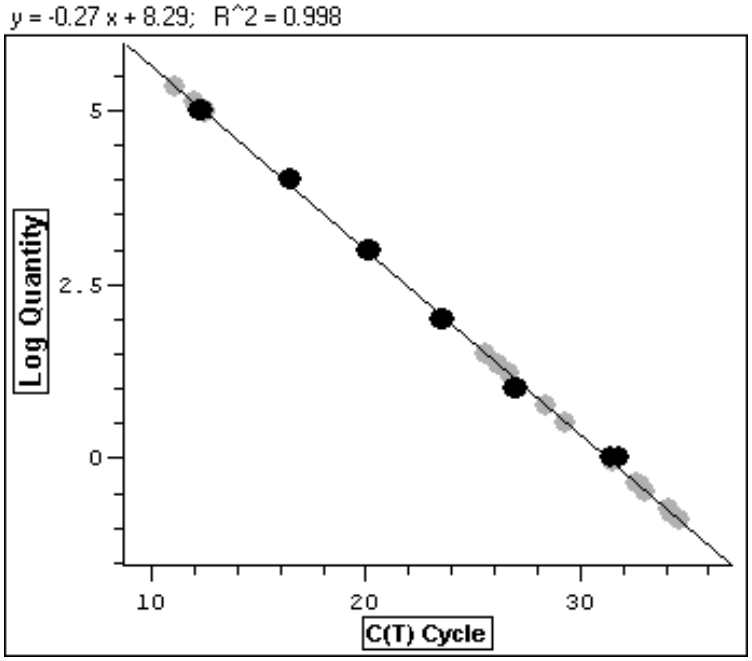

Figure 4.2: A standard curve generated from dilution series samples amplified in the qRT-PCR shown in Figure 4.1 at the threshold shown in that figure. Black dots represent dilution series samples. C(T) Cycle values for each black dot are measured during the reaction. Each sample in the dilution series is labelled with a quantity of arbitrary units. Base 10 logarithms are used, so a Log Quantity of 5 represents a unit value of 100,000. Two samples are amplified for each quantity to ensure the amplification is reliable. A regression line called the standard curve is calculated for all dilution series samples, the equation for which is shown at the top of the graph. The grey dots represent the other samples of interest in this reaction, whose C(T) values have been calculated and are then used to infer unit values based on the standard curve. The coefficient of determination r^2 is also provided for the regression line.

same amount of brain and heart tissue is being compared, or if different amounts of tissue are being controlled for. To do this, a different gene to those being investigated is selected as an internal standard and all expression levels of genes of interest are normalised to the expression of this standard gene. For this comparison to be meaningful, expression of this internal standard gene per unit of material should not change from one sample to the next (Bas et al., 2004; Bustin et al., 2005).

Because the amplification of DNA by qRT-PCR varies from reaction to reaction, it is desirable in any experiment to include not only biological replicates, where multiple biological samples are tested to measure the variation in the biological data, but also technical replicates, where a number of DNA samples from each biological replicate are amplified in several different qRT-PCRs, to provide a measure of the variation introduced by qRT-PCR amplification.

4.2.3 Quality indicators of a qRT-PCR

The reliability of any quantifications inferred using qRT-PCR should be assessed by measuring a number of quality indicators. These include the coefficient of determination, r^2, which is a measure of the fit of the standard curve to the C(T) values of the standard dilution series, the efficiency of the qRT-PCR, and the melting curve, which is a measure which can be used to determine the number of different products which have been amplified in the reaction. These indicators will now be introduced.

4.2.3.1 Coefficient of determination

As discussed in Section 4.2.2 and shown in Figure 4.2, the unit values which are recorded for samples of interest are inferred from the standard curve, a regression line which is fit to a standard dilution series. The accuracy of the quantification is dependent on the correlation of the regression line and the actual C(T) values for the standard curve dilution series. If the dilution series C(T) values do not fit the regression line well, then the quantifications inferred from this regression line will not be accurate. This correlation can be measured using the coefficient of determination, or r^2, which is a measure of the proportion of the variation in C(T) value which is accounted for by the regression line.

r^2 should be as close to 1 as possible, as this indicates that C(T) varies with input as predicted by theoretically ideal PCR kinetics. r^2 values below 1 indicate that the C(T) values of the standard curve dilution series do not perfectly match the recorded raw

fluorescent intensities for these samples, which indicates that there is some variability in the amplification of samples of different sizes which will reduce the accuracy of the inferred unit values of the experimental samples. Typically, a threshold is set for r^2 and the quantifications from a qRT-PCR with an r^2 value below this threshold are considered to be unreliable. In this chapter, r^2 values of 0.95 and above will be accepted, following Pfaffl (2001).

4.2.3.2 Efficiency of qRT-PCR

During an ideal cycle of a qRT-PCR, the amount of product is expected to double, as every strand of cDNA should be duplicated. A qRT-PCR where this doubling occurred at every cycle is considered to be 100% efficient. However, there are a number of confounding factors which may cause varying efficiencies, such as quality and purity of RNA (Fleige et al. (2006); this is of most concern when amplifying directly from total RNA rather than cDNA, but can also be a problem with cDNA amplification where many partial copies of the amplicon may have been synthesised from degraded RNA and these partial copies may compete with full length ones during amplification) and factors involving primers such as amplicon length, secondary structure of cDNA and the formation of primer-dimers (Peters et al. (2004); primer-dimers may fluoresce during amplification and so increase the signal for the cycle, appearing to cause amplification with greater than 100% efficiency, or may prevent primers from amplifying amplicons and so prevent 100% amplification, particularly in later cycles where the number of amplicons is large).

Variation in efficiency is undesirable because of the exponential nature of PCR amplification; small changes in efficiency can lead to large changes in the amount of final product, because differences in amplification at early cycles are exponentially magnified (Wong and Medrano, 2005). This is why the threshold T is chosen to be as early in the exponential phase as possible, to minimise the magnification of such variation and avoid having to correct for it (see Section 4.2.2).

The efficiency of a qRT-PCR is usually estimated from the slope of the regression line of the reaction at the chosen threshold T (see Section 2.5.3). The efficiency value is sometimes important for accurate quantification. There are two ways in which variation in efficiency can affect quantification. Different amplicons may be amplified with different efficiencies, or different amplifications of the same amplicon may have varying efficiency.

A number of early and regularly used methods for quantification of RT-PCR

assume that reactions occur with 100% efficiency or that the efficiency of different reactions is identical, such as the comparative Ct method (Schmittgen and Livak, 2008; Yuan et al., 2008). However, there are other methods available which correct for or cancel out varying efficiencies from amplifications of the same amplicon (see, for example, Pfaffl (2001)). These methods do not require efficiencies to be equal across reactions.

For standard curve comparisons, it is possible to compare RNAs which have been amplified with different efficiencies by transforming the curve units into ratios (see Section 4.3.4). It would also be possible to adjust standard curve C(T) values for a particular amplicon to be consistent with one another if they had different efficiencies by adjusting the C(T) values using the slopes for each sample. However, it is desirable that the standard curve samples are amplified with the same efficiencies as this increases confidence that the amplification is repeatable and reliable and avoids the need for adjustment of the C(T) values. The fact that different amplifications of the same amplicon have the same efficiency can be seen by observing high r^2 values (because if different samples from the standard curve dilution series were amplified at different efficiencies, it would not be possible to closely fit a regression line to the C(T) values for the dilution series) and by observing that the exponential phases for all samples follow the same trajectory (as can be seen in the example qRT-PCR curve in Figure 4.1).

4.2.3.3 Melting curves

A qRT-PCR reading (using the SYBR Green method presented here) is a measure of the total amount of double-stranded DNA in a sample, regardless of how many different PCR products are present. As the intention is to measure only a single amplicon which the primers used have been designed to amplify, it is essential that no other types of DNA are present in the sample. This includes primer-dimers, which can be created when left and right primers are bound together, although primers are usually designed to minimise this effect (see Section 2.5.4).

It is possible to see how many products are present in one sample by generating a melting curve after the qRT-PCR is completed. The samples in the reaction are heated from 60 °C to 95 °C, with the fluorescent signal from the samples being read every 1 °C. As described earlier, the qRT-PCR products are double-stranded DNA bound to SYBR Green, which only fluoresces when it is bound to double-stranded DNA but cannot bind to single-stranded DNA. As the tubes are heated, the DNA separates into

single strands, releasing the SYBR Green and causing a decrease of fluorescent signal. The changes in signal are measured and plotted on a graph.

If only one product has been amplified in a tube, it is expected that one large change of signal will be detected, shown as a peak on the melting curve. If more than one product is present, it is likely that there will be more than one peak on the melting curve, as the many products will separate into single strands at different temperatures according to their lengths and conformations. Therefore the melting curve can be used to ensure that the qRT-PCR signal represents the amplification of one product only and that tubes which contain primer-dimers or other contaminants can be discarded. A melting curve has been generated for every qRT-PCR presented in this chapter.

With the qRT-PCR method outlined and technical terms defined, it is now possible to turn to the application of this method for quantifying thalamic axonal RNAs.

4.3 Methods

4.3.1 Selection of RNAs

mRNAs from Thomas Pratt's library (see Section 1.6.1) were selected by prioritising the sequences which were cloned from the 3'UTR, 5'UTR and coding regions as opposed to the introns. Intronic clones were not prioritised because they were not likely to be part of the canonical mRNA for the identified gene; however, they may have been part of a splice variant of the mRNA or a separate mRNA and so should be investigated in future. One exception was made in the case of reticulon-1, which was cloned from an intron, and was selected because it has been linked to axonal behaviour (see Section 1.6.1). Several mRNAs from the library were not investigated because it was not possible to generate suitable primers for them. Several further mRNAs which had been identified as present or absent in other axonal systems were selected from the literature to investigate whether they were present or absent in thalamic axons.

4.3.2 Standard curve

In order to provide scales of units to measure quantities of RNA, a set of cDNA samples was used to create a dilution series. This set of cDNA samples was generated from samples of thalamic cellular RNA collected using the method described in Chapter 3, some of which were also used for qRT-PCRs. Aliquots from four of the samples listed

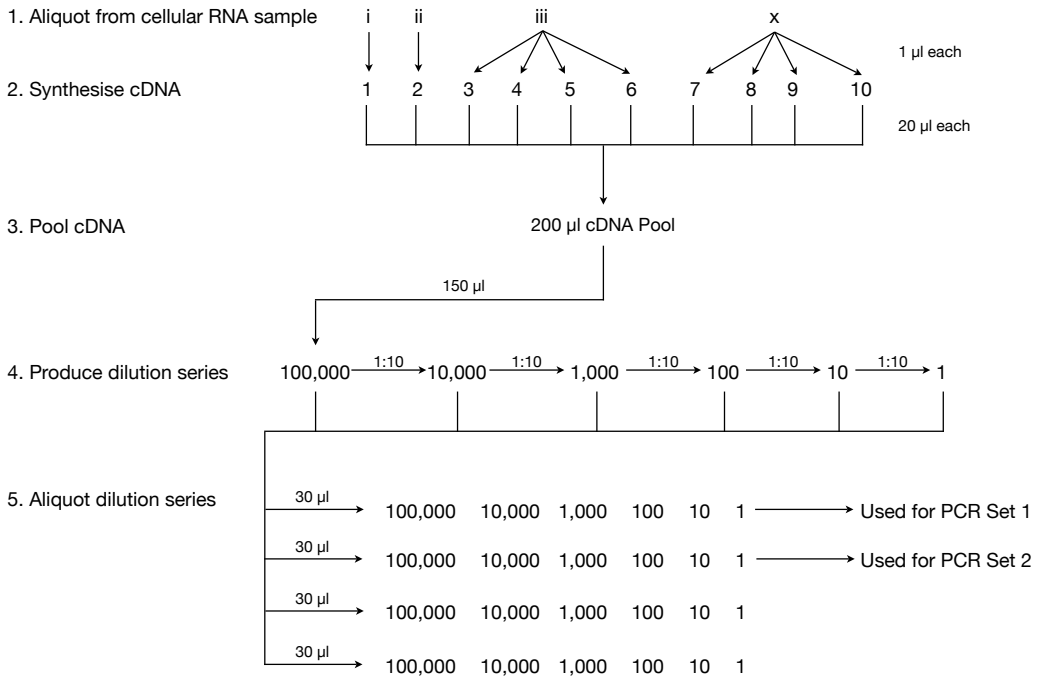

Figure 4.3: A flowchart showing the generation of cDNA samples used to produce a standard curve for use in all qRT-PCRs. Thalamic cellular RNA was taken from the extractions from cultures i, ii, iii and x, shown in Figure 4.6 below. 10 cDNA synthesis reactions were run, each containing 1μL of cellular RNA and producing a 20μL solution containing newly synthesised cDNA. These ten samples were pooled together and 150μL was removed and labelled as 100,000 units. 15μL of this solution was aliquotted into a new tube with 135μL of sterile RNase-free water, a dilution of 1:10, and labelled 10,000 units. This was repeated for four further tubes to produce 1,000, 100, 10 and 1 unit tubes. These units are arbitrary and simply reflect the dilution steps. These 135μL solutions were then aliquotted into four sets of 30μL tubes which were stored at -20°C, the first set of which was used for the Set 1 qRT-PCRs and the second set of which was used for the Set 2 qRT-PCRs described below. The other sets were unused.

in Figure 4.6 were used to produce the standard curve cDNA. The process is shown in Figure 4.3.

Ten separate cDNA synthesis reactions were run, labelled Samples i-x, each on 1μL of RNA, with 1μL taken from Sample i, 1μL from Sample ii, 4μL from Sample iii and 4μL from Sample x (see Section 2.5.1 for cDNA synthesis method). Once the cDNA synthesis reactions were complete the ten cDNA samples were pooled together. Pooling this many separate cDNA samples should minimise the impact of any variability in cDNA synthesis. 150μL of this pool of cDNA (approximately 200μL in size) was aliquotted and labelled as 100,000 units. This pool was then serially diluted to 1 part in 10 with sterile RNase-free water five times to produce separate 10,000, 1,000, 100, 10 and 1 unit samples. These units are arbitrary and simply reflect the dilution steps. These six samples of 135μL each were then separated into four sets of 30μL aliquots and a set of remainders. The first set of qRT-PCRs were run on one set of aliquots 1-10 days after the aliquots were prepared and the second set on a separate set of aliquots 209-221 days after the aliquots were prepared.

4.3.3 qRT-PCRs

Two sets of qRT-PCRs were run (see Section 2.5.3 for program). Each set of qRT-PCRs tested a different group of three biological replicates (sets of RNA samples) for the presence of selected RNAs. Each set of RNA samples contained Cells, Axons, Blank Near, Blank Far, CnoRT, AnoRT, BNnoRT, BFnoRT and noRNA samples. Each RNA was tested in a separate qRT-PCR. The Cells, Axons, Blank Near and Blank Far

---

Figure 4.4 *(following page)*: Design of qRT-PCRs for Set 1 and Set 2 experiments. One RNA was tested in each qRT-PCR experiment. All three samples in a set were tested in each qRT-PCR. For each Set, all tubes including all controls were tested for 18S rRNA, but the noRT and noRNA controls were not tested for other RNAs in Set 1 such as β-actin and β-catenin (see more concise design for these RNAs, which was also used for all other RNAs tested). In Set 2, as a further precaution, the CnoRT conditions were tested for all RNAs. The full design will now be explained by describing the plate for Set 1, 18S at the top of the figure. 39 tubes are shown (tube numbers in superscript). One set of cDNA synthesis reactions (see Figure 3.1) are labelled a sample; for example, tubes 01-09 are from Sample 1a (see Figure 4.6). Two further samples were processed simultaneously (tubes 10-18, Sample 1b; tubes 19-27, Sample 1c). Two dilution series, used to produce a standard curve, a unit scale against which samples can be quantified, are processed in every experiment (tubes 28-33, Standard curve 1; tubes 34-39, Standard curve 2). A control containing only water was processed by qRT-PCR to control for DNA and RNA contamination (tube 40, Water).

Set 1, 18S

Sample 1a: [01] C [02] CnoRT [03] A [04] AnoRT [05] BN [06] BNnoRT [07] BF [08] BFnoRT [09] No RNA
Sample 1b: [10] C [11] CnoRT [12] A [13] AnoRT [14] BN [15] BNnoRT [16] BF [17] BFnoRT [18] No RNA
Sample 1c: [19] C [20] CnoRT [21] A [22] AnoRT [23] BN [24] BNnoRT [25] BF [26] BFnoRT [27] No RNA

Standard curve 1: [28] 100,000 [29] 10,000 [30] 1,000 [31] 100 [32] 10 [33] 1
Standard curve 2: [34] 100,000 [35] 10,000 [36] 1,000 [37] 100 [38] 10 [39] 1
[40] Water

Set 1, β-actin

Sample 1a: [01] C [02] A [03] BN [04] BF
Sample 1b: [05] C [06] A [07] BN [08] BF
Sample 1c: [09] C [10] A [11] BN [12] BF
[13] 100,000 [14] 10,000 [15] 1,000 [16] 100 [17] 10 [18] 1
[19] 100,000 [20] 10,000 [21] 1,000 [22] 100 [23] 10 [24] 1
[25] Water

Set 1, β-catenin

Sample 1a: [01] C [02] A [03] BN [04] BF
Sample 1b: [05] C [06] A [07] BN [08] BF
Sample 1c: [09] C [10] A [11] BN [12] BF
[13] 100,000 [14] 10,000 [15] 1,000 [16] 100 [17] 10 [18] 1
[19] 100,000 [20] 10,000 [21] 1,000 [22] 100 [23] 10 [24] 1
[25] Water

Repeat with same design for RPS3, EphB2, MAP2...

Set 2, 18S

Sample 2a: [01] C [02] CnoRT [03] A [04] AnoRT [05] BN [06] BNnoRT [07] BF [08] BFnoRT [09] No RNA
Sample 2b: [10] C [11] CnoRT [12] A [13] AnoRT [14] BN [15] BNnoRT [16] BF [17] BFnoRT [18] No RNA
Sample 2c: [19] C [20] CnoRT [21] A [22] AnoRT [23] BN [24] BNnoRT [25] BF [26] BFnoRT [27] No RNA

Standard curve 1: [28] 100,000 [29] 10,000 [30] 1,000 [31] 100 [32] 10 [33] 1
Standard curve 2: [34] 100,000 [35] 10,000 [36] 1,000 [37] 100 [38] 10 [39] 1
[40] Water

Set 2, β-actin

Sample 2a: [01] C [02] CnoRT [03] A [04] BN [05] BF
Sample 2b: [06] C [07] CnoRT [08] A [09] BN [10] BF
Sample 2c: [11] C [12] CnoRT [13] A [14] BN [15] BF
[16] 100,000 [17] 10,000 [18] 1,000 [19] 100 [20] 10 [21] 1
[22] 100,000 [23] 10,000 [24] 1,000 [25] 100 [26] 10 [27] 1
[28] Water

Set 2, β-catenin

Sample 2a: [01] C [02] CnoRT [03] A [04] BN [05] BF
Sample 2b: [06] C [07] CnoRT [08] A [09] BN [10] BF
Sample 2c: [11] C [12] CnoRT [13] A [14] BN [15] BF
[16] 100,000 [17] 10,000 [18] 1,000 [19] 100 [20] 10 [21] 1
[22] 100,000 [23] 10,000 [24] 1,000 [25] 100 [26] 10 [27] 1
[28] Water

Repeat with same design for RhoA, Rock1, Ubiquilin-1...

conditions for each of the three samples in one group were run in one reaction, together with two sets of standard curve samples and a control containing only sterile, RNase-free water, labelled Water. After each qRT-PCR was completed, a melting curve was performed on the set of tubes, as described in Section 4.2.3.3.

The noRT and noRNA controls were only run for 18S for the first set of qRT-PCRs. Given that 18S is expected to be the most abundant RNA in the samples, it was thought that if these controls were blank for 18S, there was no need to run them for all RNAs, given the expense of qRT-PCR. However, as a precaution, for the second set of qRT-PCRs the CnoRT condition was tested for all RNAs. 18S was repeated at least once for both groups of three samples.

4.3.4 Ratio comparison

In order to compare the expression of different RNAs, mean ratios of expression between axon and cell samples and their standard deviations were calculated as follows from the Set 1 qRT-PCR results, using 18S as an internal standard.

As discussed in Section 4.5.1.3, two types of replicates were used in these qRT-PR experiments: biological replicates, where many samples of RNA are tested, and technical replicates, where each sample of RNA is tested several times. Each RNA was tested with three biological replicates, but technical replicates were only carried out for the internal standard, 18S rRNA.

4.3.4.1 Calculation of ratios

Uncontrolled ratios of axonal units to cellular units for each RNA for each biological replicate b were calculated:

$$Ratio_{RNA_b} = \frac{A_{RNA_b}}{C_{RNA_b}} \tag{4.1}$$

For 18S, the axonal and cellular units for the technical replicates (t) were averaged for each biological replicate b:

$$\bar{A}_{18S_b} = \frac{\sum_{i=1}^{n_t} A_{18S_i}}{n_t} \qquad \bar{C}_{18S_b} = \frac{\sum_{i=1}^{n_t} C_{18S_i}}{n_t} \tag{4.2}$$

where n_t is the number of technical replicates. The same could be done for the other RNAs if technical replicates for those RNAs were performed.

The standard deviations (s) and coefficients of variation (CV) for 18S cellular and axonal units for each biological replicate were calculated as follows:

$$s(C)_{18S_b} = \sqrt{\frac{\sum_{i=1}^{n_t}(C_{18S_i} - \bar{C}_{18S_b})^2}{n_t - 1}} \tag{4.3}$$

$$CV(C)_{18S_b} = s(C)_{18S_b} / \bar{C}_{18S_b} \tag{4.4}$$

$$s(A)_{18S_b} = \sqrt{\frac{\sum_{i=1}^{n_t}(A_{18S_i} - \bar{A}_{18S_b})^2}{n_t - 1}} \tag{4.5}$$

$$CV(A)_{18S_b} = s(A)_{18S_b} / \bar{A}_{18S_b} \tag{4.6}$$

CV and s for each axon-to-cell ratio for each 18S biological replicate were calculated as follows:

$$CV(Ratio)_{18S_b} = \sqrt{CV(A)_{18S_b}{}^2 + CV(C)_{18S_b}{}^2} \tag{4.7}$$

$$s(Ratio)_{18S_b} = Ratio_{18S_b} * CV(Ratio)_{18S_b} \tag{4.8}$$

Loading-controlled axon-to-cell ratios (LCR) were then calculated for each RNA, where n_b is the number of biological replicates:

$$LCR_{RNA_b} = \frac{Ratio_{RNA_b}}{Ratio_{18S_b}} \tag{4.9}$$

$$LCR_{RNA} = \frac{\sum_{i=1}^{n_b} LCR_{RNA_i}}{n_b} \tag{4.10}$$

The standard deviations for each of these ratios were calculated by combining the deviations within the set of biological replicates for each RNA with the deviations within the biological replicates for 18S:

$$s(Ratio)_{RNA} = \sqrt{\frac{\sum_{i=1}^{n_b}(LCR_{RNA_i} - LCR_{RNA})^2}{n_b - 1}} \tag{4.11}$$

$$s(Ratio)_{18S} = \sqrt{\frac{\sum_{i=1}^{n_b} s(Ratio)_{18S_i}}{n_b - 1}} \tag{4.12}$$

$$s(LCR)_{RNA} = \sqrt{s(Ratio)_{RNA}{}^2 + s(Ratio)_{18S}{}^2} \tag{4.13}$$

The LCR_{RNA} and $s(LCR)_{RNA}$ values are plotted in Figure 4.11.

4.3.4.2 Statistical comparison of ratios

To compare the set of ratios of axonal to cellular RNA expression, a Friedman analysis of variance by ranks test was used, which is the appropriate non-parametric analysis of variance test for related data (Coolican, 2004). As the standard deviations of the ratios varied considerably (from 0.07 for β-catenin to 3.22 for RPS3) it could not be assumed that the variances of the ratios was homogenous, and so it was not appropriate to use the standard F test for parametric analysis of variance.

The Friedman test involves ranking the ratios of expression for each RNA for each sample and then summing the ranks for each RNA over all samples. These summed ranks can be used to perform posthoc multiple comparisons using the following equation:

$$|R_u - R_v| \geq z_{\alpha/k(k-1)} \sqrt{\frac{n_b * k(k+1)}{6}} \tag{4.14}$$

where R_u and R_v are the summed ranks of ratios for two RNAs which are being compared, k is the total number of RNAs to be compared, α is a chosen significance level and $z_{\alpha/k(k-1)}$ is the abscissa value from the unit normal distribution above which lies $\alpha/k(k-1)\%$ of the distribution (Siegel and John, 1988). This equation can be used to compare the difference in summed ranks for each pair of RNA ratios against the critical value on the right side of the equation above. If the difference between the summed ranks for a particular pair of RNAs is greater than the critical value, the RNAs can be considered to be significantly different at $p < \alpha$.

4.3.5 Other methods

The gel electrophoresis data presented in Figures 4.7b and 4.12b was generated using the method in Section 2.3. The programs used for standard and quantitative RT-PCR and the methods for primer generation and efficiency calculation are presented in Section 2.5.

4.4 Results

4.4.1 Selection of RNAs

Figure 4.5 lists the RNAs that have been examined in these experiments, along with their Ensembl (Flicek et al., 2008) and Mouse Genome Database (Bult et al., 2008)

RNA	Ensembl Gene ID	MGI Symbol	Reason for use	Forward primer	Reverse primer	PCR product length
18S rRNA	ENSMUSG00000065257	Rn18s	Internal standard (Alvarez et al., 2000)	TCAGTTATGGTTCCTTTGGT	CGAAAGTTGATAGGGCAGAC	272
β-actin	ENSMUSG00000029580	Actb	Found in chick spinal axons (Olink-Coux et al., 1996)	CACCACACCTTCTACAATGAG	GTCTCAAACATGATCTGGGTC	118
EphB2	ENSMUSG00000028664	Ephb2	Found in chick spinal axons (Brittis et al., 2002)	AATCAAGACGTAATCAACGCC	CATCCACCGTGTTAAAGCTG	264
RhoA	ENSMUSG00000007815	Rhoa	Found in rat DRG axons (Wu et al., 2005)	GCACCTTTATAAGTGATGGCTG	GCGGTCATAATCTTCCTGTC	218
Ascc3l1	ENSMUSG00000003660	Ascc3l1	Cloned from 3'UTR	ATGTGAAGACCAATCTGCTG	ACTCTCCACTCCCTTATCTG	280
β-catenin	ENSMUSG00000006932	Ctnnb1	Cloned from 3'UTR	CTGCTCATCCCACTAATGTC	CTTTATTAACTACCACCTGGTCCT	164
BPGM	ENSMUSG00000038871	Bpgm	Cloned from 3'UTR	AACATCTGGAAGGTATCTCAGAC	TTTGCCTTGTTTCACTTTCCC	184
Synaptotagmin-13	ENSMUSG00000027220	Syt13	Cloned from 3'UTR	CAGAAGTCATCAACTACGCA	TCCTCAACTACACCGTTCTG	147
Reep5	ENSMUSG00000005873	Reep5	Cloned from 5'UTR	GCCTACATCTCAATGAAAGCC	CTTCACCACACTGTCTACCT	269
RPA1	ENSMUSG00000000751	Rpa1	Cloned from 5'UTR	AGGTCATTAACATCCGTCCC	CAACTACTTTCTGGCTTAACTTCC	269
RPS3	ENSMUSG00000030744	Rps3	Cloned from 5'UTR	CAAGAAGAGGAAGTTTGTAGCTG	CCCAAGAACATTCTGTGTCC	162
Ubiquilin-1	ENSMUSG00000005312	Ubqln1	Cloned from 5'UTR	GAGCAACCTAGAAAGTATTCCT	TTACCACCAAACTGTTCTTGAG	104
Bat2d1	ENSMUSG00000040225	Bat2d1	Cloned from coding region	GACAACCTCTGATTGCTTTACC	TGATGTAGCCCTGAATGGAC	277
RalA	ENSMUSG00000008859	Rala	Cloned from coding region	TGTACGACGAGTTTGTAGAG	GATCTGACTTGTTACCAACC	287
Reticulon-1	ENSMUSG00000021087	Rtn1	Cloned from intron, axonal protein (Steiner et al., 2004)	GAGCAGATCCAGAAGTACAC	GAAACCACAGCCATAAGCAG	184
α-tubulin	ENSMUSG00000072235	Tuba1a	Absent from chick spinal axons (Olink-Coux et al., 1996)	CAGATGCCAAGTGACAAGAC	GTGCGAACTTCATCGATGAC	136
α-tubulin (OH)	ENSMUSG00000023004	Tuba1c	Absent from chick spinal axons (Olink-Coux et al., 1996)	ATTGCCACCATCAAGACCAA	TAGATCACAAGTTTGATCTG	198
MAP2	ENSMUSG00000015222	Mtap2	Absent from P19 & rat spinal axons (Litman et al., 1993)	CTTCGGCTTATTAACCAACCA	GGCTGTCAATCTTCACATTACC	300
Rac1	ENSMUSG00000001847	Rac1	Absent from rat DRG axons (Wu et al., 2005)	GAAGATTATGACAGATTGCGTCC	GTATTTGACAGCACCGATCTC	278
Rock1	ENSMUSG00000024290	Rock1	Absent from rat DRG axons (Wu et al., 2005)	TCAAGTCTATACAACAGCGG	GATTCTTAACTTCATCCTCCATCC	284

Figure 4.5: RNAs selected for testing using qRT-PCR. Ensembl Gene IDs and Mouse Genome Informatics (MGI) symbols are provided for each RNA. Cloning locations in the "Reason for use" column refer to clones produced in Thomas Pratt's library (see Section 1.6.1). RNAs found to be present or absent in other systems were selected for use based on the references listed in the "Reason for use" column. Forward and reverse primers and the length of the product predicted to be amplified by PCR when using each pair of primers is provided for each RNA. DRG, dorsal root ganglion.

reference numbers, the reasons why these RNAs were tested, the sequences of the primers used to amplify the RNAs and the expected length of the resulting qRT-PCR products. As explained in Section 4.3.1, RNAs were selected for use because they were found in Thomas Pratt's library (see Section 1.6.1), or had previously been shown to be present or absent in other axonal systems, based on reports from the literature as indicated in the figure.

4.4.2 Collection of samples

Thalamic sections were cultured according to the method outlined in Section 3.2. Fifteen cultures were carried out, four of which did not yield sufficient quantities of axons or became contaminated. Eleven cultures were dissected and the RNA from these cultures was extracted. Figure 4.6 shows the unit values for Axons, Blank Far and Blank Near for a qRT-PCR for 18S, run as a test on each of the samples. It shows that six of the eleven samples were deemed usable and five were discarded, according to the fold differences between the axonal and blank conditions. The samples with the highest fold differences between axonal and blank signals were chosen for use, whereas samples with lower fold differences between axonal and blank signals or samples where either of the blank signals were higher than the axonal signal were discarded.

The six usable samples were tested in two different sets of qRT-PCRs, with Samples 1a, 1b and 1c forming Set 1 and Samples 2a, 2b and 2c forming Set 2. These sets of qRT-PCRs will now be considered separately.

4.4.3 Results for Set 1 samples

In this section, a series of results demonstrating the quality of the samples in Set 1 will be presented, followed by the results for the qRT-PCRs on this set of samples.

4.4.3.1 Quality of Set 1 samples

For the three samples in Set 1, Figure 4.7a shows the number of days since culturing for each of the steps of the process and the number of explants in each sample. The table in the figure shows that RNA extraction and cDNA synthesis were carried out in a timely fashion but that there was a significant amount of time between cDNA syntheses and qRT-PCRs, due to unforeseen and uncontrollable circumstances.

Sample	Axons	Blank Near		Blank Far		Use
	Units	Units	Fold decrease from axons	Units	Fold decrease from axons	
i	21.19	0.45	**47.09**	0.38	**55.76**	Sample 1a
ii	17.4	0.33	**52.73**	0.46	**37.83**	Sample 1b
iii	14.2	1.11	**12.79**	0.22	**64.55**	Sample 1c
iv	14.13	1.92	**7.36**	0.53	**26.66**	Sample 2a
v	40.78	3.33	**12.25**	1.86	**21.92**	Sample 2b
vii	5.95	0.49	**12.14**	1.43	**4.16**	Sample 2c
vi	18.4	5.91	**3.11**	11557.07	**-628.10**	Discarded
viii	20.78	15.19	**1.37**	10.09	**2.06**	Discarded
ix	10.35	8.12	**1.27**	1.41	**7.34**	Discarded
x	5.67	3.83	**1.48**	7.34	**0.77**	Discarded
xi	0.89	1.5	**0.59**	0.28	**3.18**	Discarded

Figure 4.6: A list of sets of RNA samples collected. Units are arbitrary values inferred from C(T) values generated by qRT-PCR for 18S rRNA using 100,000 unit standard curves. Samples i, ii and iii were relabelled Samples 1a, 1b and 1c and used for the first set of qRT-PCR experiments, subsequently labelled Set 1. Samples iv, v and vii were relabelled Samples 2a, 2b and 2c and used for the second set of qRT-PCR experiments, subsequently labelled Set 2. Samples were discarded where there was clear contamination (eg in the Blank Far condition for Sample vi), where either Blank Near or Blank Far signal was higher than Axonal signal (where the fold decrease between either Axons and Blank Near or Axons and Blank Far is less than 1, as for Samples x and xi) or because the differences were not as high as other samples (eg Sample vii was chosen for use above Samples viii and ix).

a

Days post culture	1a	1b	1c
Dissection	5	4	4
RNA Extraction	6	4	5
cDNA Synthesis	11	5	9
qRT-PCRs	80-90	74-84	72-82
Number of explants	15	21	23

b

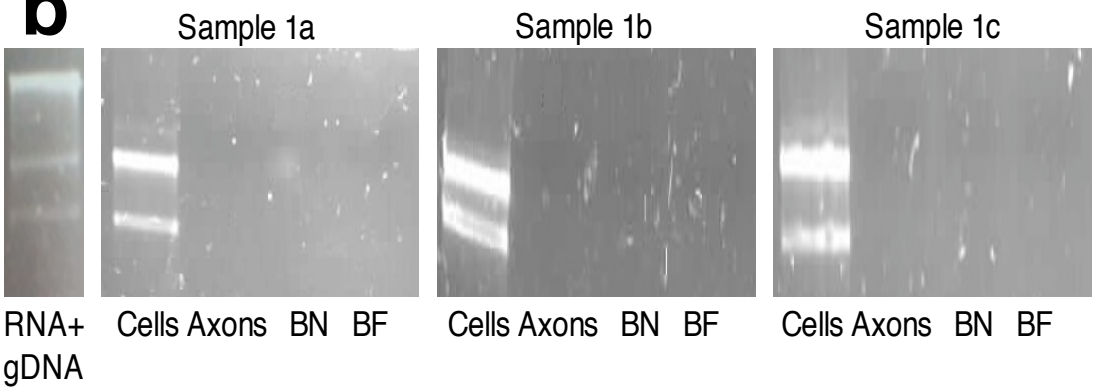

Figure 4.7: Quality of Set 1 samples, containing samples 1a, 1b and 1c. a) The days from culture to processing steps and number of explants dissected for the Set 1 samples used for qRT-PCR. qRT-PCRs were carried out over 11 days for Set 1 samples (1a, 1b and 1c). b) Quality of Set 1 RNA samples shown by gel electrophoresis. All three samples show two bands, representing 18S and 28S rRNA, and no band representing genomic DNA (gDNA), as shown in the left-most picture, which shows a sample of cellular RNA where no DNase step was performed during RNA extraction. The small quantities of RNA from axons and blanks are below the limits of detection for gel electrophoresis, but these bands are shown to demonstrate the lack of contaminating gDNA in these conditions. BN, Blank Near; BF, Blank Far.

Figure 4.7b shows pictures of gels for the Set 1 samples used for qRT-PCR, showing that the cellular conditions contained two bands representing 18S and 28S rRNA (there is insufficient RNA in axonal and blank conditions to be detected by gel electrophoresis). No contaminating gDNA was found in any condition for any sample used for qRT-PCRs.

Figure 4.8a shows an example of a qRT-PCR result for one RNA, in this case one of the qRT-PCRs for 18S for the Set 1 samples. The figure shows the C(T) and unit values for each condition for each sample. As expected, the unit values for the axonal conditions are very small compared to the unit values for the cellular conditions. However, a clear difference can be seen between the axonal conditions and all of the Blank, noRT, noRNA and Water conditions. The Axon unit values are significantly higher than the Blank Near unit values (p=0.01) and Blank Far unit values (p=0.01) but the Blank Near and Blank Far unit values are not significantly different (p=0.25), according to one-tail paired t-tests.

Figure 4.9 shows an example of a melting curve, for 18S2 in Set 1 (see Section 4.2.3.3 for a description of melting curves). The graph shows that only one product was present in all of the samples run in this qRT-PCR, with the exception of the Water control where no product was present. Similar graphs were produced for every qRT-PCR and used to calculate the melting temperatures for each product presented in Figure 4.8b. Each pair of primers used produced only a single product in most samples, including all samples where a significant signal could be detected. All primers produced a single product in at least the Cells condition, demonstrating that the primers functioned as expected and that any lack of signal in a particular tube was not due to the problems with primers. Primer dimers did form in a minority of samples where no original material was present (such as in some Blanks or noRT samples). The melting curves were used to identify such samples and omit the readings for these samples in further analyses.

Figure 4.8b show the r^2 values, efficiencies, melting curve peaks and missing standard curve values for all the qRT-PCRs carried out for Set 1. The missing standard curve values are tubes in the standard curve dilution series (which contains two tubes each for 100,000 units, 10,000 units, 1,000 units, 100 units, 10 units and 1 unit) where no signal was detected. The figure shows that melting curve peaks were consistent for RNAs which were repeated within and across sets. For example, 18S products repeatedly separated at 89 °C (see also Figure 4.13b).

The figure shows that the r^2 values for the Set 1 qRT-PCRs are all above 0.95,

a

18S	1a		1b		1c	
	C(T)	Units	C(T)	Units	C(T)	Units
Cells	5.05	63229.40	4.49	86944.65	4.58	82624.90
Axons	19.04	21.19	19.38	17.40	19.74	14.20
Blank Near	25.78	0.45	26.32	0.33	24.19	1.11
Blank Far	26.06	0.38	25.74	0.46	27.02	0.22
Cells, no RT	32.77	0.00	34.98	0.00	33.59	0.01
Axons, no RT	None	0.00	39.50	0.00	None	0.00
BN, no RT	None	0.00	None	0.00	None	0.00
BF, no RT	39.34	0.00	None	0.00	None	0.00
No RNA	36.76	0.00	None	0.00	34.32	0.00
Water	34.12	0.00				

Paired one-tail t-tests, comparing unit values:
Axons & Blank Near, p=0.01
Axons & Blank Far, p=0.01
Blank Near & Blank Far, p=0.25

b

Set 1	r^2	Efficiency	Melting curve peak (°C)	Missing standard curve values
18S 1	0.996	78%	89	
18S 2	0.996	78%	89	
α-tubulin	0.998	86%	84	
β-actin	0.998	82%	84	
β-catenin	0.999	90%	82	
EphB2	0.994	90%	87	2x1
MAP2	1.000	90%	81	1x1
RalA	0.997	86%	82	1x1
Reticulon-1	0.984	74%	84	
RPS3	0.989	86%	81	1x1
Synaptotagmin-13	0.998	86%	85	2x1

Figure 4.8: Quality of Set 1 qRT-PCRs. a) An example of a complete qRT-PCR for 18S for Set 1 samples. Cells, Axons, Blank Near and Blank Far results are shown, with corresponding No Reverse Transcriptase (noRT) controls. Water and noRNA controls are also shown. For each condition, C(T) and Unit values are given. The text shows that Set 1 Axonal Units were significantly above both Blank Near and Blank Far units according to paired one-tail t-tests. b) Quality of qRT-PCRs for Set 1, indicated by r^2 values, efficiencies, melting curve peaks and missing standard curve values. The r^2 values are coloured green where $r^2 > 0.95$ and red where $r^2 < 0.95$ (all Set 1 samples have $r^2 > 0.95$). Single melting curve peaks were found in all tubes where significant signal was detected, indicating that only one product was present in each tube. The same peak was found in all tubes for each RNA and repeated RNAs (such as 18S) produced the same melting curve peak when repeated within and across sets (see also Figure 4.13b). Missing standard curve values are readings from the two standard curve dilution series, which were run with every qRT-PCR, where no signal was detected. So, for example, for Synaptotagmin-13, no signal was detected from either of the 1 unit tubes.

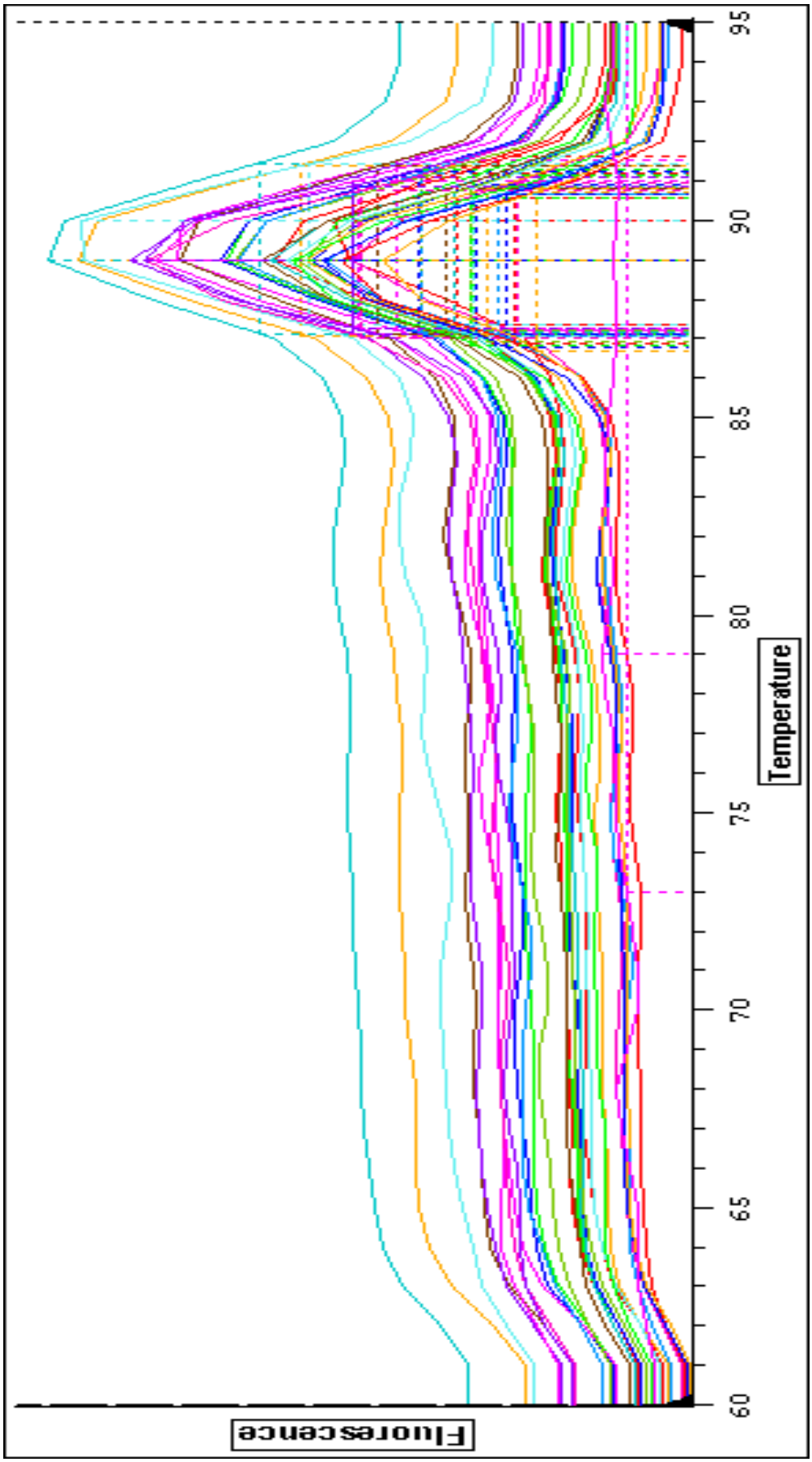

Figure 4.9: An example of a melting curve, for 18S in Set 1. Each coloured line represents a different condition. The y-axis shows change of fluorescence; the x-axis shows temperature in °C. The figure shows that the greatest change in fluorescence for all samples was at 89 °C. The flat purple line in the peak region is the Water control, where no signal was detected.

which indicates that the standard curve C(T) values are well correlated with their expected unit values and the quantifications from this set of PCRs are reliable. The efficiencies for Set 1, while somewhat below 100%, do not indicate any serious problem with these reactions. The high r^2 values indicate that each amplicon could be amplified with the same efficiency reliably. Also, it is encouraging that the efficiencies for both 18S qRT-PCRs were identical, indicating that the amplification of at least this RNA was reliable and consistent across different qRT-PCRs.

4.4.3.2 qRT-PCR results for Set 1 samples

To claim that an RNA is present in thalamic axons, it is necessary to show that a signal can be found for that RNA in the axonal conditions which is above any signal in either of the blank conditions. Figure 4.10 shows the Axon and Blank unit values for the qRT-PCRs carried out on the Set 1 samples. The unit values for each RNA are inferred from standard curves specific to each RNA and so cannot be compared directly. The figure shows that, according to one-tailed, paired t-tests, significant differences could be found between Axons and Blank Near signals, and between Axons and Blank Far signals, for 18S, β-actin, β-catenin, Reticulon-1, RPS3 and Synaptotagmin-13, and also for RNAs which have not been found in other axonal systems, α-tubulin and MAP2.

For two RNAs, RalA and EphB2, the differences between Axons and at least one of the blank conditions were not significant. However, this may be due to the variation between samples, which cannot be controlled for in this analysis (see Section 4.5.1.1 for discussion). The data for each individual sample are provided for these RNAs in the figure, and it can be seen that, for RalA, the axonal signal is above both blank signals in all three samples, and that for most blank signals a 0 unit value was recorded. For EphB2, a signal could be detected in axons in two samples and no signal was present in the blanks in any sample. This indicates that both RalA and EphB2 can be found in axons above levels of contamination and should be considered to be present in thalamic axons.

4.4.3.3 Comparison of RNAs tested on Set 1 samples

Figure 4.11 shows ratios of axonal to cellular expression for RNAs from Set 1, controlled for tissue quantity against the internal standard, 18S (see Section 4.5.1.2). These ratios were calculated using the method described in Section 4.3.4.

a

Set 1 (n=3)	Axons	Blank Near		Blank Far	
RNA	Mean Units	Mean Units	Significant difference from axons	Mean Units	Significant difference from axons
18S1	17.59 (SD 3.50)	0.63 (SD 0.42)	p<0.01	0.35 (SD 0.12)	p<0.01
18S2	16.28 (SD 3.55)	0.61 (SD 0.60)	p<0.05	0.41 (SD 0.39)	p<0.01
α-tubulin	23.44 (SD 8.25)	0.25 (SD 0.17)	p<0.05	0.30 (SD 0.12)	p<0.05
β-actin	25.38 (SD 6.83)	1.19 (SD 1.03)	p<0.05	0.90 (SD 0.80)	p<0.05
β-catenin	10.35 (SD 2.76)	0.47 (SD 0.47)	p<0.05	0.49 (SD 0.55)	p<0.05
MAP2	3.25 (SD 0.42)	0 (SD 0)	p<0.05	0 (SD 0)	p<0.05
Reticulon-1	15.27 (SD 5.50)	0.14 (SD 0.24)	p<0.05	0.13 (SD 0.22)	p<0.05
RPS3	267.99 (SD 124.08)	2.20 (SD 2.03)	p<0.05	1.43 (SD 1.40)	p<0.05
Synaptotagmin 13	15.22 (SD 5.15)	0 (SD 0)	p<0.05	0 (SD 0)	p<0.05
EphB2	4.67 (SD 4.04)	0 (SD 0)	p>0.05	0 (SD 0)	p>0.05
RalA	6.11 (SD 3.83)	0.65 (SD 1.13)	p<0.05	0 (SD 0)	p>0.05

b

Ral-A	Axons	Blank Near	Blank Far
Sample 1a	**4.00**	0.00	0.00
Sample 1b	**10.53**	1.96	0.00
Sample 1c	**3.80**	0.00	0.00

c

EphB2	Axons	Blank Near	Blank Far
Sample 1a	**6.90**	0.00	0.00
Sample 1b	**7.10**	0.00	0.00
Sample 1c	0.00	0.00	0.00

Figure 4.10: qRT-PCR results for Set 1. a) Comparison of axon and blank unit values for RNAs tested on Set 1 samples. Colouring of RNA names reflects the quality of the qRT-PCR for that RNA indicated by the r^2 value for the qRT-PCR (see Figure 4.8b). The unit values for each RNA are inferred from standard curves specific to each RNA and so cannot be compared directly. Means and standard deviations for Axons, Blank Near and Blank Far Units are shown, and significant differences between Axons and Blank Near, and Axons and Blank Far, are reported according to one-tailed paired t-tests. For the RNAs where differences were insignificant (where $p > 0.05$), full data for all samples has been provided to show where Axon signals were above Blank signals. b) RalA, c) EphB2. Axon unit values for a particular sample which were above both Blank Near and Blank Far unit values for that sample are marked in bold. 0 values where no signal was detected are coloured grey.

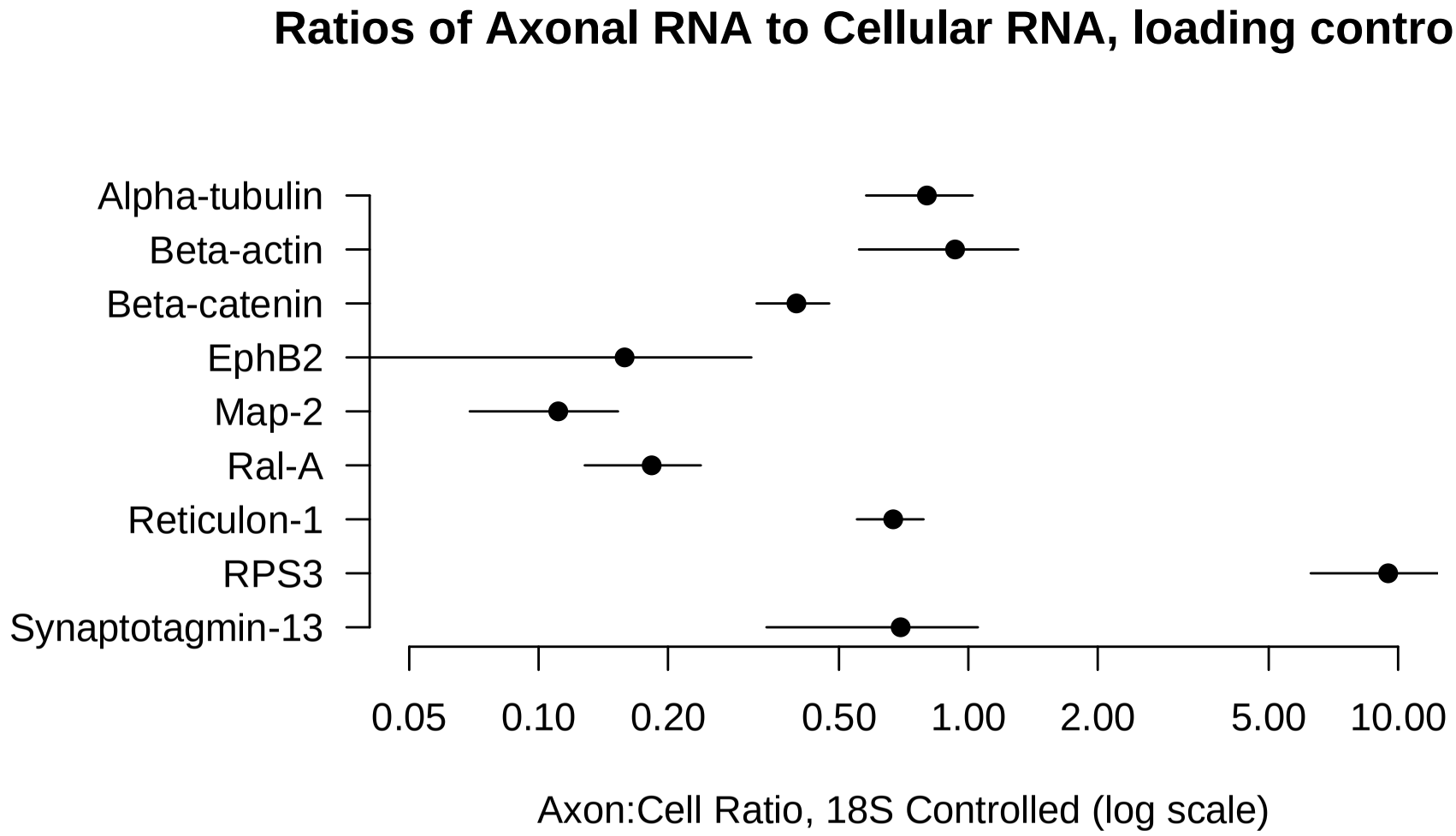

Figure 4.11: Mean ratios of Axonal RNA to Cellular RNA, controlled for tissue quantity against the internal standard 18S, for the RNAs in Set 1. Means are shown as dots. Lines represent one standard deviation on either side of the mean. A ratio of 1 indicates that an RNA has the same expression in axons as in cells.

A ratio of axonal RNA to cellular RNA equal to 1 would indicate that the RNA is expressed at the same level in axons and cells relative to 18S. Except for RPS3, with a mean ratio of 9.43, indicating an almost 10-fold increase in expression in axons compared to cells, all of the ratios are below 1. A ratio of 1 is within 1 standard deviation of the mean ratios for α-tubulin, β-actin and synaptotgamin-13. The ratios for β-catenin, EphB2, MAP2, RalA and Reticulon-1 indicate that these RNAs are expressed at a considerably lower level in axons compared to cells, with the MAP2 having a mean ratio of 0.11, or a 9-fold difference in expression between axons and cells.

There are significant differences within the set of mean ratios (Friedman's analysis of variance by ranks test, χ^2 (7) = 18.48, $p < 0.01$) but the only significant difference that could be found between RNAs with posthoc multiple comparisons was between RPS3 and MAP2 ($p < 0.05$, see Section 4.3.4.2 for calculation). If RPS3 is omitted from the analysis, significant differences can still be found using a Friedman test (χ^2 (6) = 16.81, $p < 0.01$) but the particular differences cannot be identified by posthoc tests (comparisons of all pairs of RNA are all $p > 0.05$).

Therefore, these ratios cannot be used to infer differences in axonal to cellular expression for particular pairs of RNAs other than RPS3 and MAP2. However, the ratios do indicate that, with the exception of RPS3, RNAs are mostly depleted in axons compared to cells. Also, the fact that there are differences in the ratios in the set both when RPS3 is included and when it is excluded increase confidence that the RNAs in the axonal samples did indeed come from axons rather than cellular contamination. This is because it might be expected that if the RNA came from cells alone, the ratios of expression would all be 1, or at least show the same enrichment or depletion of RNA, because the comparison would be between two samples of thalamic cells, which might be expected to express the same levels of RNA. However, this assumption needs to be confirmed experimentally.

In summary, a set of high quality qRT-PCRs have been presented in this section demonstrating the presence of 18S, α-tubulin, β-actin, β-catenin, EphB2, MAP2, RalA, Reticulon-1, RPS3 and Synaptotagmin-13 in thalamic axons, and indicating variability in the expression profile of these RNAs in axons compared to their expression in cells.

4.4.4 qRT-PCRs on Set 2 samples

In this section, a series of results testing the quality of the samples in Set 2 will be presented, followed by the results for the qRT-PCRs on this set of samples.

4.4.4.1 Quality of Set 2 samples

For the three samples in Set 2, Figure 4.12a shows the number of days since culturing for each of the steps of the process and the number of explants in each sample. The table in the figure shows that there was a significant amount of time between cDNA syntheses and qRT-PCRs for Set 2. Also, the steps up to cDNA synthesis were all later for Set 2 than for Set 1. It may be that delays in RNA extraction and cDNA synthesis affected the Set 2 samples although no systematic tests of the effects of storage have been performed. However, when the qRT-PCRs were begun for the second set, it became clear that some evaporation had occurred in the samples. As this should only have affected the water in each tube but not the DNA, the samples were ethanol precipitated again to ensure an even amount of water in each tube, which was essential to ensure that equivalent quantities of DNA were present in each tube when running each qRT-PCR, but undesirable because each ethanol precipitation causes some RNA to be lost. This subsequently lead to a loss of signal and cDNA quality, which will be discussed in Section 4.5.1.4.

Figure 4.12b shows pictures of gels for the Set 2 samples used for qRT-PCR, showing that the cellular conditions contained two bands representing 18S and 28S rRNA (there is insufficient RNA in axonal and blank conditions to be detected by gel electrophoresis). No contaminating gDNA was found in any condition for any sample which was tested and used for qRT-PCRs.

Figure 4.13a shows one of the 18S results for the three samples in Set 2. It shows the axon unit values are all above the unit values for the Blanks and the noRT, noRNA and Water controls for all three samples. This shows that no significant contaminating DNA was introduced into the reactions during culture, RNA extraction, cDNA synthesis or qRT-PCR. However, although the axon unit values are all higher than the blank unit values, the difference is not statistically significant (Axons and Blank Near, p=0.1, Axons and Blank Far, p=0.1) due to the large variation in axon unit values (mean = 20.29, standard deviation = 18.21). Despite this, as these were the best samples that it was possible to obtain in the time available (see Section 4.4.2), these three samples were used for qRT-PCR. This is discussed further in Section 4.5.1.1.

a

Days post culture	2a	2b	2c
Dissection	5	6	5
RNA Extraction	6	8	6
cDNA Synthesis	20	18	13
qRT-PCRs	190-202	188-200	141-153
Number of explants	17	18	19

b

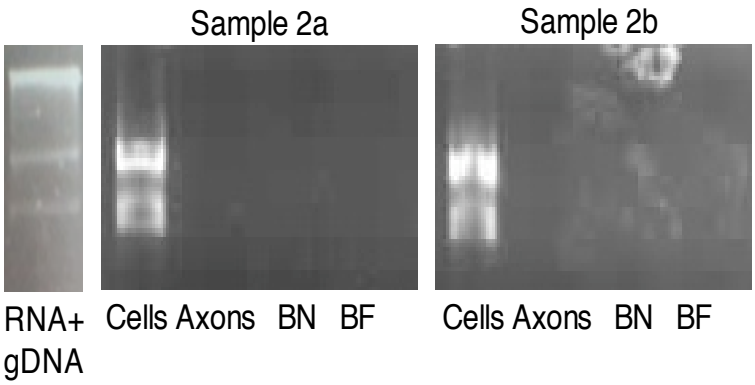

Figure 4.12: Quality of Set 2 samples, containing samples 2a, 2b and 2c. a) The days from culture to processing steps and number of explants dissected for the Set 2 samples used for qRT-PCR. qRT-PCRs were carried out over 13 days for Set 2 samples (2a, 2b and 2c). b) Quality of Set 2 RNA samples shown by gel electrophoresis (Sample 2c not tested). Each sample shows two bands, representing 18S and 28S rRNA, and no band representing genomic DNA (gDNA), as shown in the left-most picture, which shows a sample of cellular RNA where no DNase step was performed during RNA extraction. The small quantities of RNA from axons and blanks are below the limits of detection for gel electrophoresis, but these bands are shown to demonstrate the lack of contaminating gDNA in these conditions. BN, Blank Near; BF, Blank Far.

a

18S	2a		2b		2c	
	C(T)	Units	C(T)	Units	C(T)	Units
Cells	6.69	53462.80	6.23	62644.59	4.54	41747.43
Axons	30.31	14.13	27.27	40.78	23.26	5.95
Blank Near	36.03	1.92	34.45	3.33	28.52	0.49
Blank Far	39.71	0.53	36.12	1.86	26.27	1.43
Cells, no RT	32.77	0.00	34.98	0.00	31.54	0.12
Axons, no RT	47.67	0.00	47.40	0.01	36.53	0.00
BN, no RT	None	0.00	None	0.00	48.54	0.00
BF, no RT	None	0.00	None	0.00	37.41	0.00
No RNA	None	0.00	None	0.00	33.47	0.01
Water	None	0.00				

Paired one-tail t-tests, comparing unit values:
Axons & Blank Near, p=0.1
Axons & Blank Far, p=0.1
Blank Near & Blank Far, p=0.23

b

Set 2	r^2	Efficiency	Melting curve peak (°C)	Missing standard curve values
18S 1	0.982	55%	89	1x100
18S 2	0.975	51%	89	
18S 3	0.974	51%	89	
α-tubulin (OH)	0.860	55%	84	1x1000, 2x100, 2x10, 2x1
β-actin	0.915	48%	84	2x1
β-catenin	0.961	70%	82	1x10, 2x1
Ascc3l1	0.964	58%	88	2x10, 2x1
Bat2d1	0.960	86%	83	2x10, 2x1
Bpgm	0.932	66%	84	1x10, 2x1
Rac1	0.950	73%	82	2x10, 2x1
Reep5	0.960	78%	84	2x10, 2x1
RhoA	0.967	91%	82	1x10
Rock1	0.932	55%	80	2x10, 2x1
RPA1	0.992	66%	84	1x1000, 2x100, 2x10, 2x1
RPS3	0.962	74%	81	2x10, 2x1
Ubiquilin 1	0.933	66%	80	2x10, 2x1

Figure 4.13: Quality of Set 2 qRT-PCRs. a) An example of a complete qRT-PCR for 18S for Set 2 samples. Cells, Axons, Blank Near and Blank Far results are shown, with corresponding No Reverse Transcriptase (noRT) controls. Water and noRNA controls are also shown. For each condition, C(T) and Unit values are given. For the three samples in Set 2, Axonal Units were all above Blank Near and Blank Far units, but due to the wide variation in Axonal Units the differences between the axonal and blank conditions were not significant. b) Quality of qRT-PCRs for Set 2, indicated by r^2 values, efficiencies, melting curve peaks and missing standard curve values. The r^2 values are coloured green where $r^2 > 0.95$ and red where $r^2 < 0.95$. Single melting curve peaks were found in all tubes where significant signal was detected, indicating that only one product was present in each tube. The same peak was found in all tubes for each RNA and repeated RNAs (such as 18S) produced the same melting curve peak when repeated within and across sets (see also Figure 4.8b). Missing standard curve values are readings from the two standard curve dilution series, which were run with every qRT-PCR, where no signal was detected. So, for example, for BPGM in Set 2, no signal was detected from 1 of the 10 unit tubes and both of the 1 unit tubes.

Figure 4.13b show the r^2 values, efficiencies, melting curve peaks and missing standard curve values for all the qRT-PCRs carried out for Set 2. The figure shows that melting curve peaks were consistent for RNAs which were repeated within and across sets. For example, 18S products always separated at 89 °C, twice for Set 1 (see Figure 4.8b and three times for Set 2 (see Figure 4.9 for an example of a melting curve).

The figure shows that most r^2 values for the Set 2 qRT-PCRs fall above 0.98 but that five of the sixteen values fall below 0.95. The r^2 values for β-actin, BPGM, Ubiquilin-1, Rock1 and α-tubulin(OH) are all below 0.95, which means the quantifications for these five qRT-PCRs cannot be considered to be reliable.

In addition, the efficiencies for Set 2 are considerably lower than those for Set 1, and, significantly, unlike the melting curve peaks, the efficiencies for RNAs which were repeated such as 18S and β-actin are not the same in both sets. This suggests that something in the samples interfered with the efficiency of the reactions, which means that these low efficiencies cast further doubt on the validity of quantifications from this set.

In addition, many standard curve values could not be detected for this set, which may indicate that the standard curve cDNA had degraded (which would explain why standard curve values were missing for β-actin and β-catenin in Set 2 but not in Set 1), or that the RNAs were of such low abundance that they could not be detected in some of the higher dilution standard curve samples (see, for example, RPA1). The failure to detect the whole standard curve for some RNAs means that the unit values at the lower end of the scale for these RNAs may not be accurate. For example, Figure 4.14 shows that Bat2d1 has a mean axonal unit value of 2.58. However, as neither of the 10 unit or 1 unit standard curve samples were detected, the mean value has been inferred from the samples for the range 100 - 100,000, and cannot be considered to be accurate.

The low r^2 values, low efficiencies and several missing standard curve values for Set 2 shown in Figure 4.13b indicate that the quantifications resulting from this set are not reliable. As a result, in what follows, while these quantifications will be considered, these qRT-PCRs will be interpreted as standard RT-PCRs, examining only presence or absence of signal in Axons, Blank Near and Blank Far conditions, and no comparison of RNA quantity will be presented.

4.4.4.2 qRT-PCR results for Set 2 samples

Figure 4.14 shows the Axon and Blank unit values for the qRT-PCRs carried out on the Set 2 samples. As with the Set 1 results, the unit values for each RNA are inferred from

a

Set 2 (n=3)	Axons	Blank Near		Blank Far	
RNA	Mean Units	Mean Units	Significant difference from axons	Mean Units	Significant difference from axons
18S1	19.31 (SD 21.42)	1.50 (SD 1.14)	p>0.05	2.90 (SD 2.28)	p>0.05
18S2	17.54 (SD 13.52)	2.07 (SD 1.40)	p>0.05	1.26 (SD 1.57)	p>0.05
18S3	14.97 (SD 12.35)	4.51 (SD 3.83)	p>0.05	0.16 (SD 0.15)	p>0.05
Bat2d1	2.58 (SD 4.47)	0 (SD 0)	p>0.05	0 (SD 0)	p>0.05
β-actin	13.18 (SD 14.11)	8.31 (SD 7.22)	p>0.05	2.55 (SD 4.42)	p>0.05
β-catenin	5.14 (SD 4.45)	1.27 (SD 2.19)	p>0.05	0 (SD 0)	p>0.05
Reep5	1.19 (SD 2.05)	0 (SD 0)	p>0.05	0 (SD 0)	p>0.05
RhoA	0.32 (SD 0.56)	0 (SD 0)	p>0.05	0 (SD 0)	p>0.05
RPS3	4.74 (SD 5.07)	0 (SD 0)	p>0.05	0 (SD 0)	p>0.05
Ubiquilin-1	49.06 (SD 42.65)	0 (SD 0)	p>0.05	0 (SD 0)	p>0.05
Ascc3l1	0 (SD 0)	0 (SD 0)	p>0.05	0 (SD 0)	p>0.05
Bpgm	0 (SD 0)	0 (SD 0)	p>0.05	0 (SD 0)	p>0.05
Rac1	0 (SD 0)	0 (SD 0)	p>0.05	0 (SD 0)	p>0.05
Rock1	0 (SD 0)	0 (SD 0)	p>0.05	0 (SD 0)	p>0.05
RPA1	0 (SD 0)	0 (SD 0)	p>0.05	0 (SD 0)	p>0.05
α-tubulin-OH	0 (SD 0)	0 (SD 0)	p>0.05	0 (SD 0)	p>0.05

b

18S 1	Axons	Blank Near	Blank Far
Sample 2a	**11.98**	2.53	1.16
Sample 2b	**43.43**	1.69	5.47
Sample 2c	**2.52**	0.27	2.05

c

18S 2	Axons	Blank Near	Blank Far
Sample 2a	**26.48**	2.44	0.00
Sample 2b	**24.16**	3.24	3.01
Sample 2c	**1.99**	0.52	0.76

d

18S 3	Axons	Blank Near	Blank Far
Sample 2a	**17.79**	4.76	0.00
Sample 2b	**25.67**	8.20	0.19
Sample 2c	**1.45**	0.56	0.29

e

Bat2d1	Axons	Blank Near	Blank Far
Sample 2a	0.00	0.00	0.00
Sample 2b	**7.74**	0.00	0.00
Sample 2c	0.00	0.00	0.00

f

β-actin	Axons	Blank Near	Blank Far
Sample 2a	**28.06**	11.86	0.00
Sample 2b	*11.49*	13.07	7.66
Sample 2c	0.00	0.00	0.00

g

β-catenin	Axons	Blank Near	Blank Far
Sample 2a	**7.74**	0.00	0.00
Sample 2b	**7.68**	3.80	0.00
Sample 2c	0.00	0.00	0.00

h

Reep-5	Axons	Blank Near	Blank Far
Sample 2a	0.00	0.00	0.00
Sample 2b	**3.56**	0.00	0.00
Sample 2c	0.00	0.00	0.00

i

RhoA	Axons	Blank Near	Blank Far
Sample 2a	0.00	0.00	0.00
Sample 2b	**0.96**	0.00	0.00
Sample 2c	0.00	0.00	0.00

j

RPS3	Axons	Blank Near	Blank Far
Sample 2a	**4.14**	0.00	0.00
Sample 2b	**10.09**	0.00	0.00
Sample 2c	0.00	0.00	0.00

k

Ubiquilin-1	Axons	Blank Near	Blank Far
Sample 2a	**69.83**	0.00	0.00
Sample 2b	0.00	0.00	0.00
Sample 2c	**77.34**	0.00	0.00

Figure 4.14: Comparison of axon and blank unit values for RNAs tested on Set 2 samples. Colouring of RNA names reflects the quality of the qRT-PCR for that RNA indicated by the r^2 value for the qRT-PCR (see Figure 4.13b). The unit values for each RNA are inferred from standard curves specific to each RNA and so cannot be compared directly. Means and standard deviations for Axons, Blank Near and Blank Far Units are shown, and significant differences between Axons and Blank Near, and Axons and Blank Far, are reported according to one-tailed paired t-tests. For the RNAs where differences were insignificant (where $p > 0.05$) and signal was detected in at least one condition, full data for all samples has been provided to show where Axon signals were above Blank signals. b) 18S 1, c) 18S 2, d) 18S 3, e) Bat2d1, f) β-actin, g) β-catenin, h) Reep5, i) RhoA, j) RPS3, k) Ubiquilin-1. Axon unit values for a particular sample which were above both Blank Near and Blank Far unit values for that sample are marked in bold. Axon unit values for a particular sample which are below either Blank Near or Blank Far unit values for that sample are italicised. 0 values where no signal was detected are coloured grey.

standard curves specific to each RNA and so cannot be compared directly. Also, as established in Section 4.4.4.1, the quantifications from these qRT-PCRs are not reliable and should be interpreted cautiously.

The figure shows that, according to one-tailed, paired t-tests, no significant differences could be found between Axons and Blank Near signals, or between Axons and Blank Far signals, for any RNA. This is perhaps unsurprising, as it was known that no significant difference could be found between these signals when the set of samples was first collected due to the wide variation in axonal signals (see Section 4.4.4.1) and these samples subsequently degraded after this first analysis. The figure shows the complete data sets for the RNAs where a signal was detected in any one condition (the RNAs where no signal was detected in Axons, Blank Near and Blank Far, which are Ascc3l1, BPGM, Rac1, Rock1, RPA1 and α-tubulin-OH, are considered to be absent from thalamic axons).

These full data sets show that where signals were found in the Blank Near or Blank Far conditions, the Axonal signal was above the blank signals, for all samples for 18S 1, 18S 2, 18S 3 and β-catenin. This is not true for β-actin, where the signal for Sample 2b was below the Blank Near signal for that sample, although the quantification for β-actin is not reliable because the r^2 value for this qRT-PCR was below the acceptable threshold. Indeed, because of the general doubts over the quality of these samples (discussed in Section 4.4.4.1), any unit value above 0 for a particular condition can only be used to indicate the presence of a signal in that condition. This means that it cannot be concluded that 18S, β-actin and β-catenin were present above contamination in these samples, although it is encouraging that axonal signals were detected in at least two samples for each of these RNAs.

For the remaining RNAs, Bat2d1, Reep5, RhoA, RPS3 and Ubiquilin-1, no signal was detected in either the Blank Near or Blank Far conditions for any sample, which indicates that signal detected in the axons is not from contamination. Signal was detected in two out of three samples for RPS3 and Ubiquilin-1 but only one sample for Bat2d1, Reep5 and RhoA. While the absence of these RNAs from at least one sample is concerning, it can be tentatively concluded that these RNAs are present in thalamic axons, although further confirmation with RNA samples of higher quality is desirable.

β-actin, β-catenin and RPS3 were repeated in Set 2 to confirm that they were present in both sets of samples. As discussed above, these RNAs were detected in both sets, although the signals found in Set 2 were considerably smaller than those

found in Set 1 and could not be statistically differentiated from the blank signals, but it is believed this is due to the poor quality of the Set 2 samples.

In conclusion, these two sets of qRT-PCRs provide good evidence for the presence of 18S, α-tubulin, β-actin, β-catenin, MAP2, Reticulon-1, RPS3 and Synaptotagmin 13 RNAs, and the absence of Ascc3l1, BPGM, Rac1, Rock1 and RPA1 RNAs in thalamic axons, and also suggest the presence of Bat2d1, EphB2, RalA, Reep5, RhoA and Ubiquilin-1 RNAs in these axons.

4.5 Discussion

There are several aspects of the method described in this chapter, and the results acquired using the method, which require further discussion. The qRT-PCR method has been modified in a number of ways which require justification, and the quality and validity of the results needs to addressed. Once these subjects have been considered, the presence or absence in thalamic axons of the RNAs investigated here can be put into context.

4.5.1 Application of qRT-PCR method

A number of decisions were made in the application of qRT-PCR to the detection of RNAs in axons which need to be justified. These decisions will now be explained.

4.5.1.1 Comparing axons and blanks

The primary purpose of using qRT-PCR rather than standard RT-PCR for these experiments is to discriminate between very small signals, such as those acquired from the Axons, Blank Near and Blank Far conditions, which it would not be possible to do with standard RT-PCR. Therefore, unit values for Axons, Blank Near and Blank Far have been compared for each RNA tested over each set of samples using one-tailed t-tests. These unit values are inferred from a standard curve for the RNA. The primary criterion for the presence of an RNA in axons is to find a significant difference between the signal from the axons and both of the two blank conditions.

As discussed in Section 4.2.2, variation in quantity of tissue is often controlled for using an internal standard. This does not make sense for the comparison of axons to blanks because it is not known what contaminating tissue may be present in the blanks and so it is expected that the internal standard will reflect the amount of contamination

reliably. This means that variation in number and size of explants between samples is not directly controlled for, although variation within samples is accounted for by taking the same number of pieces of insert for each of the Cells, Axons, Blank Near and Blank Far conditions. This lack of control for variation between samples does not matter where axonal conditions are of good quality, because the difference between these conditions and the blank conditions should be much larger than any variance caused by varying numbers of explants, as is the case for the Set 1 samples (see Figures 4.8 and 4.10). However, it may affect samples of poorer quality, such as those of Set 2, where it may be that the wide variation in axonal signal and the small signal from Sample 2c seen in Figure 4.13a meant that differences between axons and blanks could not be statistically distinguished.

It is not clear how this problem could be addressed, although it is probably best to simply ensure that axonal samples are of higher quality than those used for Set 2. The unit values could not be weighted by number of explants, for example, as the number of explants is not a reliable indicator of amount of axonal tissue in each sample, because the amount of axonal tissue dissected from each explant will depend on how much axonal tissue grew from the explant and how much could be dissected without contaminating the sample. However, it is not thought that this problem poses a significant difficulty for future applications of the method, providing samples of high quality are collected and processed promptly.

4.5.1.2 Internal standard for quantity of tissue

Although the primary purpose of the use of qRT-PCR is to detect differences between axons and blanks, it is also possible to compare cellular and axonal signals, and also to compare different RNAs, through the use of an internal standard, as presented in Section 4.4.3.3. Because each RNA is measured on a standard curve scale specific to the RNA, the units for one RNA can not be translated into units for another RNA. These units must be cancelled out by calculating ratios of axonal to cellular expression. These ratios can then be controlled for tissue quantity using the internal standard and compared.

As explained in Section 4.2.2, an internal standard gene is chosen to represent the amount of biological material in the test sample, so that any variation in amount of tissue across different samples can be controlled for. To study axonal RNA using qRT-PCR, an internal standard is required which is expressed in cells and axons at the same or similar levels. For these experiments, the ribosomal RNA 18S has been

used as a internal standard. It is known that ribosomes are present in axons (Bassell et al., 1998; Alvarez et al., 2000) and so the presence of 18S is expected. 18S has been shown to be the most stable indicator of amount of material compared to other standard controls such as β-actin and GAPDH in a number of studies on human cell populations (Bas et al., 2004; Goidin et al., 2001). There are also particular reasons for considering β-actin and GAPDH to be unsuitable as axonal internal standards. β-actin is known to be present in axons, as is 18S, but its expression is known to vary at the growth cone and so it is not suitable as an internal standard (see Section 1.5.5). It is not known whether GAPDH is present in axons or not, and therefore it cannot be relied on as an internal standard; given its roles in cellular processes such as glycolysis, transcription activation and apoptosis (Chuang et al., 2005) it would seem unlikely that it would be be present in axons as well, although the finding that GAPDH is involved in Src-dependent retrograde transport (Tisdale and Artalejo, 2007) might suggest otherwise, as the same mechanism is known to function in axons (Hüttelmaier et al., 2005). Nevertheless, given the lack of knowledge about GAPDH in axons at present, 18S remains the best choice for an axonal internal standard.

One of the implications of choosing 18S as an internal standard is the requirement to use random hexamers to prime the cDNA synthesis reaction, rather than oligo dT primers, because ribosomal RNA does not have a poly-A tail. In fact, random hexamers are known to be more efficient than oligo dTs and so are the best choice for cDNA synthesis regardless of choice of internal standard (Peters et al., 2004). A number of sources suggest that gene specific primers are ideal for cDNA synthesis (Peters et al., 2004; Wacker and Godard, 2005) but this is not feasible for this study because sufficient mRNA would be required to perform separate cDNA synthesis reactions for each RNA of interest and this quantity of mRNA cannot be easily acquired from axons.

4.5.1.3 Cycle number and replicates

Finally, the issues of cycle number and replicates must be addressed. Each qRT-PCR was run for 50 cycles to ensure that all reactions involving very small amounts of cDNA reached plateau. Rameckers et al. (1997) show that 30-35 cycles are not sufficient to successfully amplify small amounts of cDNA, particularly at less than perfect efficiency, and claim that using as high as 60 or 70 cycles should pose no problem as long as appropriate negative controls are performed to control for contaminants, as they have been here. In fact, for the qRT-PCRs presented in this chapter, 40 cycles would have been sufficient and should be considered sufficient for future applications

of the method. Also, the risk of amplifying contaminants is not as serious a problem for qRT-PCR as for standard RT-PCR, because it does not rely on end-point detection (measuring only the end products of a PCR) and so contaminants can be separated from amplicons by examining quantities and melting temperatures of products in experimental and control samples.

As described in Section 4.2.2, two types of replicates are desirable in a qRT-PCR experiment; biological replicates, where several samples of tissue are tested, and technical replicates, where the same sample is tested multiple times. Three biological replicates have been used for each set of RNAs tested for these experiments. However, because so few qRT-PCRs could be performed on each sample, and because so many RNAs were candidates for presence in axons, technical replicates were only performed for one RNA, 18S. It would be desirable to perform more technical replicates for each RNA, but given the difficulty of acquiring the samples, and the fact that the most important result of the method is to determine the presence or absence of the RNA in axons rather than the precise quantity of RNA in the axons, it is thought that a single qRT-PCR is sufficient for each RNA in this study.

4.5.1.4 Quality of Set 2 samples

As presented in Section 4.4.4.1, Figure 4.13b shows that while several indicators demonstrate that the samples used for the qRT-PCRs in Set 1 were of high quality (see Figure 4.8b), the Set 2 qRT-PCRs had a number of problems. The coefficients of determination (r^2 values) were questionable or unacceptable for most qRT-PCRs and the efficiencies of the reactions were almost all much lower than those for the Set 1 qRT-PCRs. Also, it was not possible to amplify many samples in the standard curve dilution series. This indicates that the standard curve dilution series used for these experiments had degraded and was not suitable for use. In addition, the Set 2 samples themselves were known not to be as high quality as those of Set 1 after cDNA synthesis and had degraded between cDNA synthesis and qRT-PCRs (see Section 4.4.4.1).

These problems mean that the quantifications for Set 2 cannot be considered reliable. However, this does not mean that the results are unusable. If a signal is found for a particular RNA in axons but no signal is found in either blank condition, this result can be treated as a standard RT-PCR and considered to indicate the presence of that RNA in axons. Using this criterion, the Set 2 data indicates that Bat2d1, Reep5, RhoA, Ubiquilin-1 and RPS3 are present in thalamic axons, and Ascc3l1, BPGM, Rac1, Rock1 and RPA1 are not. However, while signal was detected in axons for 18S,

β-actin and β-catenin in this set, nothing further can be concluded about these RNAs because signal was also detected in at least one of the blank conditions. The evidence for the presence of these RNAs in axons is solely to be found in the Set 1 data, but it is encouraging that the Set 2 data at least does not contradict this Set 1 data, as all of the repeated RNAs (18S, β-actin, β-catenin and RPS3) were detected in axons.

4.5.2 Presence of RNAs

What do the two sets of qRT-PCR results indicate about the presence or absence of RNAs in thalamic axons? Figure 4.10 shows that, for Set 1, there are significant differences between the axonal samples and blank samples for all the tested RNAs except EphB2 and RalA, which indicates that all of these RNAs were present in these samples of thalamic axons. For EphB2 and RalA, where no significant difference between axons and blanks could be found, it was the case that no signal was present in the blank conditions at all, and therefore it is reasonable to conclude that these RNAs are also present in thalamic axons.

For Set 2, while the quantifications are not reliable and no significant differences can be found between axons and blanks, there are several RNAs where a signal was detected in axons and no signal was detected in either of the blanks (Bat2d1, Reep5, RhoA, RPS3, Ubiquilin-1) and several more where no signal was detected in any of the samples (Ascc3l1, BPGM, Rac1, Rock1, RPA1, α-tubulin-OH). This indicates that the first group of RNAs is present in axons but the second group is not.

Therefore, to summarise, it can be concluded that the qRT-PCRs presented here provide evidence for the presence of 18S, α-tubulin, β-actin, β-catenin, Bat2d1, EphB2, MAP2, RalA, Reep5, RhoA, RPS3, Reticulon-1, Synaptotagmin-13 and Ubiquilin-1 RNAs in thalamic axons, and indicate the absence of Ascc3l1, BPGM, Rac1, Rock1 and RPA1 from these same axons.

Of these mRNAs, α-tubulin, β-actin, RhoA and EphB2 proteins have well characterised roles in axon growth and guidance and the identification of their mRNAs in thalamic axons supports the case for the involvement of the proteins in thalamic axon development. α-tubulin and β-actin are core components of the cytoskeleton, with α-tubulin forming microtubules and β-actin forming actin filaments. RhoA is an intermediary between Sema3A and actin filaments, with a crucial role in axon collapse in some systems (see Section 1.5.4). The identification of RalA here indicates that a wider survey of the small GTPases would be of interest in these axons and in other

axonal systems, especially since RalA has been shown to regulate neurite branching in rat sympathetic neurons (Lalli and Hall, 2005).

EphB2 is the only guidance cue-related molecule which has been investigated here, but the identification of the mRNA for this receptor suggests that the mRNAs for other receptors known to be present in thalamic axons should be investigated, such as EphA2, DCC, Robo1 and Robo2. In addition, while the regulation of mRNAs for cytoskeletal proteins such as β-actin has been investigated in some detail, very little is known about how new receptors are translated in response to guidance cues (as shown by Brittis et al. (2002)). Thalamic axons may prove to be a good model of this behaviour given the variety of responses to guidance cues by different populations of thalamic axons (see Section 1.4.2.4).

The identification of RPS3 mRNA and 18S rRNA in thalamic axons in these experiments strongly suggests the presence of ribosomes in these axons, and indicates that further experiments should be carried out to detect the location of these ribosomes in these axons and to demonstrate that protein synthesis occurs at these locations. Many mRNAs for ribosomal proteins were identified by Willis et al. (2007) in their survey of regenerating rat dorsal root ganglion axons, which suggests that other ribosomal protein mRNAs will be found in developing thalamic axons. Similarly, the identification of reticulon-1 mRNA in these experiments suggests that the reticulon proteins should be investigated further in thalamic axons, as reticulon-1 has been shown to colocalise and interact with spastin, which is involved in microtubule dynamics and vesicle transport in axons (Mannan et al., 2006; Steiner et al., 2004), and reticulon-4 is known to trigger growth cone collapse (although this is via oligodendrocytes; Yang and Strittmatter (2007)).

The functions of ubiquilin-1 and synaptotagmin-13 in axons is less clear, although synaptotagmin-13 has been shown to bind to neurexin 1α (Fukuda and Mikoshiba, 2001), and neurexins are required in axons for presynaptic terminals to form (Dean et al., 2003). Similarly, the β-amyloid precursor protein (APP), the precursor of β-amyloid, which is the peptide that clusters together in plaques and causes Alzheimer's disease, is expressed in neuronal processes and is required for neurite outgrowth (Young-Pearse et al., 2008), and ubiquilin-1 is required to transport APP from intracellular compartments to the cell surface (Hiltunen et al., 2006), and so it is possible that it performs a similar function in axons. The remaining RNAs, Bat2d1 and Reep5, have been identified in large surveys of gene expression and have not yet been investigated in their own right, and so it is not possible to speculate on what might

be their roles in axonal function.

These results mostly agree with the literature on RNAs in other axonal systems, in that 18S (Alvarez et al., 2000), β-actin (Bassell et al., 1998), EphB2 (Brittis et al., 2002) and RhoA (Wu et al., 2005) were all found to be present in thalamic axons, whereas Rock1 and Rac1 were not (Wu et al., 2005). In addition, seven of these RNAs (Bat2d1, RalA, Reep5, RPS3, Reticulon-1, Synaptotagmin-13 and Ubiquilin-1) have never been identified in any axonal system prior to this study, and none of the RNAs identified here (or any other RNAs) have previously been identified in thalamic axons. There are also two mRNAs which have been found in thalamic axons which have not been found in other axonal systems, namely α-tubulin and MAP2. It is possible that these mRNAs are present in thalamic axons but not other systems; however, it is also possible that they are absent from thalamic axons and the detection of these mRNAs is due to the presence of contaminating cellular or dendritic mRNA in the axonal samples. These alternatives will now be considered.

4.5.2.1 α-tubulin

α- and β-tubulin are crucial proteins in developing neurites, as they form the backbone of microtubules which are central parts of the neurite cytoskeleton and which are heavily involved in growth cone turning (see Section 1.5.1). Therefore, given the presence of the mRNA for the similarly crucial β-actin (see Section 1.5.5), it is perhaps not surprising that α-tubulin mRNA might be found in axons. Indeed, β-tubulin has already been shown to be synthesised in distal rat sympathetic ganglion axons (Eng et al., 1999).

Despite this, α-tubulin was found to be absent from sympathetic ganglion axons in chick using qRT-PCR by Olink-Coux and Hollenbeck (1996) and in rat using in situ hybridisation by Bruckenstein et al. (1990). This result does not necessarily negate the result presented here, because it may be that thalamic axons, or axons in the brain in general as opposed to the spinal cord, behave differently to sympathetic ganglion axons. Indeed, α-tubulin mRNA has been found in Aplysia central nervous system neurites (Moccia et al., 2003).

In fact, the discrepancy between the results presented here and those in the literature can be accounted for by examining the primers used. The primers used here for α-tubulin for the Set 1 qRT-PCR results were designed de novo from the α-tubulin mRNA sequence and did not match the primers used by Olink-Coux and Hollenbeck (1996). The primers used were designed to bind to mouse α-tubulin 1a, whereas the

primers used by Olink-Coux and Hollenbeck (1996) were designed to bind to chick α-tubulin 5 (tba5_chick), which is the homologue of mouse α-tubulin 1c. However, the discrepancy between the results presented by Olink-Coux and Hollenbeck (1996) and those presented here cannot be accounted for by the fact that they were designed to bind to two different variants of α-tubulin, because both α-tubulin 1a and α-tubulin 1c contain binding sites for both the primers used in this thesis and the primers used by Olink-Coux and Hollenbeck (1996) and are homologous throughout the regions amplified by both pairs of primers.

A further qRT-PCR using primers which were homologous in mice to the primers used by Olink-Coux and Hollenbeck (1996) in chicks (labelled α-tubulin (OH) in Figures 4.5, 4.13 and 4.14) showed that it was not possible to detect α-tubulin in thalamic axons using these primers, although a signal could be detected in thalamic cells (in agreement with Olink-Coux and Hollenbeck (1996), who found a signal in chick sympathetic ganglion cells with these primers). This indicates that differences in the primers led to a difference in detection. Either something prevents the primers used by Olink-Coux and Hollenbeck (1996) from binding to either α-tubulin variant efficiently (perhaps this region is folded in such a way to interfere with binding with another RNA, or a protein is already bound to this region), or the primers used in this thesis may be binding to something other than α-tubulin. While this cannot be ruled out, a BLAST search for these primers against the mouse genome reveals no other known gene sequence which matches the sequences of both primers. Therefore it seems likely that the primers used by Olink-Coux and Hollenbeck (1996) were less efficient than the primers used in this thesis and, while these primers could amplify mRNA in cells, they were not able to amplify the very small quantities of α-tubulin mRNA present in axons.

In addition, in a separate experiment to their α-tubulin in situ hybridisation, Bruckenstein et al. (1990) were unable to detect any poly(A) RNA in axons, although they were able to detect some in dendrites, which indicates that their in situs were not sufficiently sensitive to detect axonal RNA in general, and so their failure to detect α-tubulin may simply reflect a lack of sensitivity of their in situ technique.

Finally, in their recent cDNA microarray survey of rat dorsal root ganglion axonal RNAs, Willis et al. (2007) et al repeatedly identified α-tubulin as one of the RNAs present in these axons. Therefore it seems reasonable to conclude that α-tubulin mRNA can be found in thalamic axons.

4.5.2.2 MAP2

A very small quantity of MAP2 was detected in the qRT-PCRs presented here (see Figure 4.10). MAP2 had the lowest ratio of axon-to-cell expression of all the RNAs tested, with 9-fold lower expression in axons than cells (see Figure 4.11).

MAP2 is often used as a marker to differentiate axons and dendrites (Dehmelt and Halpain, 2004). This is supported by a series of papers showing that MAP2 protein and mRNA is present in dendrites but absent from axons of cultured sympathetic neurons (Higgins et al., 1988; Bruckenstein et al., 1990), hippocampal neurons (Caceres et al., 1984a; Bruckenstein et al., 1990) and P19 neuronal cells (Aronov et al., 2001). These *in vitro* results are supported by a number of *in situ* studies in cerebral cortex, hippocampus and cerebellum (Caceres et al., 1984b; Camilli et al., 1984; Huber and Matus, 1984). Aronov et al. (2001) also shows that when the 3'UTR of the axonal marker tau is replaced with the 3'UTR of MAP2, the tau construct is found in dendrites but not axons (see discussion in Section 1.5.3).

These results suggest that the MAP2 found in the axonal samples presented here came from some other source, either dendrites or cells, and therefore the other detected RNAs cannot reliably be considered axonal RNAs. However, there are a number of reasons why the qRT-PCR results presented here may be accurate and that very small amounts of MAP2 mRNA are present in axons.

Firstly, MAP2 is found in a number of different isoforms of high molecular weight (MAP2a and MAP2b) and low molecular weight (MAP2c) (Langkopf et al., 1994). The high molecular weight isoforms are the forms which are found in dendrites but not axons. However, the low molecular weight isoform MAP2c has been found in developing axons (Meichsner et al., 1993; Tucker et al., 1988) and so it is not surprising to find it expressed in developing thalamic axons. The MAP2 primers used for these qRT-PCRs identified a sequence present in both MAP2b and MAP2c. In light of this, it is likely that the signal detected here is for the short MAP2c isoform rather than the long MAP2b isoform, and that therefore this signal should not be considered to invalidate the other results.

In addition, it is possible that the signal detected here is from the long MAP2b isoform. Firstly, some of the early results cited above do show very small amounts of staining for high molecular weight MAP2 in axons, although it is much lower than the staining in dendrites (see for example Caceres et al. (1984b)), and it may be that there was a very small amount of MAP2b present which was below the limits of detection

of the methods used in previous studies. Secondly, E14.5 thalamic axons have not previously been tested for MAP2b and it may be that this system behaves differently to previously tested systems, which were all tested at later points in development.

One reason for considering this possibility is that all of the results listed above are from cultures containing axons and dendrites. Higgins et al. (1988), in addition to showing the absence of MAP2 in such a culture, show that in cultures where dendrite growth is suppressed, MAP2 protein is found in axons. This peculiar effect appears not to have been investigated further, but it may be that in the cultures presented here a similar effect took place.

To summarise, it is not clear whether the MAP2 signal detected here has come from MAP2b sourced from cells or dendrites, MAP2c sourced from axons, or a novel MAP2b signal from axons, but it is most likely that the signal is from MAP2c as this is known to be expressed in developing axons. The matter could be settled by running more qRT-PCRs on similar axonal samples using primers designed specifically for MAP2b. But it seems reasonable to conclude that, given the small amount of signal, this result should not be considered to compromise the other qRT-PCR results.

4.5.3 Comparison of RNAs

The main reason for using quantitative RT-PCR rather than standard RT-PCR for these experiments was to detect very small differences in RNA quantity. For example, in a standard RT-PCR it would not be possible to distinguish between axons and blanks where a small blank signal is detectable, because both reactions would plateau at similar levels which do not represent the actual quantities of RNA in the original samples. The quantitative data from qRT-PCR allows the axon and blank signals to be distinguished.

In addition to this primary use, the quantitative data can be used to compare the expression of different RNAs in axons and cells. Using the method described in Section 4.3.4, ratios of axonal to cellular expression can be produced, which are controlled for tissue quantity by standardising each ratio against the ribosomal RNA 18S (see Section 4.5.1.2 for justification of the use of 18S as internal standard). The ratios for the qRT-PCRs in Set 1 are shown in Figure 4.11. No comparison of ratios has been made for Set 2 because the quality of the quantitative data from this set of qRT-PCRs is questionable (see Section 4.5.1.4).

These ratios must be interpreted with care. For example, MAP2 shows 9-fold

less expression in axons than in cells, compared to a 2.5-fold decrease of β-catenin expression. But this does not mean that there is 3.6 times less MAP2 than β-catenin in axons, because the cellular expression of these two RNAs may not be equivalent. However, the ratio does indicate that there is 3.6 times less enrichment of MAP2 in axons than of β-catenin when compared to cellular expression, which may reflect a real difference in cellular and axonal metabolism.

Indeed, the fact that the expression ratios for different RNAs vary supports the case that axonal RNA has been detected rather than potential contaminating cellular RNA. Assuming that different samples of cellular RNA will exhibit the same profiles of gene expression, it would be expected that a comparison of cellular RNA to cellular RNA would not show any variation in expression ratios. As the ratios of expression in the Set 1 RNAs do vary, with one showing enrichment and the others showing different levels of depletion, this suggests that the RNAs shown here have come from a different type of tissue, thalamic axonal tissue, in which genes are expressed at different levels to their expression in thalamic cells.

The ratios shown here indicate that overall there is less of an enrichment for the RNAs tested in axons than there is in cells (with the exception of the enriched RPS3). This perhaps explains why RNAs were not detected in axons for many years (Alvarez et al., 2000). It appears that a very small quantity of RNA is required in axons for sufficient protein to be locally translated. It is also worth speculating that this might reflect requirement for the RNAs in the growth cone but not in the main body of the axon. Ribosomes are found all the way along axons and in growth cones, and some RNAs such as GAP-43 mRNA have also been found in axons and growth cones (Smith et al., 2004). However, if an RNA was only found in growth cones, it would appear to be depleted when measured against the expression of 18S, because 18S, as part of the ribosome, should be found all the way along the axon. Therefore the depletions seen in the axon:cell expression ratios may reflect the fact that the RNAs are only expressed in part of the axon.

4.6 Conclusion

In this chapter, the results from a study of RNAs in developing thalamic axons using the method described in Chapter 3 and the current chapter have been presented. Evidence has been provided for the presence of several novel RNAs in these axons, many of which already have intriguing connections with axonal function which are worthy of

further investigation. This evidence indicates that the roles demonstrated for β-actin mRNA (Leung et al., 2006; Yao et al., 2006) and hypothesised for RalA, Reticulon-1, RPS3, Synaptotagmin-13 in other axonal systems (see Section 1.6.1) are also worth investigating in thalamic axons. They also suggest that the speculations about β-catenin function in axons in Section 1.6.2 could be tested in thalamic axons. Despite some problems with sample quality, it has been shown here that it is possible to generate high quality quantifications of RNA from axonal samples and to use these quantifications to infer the presence or absence of these RNAs in axons. This method should be applicable to any system where axons can be isolated from other tissue.

Chapter 5

In situ hybridisations for β-catenin and other RNAs in thalamic axons

5.1 Introduction

Several RNAs have previously been identified in axons using in situ hybridisation, where a detectable probe is bound to an RNA of interest in a tissue sample (Bassell et al., 1998; Wu et al., 2005; Aronov et al., 2001). This chapter describes a number of attempts to use in situ hybridisation to identify β-catenin mRNA in thalamic axons. β-catenin mRNA was chosen for investigation from the mRNAs identified in Thomas Pratt's mRNA library (see Section 1.6.1) due to the known presence of β-catenin protein in growth cones, and its known roles in cell adhesion and Wnt-signalling-related pathways, which are required for Slit and neurotrophin growth cone signalling (see Section 1.6.2 for details). In addition, β-catenin mRNA has been shown to be present in thalamocortical axons in Chapter 4. Many probes, cultures and in situ protocols have been attempted in order to demonstrate the presence of β-catenin mRNA in thalamic growth cones, each of which will be considered in what follows. In the process, it will also be shown that β-actin mRNA and 18S rRNA are present in thalamic axons and growth cones.

5.2 Materials and methods

5.2.1 Probes

In situ hybridisation requires a labelled probe which will bind to an mRNA of interest by complementary base-pairing. These probes can be DNA or RNA molecules, can be of varying lengths and can be synthesised with different labels.

Long β-actin (βActL) Antisense probes were synthesised using a control template from Ambion (Catalogue number 7423) which complements and is intended to bind to a 249bp fragment of mouse β-actin mRNA.

Long β-catenin (βCatL1 and βCatL2) Antisense and Sense probes were synthesised using two separate templates constructed for this project according to the methods in Section 2.3.2. The probes were constructed from the i3156732 clone of β-catenin from the I.M.A.G.E. Consortium (Lennon et al., 1996). βCatL1 was constructed from the full i3156732 clone; βCatL2 was constructed from a subclone of the i3156732 clone containing only the β-catenin 3'UTR.

Clones were inserted into a vector and amplified. βCatL1 was inserted into pCMV-SPORT6 (Invitrogen) whereas βCatL2 was inserted into pBSIIKS(+) (Stratagene). The clones were then linearised to produce Antisense and Sense cDNA templates for each probe; these cDNA templates were then transcribed into digoxigenin-labelled RNA probes. The βCatL1 Antisense template was cut using SalI (Roche, Catalogue Number 10348783001) and transcribed from a T7 promoter. The βCatL1 Sense template was cut using NotI (Roche, Catalogue Number 11014706001) and transcribed from an SP6 promoter. The βCatL2 Antisense template was cut using PstI (Roche, Catalogue Number 10621625001) and transcribed from a T7 promoter. The βCatL2 Sense template was cut using NotI and transcribed from a T3 promoter. T7 (Roche, Catalogue Number 10881767001), T3 (Roche, Catalogue Number 11031163001) and SP6 (Roche, Catalogue Number 10810274001) RNA Polymerases were used for transcription. See Figure 5.2 for probe maps.

All oligoprobes were designed with OligoArray software (Rouillard et al., 2003) and synthesised by MWG. OligoArray tests for specificity of designed oligos by attempting to align input sequences (eg β-catenin 3'UTR) against a reference genome with the sequence alignment software BLAST (Altschul et al., 1990), only keeping those parts of the input sequence which do not match any other sequence in the genome. Only the forward strand of input DNA is searched as this is the strand which will produce labelled probes during reverse transcription. The smallest BLAST word

size possible (7) is used to detect the maximum number of sequence similarities.

Labelling of all probes was carried out by *in vitro* transcription, as described in Chapter 2.

5.2.2 Cultures

Two different culture methods were used to generate thalamic axons for testing using in situ hybridisation, one based on dissociated thalamic cells and one based on thalamic explants. These methods are now described.

5.2.2.1 Dissection of thalami

Thalamic explants for both culture systems were dissected as follows. Embryonic mouse brains (CBA or CD1 strains, E14.5) were dissected in ice-cold EBSS. The midbrain and hindbrain were cut away from the forebrain and cut in half along the sagittal plane. Each half was laid flat, allowing the thalamus to be seen and dissected. These whole thalami were then cultured as described below.

5.2.2.2 Coverslips

Coverslips for both culture systems were prepared as follows. Coverslips were sterilised by heating, placed in Nunclon 4-well dishes (well area $1.9cm^2$, VWR, UK), coated for at least two hours with 0.1mg/mL poly-L-lysine (from 10mg/mL solution, Sigma, UK), washed three times with distilled water, coated for at least one hour with 1 μg/mL fibronectin (from 1mg/mL solution, Sigma, UK) and briefly washed once with basal culture medium (see Section 2.2.2 for recipe).

5.2.2.3 Dissociated culture

Thalami were dissociated using a Worthington Papain Dissociation Kit (Lorne Laboratories, USA) according to the manufacturer's instructions, and plated on glass coverslips (see Section 5.2.2.2). The density of dissociated cells was calculated using a haemocytometer. Cells were plated at a density of 1,500 cells/mL, diluted in basal culture medium, and incubated at 37 °C in 95% oxygen, 5% carbon dioxide for two days.

5.2.2.4 Explant culture

Thalami from E14.5 mouse brains were sliced into roughly 50-70 pieces each using a sterile blade (Altomed, UK, Catalogue Number A10136). Thalamic pieces were plated on coverslips prepared as described in Section 5.2.2.2, with all the pieces from one thalami being plated on one coverslip. As far as possible, pieces were evenly distributed across the coverslip. Explants were incubated at 37°C in 95% oxygen, 5% carbon dioxide for 4-6 days.

5.2.3 In Situ Protocols

Several different protocols which were used to detect RNA in thalamic axons are now described. The recipes for the solutions for these protocols can be found in Section 2.4.2. All treatments were performed at room temperature unless otherwise stated.

5.2.3.1 Colorimetric wax section in situ protocol

E14.5 mouse heads were fixed in 4% paraformaldehyde, washed three times in 1xPBS, embedded in wax and sectioned. Slides containing wax sections were treated twice with histoclear for ten minutes, twice with 100% ethanol for five minutes, twice with 70% ethanol for five minutes and once with 2xSSC for five minutes. Slides were permeabilised in 5μg/mL Proteinase K for 7.5 minutes and washed with 2xSSC for thirty minutes. Slides were fixed with 4% paraformaldehyde for fifteen minutes and treated with 0.2M HCl for fifteen minutes. Slides were acetylated in 1xTEA for thirty seconds followed by 3μL/mL acetic anhydride in 1xTEA for ten minutes. Slides were pre-hybridised in hybridisation mixture in a humid chamber for thirty minutes and hybridised with probe (120ng per slide) at 50°C overnight.

After hybridisation, slides were washed with 2xSSC at 50°C for ten minutes, 2xSSC/50% formamide at 60°C for forty-five minutes and 4xSSC at 50°C for five minutes. Slides were treated with RNAse A (2μg/mL) in 4xSSC at 37°C and washed with 2xSSC at 50°C for thirty minutes, 1xPBS/0.1% Triton-X at room temperature for ten minutes, 1xPBS/0.1% Triton-X/1% BSA at room temperature for thirty minutes. Anti-DIG AP antibody (1:2000) in 1xPBS/0.1% Triton-X/1% BSA was applied at 4°C overnight. Slides were washed in 1xPBS/0.1% Triton-X three times for twenty minutes and Buffer 3 for five minutes. NBT/BCIP (1:1000) in Buffer 3 was applied overnight to stain antibody. Slides were rinsed in distilled water and mounted with Aquamount under glass coverslips.

5.2.3.2 Fluorescent axon in situ protocol

This protocol was kindly provided by Samie Jaffrey (Weill Cornell Medical College; protocol used for axonal in situs in Wu et al. (2005)). Cultured axons were fixed in 4% paraformaldehyde/1xTBS overnight and washed twice for five minutes in 1xTBS. The axons were permeablised for ten minutes in 0.5% Triton X-100 in 1xTBS, fixed for another five minutes in 4% paraformaldehyde/1xTBS and washed three times for five minutes in 0.1% Triton X-100/1xTBS. Axons were acetylated for ten minutes in fresh acetylation solution, washed three times for five minutes in 0.1% Triton X-100/1xTBS and pre-hybridised for 20 minutes in 4xSSC/50% formamide. Probes were hybridised overnight at 60 °C in hybridisation buffer.

After hybridisation, axons were washed in 40% formamide/1xSSC for twenty minutes at 37 °C, then three times for five minutes in 1xSSC, three times for five minutes in 0.1xSSC and thirty minutes with Antibody Blocking Solution. Primary anti-digoxigenin antibody (Clone DI-22, Sigma, UK), diluted 1:500 in Antibody Blocking Solution, was applied to the axons overnight at 4 °C and washed with three five minute washes in 0.1% Triton X-100/1xTBS. Secondary antibody (Molecular Probes, Alexa), diluted 1:1000 in Antibody Blocking Solution, was applied for 1 hour at 4 °C in the dark and washed with three five minute washes in 0.1% Triton X-100/1xTBS in the dark. Coverslips were then dipped in distilled water, air dried and mounted in Mowiol on glass slides.

5.2.3.3 Colorimetric axon in situ protocol

Cultured explants were fixed in 4% paraformaldehyde/1xPBT, pH 9.5, for 1 hour and washed twice for five minutes in 1xPBS. The explants were permeabilised in 20μg/mL proteinase K in PBS at 37 °C, washed in 0.2% glycine in PBS and washed twice for five minutes in 1xPBS. Explants were fixed for another 20 minutes in 4% paraformaldehyde/1xPBS and washed twice for five minutes in 1xPBS. Explants were pre-hybridised in hybridisation mixture at 70 °C in a humid chamber (humidified with 50% formamide/2xSSC). For each probe, 20μL of probe in hybridisation mixture (1ng/μL) was placed on a hydrophobic slide. Coverslips containing explants were placed on top of probe mixtures and placed in a humid chamber overnight for hybridisation.

After hybridisation, explants were washed for five minutes in 2xSSC (pH 4.5) and twice for fifteen minutes in 50% formamide/2xSSC at 65 °C. The explants were then

washed three times for 10 minutes in PBS/0.1% Tween and pre-blocked for 1 hour in 1% Boehringer block (Roche, UK). Anti-digoxigenin alkaline phosphatase (Roche, UK) in Boehringer block (1:500) was applied to explants at 4 °C overnight and washed with three five minute washes in PBS/0.1% Tween and one ten minute wash in Buffer 3. Explants were stained with NBT/BCIP (Roche, UK) in Buffer 3 (1:50). When staining was considered complete, the coverslips were dipped in water and mounted in 10μL Mowiol mounting solution.

5.2.3.4 Image processing

Images of colorimetric staining of axons (Figures 5.8, 5.12 and 5.15), where background intensities varied across different images, were normalised to the same background intensity using ImageJ, so that staining across images could be compared (Abramoff et al., 2004). For Figures 5.12 and 5.15, the mean pixel intensity of an area of background was calculated for each image. The image with highest mean pixel intensity was chosen as a standard. Each other image was then lightened to match the mean pixel intensity of the background of the chosen standard. For each image, each pixel in the image was multiplied by a scale factor to lighten the image. The scale factor was the ratio of the mean pixel intensity of background of the standard image compared to the mean pixel intensity of background of the image to be modified. Different background levels were used for long probes and oligoprobes. For Figure 5.8, the images were darkened rather than lightened by matching to the image with the lowest mean pixel intensity and also processed using ImageJ's Sharpen facility to make the axons visible.

For quantification and statistical analysis of staining, axons from multiple images of a single in situ hybridisation were traced using ImageJ (see Figure 5.17 for example trace) and the intensities of pixels along each axon were recorded. As many axons as possible were selected, provided the following criteria were satisfied: axons were selected where no crossover with other axons or cells could be seen, and where the axon could be seen along its entire length above background levels, so that the length of the axon could be traced with accuracy. These pixel intensity traces were then analysed using the R program listed in Appendix A. As with image normalisation, long probes and oligoprobes were treated as separate sets of images.

So that different axons could be compared, the intensity and position of each pixel along each axon were converted to percentages. Positions of pixels were converted to percentages of axon length, and intensity was converted to percentages of the highest

pixel intensity for all axons in the set (either long probes or oligoprobes). Each trace was then split into bins of 5% axon length; for example, all of the pixels in the first 5% of the length of the axon for an image were placed in the first bin. The means of the pixel intensities for all pixels in each bin for each image were calculated, and an overall mean pixel intensity and standard error of the mean calculated for each bin over all images. The sets of mean pixel intensities for each bin and image for different probes could then be compared using a one-tailed Wilcoxon rank sum test for independent, non-parametric distributions and the results plotted using the errbar function in the R Hmisc package (Harrell, 2005). The Wilcoxon rank sum test was conservatively used instead of Student's t test as some (but by no means all) of the distributions of binned intensities were skewed away from normality. The set of p-values for each pair of probes (20 p-values for each set) were adjusted using Bonferroni's correction to reduce the chance of making Type I errors with multiple tests.

5.3 Results

In this section, a series of in situ hybridisation experiments are presented, designed to test for the presence or absence of β-catenin mRNA in thalamic axons. Several different probes, culture systems and protocols have been used for these experiments. The design of all the probes used is given, followed by the results acquired with two different long probes and a set of oligoprobes. Finally, a statistical analysis of the images acquired with these probes is presented, which demonstrates the presence of β-catenin, β-actin and 18S RNAs in thalamic axons.

5.3.1 Probe design

A series of in situ hybridisations were performed using long riboprobes designed to bind to β-catenin mRNA. Two separate long DNA templates were designed both of which were based on a clone from the I.M.A.G.E. Consortium (Lennon et al., 1996) which matched part of the β-catenin mRNA sequence. Each template was used to produce two separate RNA probes by *in vitro* transcription, one for each of the two strands of the DNA template (see Figure 5.1 for diagram and Figure 5.2a/b for probe maps). One of these probes should therefore be the same as part of the β-catenin mRNA sequence and is labelled the sense probe. The other probe should be complementary to the β-catenin mRNA sequence and is labelled the antisense probe.

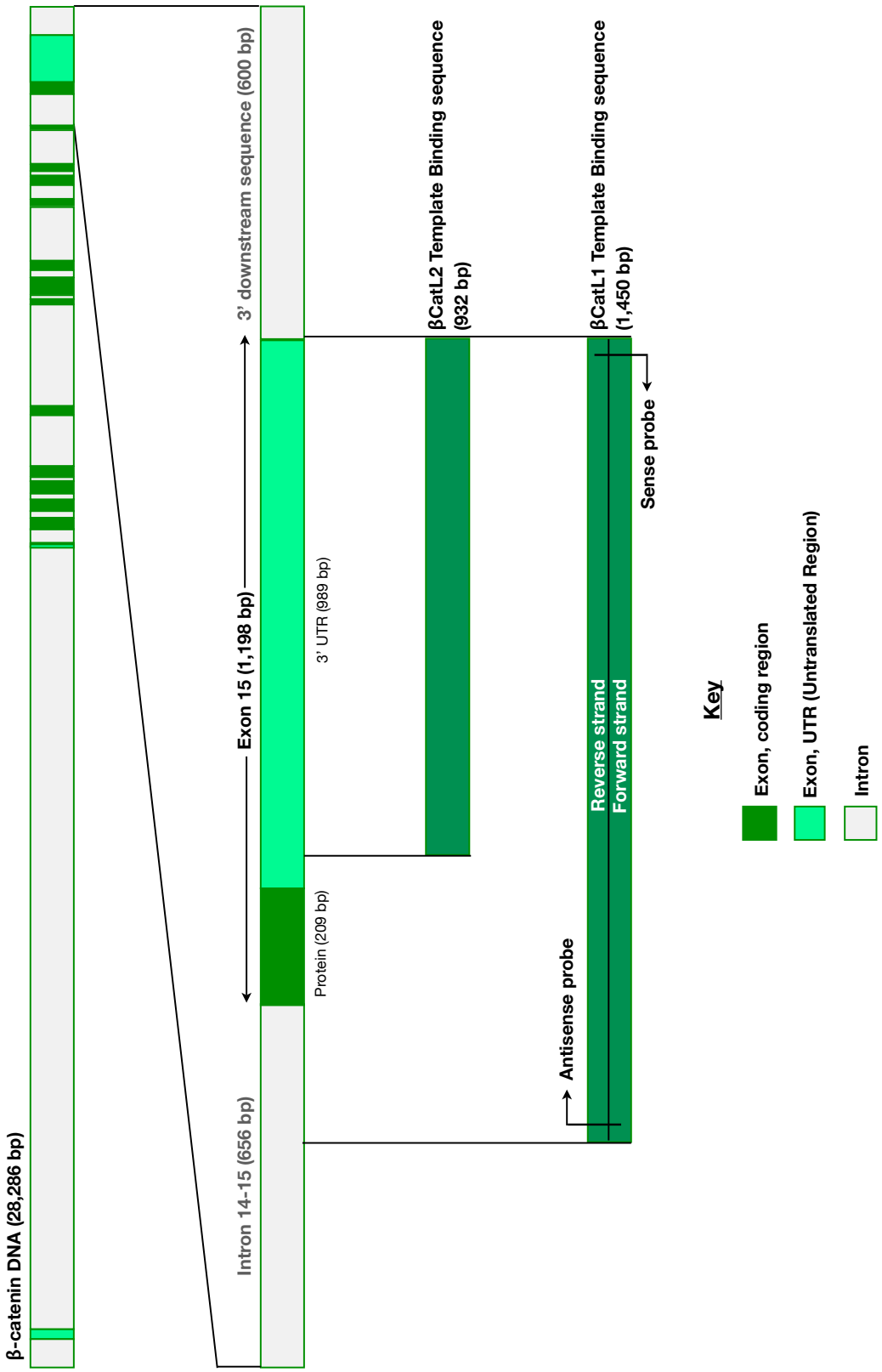

Figure 5.1: Long in situ riboprobes were designed to bind to the 3'UTR of β-catenin. Mouse β-catenin DNA (top, MGI Symbol Ctnnb1, Ensembl Ref ENSMUSG00000006392) has 15 exons, the last of which contains the 3'UTR (shown magnified in the centre of the diagram). The two long probes used for in situ hybridisations both bind to this 3'UTR. pβCatL1 binds part of the intron between Exons 14 and 15 as well as both the coding region and 3'UTR of Exon 15. pβCatL2 binds only the 3'UTR. The antisense probes are transcribed from the forward strand of the DNA, whereas the sense probes are transcribed from the reverse strand.

The antisense probe is used to detect β-catenin mRNA in situ, whereas the sense probe is used as a negative control. The use of antisense and sense probes is discussed further in Section 5.4.1.3.

Figure 5.1 shows the design of the two long riboprobes used to detect β-catenin using in situ hybridisation. The figure shows that both probes bind to the 3'UTR of β-catenin, which is found in the last exon of the gene, Exon 15. This exon also contains a protein-coding region upstream of the 3'UTR.

The two probe templates are denoted as βCatL1 and βCatL2, where L stands for Long probe. The first probe template, βCatL1, matches the entire 3'UTR but also matches the protein coding region of Exon 15 and part of the intron between exons 14 and 15. Because of problems using this probe template (which will be shown in the following sections), the second probe template, βCatL2, was designed to match the 3'UTR only, although it does not match the entire 3'UTR as βCatL1 does. Both probes match only the NCBI reference and Celera alternative β-catenin genomic sequence when BLASTed against the NCBI mouse build 37 genome database using the default parameters (E=0.01). The probe maps for both probes can be seen in Figure 5.2a/b.

In addition to these two probes, a β-actin cDNA template was purchased from Ambion, which was used to make a β-actin antisense probe for use as a positive control. This probe is denoted βActL Antisense from this point forward. As this template only had RNA polymerase promoters at one end, it was not possible to make a sense probe for β-actin using this template.

Figure 5.2 shows the sequences of thirteen oligoprobes used to detect 18S rRNA and β-catenin, β-actin and RPS3 mRNAs. For each RNA, three separate oligoprobes intended to bind to different parts of the RNA molecules were used, to maximise any signal present. All oligoprobes were tested for specificity by the oligo design software OligoArray by running BLAST against the mouse genome on each sequence that the oligoprobes were intended to bind to against, with only unique parts of these sequences used to find suitable oligos (see Section 5.2.1 for details). A single control probe was designed, called Scrambled, which was a randomised sequence of nucleotides which did not match any part of the mouse genome (BLAST returned no hits against Ensembl release 47 of the mouse genome, E=1e-10). RPS3 oligoprobes were not used for axonal in situ hybridisations but were used for the in situ hybriidsations on coronal sections presented in Chapter 6.

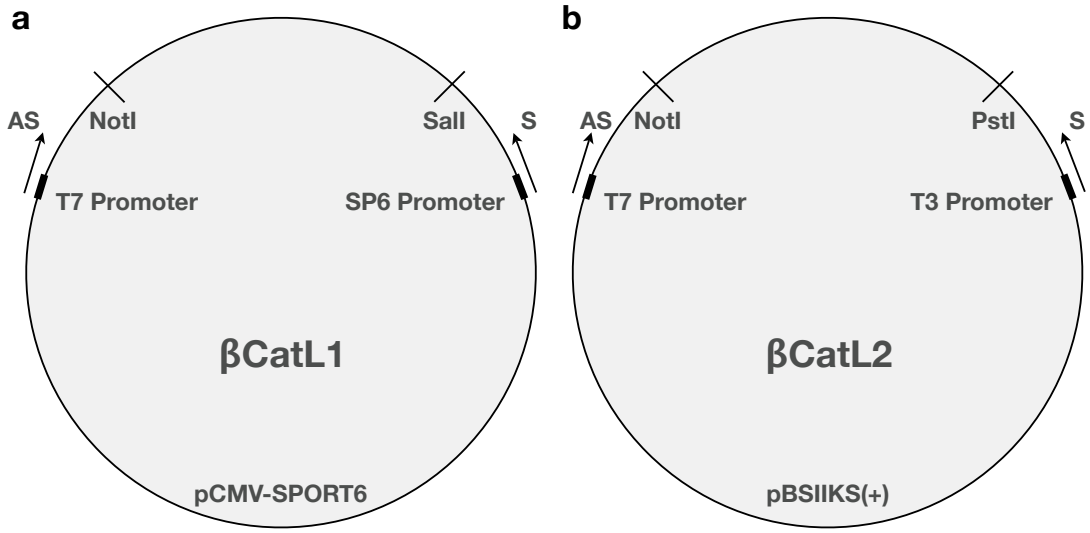

c

RNA	Sequence
18S	**CCTTTAACGAGGATCCATTGGAGGGCAAGTCTGGTGCCAG**CTATAGTGAGTCGTATTACA
	TCTGCCCTATCAACTTTCGATGGTAGTCGCCGTGCCTACCCTATAGTGAGTCGTATTACA
	GGGGGGGATGCGTGCATTTATCAGATCAAAACCAACCCGGCTATAGTGAGTCGTATTACA
β-actin	**GGCCTGTACACTGACTTGAGACCAATAAAAGTGCACACCT**CTATAGTGAGTCGTATTACA
	TCCCCCCAACTTGATGTATGAAGGCTTTGGTCTCCCTGGGCTATAGTGAGTCGTATTACA
	ACATCCCCCAAAGTTCTACAAATGTGGCTGAGGACTTTGTCTATAGTGAGTCGTATTACA
β-catenin	**TCACAAGATGGCGTTATCAAACCCTAGCCTTGCTTGTTCT**CTATAGTGAGTCGTATTACA
	CATTGTGATTGGCCTGTAGAGTTGCTGAGAGGGCTCGAGGCTATAGTGAGTCGTATTACA
	GGTGGGAATGGTTTTAGGCCTGTTTGTAAATCTGCCACCACTATAGTGAGTCGTATTACA
RPS3-1	**TGCCTACAGCATAACAGGGTCTTGGCAGCTGCATCTGGAG**CTATAGTGAGTCGTATTACA
RPS3-2	**GAAATCCTGCCCACGACCCCCATCTCCGAACAGAAGGGTG**CTATAGTGAGTCGTATTACA
RPS3-3	**GACAGGGTGTGCTGGGCATCAAAGTGAAGATCATGCTGCC**CTATAGTGAGTCGTATTACA
Scrambled	**GCGCGGATAGTCTGGAGGTCGATAGTATCACCGCTAGCAT**CTATAGTGAGTCGTATTACA

Figure 5.2: a,b) Probe maps for β-catenin long probes. Maps not to scale. AS, Antisense; S, Sense. a) βCatL1 probe in pCMV-SPORT6 vector. Antisense strand cut with SalI and transcribed from T7 promoter. Sense strand cut with NotI and transcribed from SP6 promoter. b) βCatL2 probe in pBSIIKS(+) vector. Antisense strand cut with PstI and transcribed from T7 promoter. Sense strand cut with NotI and transcribed from T3 promoter. c) Sequences of oligoprobes used for in situ hybridisations. Probes for 18S, β-actin, β-catenin and the scrambled control probe used in the present chapter are shown. Also shown are probes for RPS3, as used for in situ hybridisations on coronal sections in Chapter 6. Probe sequences are shown in bold, with the T7 promoter sequence in normal type.

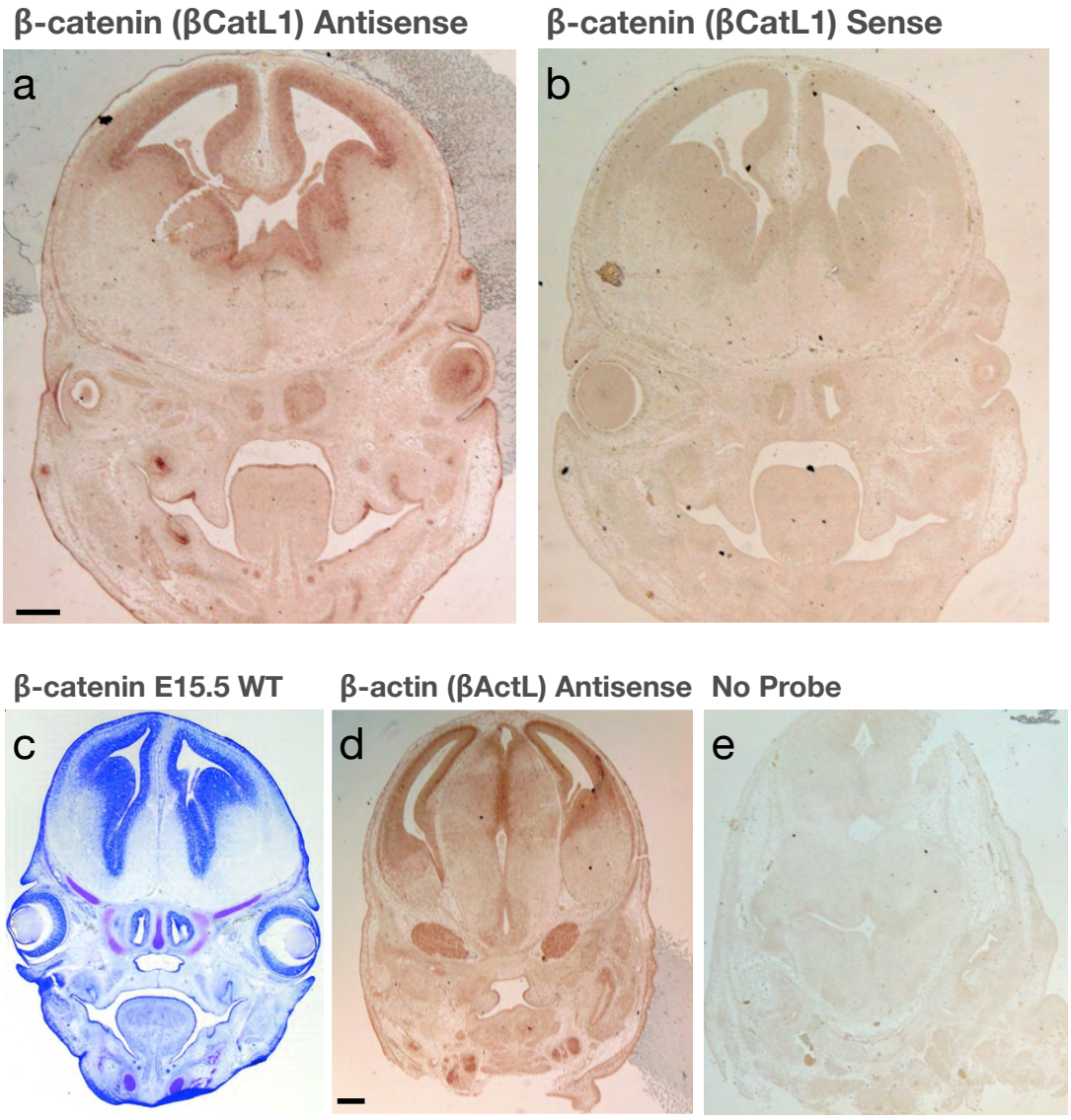

Figure 5.3: On coronal sections of E14.5 mouse heads, in situ hybridisations for (a) βCatL1 Antisense probe, (b) βCatL1 Sense probe, (d) βActL Antisense probe and (e) no probe show that both the βCatL1 Antisense and βActL Antisense probes stain areas of the cortex whereas the βCatL1 Sense probe does not substantially stain any region of the section, indicating that the three probes function as expected. (c) shows expected pattern of expression for β-catenin in E15.5 wild-type mouse, taken from Chenn and Walsh (2002), in close agreement with the expression in (a). Scale bars, 500μm; bar in (a) for (a) and (b); bar in (d) for (c), (d) and (e).

5.3.2 βCatL1

In this section, results for the first long probe for β-catenin (βCatL1) are presented, showing its use with several different culture systems and in situ hybridisation protocols.

5.3.2.1 βCatL1 on coronal sections

To confirm that the βCatL1 Antisense and Sense probes functioned as expected, they were tested on wax coronal sections of E14.5 mouse heads. Figure 5.3 shows four coronal sections, stained with the βCatL1 Antisense probe, the βCatL1 Sense probe, the βActL Antisense probe and with no probe. The figure shows that both the βCatL1 Antisense- and βActL Antisense-treated sections are strongly stained across the cortex, whereas the same strength of staining cannot be seen on either the βCatL1 Sense-treated section or the unstained section.

The βCatL1 Antisense- and βActL Antisense-treated sections show a similar level of staining, indicating that the βCatL1 template could be used to produce antisense probe of a similar quality to a commercial template. These pictures also indicate that the two probes bind specifically to particular mRNAs, because similar levels of staining were not seen with the βCatL1 Sense probe. The βCatL1 Antisense expression pattern is in close agreement with that seen in the literature (see, for example, Chenn and Walsh (2002), shown in Figure 5.3c).

Given that these results show that these probes appear to function correctly, they were used for further in situs on thalamic axons.

5.3.2.2 βCatL1 Probe on dissociated axons

Figure 5.4 shows the results of an in situ hybridisation staining for βCatL1 Antisense, βCatL1 Sense and βActL Antisense probes using the fluorescent protocol described in Section 5.2.3.2 on dissociated thalamic cells (see Section 5.2.2.3). The figure shows

---

Figure 5.4 *(following page)*: βCatL1 Antisense probe stains axons of dissociated E14.5 mouse thalamic cells above staining with βCatL1 Sense probe. However, βActL probe only shows background staining. Probes diluted 1:10 in hybridisation buffer. (a,c,e,g) Probes shown in green, GAP-43 in red and TOPRO in blue. (b,d,f,h) Probe stain only. (a,b) βCatL1 Antisense probe. (c,d) βCatL1 Sense probe. (e,f) βActL probe. (g, h) No probe. (i-l) Magnified single cells and axons (shown in white boxes in (a-d)), stained with (i,j) βCatL1 Antisense probe and (k,l) βCatL1 Sense probe. (i,l) Probe in green, GAP-43 in red and TOPRO in blue. (j,k) Probe stain only. Scale bar, 20μm.

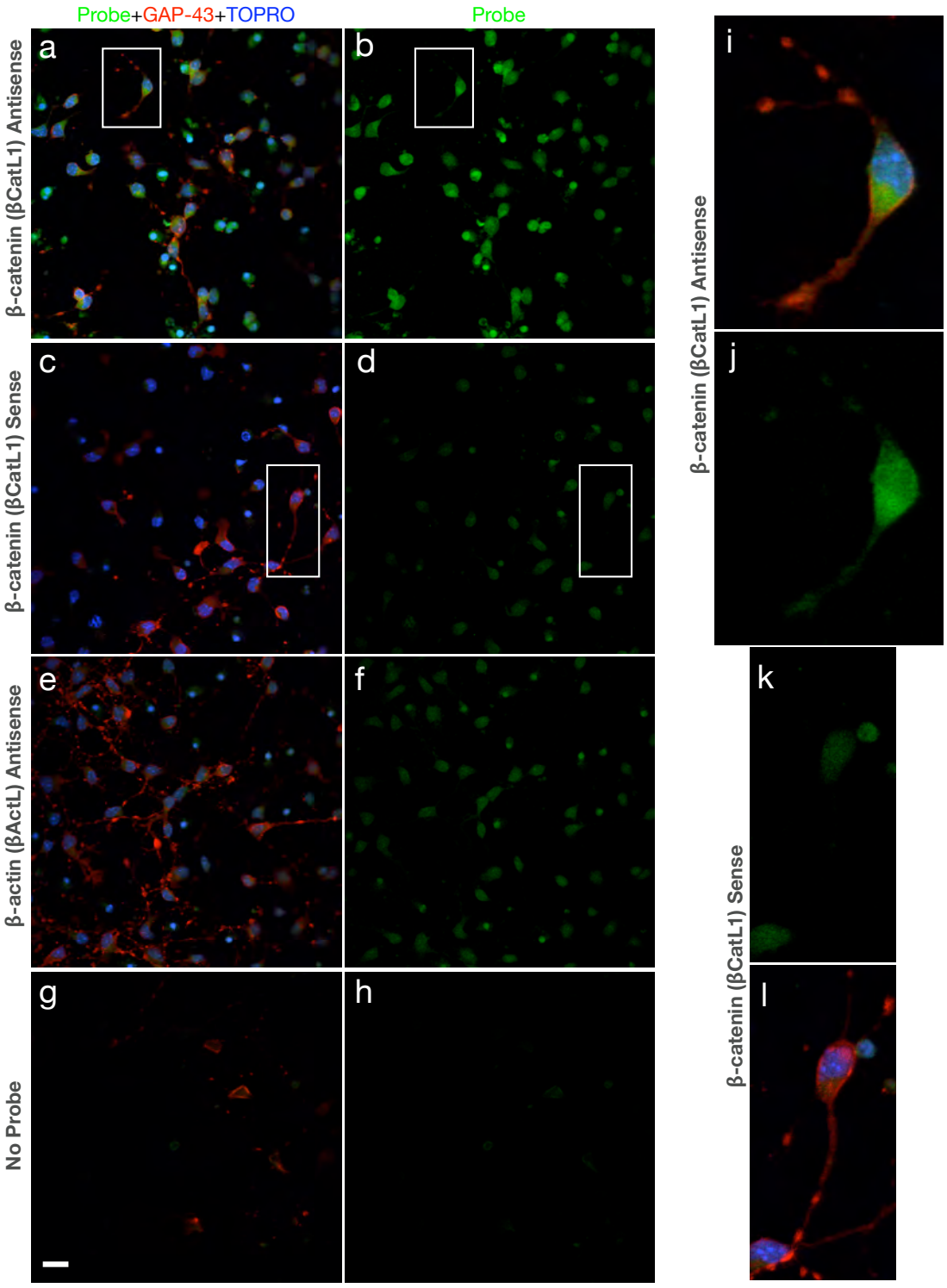
Probe+GAP-43+TOPRO
Probe
β-catenin (βCatL1) Antisense
β-catenin (βCatL1) Sense
β-actin (βActL) Antisense
No Probe
β-catenin (βCatL1) Antisense
β-catenin (βCatL1) Sense
a
b
c
d
e
f
g
h
i
j
k
l

that signal can be detected for the βCatL1 Antisense probe above the level of both the βCatL1 Sense probe and no probe control staining, indicating that β-catenin is present in the cells of these cultures. The magnifications show that there is also some evidence of β-catenin in the neurites of these cells. However, the βActL Antisense probe did not stain the cells or axons above background levels.

To try to improve this result and detect βActL Antisense probe, another in situ hybridisation was performed using 40% more probe than in the previous figure, the results of which are shown in Figure 5.5. The figure shows that βActL Antisense could now be detected in axons above the background staining shown where no probe was applied. However, the same improvement in staining could not be seen for the βCatL Antisense probe above the βCatL Sense probe. The staining of cells is slightly higher for the βCatL Antisense probe than for the βCatL Sense probe and the no probe condition, but no axonal staining can be detected (see magnified images of single cells and axons for examples).

Further attempts to replicate the result shown in Figure 5.4 failed to improve the staining of βCatL Antisense and βActL Antisense probes above the level of background or the βCatL Sense probe (see Figure 5.6 for an example, where no difference in staining between any of the four conditions can be seen).

These three figures illustrate that the neurites of dissociated cultured thalamic cells are very short, which means it is not possible to determine axons from dendrites. The neurites are also difficult to distinguish from each other and to trace to their parent cells because the cells are plated at high densities. The cells in the cultures presented in the above figures were plated at 1500 cells per mm^2 and cultured for 2 days. When cultured at 1000 cells per mm^2, cells did not survive even for two days and did not produce neurites. Cells also died when cultured for longer than 2 days (see also Asavaritikrai et al. (2003)). Therefore this culture system was not of sufficient quality to detect axonal staining.

Figure 5.5 *(following page)*: Increasing probe dilution from 1:10 to 1.4:10 (an increase of 40%) improves βActL Antisense staining but not βCatL Antisense staining above βCatL Sense staining. (a,c,e,g) Probes shown in green, GAP-43 in red and TOPRO in blue. (b,d,f,h) Probe stain only. (a,b) βCatL1 Antisense probe. (c,d) βCatL1 Sense probe. (e,f) βActL probe. (g, h) No probe. (i-l) Magnified single cells and axons (shown in white boxes in (a-d)), stained with (i,j) βCatL1 Antisense probe and (k,l) βCatL1 Sense probe. (i,l) Probe in green, GAP-43 in red and TOPRO in blue. (j,k) Probe stain only. Scale bar, 20μm.

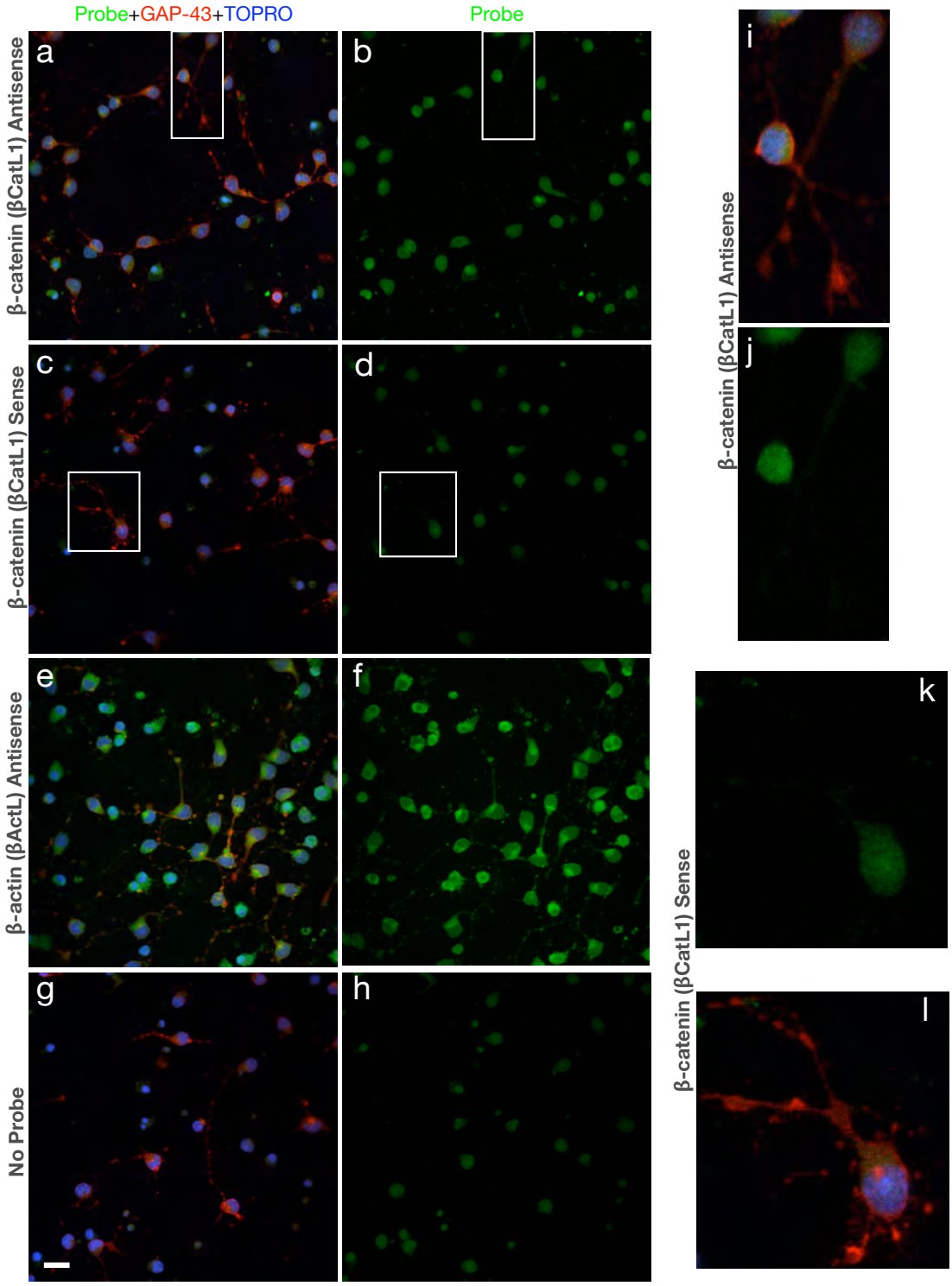
Probe+GAP-43+TOPRO
Probe
β-catenin (βCatL1) Antisense
β-catenin (βCatL1) Sense
β-actin (βActL) Antisense
No Probe
β-catenin (βCatL1) Antisense
β-catenin (βCatL1) Sense
a
b
c
d
e
f
g
h
i
j
k
l

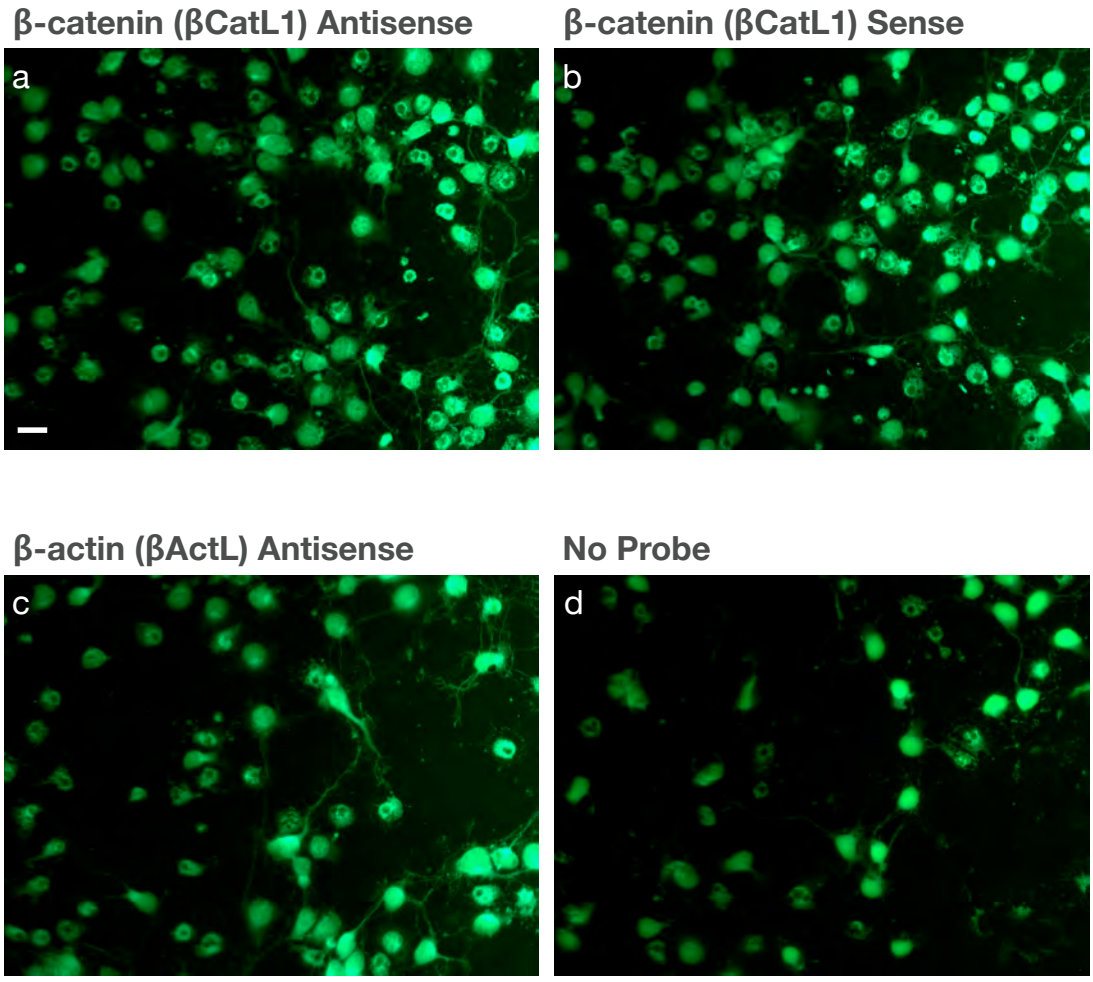

Figure 5.6: βCatL1 Antisense and βActL Antisense staining could not be replicated reliably. Further attempts using the same probes, culture and protocol as Figures 5.4 and 5.5 did not produce strong staining for βCatL1 Antisense and βActL Antisense probes compared to βCatL Sense or no probe, as shown in this example, where no substantial difference in staining can be seen between any pair of the four conditions. (a) βCatL Antisense, (b) βCatL Sense, (c) βActL Antisense, (d) No Probe. Pictures taken with 9 second exposure. Scale bar, 20μm.

5.3.2.3 βCatL1 Probe on explant cultures

Because it was not possible to obtain reliable differences in staining with any probes using the fluorescent protocol described in Section 5.2.3.2, it was decided that further in situs should be performed using a colorimetric protocol which was known to work in the lab (see Section 5.2.3.3 for method). Also, because the dissociated cell culture method had failed to yield sufficient neurite growth, an explant culture system was used to produce neurites (see Section 5.2.2.4 for method).

In this system, where whole thalami were sliced into between 50-70 pieces and plated on glass coverslips, the explants survived for many days and produced substantial neurite growth after three days. An advantage of this system is that some cells were dissociated from the explants during the vigorous dissection procedure and were also plated with the explants. These dissociated cells were found to grow neurites which were as long or longer than those found in the earlier dissociated cell cultures. Figure 5.7 shows an example of an explant and a dissociated cell from this culture system stained with the axonal marker neurofilament (for other examples, see the remaining figures in this chapter). The figures shows that considerable axonal growth could be found from both explants and dissociated cells. Therefore this culture system was used for all further in situ hybridisation experiments.

Figure 5.8 shows the results of a colorimetric in situ with the βCatL1 Antisense and βActL Antisense probes on dissociated cells and their axons in an explant culture. The figure shows that the βActL Antisense probe stained cells and axons above the background level shown for no probe staining, confirming that this probe was functional. The figure also shows light staining above background for both the βCatL1 Antisense and βCatL1 Sense probes, but no substantial difference between these two probes. This figure therefore mirrors the result acquired using the fluorescent in situ protocol shown in Figure 5.5.

Because it had not been possible to acquire a successful repeatable result using the βCatL1 probes with two different protocols, and because βCatL1 was a very long probe containing sections of RNA which may interfere with its binding to endogenous β-catenin mRNA, it was decided that new probes for β-catenin should be designed.

5.3.3 βCatL2

In this section, results for the second long probe for β-catenin (βCatL2) are presented.

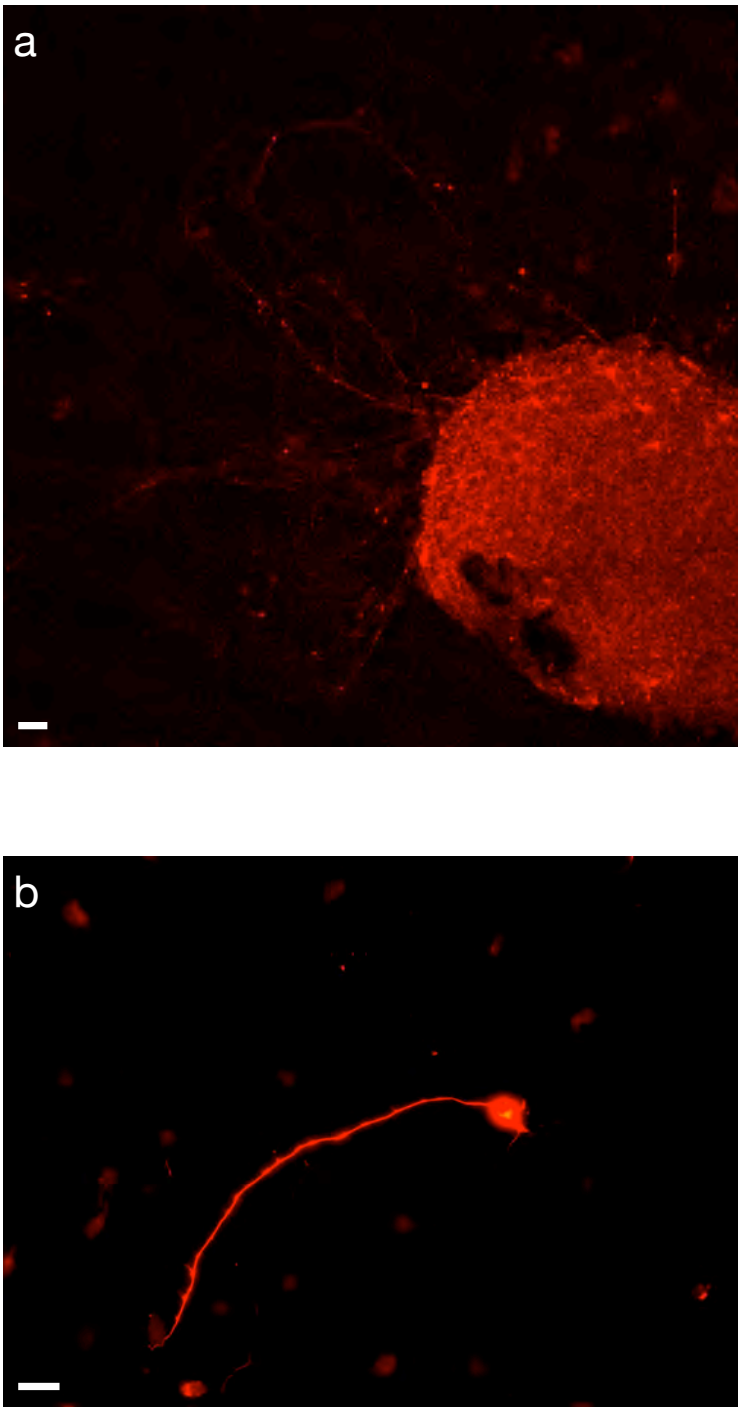

Figure 5.7: Explant culture produces substantial axonal growth from both explants and dissociated cells. (a) Confocal image of E14.5 mouse thalamic explant stained with axonal marker neurofilament. Both explant and axons are clearly stained and substantial axonal growth from the explant can be clearly seen. (b) Fluorescent image of single dissociated cell from the same culture system, stained with neurofilament, shows considerable axonal growth. Scale bars both 20μm.

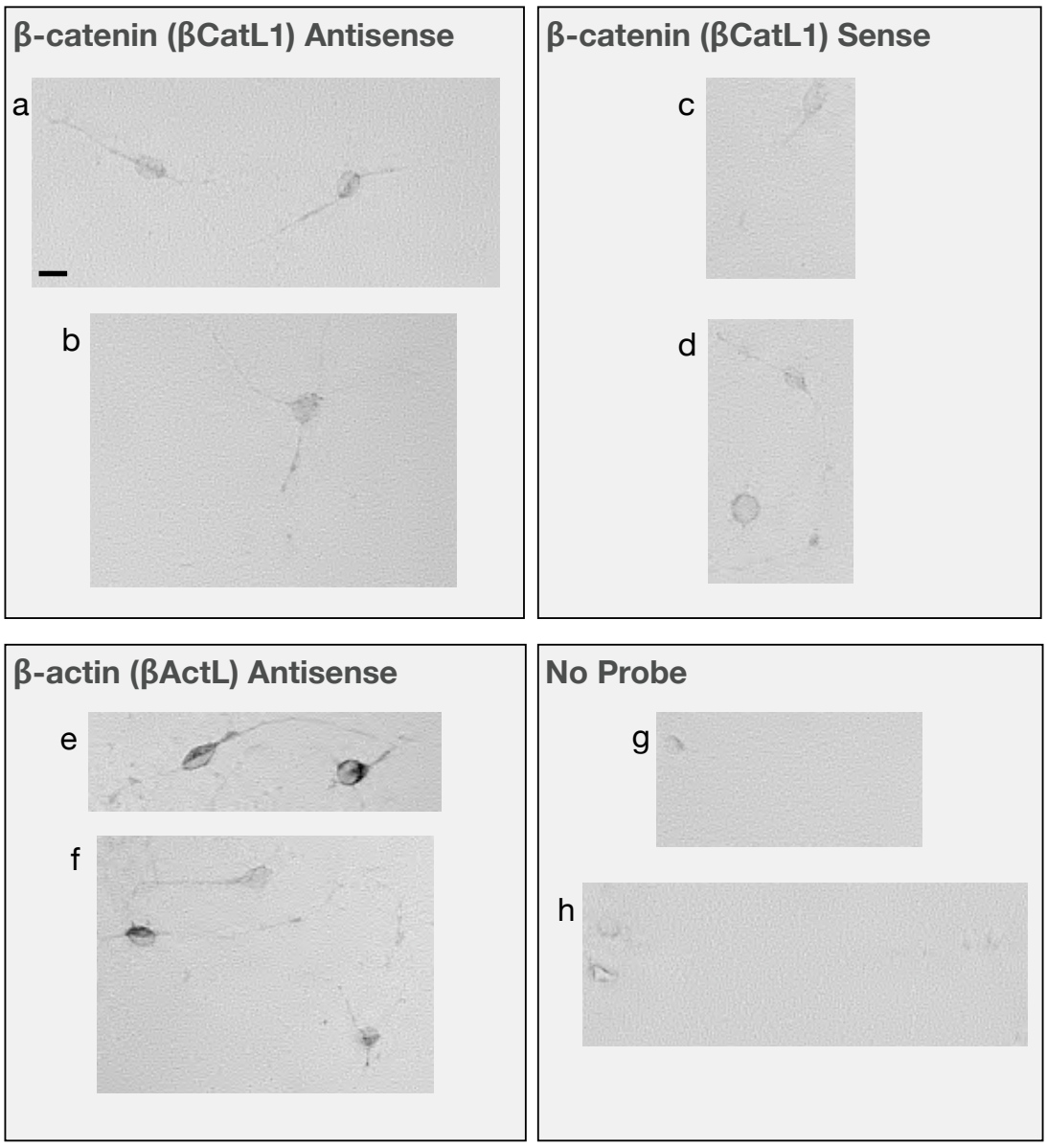

Figure 5.8: Dissociated E14.5 mouse thalamic cells from explant cultures, stained for 3 hours with (a,b) βCatL1 Antisense probe, (c,d) βCatL1 Sense probe, (e,f) βActL Antisense probe and (g,h) No probe. Both βCatL1 probes and βActL Antisense probe stained axons above background. βActL Antisense probe stains cells and axons. However, no clear difference in staining can be seen between βCatL1 Antisense and βCatL1 Sense probes. Scale bar, 20μm.

5.3.3.1 βCatL2 Probe on explant cultures

The template used to make βCatL2 Antisense and βCatL2 Sense probes was designed to match only the 3'UTR of β-catenin, and does not include the coding and intronic regions that are part of the βCatL1 template (see Section 5.3.1), based on the hypothesis that the intronic region may have been interfering with the ability of the probe to bind to β-catenin mRNA in axons in situ.

Using these probes, it was possible to successfully and repeatedly detect a signal for the βCatL2 Antisense probe in explants and single cells above the control levels detected for the βCatL2 Sense probe and with no probe, as shown in Figures 5.9, 5.10 and 5.11. However, some refinement was required to detect a signal in processes above control levels. Once bound to mRNA in situ, the digoxigenin-labelled probe is bound to anti-digoxigenin alkaline phosphatase. Alkaline phosphatase catalyses the conversion of the colorimetric stain NBT/BCIP into a purple precipitate, so when tissue samples are treated with NBT/BCIP the presence of alkaline phosphatase, and therefore digoxigenin-labelled probe bound to mRNA, can be visualised by observing this precipitate.

Figure 5.9 shows that staining for 3 hours, while sufficient to detect signal above control levels in explants and single cells, was not sufficient to detect signal in processes above control levels, with no processes in any conditions being clearly stained. However, staining for 24 hours, as shown in Figure 5.10, caused the processes to be saturated, with all processes clearly visible and stained above background in all four conditions, and no substantial difference in staining detectable between the two Antisense probes and the control probes.

Therefore, cultures were stained for 10 hours, which enabled the processes to be stained above background but below saturation levels for both the βCatL2 Antisense and βActL Antisense probes, as shown in Figure 5.11. While the processes in both the βCatL2 Sense and No Probe conditions are visible, several processes, including axons, can be seen to be stained above these control levels for both βCatL2 Antisense and βActL Antisense conditions. In particular, several axons in these two conditions show punctate staining both along the axon and at the growth cone (marked with arrowheads in the figure; absence of punctate staining in βCatL2 and No Probe conditions is also shown with arrowheads).

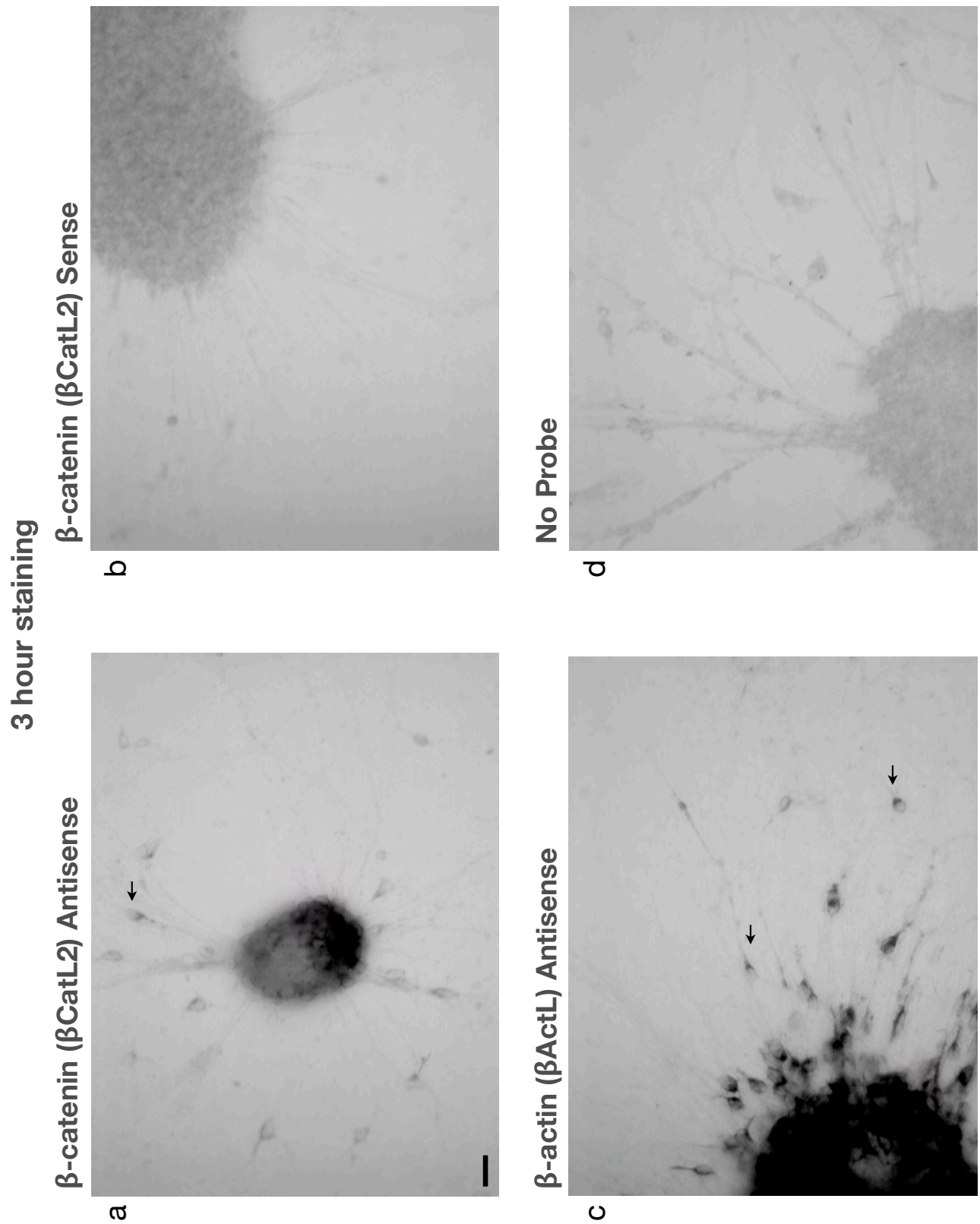

Figure 5.9: βCatL2 probes successfully and reliably stain thalamic explants and cells after 3 hours of staining. (a) βCatL2 Antisense and (c) βActL Antisense probes can be reliably detected both in explants and in single cells separated from the explants (see arrows). (b) βCatL2 Sense probe is detectable only slightly above (d) no probe background signal and substantially below the βCatL2 Antisense probe. However, no substantial staining of processes can be observed. Scale bar, 20μm.

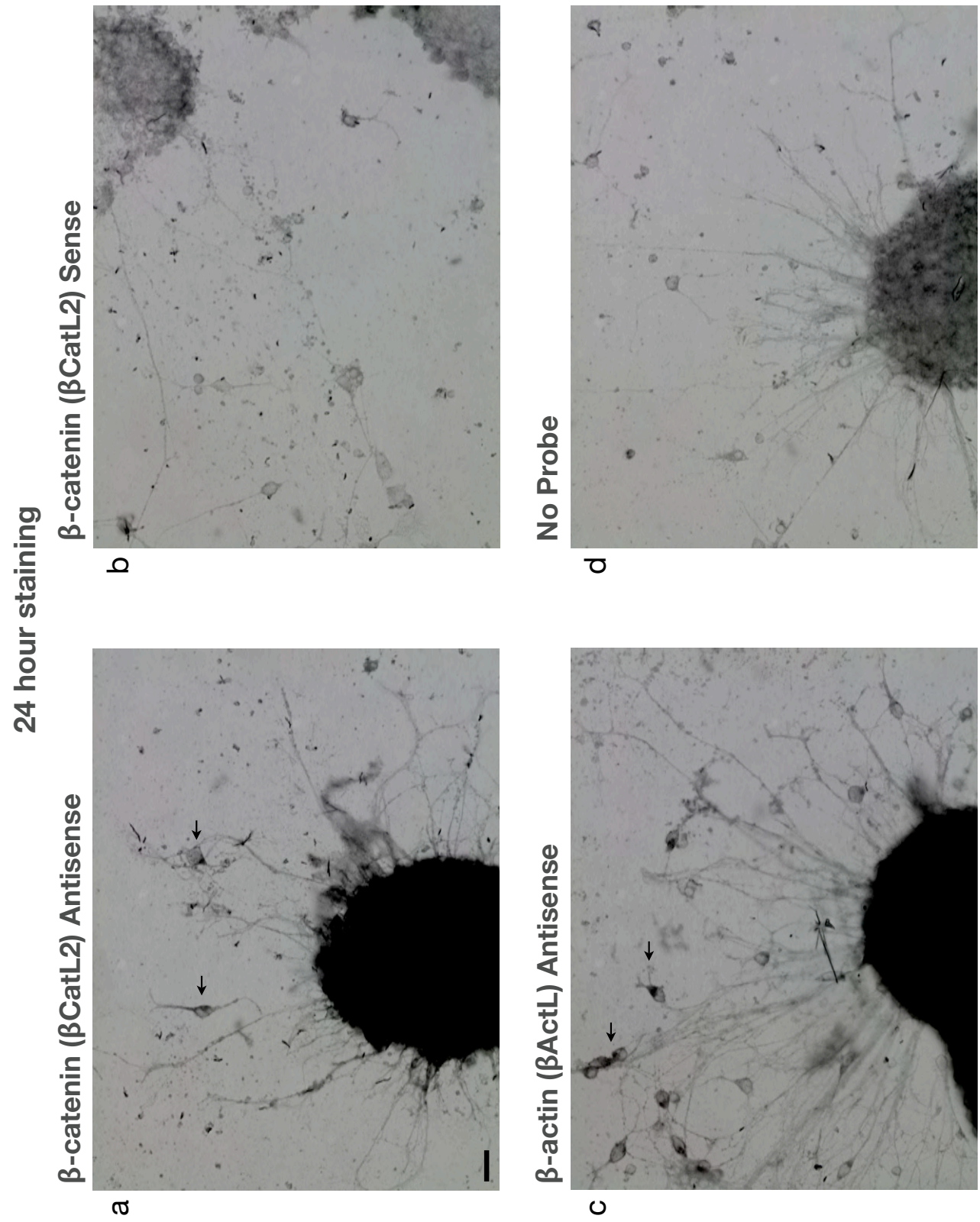

Figure 5.10: Repeating the in situ hybridisation shown in Figure 5.9 but staining for 24 hours produces the same high level of staining for (a) βCatL2 Antisense and (c) βActL Antisense probes above the levels for (b) βCatL2 Sense and (d) No Probe, in both explants and single cells (see arrows). However, processes are now stained in all four conditions, making it difficult to detect staining of processes for βCatL2 Antisense and βActL Antisense above control levels. Scale bar, 20μm.

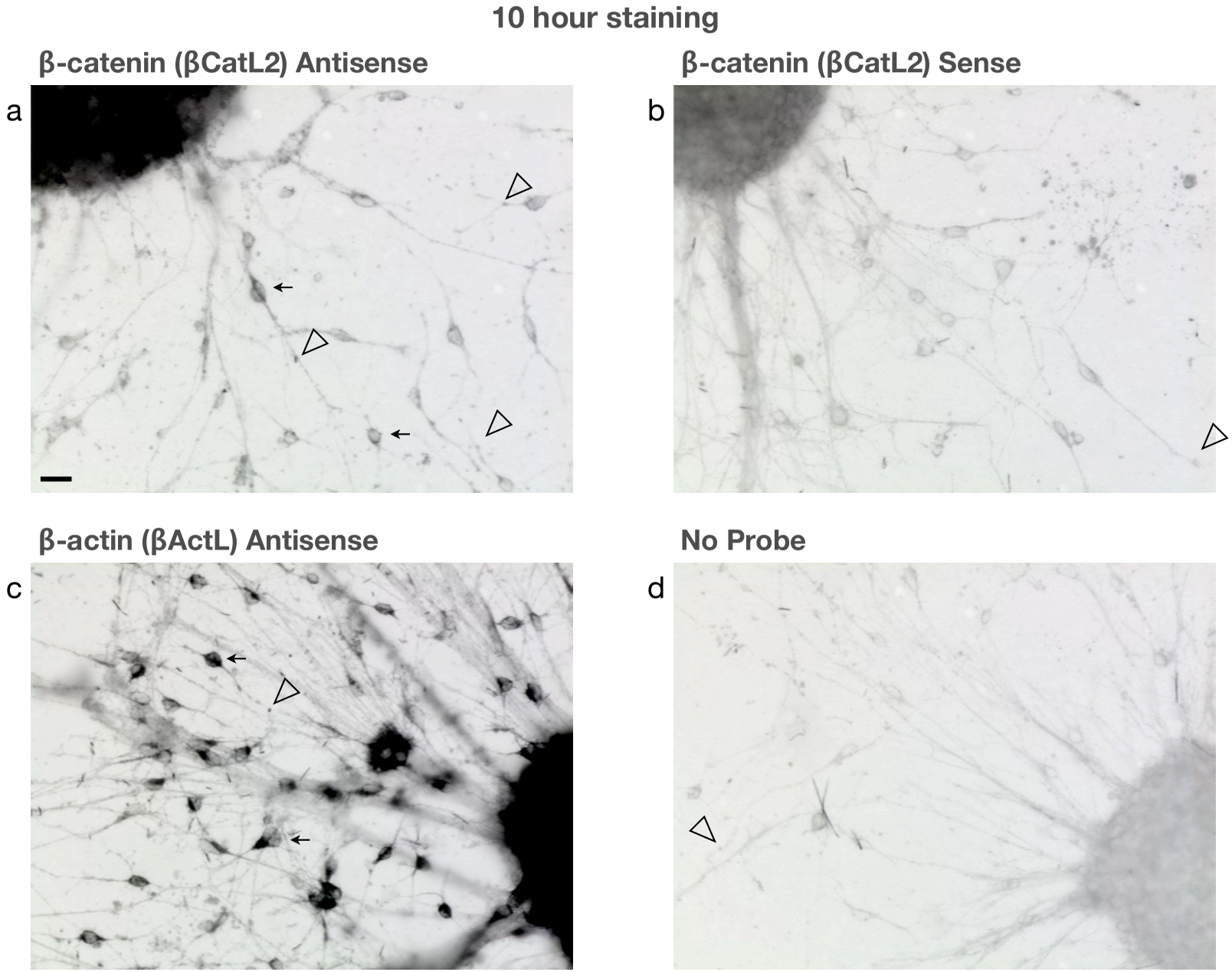

Figure 5.11: Repeating the in situ hybridisation shown in Figures 5.9 and 5.10 but staining for 10 hours stains explants, cells (arrows) and processes (arrow heads) for both (a) βCatL2 Antisense and (c) βActL Antisense above control levels for (b) βCatL2 Sense and (d) No Probe. Arrow heads show evidence of punctate staining in βCatL2 Antisense and βActL Antisense conditions but not βCatL2 Sense and No Probe conditions. Scale bar, 20μm.

5.3.3.2 βCatL2 Probe on axons

The difference in staining in processes between the two Antisense probes and the control conditions shown in Figure 5.11 is clearly small when compared to the difference in explant or cell staining. Does this truly reflect the presence of β-catenin and β-actin in these processes? Can this staining be reliably seen across many different axons? Figure 5.12 shows a number of different cells with axons, taken from the same in situ hybridisation shown in Figure 5.11. There is clear punctate staining for both the βActL and βCatL2 Antisense probes. In particular, the βCatL2 Antisense probe appears to stain the growth cone repeatedly. This staining is also above the levels seen in the growth cones and axons stained with βCatL2 Sense probe and no probe, but the difference is small in all cases, and some light staining can be seen in the processes stained with both βCatL2 Sense probe and with no probe.

Several attempts were made to improve the staining shown here, by increasing the pH of the fixative (as recommended by Basyuk et al. (2000)) or modifying the hybridisation temperature, but these modifications either did not improve the signal or were too stringent for the neurites projecting from the explants or from dissociated cells to survive the protocol. Attempts were also made to detect a signal using fluorescent antibodies rather than a colorimetric stain, by hybridising the probes using the method shown in Section 5.2.3.3 (as this hybridisation was known to work) but then detecting these probes using the method shown in Section 5.2.3.2. As shown in Figure 5.13, these attempts also failed, with no detectable difference visible between any of the probes, even in explants.

Therefore Figures 5.11 and 5.12 show the best result for β-catenin and β-actin staining in thalamic axons that it was possible to acquire in the time available. Conclusions about these results will be drawn after further analysis of the images has been presented in Section 5.3.5.

5.3.4 Oligoprobes

Figure 5.15 shows the results of a colorimetric in situ hybridisation using the oligoprobes presented in Section 5.3.1. The figure shows that 18S, β-catenin and β-actin oligoprobes could be detected above the signal detected for the Scrambled control probe in explant and single cells, demonstrating that the oligoprobes were functional. The figure also shows that the 18S and β-catenin probes can be detected above the level of the Scrambled probe in axons. However, only very slight staining above background

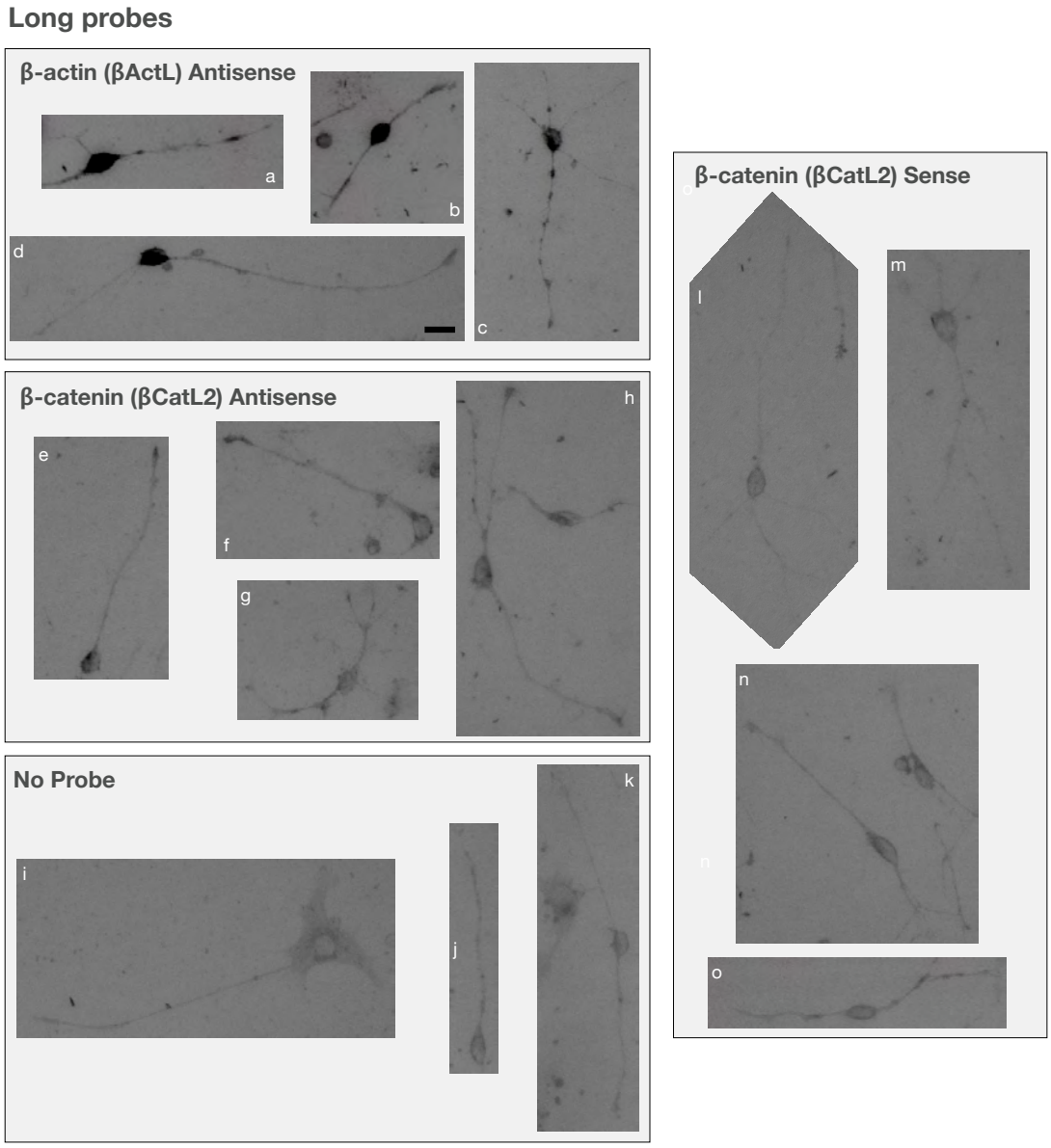

Figure 5.12: Single cells with axons from the same in situ hybridisation shown in Figure 5.11. (a-d) βActL Antisense, (e-h) βCatL2 Antisense, (i-k) No Probe, (l-o) βCatL Sense. Punctate staining can be seen for βActL and βCatL2 Antisense probes along axons, above control levels. Scale bar, 20μm.

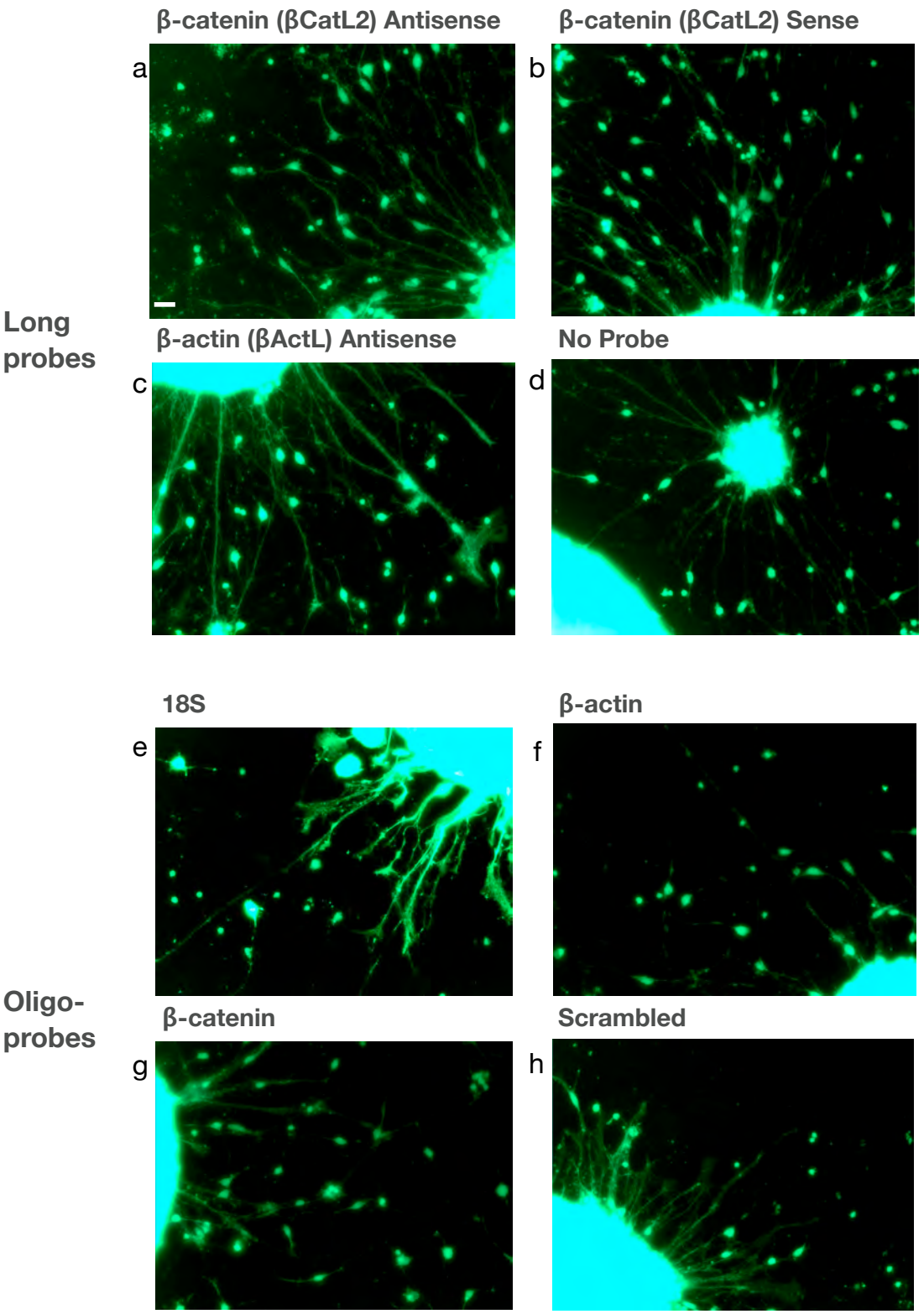

Figure 5.13: Probes hybridised according to the method in Section 5.2.3.3 but bound to fluorescent antibodies as described in Section 5.2.3.2 could not be detected on thalamic explant cultures above background levels. (a) βCatL2 Antisense probe, (b) βCatL2 Sense probe, (c) βActL Antisene probe, (d) No probe, (e) 18S Oligoprobes, (f) β-actin Oligoprobes, (g) β-catenin Oligoprobes, (h) Scrambled oligoprobe. Pictures taken at 9 second exposure. No difference can be seen in explants, cells or axons between any pair of probes. Scale bar, 20μm.

can be seen in axons for the β-actin oligoprobes.

Figure 5.15 shows a set of cells with axons from the same in situ hybridisation shown in Figure 5.14. The figure shows that the 18S oligoprobes can be reliably and strongly detected throughout cells and axons. It also shows that the β-actin and β-catenin oligoprobes can be detected in cells, but there is only slight staining in axons above the level of the Scrambled control probe. However, it was possible to detect staining of the growth cone for β-catenin in some axons (see pictures i and j in the figure) similar to that seen in Figure 5.11. These results are further analysed in Section 5.3.5 below.

5.3.5 Image Analysis

The pictures shown in the previous sections appear to demonstrate differences in staining between experimental and control probes. In this section, these differences will be quantified and shown to be statistically significant, following the method described in Section 5.2.3.4.

All of the axons analysed here were taken from the same in situ hybridisation shown in Figures 5.11, 5.12, 5.14 and 5.15. As many axons as possible were selected from this in situ, following the criteria listed in Section 5.2.3.4. Axons were traced as shown in Figure 5.17a and the intensities of the pixels in the trace were recorded. The number of axons traced for each probe are shown in Figure 5.16. The means and standard error of the mean of pixel intensities for all images in each 5% bin are given as percentages of the maximum intensity found for each set of probes. These means and standard errors of the mean are plotted for eight different pairs of probes in Figures 5.17, 5.18, 5.19 and 5.20.

Figure 5.17 shows that there is significant staining for the βCatL2 Antisense probe above both the βCatL2 Sense and No Probe controls at the cell (in the leftmost bins) and the growth cone (in the rightmost bins), but not along the bulk of the axon. Conversely, Figure 5.18 shows that there is significant staining for the βCatL probe in the cell and along the axon, but not in the growth cone, compared to the βCatL2 Sense and No Probe controls. These plots demonstrate that at least a small quantity of β-catenin mRNA is present in thalamic growth cones and that β-actin mRNA is present in thalamic axons.

Figure 5.19 shows that the same significant different in staining cannot be seen for either the β-catenin or β-actin oligoprobes above the staining for the Scrambled

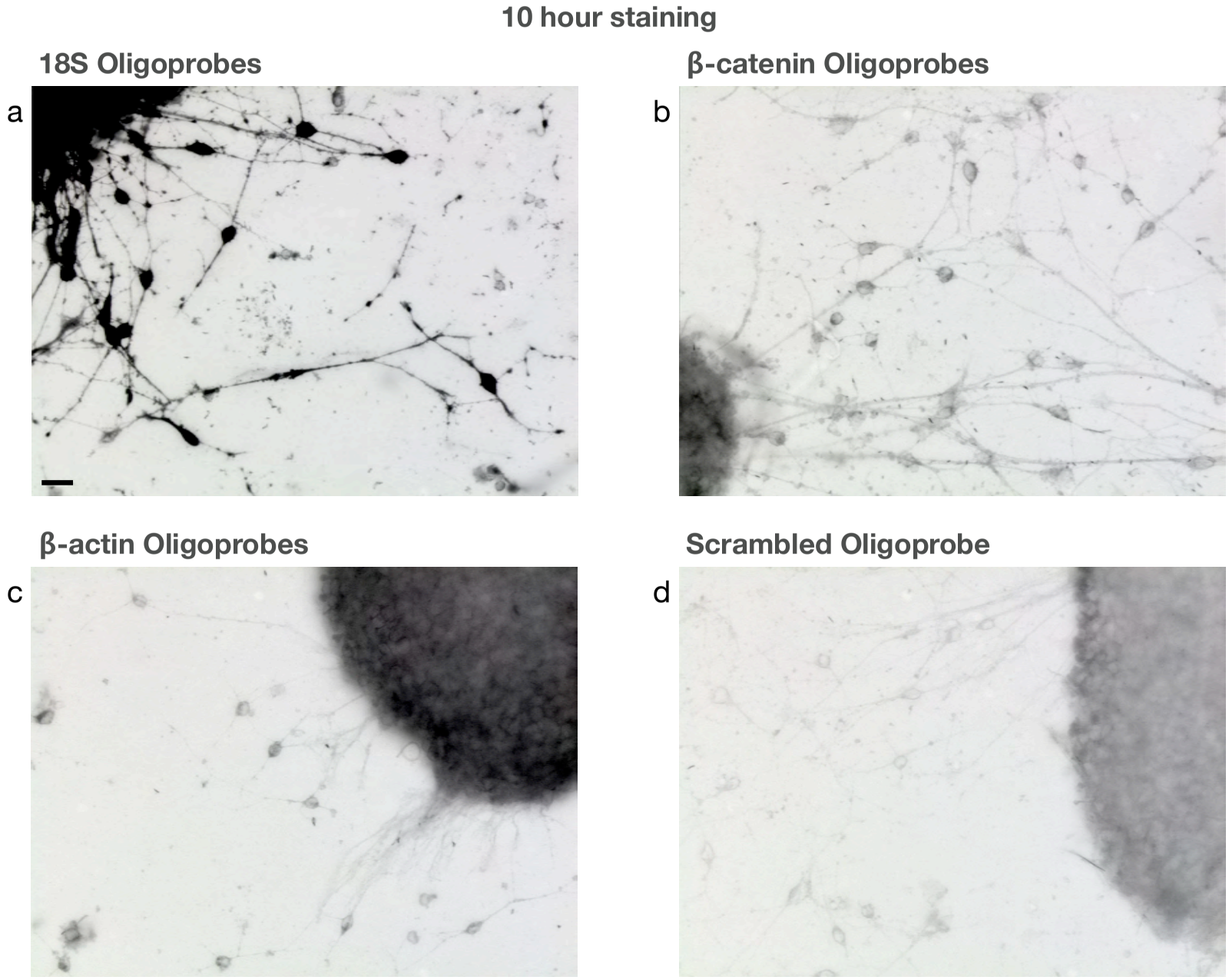

Figure 5.14: Oligoprobes for (a) 18S, (b) β-catenin and (c) β-actin can be detected in E14.5 mouse thalamic explants, cells and axons using colorimetric in situ hybridisation, above the levels seen for the Scrambled control probe (d). Scale bar, 20μm.

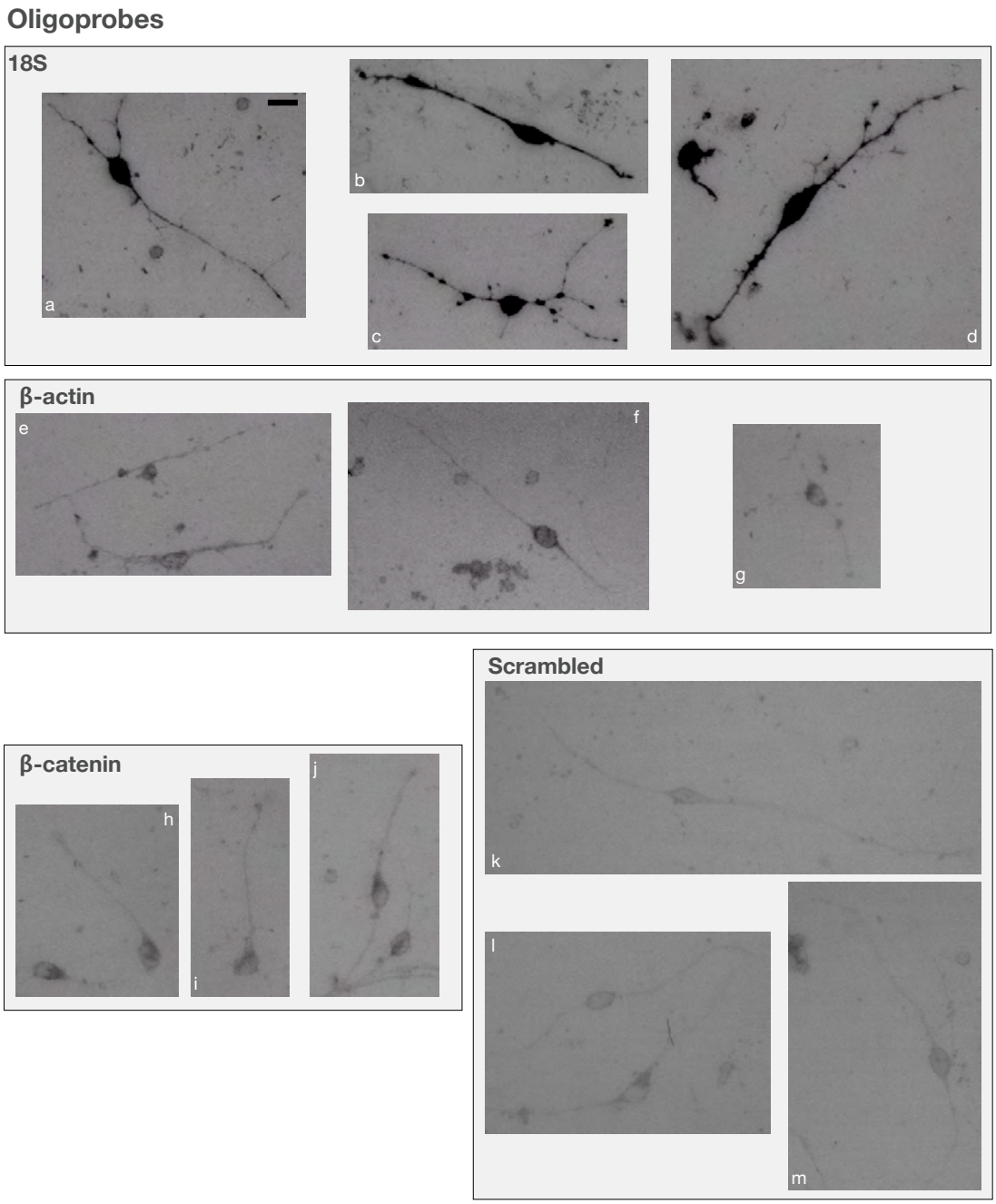

Figure 5.15: Oligoprobes detected on E14.5 mouse thalamic explants using colorimetric in situ hybridisation. Staining in explants, cells and axons is apparent for (a) 18S, (b) β-catenin and (c) β-actin when compared to (d) Scrambled oligoprobe, although axonal staining is slight for β-actin and β-catenin. Scale bar, 20μm.

control oligoprobe, indicating that these mRNAs cannot be detected reliably with these oligoprobes. However, Figure 5.20a shows that the 18S oligoprobes do stain significantly above the levels of the Scrambled control probe in the cell and along the entire length of the axon. An increase in staining can be seen at the growth cone (see 90-95% bin).

Finally, the staining for the two long probe controls (βCatL2 and No Probe) is not significantly different, as seen in Figure 5.20b, further indicating that the significant staining seen in the other figures shows genuine staining and is not an artifact of image collection and processing. Therefore it can be concluded that this analysis of the in situ hybridisations shown in this chapter demonstrate the presence of β-catenin mRNA in thalamic growth cones, β-actin mRNA in thalamic axons and 18S rRNA in thalamic axon and growth cones.

5.4 Discussion

In this chapter, a series of attempts to identify mRNAs in thalamic axons using in situ hybridisation has been presented. In this discussion, the probes, cultures and protocols used will be considered and several conclusions will then be drawn about the presence of RNAs in thalamic axons based on the results presented above.

5.4.1 Technical considerations

In this section, the choice of RNAs used for the in situ hybridisations is defended, and the choices of probe type, culture and protocol are explained.

5.4.1.1 Selection of RNAs

The RNAs investigated here are β-catenin, β-actin and 18S. All three of these RNAs have been shown to be present in samples of thalamic axonal RNA in Chapter 4. As discussed in Section 1.5.5, β-actin has previously been shown to be in axons of other systems (Bassell et al., 1998) and ribosomes, which contain 18S rRNA, have been shown to be present in axons (Wu et al., 2005; Alvarez et al., 2000). However, β-actin and 18S have not been previously shown to be present in thalamic axons and therefore the demonstration of their presence in thalamic axons here is a novel result. In particular, demonstrating the presence of 18S mRNA in thalamic axons would support its use as an internal standard in the PCR experiments presented in Chapter 4.

Probe	Axons (n)		0-5%	6-10%	11-15%	16-20%	21-25%	26-30%	31-35%	36-40%	41-45%	46-50%
βCatL2 Antisense	12	Mean	58.77	49.60	34.87	30.82	31.11	31.42	29.36	29.34	27.93	30.05
		S.E.M.	4.81	4.74	2.67	1.61	2.08	2.46	1.89	1.58	1.63	1.77
βCatL2 Sense	15	Mean	39.61	37.46	30.92	28.37	28.16	28.16	28.20	27.67	26.26	26.36
		S.E.M.	1.54	2.13	1.56	1.16	1.27	1.23	1.58	1.15	0.91	0.89
βActL	11	Mean	98.24	79.72	59.45	48.93	44.75	37.91	35.85	36.36	38.99	36.23
		S.E.M.	1.55	6.09	6.20	3.49	3.00	1.98	2.14	2.33	2.70	3.59
No Probe	6	Mean	34.09	34.35	28.49	27.38	27.64	26.33	26.22	25.58	24.32	26.86
		S.E.M.	1.18	1.13	1.33	0.80	0.92	0.81	1.23	0.45	0.58	1.22
β-Catenin Oligo	7	Mean	39.69	32.42	23.43	19.81	19.02	19.64	16.40	16.13	16.72	16.54
		S.E.M.	3.37	3.87	2.55	0.83	1.44	1.61	1.68	1.47	1.31	1.03
β-Actin Oligo	6	Mean	44.19	36.64	25.73	23.00	20.59	23.84	24.25	26.04	24.90	22.61
		S.E.M.	5.42	4.35	1.73	2.52	3.24	3.96	3.14	4.41	3.66	3.47
18S	6	Mean	100.00	99.54	87.32	74.17	68.42	73.28	67.74	55.85	57.47	53.92
		S.E.M.	0.00	0.32	2.89	2.43	8.72	7.92	6.97	4.16	5.66	8.52
Scrambled	7	Mean	22.32	22.44	18.64	15.85	14.72	14.23	13.82	13.58	14.42	13.34
		S.E.M.	1.64	3.24	2.36	1.45	1.13	0.78	1.18	1.03	1.16	1.19

Probe			51-55%	56-60%	61-65%	66-70%	71-75%	76-80%	81-85%	86-90%	91-95%	96-100%
βCatL2 Antisense		Mean	29.09	27.99	29.17	28.74	29.24	30.04	32.89	38.62	42.88	37.35
		S.E.M.	1.60	1.20	1.12	1.32	1.47	1.43	1.38	2.35	2.45	2.32
βCatL2 Sense		Mean	25.44	26.61	26.35	27.37	27.63	27.41	27.13	27.12	28.72	26.57
		S.E.M.	0.87	1.00	1.02	1.00	1.39	1.22	0.94	0.75	0.83	1.11
βActL		Mean	34.58	32.66	35.18	34.11	39.39	40.80	32.21	31.19	32.37	30.32
		S.E.M.	1.54	2.05	1.86	2.38	4.81	4.18	2.56	1.72	1.90	2.59
No Probe		Mean	25.38	25.28	24.61	26.80	26.54	25.82	28.04	29.33	30.02	24.44
		S.E.M.	1.16	1.29	0.94	1.54	1.32	1.44	1.19	1.40	1.33	0.66
β-Catenin Oligo		Mean	16.54	17.65	15.61	15.11	16.28	17.24	16.91	19.51	21.68	15.59
		S.E.M.	0.83	1.22	0.63	0.69	1.53	1.82	1.77	1.96	1.42	2.22
β-Actin Oligo		Mean	26.34	22.40	20.92	20.71	21.25	24.62	22.37	23.41	25.69	21.41
		S.E.M.	4.04	3.61	3.37	4.06	3.65	4.53	3.64	3.99	2.83	3.50
18S		Mean	55.80	57.23	57.31	49.80	43.73	48.99	49.73	38.84	66.96	37.59
		S.E.M.	8.44	10.79	10.38	11.59	8.56	6.79	8.29	5.30	7.34	5.17
Scrambled		Mean	14.20	13.95	15.28	13.94	14.88	16.30	15.69	17.13	17.60	15.74
		S.E.M.	0.94	0.89	0.66	0.83	1.12	1.36	1.16	1.47	1.29	1.16

Figure 5.16: Summary of axonal in situ hybridisation image analysis. Images for long probes (βCatL2 Antisense, βCatL2 Sense, βActL and No Probe control) and oligoprobes (β-Catenin Oligo, β-Actin Oligo, 18S and Scrambled) were traced and the pixel intensities along the trace were binned along the length of the axons in 5% bins and averaged for each image. The table shows the number of images of axons traced for each probe, and the means and standard errors of the mean (S.E.M.) of the average pixel intensities for each 5% bin across the set of images for each probe. The intensities are given as percentages of the maximum pixel intensity found for all the probes in each set of probes, with long probes and oligoprobes treated as separate sets and so measured against different maximum intensities.

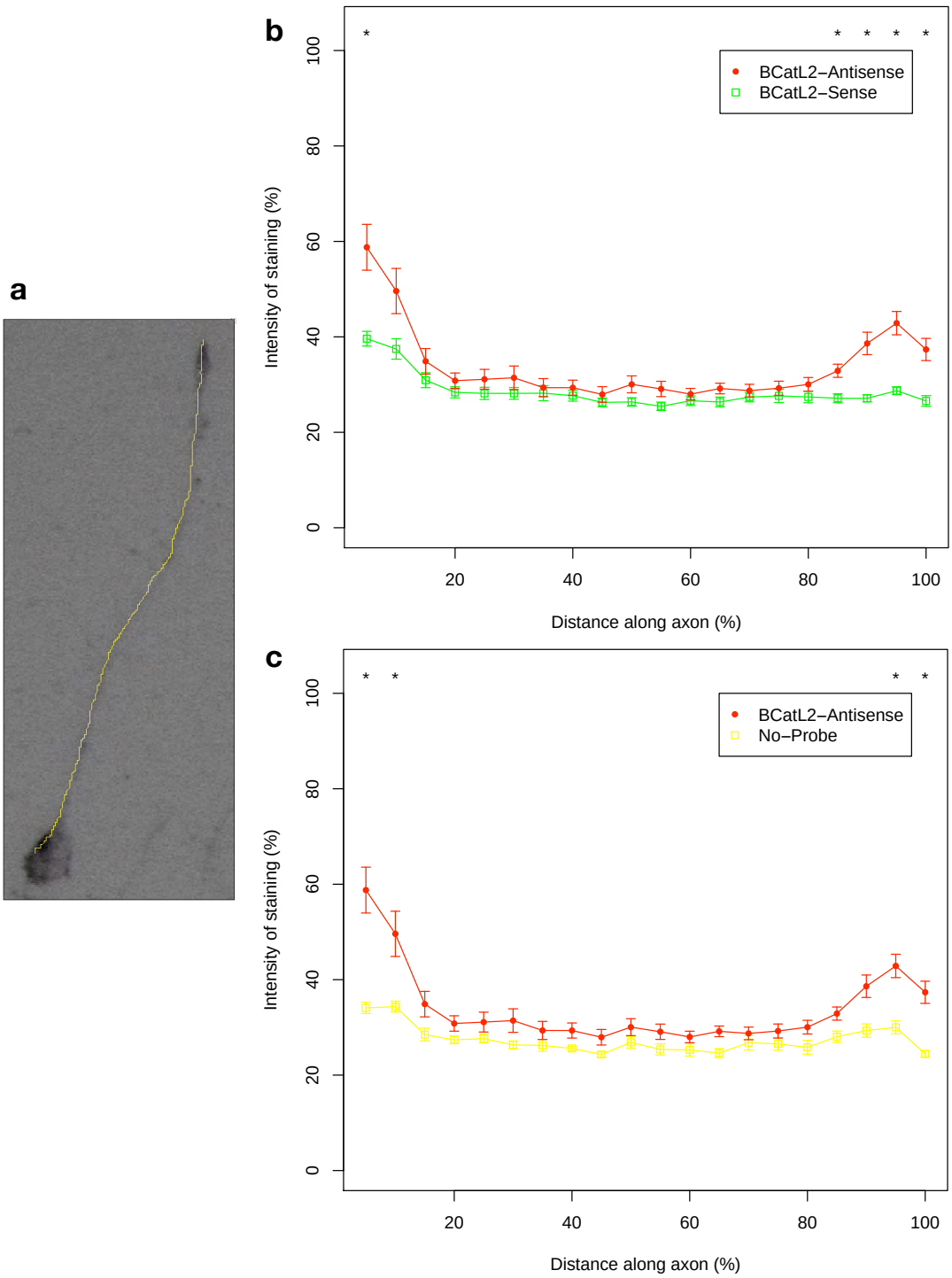

Figure 5.17: Comparison of staining along multiple axons for β-catenin long probe. a) Example of axon trace. Axons were traced by hand from a region of high staining in the cell (to measure the level of cellular staining) to the edge of the growth cone. b-c) Comparisons of βCatL2 Antisense staining to controls. The x-axes show distance along axons in bins of 5%; therefore the left side of each plot represents the cell and the right side of each plot represents the growth cone. The y-axes show intensity of axon staining as a percentage of the highest intensity seen over all axons for all long probes. Each asterisk indicates there is a significant difference between the intensities for the two probes in the corresponding 5% bin, at the $p<0.05$ significance level. The absence of an asterisk indicates $p>=0.05$. p values calculated using a one-tailed Wilcoxon rank sum test with Bonferroni correction. The plots show that βCatL2 Antisense staining is significantly above staining for b) βCatL2 Sense and c) No Probe in the cell and the growth cone, but not along the trunk of the axon. Number of axons in each sample: βCatL2 Antisense, 12; βCatL2 Sense, 15; No Probe, 6.

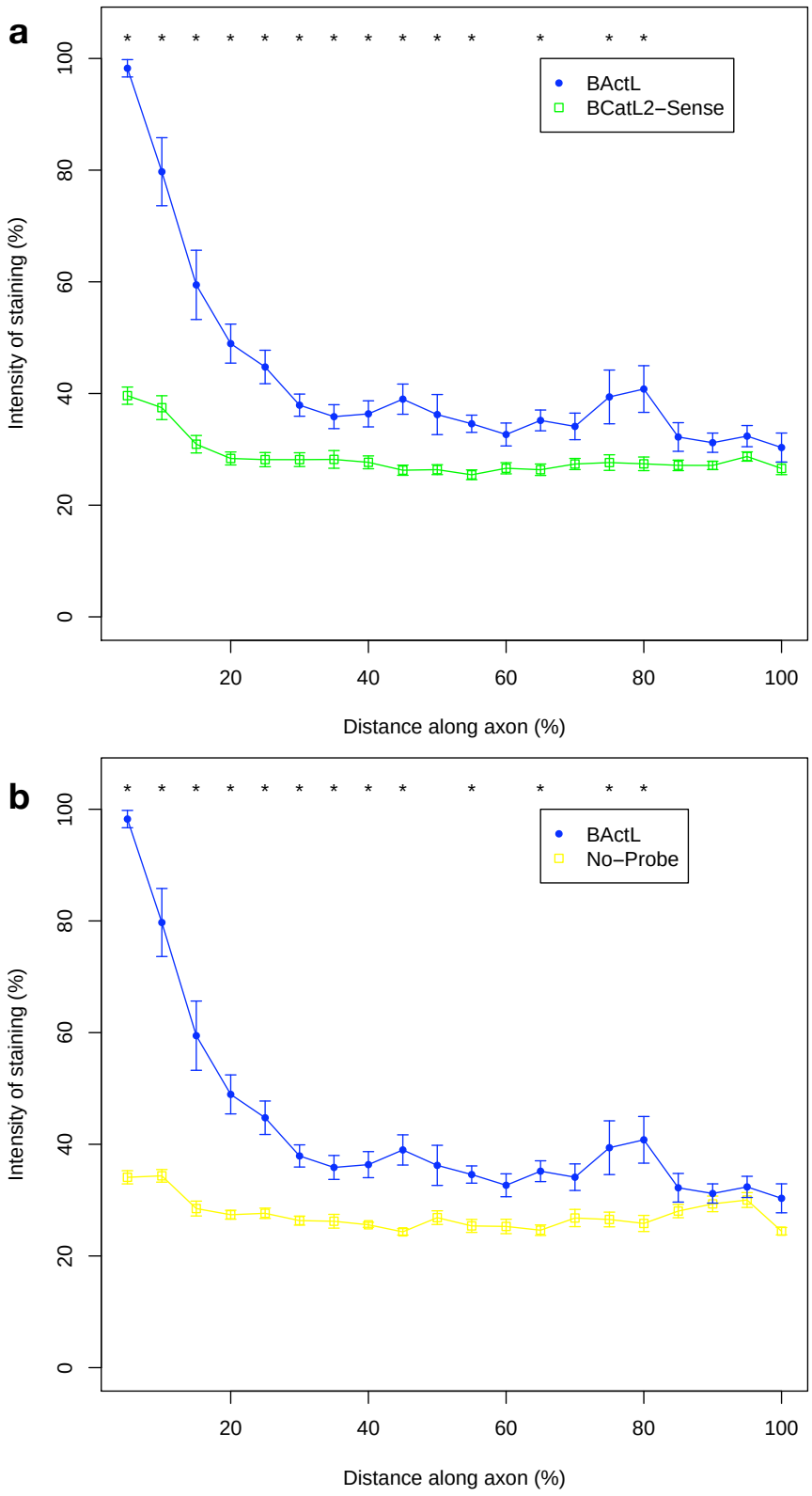

Figure 5.18: Comparison of staining along multiple axons for β-actin long probe. See Figure 5.17 for description of plots. βActL significantly stains axons, but not growth cones, above the level of b) βCatL2 Sense and c) No Probe controls. Number of axons in each sample: βActL, 11; βCatL2 Sense, 15; No Probe, 6.

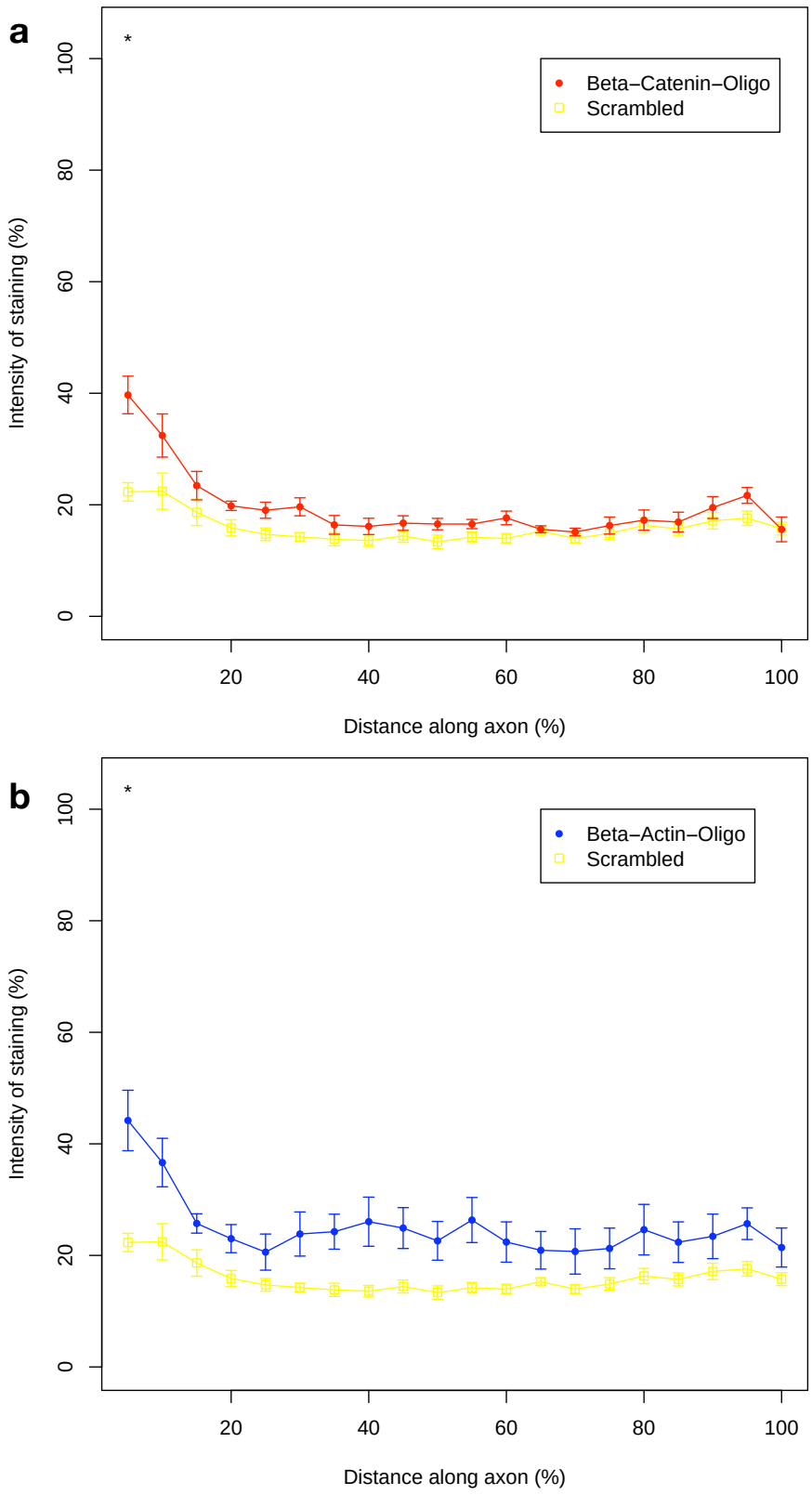

Figure 5.19: Comparison of staining along multiple axons for β-catenin and β-actin oligoprobes. See Figure 5.17 for description of plots. Neither a) β-catenin oligoprobes or b) β-actin oligoprobes stain axons significantly above the level of the Scrambled control oligoprobe, except in the cell body. Number of axons in each sample: β-Catenin Oligo, 7; β-Actin Oligo, 6; Scrambled, 7.

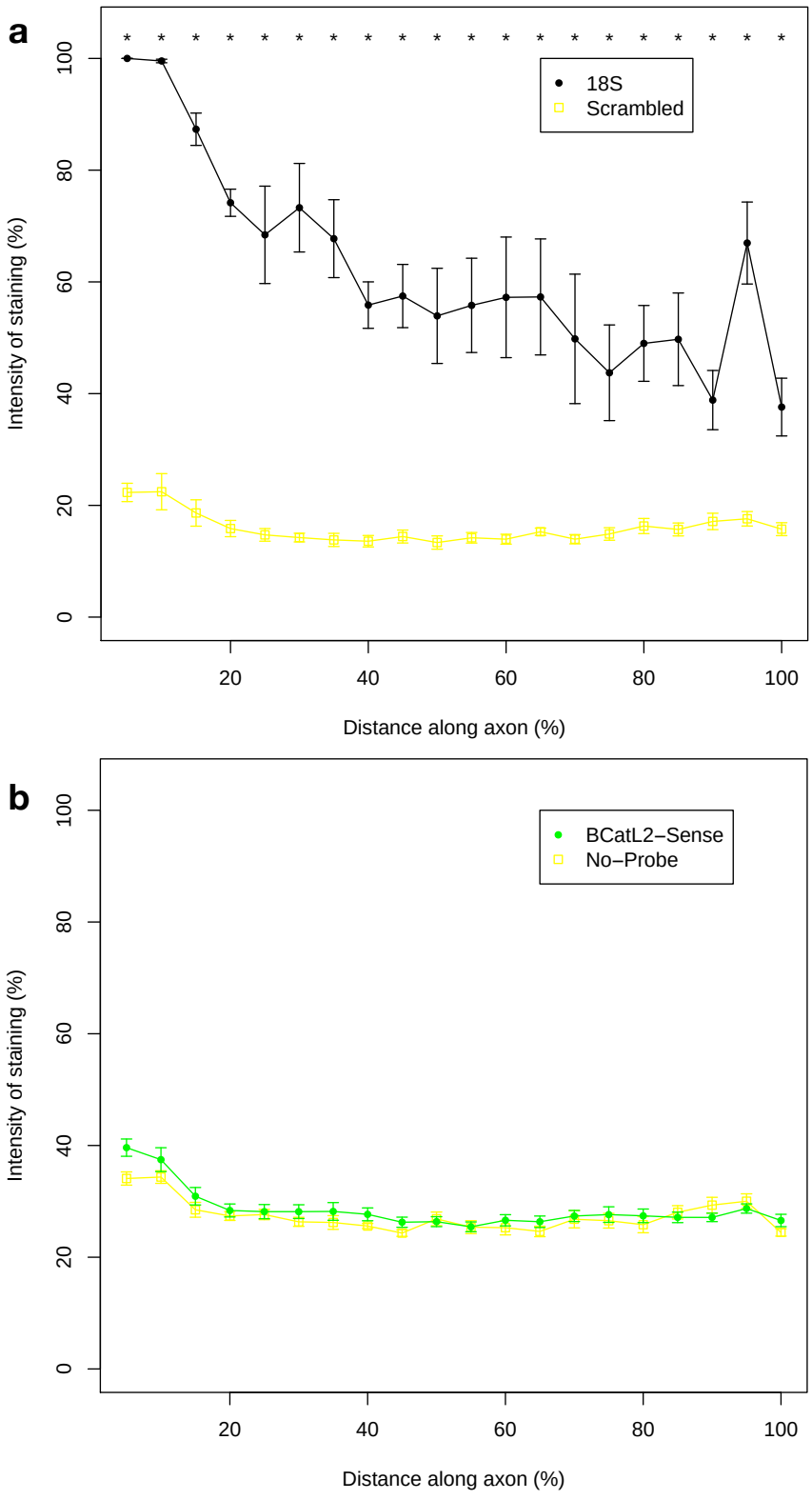

Figure 5.20: Comparison of staining along multiple axons for 18S oligoprobes and long probe controls. See Figure 5.17 for description of plots. a) 18S significantly stains cells, axons and growth cones above the level of the Scrambled control oligoprobe. An increase in staining can be seen at the growth cone (90-95% bin). b) βCatL2 Sense and No Probe control stains are not significantly different according to one-tailed Wilcoxon rank sum test with Bonferroni correction in either direction. Number of axons in each sample: 18S, 6; Scrambled, 7; βCatL2 Sense, 15; No Probe, 6.

In contrast, β-catenin mRNA has never been shown to be present in any axonal system. However, as described in 1.6.2, several lines of evidence indicate that β-catenin mRNA may be present in axons; β-catenin protein has been found in other axonal systems, β-catenin is central to cell adhesion behaviour which may also play a role in axon guidance, and β-catenin has been implicated in the regulation of both the Slit/Robo and Eph/ephrin guidance cue systems. In this thesis, it has been shown that β-catenin mRNA was cloned in a library of axonal mRNA and was successfully amplified by qRT-PCR using the method described in Chapters 3 and 4. Therefore, a series of in situ hybridisations for β-catenin were carried out, firstly to add weight to the evidence presented in Chapter 4 for the presence of β-catenin mRNA in thalamic axons, and secondly to see if β-catenin is localised to a particular region of the axon or growth cone.

The β-catenin and β-actin probes were all designed to bind to the 3'UTR of the RNAs, as this region has been shown to be required for several mRNAs, including β-actin, EphB2, tau and RhoA, to be translated in axons (see Sections 1.5.3, 1.5.4 and 1.5.5).

5.4.1.2 Selection of Probe Type

The probes used for the experiments presented here were short and long RNA probes. Single short RNA probes, or oligoprobes, 50 base pairs in length, have been used successfully for axonal in situ hybridisation by the Jaffrey lab (Hengst et al., 2006; Wu et al., 2005). Long RNA probes, or riboprobes, of 500-1000 base pairs in length, have been used by the Ginzburg lab (Aronov et al., 2002; Litman et al., 1994). In each case, cDNA templates must be produced which can be used to transcribe labelled RNA strands. This is done by incorporating labelled uracil bases into the *in vitro* transcription mix. The RNA probes used here were transcribed using digoxigenin-labelled uracil bases. Digoxigenin is commonly used to label in situ probes and was used by Jaffrey, Ginzburg and Bassell in their axonal in situ hybridisations.

RNA oligoprobes are ideal for the purpose of rapidly characterising many RNAs using in situ hybridisation, because the cDNA templates used to make them can be synthesised quickly and cheaply and labelled oligoprobes can be rapidly transcribed from these templates. Long riboprobes are not suitable for this purpose; although the transcription of labelled probes is performed in the same way as for the oligoprobes, the construction of a cDNA template from a clone is time-consuming and expensive and it would not be feasible to use these probes to validate large numbers of RNAs.

However, here, where β-catenin was thought to be of particular interest, it was decided to use long riboprobes to attempt to detect β-catenin, as a clone for β-catenin was readily available and in situ hybridisation with long riboprobes was well-established in the laboratory, whereas RNA oligoprobes were untested.

Another reason for preferring long probes to short probes is that long probes will contain more labelled bases than short probes and so may be easier to detect. This problem can be partly alleviated by including multiple short probes in the same mixture which will bind to different parts of the mRNA. In these experiments, three different oligoprobes have been used for each RNA (see Section 5.3.1).

Whereas the Jaffrey lab use 50 base pair oligoprobes (Wu et al., 2005), 40 base pair oligoprobes were used for the in situ hybridisations presented here. This was because each oligoprobe required a T7 promoter region to be synthesised to the end of the probe, to enable the probe to be transcribed using T7 RNA polymerase, making each oligoprobe 60 base pairs in length. The price of synthesis by MWG increased considerably for oligoprobes over 60 base pairs in length, and so it was not economically possible to make multiple longer oligoprobes.

The Bassell lab use multiple DNA oligoprobes for their axonal in situ hybridisations (eg Antar et al. (2006); Zhang et al. (2001); Bassell et al. (1998)). The probes are constructed with amino-modified thymidine bases which are able to bind to digoxigenin, using a DNA synthesiser. While the results from these probes appear to be specific and strong, no DNA synthesiser was available to be used to construct probes in this way, and purchasing amino-modified or digoxigenin-labelled DNA oligoprobes was prohibitively expensive. Therefore DNA probes have not been used for these experiments.

5.4.1.3 Selection of controls

To conclude that an RNA of interest is present in axons, it is not sufficient to only stain the axons using a labelled probe designed to bind to the RNA. It may be that the probe has not bound specifically to the RNA of interest, or that the fluorescent antibodies or colorimetric stain used has not bound specifically to the labelled probe. Extra probes should be used to control for these possibilities.

For oligoprobes, a scrambled probe should be constructed which is confirmed (using BLAST) not to bind to any known RNA molecule. If this probe is labelled and detected as the other probes are and no signal is detected once the protocol is complete, this indicates that the scrambled probe did not bind to any RNA and that

any stain is indiscriminate. This means that any stain for other probes above the level shown for the scrambled probe can be considered to reflect accurate staining for those other probes.

For long probes, it is not possible to construct scrambled probes of the required length efficiently. However, suitable controls can be constructed using the double-stranded DNA vectors which are used to construct cDNA probe templates. If the sequence of the RNA of interest is defined as the sense strand, the probe which will be used to bind to this RNA should be the antisense strand. This antisense strand is constructed using one strand of the DNA vector. However, the other strand of the vector can be used to construct sense probes. These sense probes should not bind to any RNA, unless the antisense strand is endogenously transcribed. While it is customary to compare antisense probes to sense probes from the same transcript, it is also possible to compare antisense probes with sense probes for other genes, as has been done with βActL and βCatL2 Sense here.

The use of scrambled or sense probes is sufficient to establish that the other oligos or antisense probes have bound to RNA. In addition, a condition where no probe is used but the protocol is otherwise the same has been used to demonstrate a baseline level of background staining, to determine if the scrambled or sense probes have produced any staining at all.

5.4.1.4 Cultures and Protocols

Two culture systems were used for these experiments; dissociated thalamic cells and thalamic explants. Dissociated thalamic cells plated on fibronectin-coated glass coverslips were not able to survive for more than two days and so did not grow axons of substantial length. However, thalamic explants plated on the same substrate were able to survive for at least a week, producing substantial axonal growth. In addition, single cells in these explant cultures were able to grow longer axons than those in the dissociated cell cultures. This suggests that the explants contained factors which enabled the survival of thalamic cells and the growth of thalamic axons. It may be that thalamic cells require interactions with other thalamic cells to survive, but it seems more likely that secreted factors are involved given that single cells were able to survive and grow axons away from thalamic explants.

Although the explant cultures were more robust than dissociated cell cultures, it still proved difficult to preserve a large number of explants and cells throughout the full length of an in situ hybridisation protocol, and it was not possible in the time available

to improve on the staining shown here without damaging the cultured explants and cells. This is regrettable given the small levels of staining observed, and the failure to achieve a high quality fluorescent staining of axons. It is clear that the sensitivity required for axonal in situs is far above that of in situs on sections; the βCatL1 probes worked well on coronal sections (see Figure 5.3) but could not be used reliably on either axonal culture system with either fluorescent or colorimetric protocols.

It may be that the addition of serum, which was not attempted with in situ hybridisations but which proved crucial for the qRT-PCR experiments, as shown in Chapter 3, would improve the growth and stability of axons in explant cultures. Alternatively, other protocols such as those of Bassell et al. (1998) or Aronov et al. (2002) could be attempted in place of the Wu et al. (2005) protocol used here. It would also be of interest to attempt an in situ with DNA probes synthesised to incorporate DIG-labelled thymine bases, as is done by the Bassell lab.

5.4.2 Presence of mRNAs in thalamic axons

Figures 5.4, 5.11, 5.12, 5.14 and 5.15 provide evidence that 18S rRNA, β-actin mRNA and β-catenin mRNA are present in thalamic axons, in agreement with the evidence presented in Chapter 4. It also appears that β-catenin can be found in particular at the growth cone (see Figure 5.12). Statistical analysis of these results demonstrates significant signal for β-catenin mRNA in thalamic growth cones but not axons (see Figure 5.17), for β-actin mRNA in thalamic axons but not growth cones (see Figure 5.18) and for 18S rRNA in thalamic axons and growth cones (see Figure 5.20). This analysis also supports what is apparent from the pictures, that there is a small but significant increase in β-catenin mRNA at the growth cone. An increase at the growth cone can also be seen for 18S rRNA, but not for β-actin mRNA, with either long probes or oligoprobes.

These results support the case for the presence of β-catenin in thalamic growth cones in Section 1.6.2.1; given the presence of β-catenin mRNA in thalamic growth cones, the known role of β-catenin in Slit functioning, and the requirement for Slit to induce thalamic axons to turn away from the hypothalamus, it is highly likely that β-catenin is essential for this turning event to occur. It also seems likely that β-catenin is involved in the response of thalamic axons to ephrin-A5 in the ventral telencephalon.

The results also support the hypothesis that β-catenin is locally translated at the growth cone, in common with other molecules such as β-actin and RhoA. This suggests

that GSK-3β regulation of β-catenin should be investigated at the growth cone. β-catenin accumulates in the cell when GSK-3β is inhibited, but it is unclear if this is due to β-catenin protein transport or due to synthesis of new β-catenin protein. The presence of β-catenin mRNA at the growth cone indicate that the latter may be the case, but this requires detailed investigation of both β-catenin mRNA and GSK-3β at the growth cone.

In addition, the results lend further support to the results presented in Chapter 4, in that they provide another demonstration of the presence of β-catenin, β-actin and 18S RNAs in thalamic axons, but also that the level of staining matches the general pattern seen when comparing ratios of axon-to-cell expression in the PCR experiments (see Section 4.4.3.3), with 18S staining being more intense than β-actin staining and β-catenin staining.

The differences in staining between the probes are intriguing. β-actin mRNA has been shown to be expressed along the whole axon and growth cone in other systems such as rat cortical neurons (Bassell et al., 1998); however, other RNAs such as EphA2 have been shown not to be expressed in the axon but are only found in the growth cone (see Section 1.5.3). Here, β-catenin mRNA appears to follow the pattern of EphA2; there is no significant staining in the axon, but there is a noticeable and significant rise in staining at the growth cone (see Figure 5.17). In contrast, β-actin mRNA is found along the axon but not in the growth cone.

It may be that this apparent difference is the result of variation in in situ protocols and probes in the literature and in the experiments presented in this thesis, but it may also reflect a genuine difference in biological function. It may be that some RNAs are distributed across the axon whereas others are restricted at the growth cone; β-actin and RhoA, while they have been identified in the growth cone, may have additional cytoskeletal roles along the whole axon, whereas the majority of β-catenin and EphB2 mRNAs, which have mostly membrane-bound roles, may be restricted to the growth cone. Further investigation of mRNAs in thalamic axons, in particular time-sensitive investigations of mRNA transport and new synthesis such as those carried out by Leung et al. (2006), are required before this issue can be resolved.

It should be noted that this data is congruent with that presented in Section 4.4.3.3, where β-actin was shown to have a higher axon:cell expression ratio (relative to 18S) compared to β-catenin. This is what would be expected if β-actin is expressed throughout the axons, whereas β-catenin is only expressed at growth cones, as the growth cones form a smaller percentage of the total quantity of tissue compared to the

axons. It may be that expression of β-catenin in growth cones is actually more dense than β-actin in axons, but due the large volume of axonal tissue compared to growth cone tissue there is a greater quantity of β-actin present overall.

Why is there apparent β-actin staining in the growth cones of the axons shown in Figure 5.12(a-d), but this cannot be detected statistically with a larger population of axons? This may be a problem with the method of image analysis; tracing a line through the axon and growth cone covers most of the axon but only a small portion of the growth cone, and it may be that there is staining in the growth cone which is less dense than that in the axon and so is not detected using this analysis method. Alternatively, the population of axons chosen for analysis may be heterogenous. The pictures in the figure were chosen to show the best staining achieved over all axons for β-actin and β-catenin. It is known that the population of thalamic cells is heterogeneous, because they differentiate into many nuclei (see Section 1.3.3) and because axons from different parts of the thalami behave differently in the same environment (see Section 1.4.2). Therefore it may be that β-actin and β-catenin mRNAs are differently expressed within the population of cells and explants examined here, given that the cells come from very small pieces of thalamus. This point will be returned to in Chapter 6. However, this should not affect the results presented in Chapter 4, where whole thalami (and whole axonal carpets) were cultured and dissected, and so the whole population of thalamic cells should be represented.

Nevertheless, it may be that the analysis shown here represents a real difference in biological function. If so, it agrees with reports that β-actin mRNA is not localised to the growth cone in minimal essential medium or even when stimulated with NGF, but it is localised to the growth cone when stimulated by BDNF and neurotrophin-3 (Zhang et al., 1999). It also appears that β-actin mRNA is upregulated in the growth cone when stimulated with netrin-1, but that expression is low prior to stimulation (Leung et al. (2006); see Figure 1.12). Therefore it may be that while a small quantity of β-actin mRNA is present in growth cones, it is transported to the growth cone from the axon upon stimulation. Unfortunately, while these studies did quantify differences in growth cone expression under various conditions, they did not quantify differences in axonal and growth cone expression. It would be of great interest to compare axonal and growth cone expression levels of β-actin mRNA, as it would indicate whether stimulation causes a general upregulation of β-actin in axons and growth cones, or whether there may be transportation of mRNA from axon to growth cone upon stimulation. This is particularly of interest given the apparent small increase in β-actin expression just

prior to the growth cone in these in situs (see 75% to 80% bin in Figure 5.18), which may represent an area in the axon or perhaps the C-domain of the growth cone, and raises the possibility that β-actin mRNA is sequestered at the base of the growth cone and transported into the growth cone upon stimulation.

The image analysis clearly shows that β-catenin mRNA is expressed in thalamic growth cones without stimulation. These same growth cones should now be tested for β-catenin mRNA expression under stimulation with guidance cues such as Slit1/2 and ephrin-A5, which are likely to be involved in regulating β-catenin in thalamic growth cones (see Section 1.6.2.1 for discussion), and with the neurotrophins BDNF, neurotrophin-3 and NGF. This will reveal if β-catenin mRNA responds to stimulation as β-actin mRNA does, although it might be expected that the particular responses of these mRNAs to the same stimuli will vary, given their opposite expression without stimulation. For example, β-actin mRNA expression does not change in the presence of NGF, but β-catenin protein is known to be downregulated by NGF in mouse DRG growth cones (Zhou et al., 2004b). It may be that the regulation of these mRNAs and proteins is intertwined, with adherens junctions containing β-catenin forming to stabilise the actin cytoskeleton, and the same junctions being dismantled to allow the cytoskeleton to respond to stimulation.

The localisation of β-catenin mRNA to thalamic growth cones also suggests that its 3'UTR should be investigated for targeting elements such as those found in the EphA2, tau, MAP2 and β-actin mRNAs, and constructs containing any predicted elements should be introduced into thalamic cells to test if they are transported to the growth cone. It will be of interest to see if the β-catenin mRNA is transported in the same protein complexes as β-actin, or if other proteins may be involved in the regulation of other axonal mRNAs such as β-catenin.

Chapter 6

Visualising RNA in the Thalamus and Internal Capsule with In Situ Hybridisation

6.1 Introduction

In previous chapters, RNAs have been shown to be present in axons grown in vitro. In this chapter, in situ hybridisations on vibratome sections are presented in order to visualise RNA in vivo, focussing on the thalamus and on the internal capsule which contains axons grown from the thalamus to the cortex and also from the cortex to the thalamus. These regions have been studied at two different stages of development to see if any difference in levels of RNA could be detected during the development of the thalamocortical and corticothalamic projections. These in situ hybridisations are now presented.

6.2 Materials and methods

The in situ hybridisations presented here were all performed on 100μm-thick coronal sections, cut using a vibratome, from the heads of E14.5 mice (CD1 strain). Heads were fixed in 4% paraformaldehyde in PBT, pH 9.5, at 4°C overnight, washed three times in 1xPBS for ten minutes and stored in 1xPBS + sodium azide at 4°C until they were sectioned. Before sectioning, heads were embedded in 3% agarose in DEPC-treated water. Sections were cut onto SuperFrost Plus slides (VWR) and dried overnight before in situ hybridisation commenced.

The probes used for the in situ hybridisations were all used for the in vitro in situs presented in Chapter 5. Details of their construction and design can be found in Sections 5.2.1 and 5.3.1.

6.2.1 Vibratome in situ hybridisation protocol

This protocol was kindly provided by Lynda Erskine (University of Aberdeen, UK; Thompson et al. (2006)). All treatments were performed at room temperature unless otherwise stated.

Slides were washed with PBT for five minutes, dehydrated with 50% and 100% methanol in PBT for five minutes each, rehydrated with 75%, 50% and 25% methanol in PBT for five minutes each and washed with PBT twice for five minutes. Slides were treated with 6% hydrogen peroxide in PBT for one hour and washed three times in PBT for five minutes each. Slides were treated with 5 μg/mL Proteinase K in PBT for ten minutes and washed with fresh 2mg/mL glycine in PBT for ten minutes followed by two five minute PBT washes. Slides were post-fixed in 4% paraformaldehyde in PBT for twenty minutes and washed twice for five minutes in PBT. Slides were pre-hybridised in pre-heated hybridisation mixture at 65 °C for sixty minutes. Probes were prepared in hybridisation mixture at dilutions of 15μl/mL and denatured at 85 °C for five minutes. 100 μl of probe mixture was added to each slide, covered with a plastic coverslip and left to hybridise in a humid chamber containing filter paper soaked in 50% formamide at 65 °C overnight.

After hybridisation, slides were washed three times with pre-heated Solution 1 for twenty minutes at 65 °C, three times with pre-heated Solution 3 for twenty minutes at 60 °C and three times with 1xTBST for five minutes at room temperature. Slides were incubated in 10% sheep serum in TBST for sixty minutes and then incubated in anti-digoxigenin alkaline phosphatase in 1% sheep serum in TBST (1:2000) at 4 °C overnight.

Slides were washed five times in 1xTBST for ninety minutes at room temperature and three times in 1xNTMT for ten minutes at room temperature. Slides were incubated in NBT/BCIP in 1xNTMT (1:50) at 4 °C for 25 hours. Slides were washed twice with 1xNTMT for ten minutes, then washed in 1xPBT, pH 5.5, for ten minutes, washed twice in 1xPBT for ten minutes, postfixed with 4% paraformaldehyde in 1xPBS for thirty minutes and washed twice in 1xPBS for ten minutes. Slides were mounted in 90% glycerol in PBS.

6.3 Results

Colorimetric in situ hybridisations on coronal vibratome sections of mouse E14.5 and E15.5 brain were carried out. Figures 6.1 and 6.2 show the results for E14.5 sections; Figure 6.3 and 6.4 show the results for E15.5 sections. β-catenin (βCatL2) Antisense, β-catenin (βCatL2) Sense and β-Actin (βActL) Antisense long probes, and 18S, RPS3 and Scrambled oligoprobes were tested at each age. The figures show images of whole coronal sections where the thalamus was visible and also higher magnifications of the internal capsules in these sections where it was possible to clearly see these regions (some regions in Figure 6.2 are not visible). The slides were stained for 25 hours, saturating most of the section, in order to attempt to stain any small amounts of RNA which may be present in the internal capsule. Figure 6.5 shows magnifications of the thalami shown in Figures 6.1 and 6.3.

Figure 6.1 shows that both the β-catenin and β-actin Antisense long probes heavily stained E14.5 coronal sections of mouse brain far above the level seen for the β-catenin Sense probe. The thalamus is heavily stained for both probes, with some heterogeneity of staining apparent in both cases (see Figure 6.5 for magnifications). There are vertical strips of heavy β-catenin staining in the medial ventricular zone and heavy staining lateral to the ventricular zone but only light staining within the majority of the ventricular zone itself. In contrast, β-actin is heavily stained in most of the ventricular zone with light strips of staining medial and lateral to the ventricular zone. β-actin stains particularly heavily ventromedially. The epithalamus is stained similarly to the thalamus for β-actin but is more heavily stained than the thalamus for β-catenin. However, the internal capsules, which are the white, cell free regions in the sections, and which contain the thalamocortical and corticothalamic tracts, are not stained, despite the long exposure times. While there is some dark punctate staining in some areas of the internal capsule, the same punctate staining can be seen in the images of the control internal capsule, and so should be considered an artefact of the protocol rather than a reflection of the presence of RNA.

Figure 6.2 shows that the 18S oligoprobes and, to a lesser extent, the RPS3 oligoprobes stained E14.5 coronal sections of mouse brain above the level of the Scrambled control probe. Staining of the sections is broadly uniform for both probes and as with the long probes, the internal capsule is not stained above control levels.

Figure 6.3 shows that the β-catenin and β-actin Antisense long probes both stain E15.5 coronal sections of mouse brain far above the level of the β-catenin Sense probe.

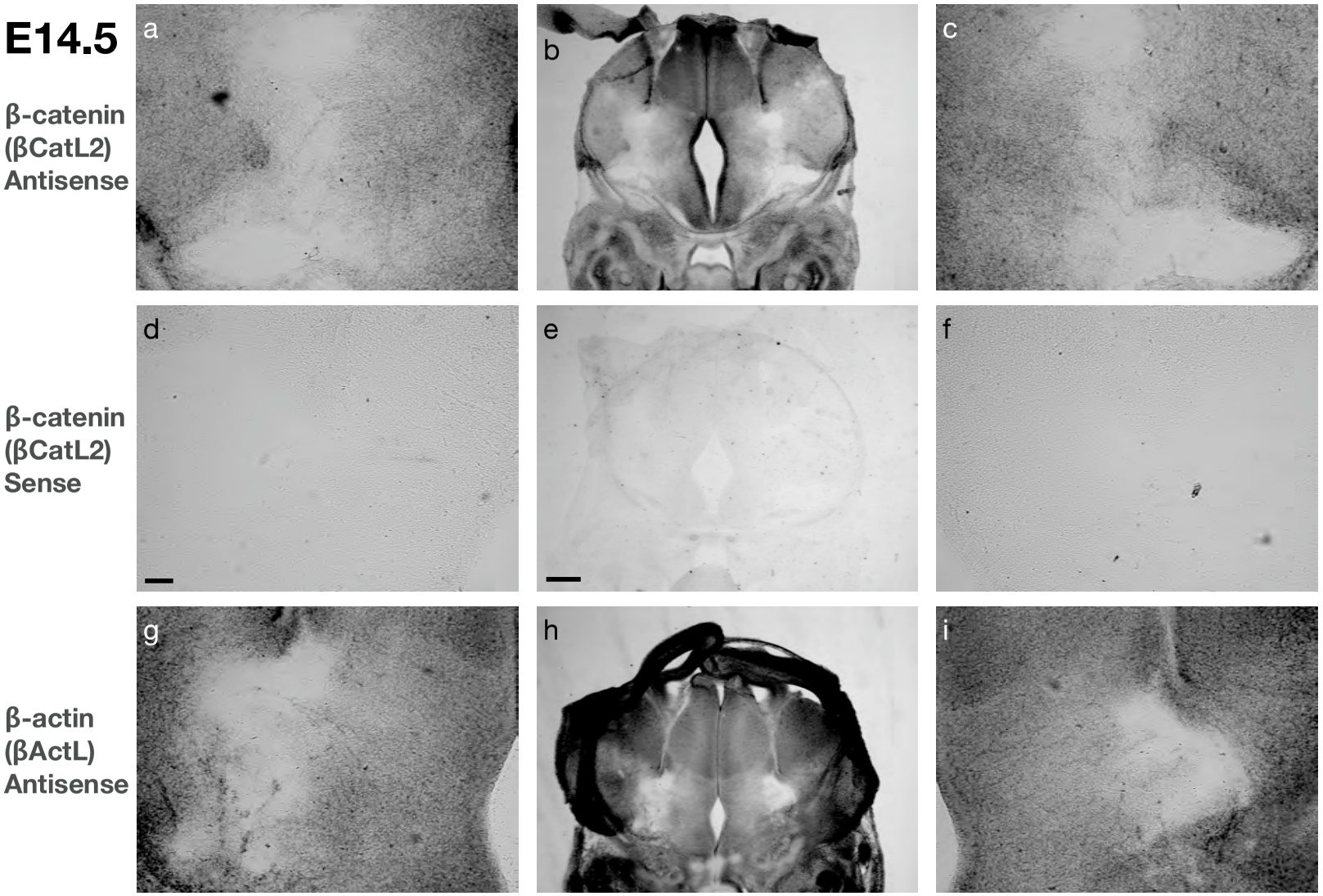

Figure 6.1: β-catenin and β-actin mRNAs are expressed in E14.5 thalamus but not internal capsule. βCatL2 Antisense (a-c) and βActL Antisense (g-i) probes can be detected above levels for control probe βCatL2 Sense (d-f). (b,e,h) Coronal sections. (a,d,g) Magnifications of left internal capsule. (c,f,i) Magnifications of right internal capsule. Scale bar in d) for a,d,g,c,f,i), 100μm; scale bar in e) for b,e,h), 500μm.

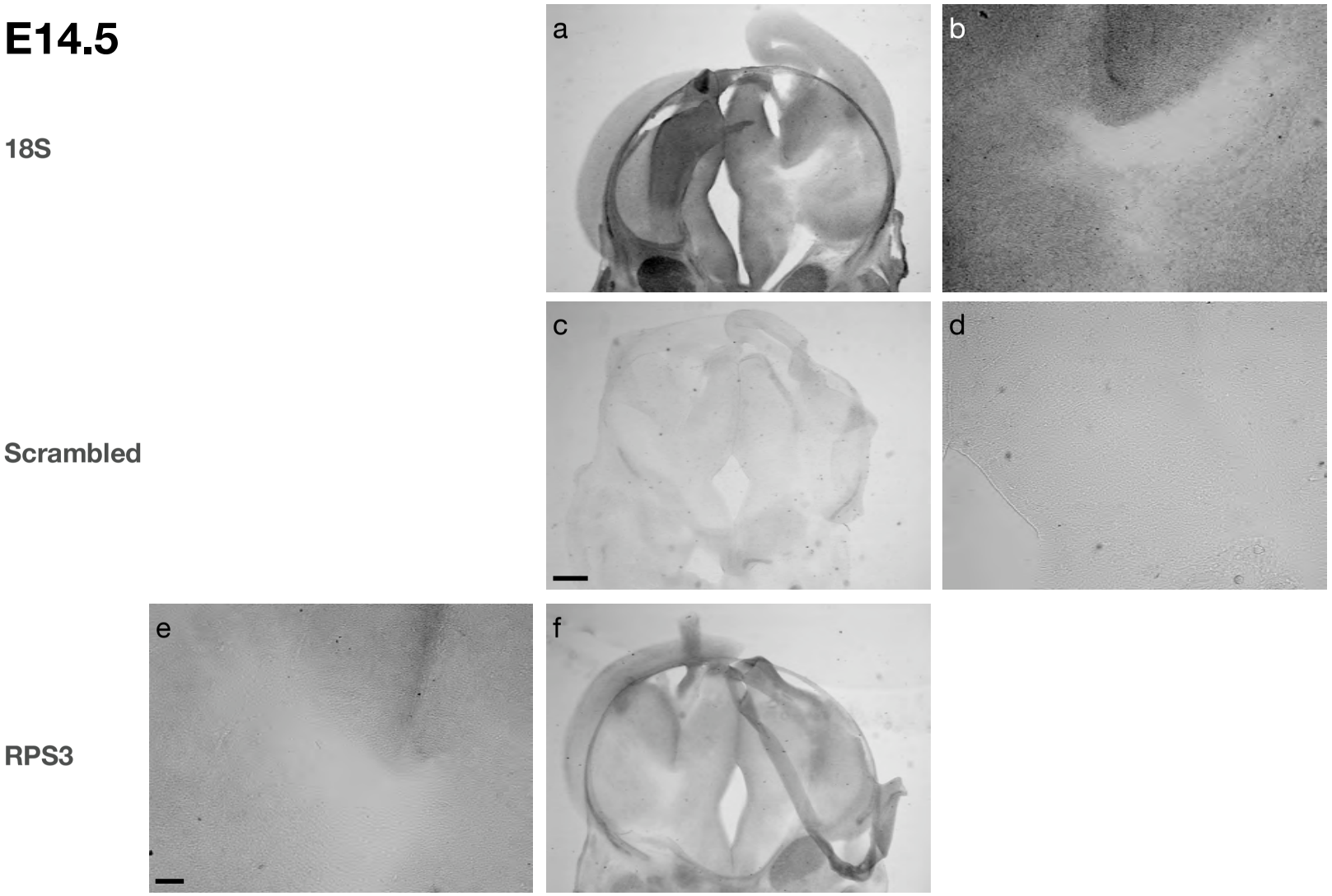

Figure 6.2: 18S rRNA and RPS3 mRNA are expressed in E14.5 thalamus but not internal capsule. 18S (a-b) and RPS3 (e-f) probes can be detected above levels for Scrambled control probe (c-d). (a,c,f) Coronal sections. (e) Magnification of left internal capsule. (b,d) Magnifications of right internal capsule. Scale bar in e) for b,e,d), 100μm; scale bar in c) for a,c,f), 500μm.

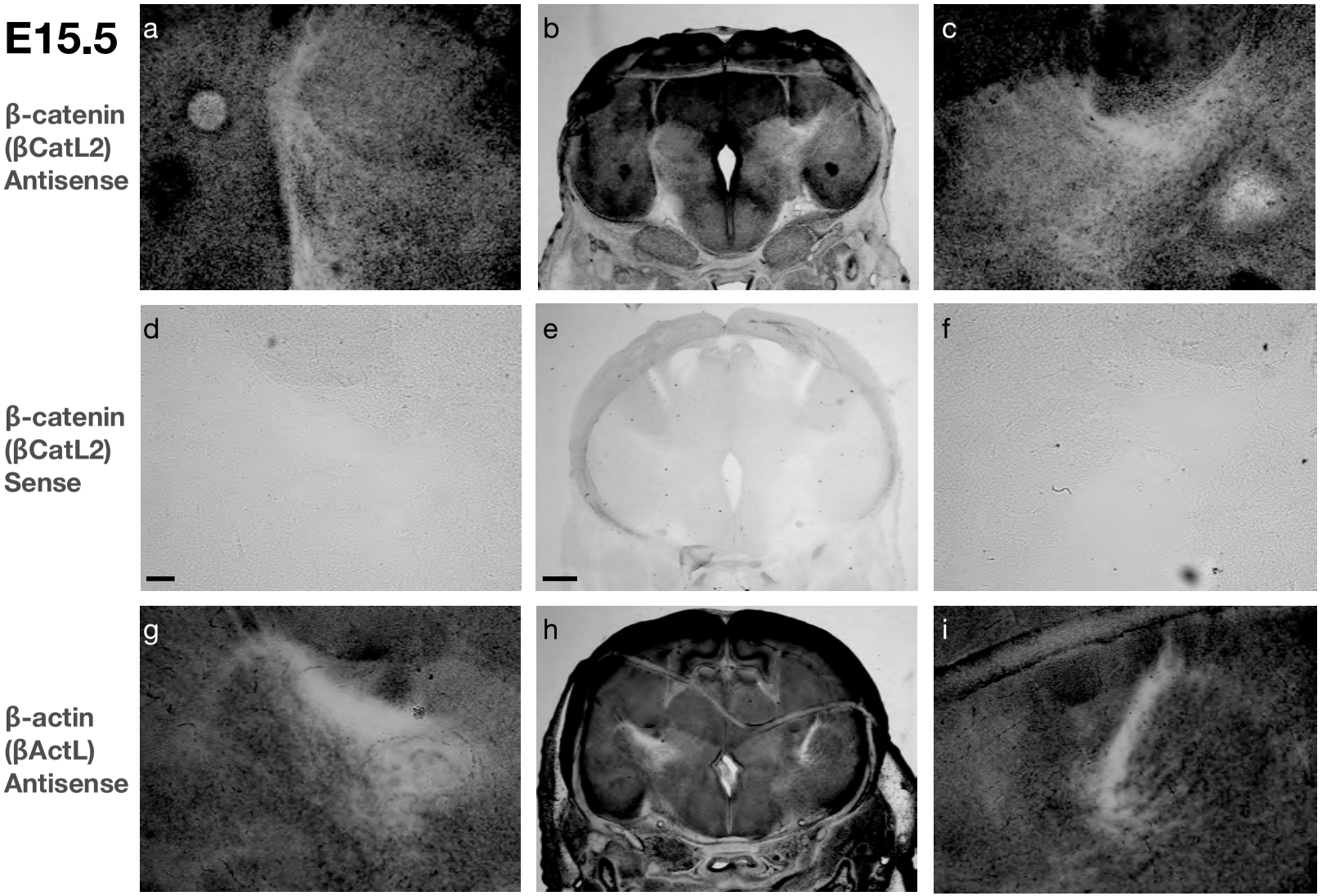

Figure 6.3: β-catenin and β-actin mRNAs are expressed in E15.5 thalamus but not internal capsule. βCatL2 Antisense (a-c) and βActL Antisense (g-i) probes can be detected above levels for control probe βCatL2 Sense (d-f). (b,e,h) Coronal sections. (a,d,g) Magnifications of left internal capsule. (c,f,i) Magnifications of right internal capsule. Scale bar in d) for a,d,g,c,f,i), 100μm; scale bar in e) for b,e,h), 500μm.

As with the E14.5 sections, heavy ventromedial staining for β-actin can be seen in the thalamus (see Figure 6.5 for magnification). β-catenin is considerably upregulated in the thalamus compared to the rest of the section, and variation in thalamic staining is visible, with light and dark patches intermingled across the thalami and dorsal regions particularly heavily stained (see Figure 6.5 for magnification). Once again, however, no clear staining can be seen in any of the internal capsules above control levels.

Figure 6.4 shows that both the 18S and RPS3 oligoprobes stain E15.5 coronal sections of mouse brain above the levels seen for the Scrambled control oligoprobe. Staining is uniform across the thalamus for both probes except for strong staining for RPS3 in the epithalamus. However, as with all the other pictures, no clear staining can be seen in the internal capsule above control levels apart from cellular staining.

6.4 Discussion

These experiments were undertaken to confirm the expected expression of β-catenin, β-actin, 18S and RPS3 RNAs in the thalamus at embryonic days E14.5 and E15.5, when thalamocortical axons begin to grow from the thalamus to the cortex, and also to attempt to detect these RNAs in the internal capsule. β-catenin, β-actin and 18S were chosen because these probes had been examined in detail in the work presented in Chapters 4 and 5. RPS3 (see Section 1.6.1) was chosen in addition, from all of the RNAs identified in the qRT-PCR experiments presented in Chapter 4, because of its high axon:cell ratio of expression shown in Section 4.4.3.3, which may indicate that it has a significant role to play in the development of thalamocortical axons.

The results shown here demonstrate that β-catenin, β-actin, 18S and RPS3 RNAs are expressed in the thalamus while the thalamocortical tract is growing towards the cortex. This is not surprising given the central roles of these molecules in cytoskeletal, adhesive and translation behaviour. However, they also show that β-catenin mRNA appears to be upregulated in the thalamus during this time, which may indicate a particular requirement for β-catenin mRNA in the thalamus. It may be that this mRNA is transported from thalamic cells to the growth cones of the axons of these cells, in order for these growth cones to respond to guidance cues such as Slit and ephrin-A5, as discussed in Sections 1.6.2 and 5.4.2.

No staining in the internal capsule can be seen in any of the images above the levels seen in the control images. This is not surprising given that only very small quantities of RNA have been detected in axons in culture compared to that which can

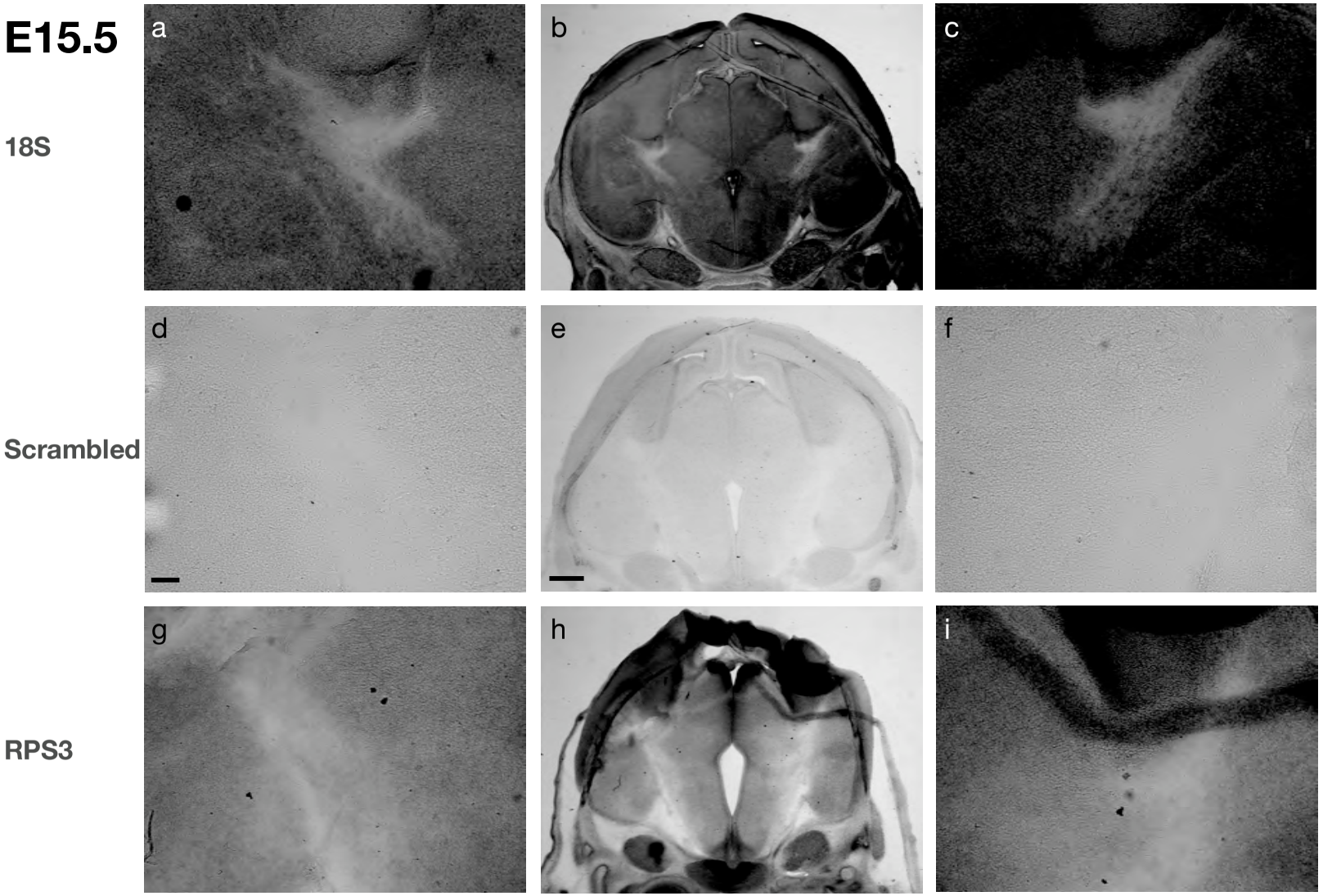

Figure 6.4: 18S rRNA and RPS3 mRNA are expressed in E15.5 thalamus but not internal capsule. 18S (a-c) and RPS3 (g-i) probes can be detected above levels for Scrambled control probe (d-f). (b,e,h) Coronal sections. (a,d,g) Magnifications of left internal capsule. (c,f,i) Magnifications of right internal capsule. Scale bar in d) for a,d,g,c,f,i), 100μm; scale bar in e) for b,e,h), 500μm.

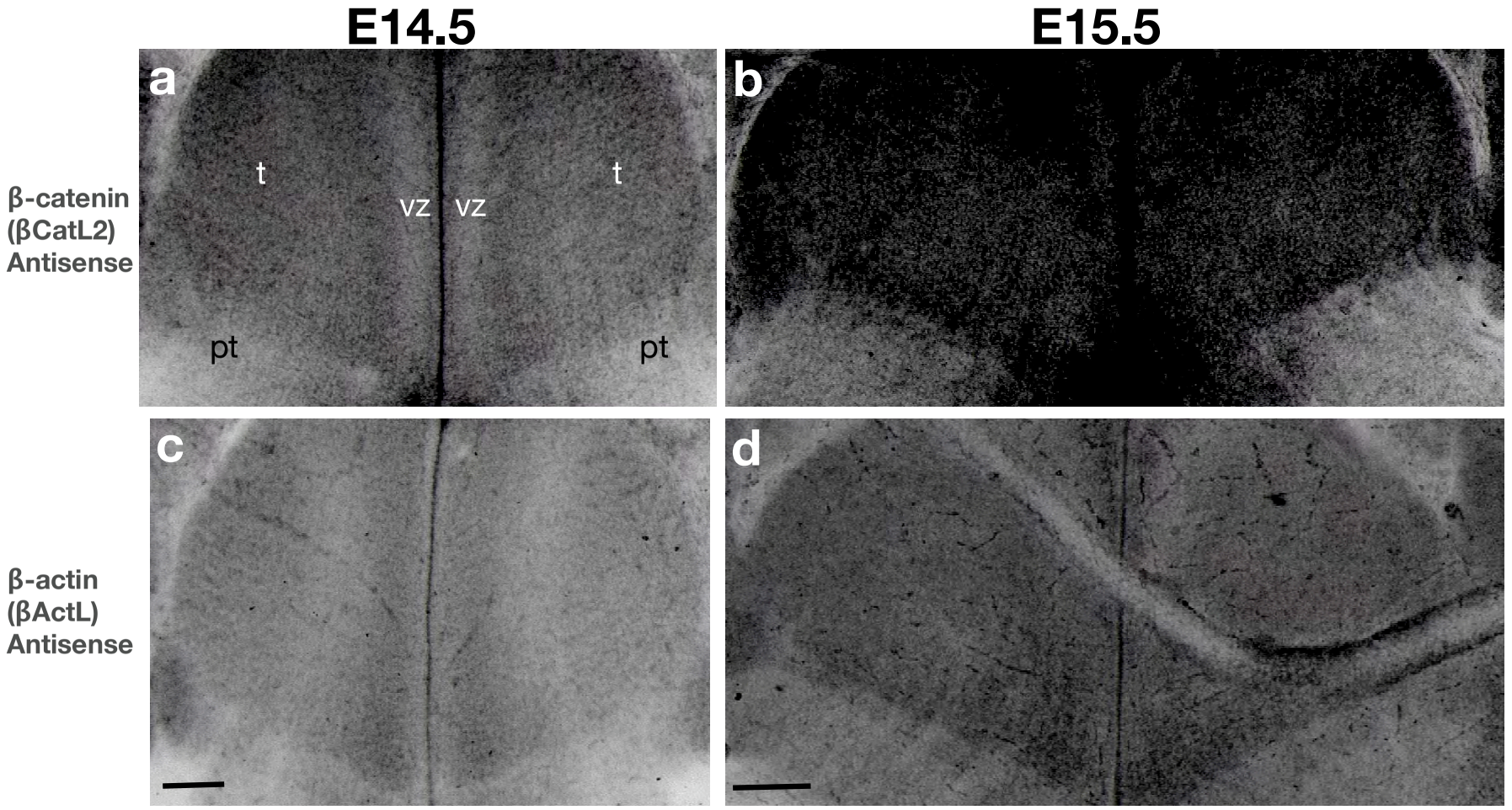

Figure 6.5: Small variation in β-catenin mRNA and β-actin mRNA expression can be observed in E14.5 and E15.5 thalamus. a-d) Magnifications of thalami from pictures shown in Figures 6.1 and 6.3. a) βCatL2 Antisense, E14.5; light vertical strips of low staining can be seen medially in the ventricular zone (vz), and heavier staining can be seen laterally in the thalamus (t). b) βCatL2 Antisense, E15.5; light and dark patches are distributed across the thalamus. c) βActL Antisense, E14.5; there is heavy staining in the ventricular zone and laterally in the thalamus, but only light staining in a central strip on the edge of the ventricular zone. d) βActL Antisense, E15.5. The ventricular zone is heavily stained compared with the rest of the thalamus. vz, ventricular zone; t, thalamus; pt, prethalamus. Scale bar in c) for a) and c); scale bar in d) for b) and d); both 100μm.

be detected in cells. However, this does highlight a problem with the investigation of axonal RNA; almost all results published so far are based on *in vitro* studies, rather than *in vivo* studies. There remains no reliable method of identifying and manipulating axonal RNA *in vivo* in such a way that the axonal RNA can be discriminated from cellular RNA. This point will be returned to in Section 7.3.2.

Finally, there is some evidence for heterogeneity of β-actin mRNA and β-catenin mRNA expression across the thalamus, with patches of light and dark staining being visible at E14.5 and E15.5. Therefore it is possible that there is heterogeneous expression of β-actin and β-catenin mRNA in thalamic axons and growth cones. This may account for some of the difficulty of achieving significant in situ hybridisation staining in axons, as discussed in Chapter 5, as it may be that only a subset of axons within the population express the mRNAs in question. It also suggests that it would be useful to further investigate the staining of the regions of the thalamus, and to find some way of discriminating between prospective nuclei at early embryonic ages, in order to investigate the populations of axons which they produce.

Most notably, it appears that expression of β-catenin mRNA and β-actin mRNA is different in the ventricular zone compared to the rest of the thalamus, with β-catenin mRNA having low expression in the ventricular zone but high expression on either side of the zone, and β-actin mRNA having high expression in the ventricular zone but low expression on either size of the zone (although there is high β-actin mRNA expression on the lateral side of the thalamus). This is congruent with evidence that β-catenin protein is expressed in precursor cells in the cortical ventricular zone and prevents cells from differentiating, whereas it is downregulated in differentiated cells as they travel through and exit the ventricular zone (Woodhead et al., 2006; Chenn and Walsh, 2002). This suggests that β-catenin has the same function in thalamic precursors as it does in cortical precursors, as it appears to be highly expressed at the medial edge of the ventricular zone where the precursors are located but is not highly expressed in the majority of the ventricular zone itself. In contrast, β-actin mRNA appears to be highly expressed as the cells progress through the ventricular zone, which is perhaps expected as the cytoplasm of these cells is highly active at this point.

It is possible that β-catenin and β-actin are actually antagonistic at this point in development, as is suggested by the staining patterns in Figure 6.5. In motile cells, there is more requirement for actin filaments in order for the cells to move, whereas in stable cells, there is more requirement for adherens junctions containing β-catenin to stabilise the actin cytoskeleton. However, this requires further investigation, especially

as the contrast between the staining patterns is not precise, with the strips of β-actin staining extending more laterally than those for β-catenin staining.

Chapter 7

Conclusions

7.1 Introduction

In this final chapter, the implications of the results presented in earlier sections will be discussed. The focus is on the conclusions which can be drawn from these results; for discussion of the interpretation of the data and the usefulness of the qRT-PCR and in situ hybridisation techniques, please see the discussions of the earlier chapters. The presence of a number of RNAs in thalamic axons will be discussed, followed by a consideration of further work which may arise from the results presented in this thesis.

7.2 Identification of RNAs in thalamic axons

The qRT-PCR experiments presented in Chapter 4 and the in situ hybridisation experiments presented in Chapter 5 have demonstrated the presence of multiple RNAs in thalamic axons, in particular the mRNA for β-catenin. This is the first time that RNAs have been identified in thalamic axons.

The work presented here is consistent with the idea that thalamocortical axons function via the same general mechanisms as axons of other systems and can be investigated using the same methods as are used to investigate those other systems. In particular, it strongly suggests that thalamocortical growth cones require local protein synthesis to navigate to their targets. Many of the other RNAs which have been identified in thalamic axons, namely β-actin, 18S, α-tubulin, EphB2, MAP2c and RhoA, have been identified in other axonal systems, and local translation of β-actin and RhoA in other systems has been shown to be crucial for axons in these systems to respond to guidance cues. Therefore it is expected that thalamocortical axons will

function in the same way, although this remains to be investigated.

The identification of β-catenin mRNA in thalamic growth cones is significant, for the reasons outlined in Section 1.6.2. β-catenin protein has been identified in axons of other systems and the actions of both Slit and ephrin-A5 have been implicated in the binding of N-cadherin to β-catenin, which is required for adherens junctions to form. β-catenin is also regulated by proteins which are linked to microtubule regulation such as GSK-3β which are downstream of growth cone trophic factors such as the neurotrophins and may therefore be involved in the regulation of the growth cone cytoskeleton. Slits, ephrin-A5 and several neurotrophins are known to be crucial for navigation of thalamocortical axons across the diencephalic-telencephalic boundary, through the ventral telencephalon and into the cortex. Therefore the presence of β-catenin mRNA in thalamic axons strongly suggests that this protein is important for these navigation events to take place, and that these events require local protein synthesis of β-catenin, although these hypotheses require validation. The in situ hybridisation results in Chapter 5 also suggest that β-catenin mRNA is mostly found in the growth cone and not in the length of the axon, as is the case for EphA2 in spinal cord axons (Brittis et al., 2002) but in contrast to β-actin mRNA, which is found in axons and growth cones in some axonal systems (Zhang et al., 1999; Leung et al., 2006) but has only been found in thalamic axons and not growth cones in this study. If this is correct, it further suggests that mRNAs are targeted to axonal regions, most likely through their 3'UTR (as has been shown for EphA2, tau and β-actin).

Several novel mRNAs have been identified here which have not been identified in any axonal system, namely Bat2d1, RalA, Reep5, RPS3, Reticulon-1, Synaptotagmin-13 and Ubiquilin-1; in addition, several RNAs appear to be absent from thalamic axons, namely Ascc3l1, BPGM, Rac1, Rock1 and RPA1. Of these mRNAs, little is known about Bat2d1, Reep5, Ascc3l1 and BPGM which have mostly been reported in large surveys of gene expression and have not yet been investigated in depth in their own right, and so little further can be said of them here. However, it is encouraging that, of the absent RNAs, Rock1 and Rac1 also appear to be absent from rat dorsal root ganglion cells (Wu et al., 2005) and RPA1 is a DNA replication and repair protein (Binz et al., 2004) and is therefore unlikely to be involved in axon development; of the present RNAs, Reticulon-1, RalA, Synaptotagmin-13 and RPS3 have all been directly or indirectly linked to axon growth. Reticulon-1 is associated with the microtubule- and vesicle-regulating protein spastin, which is involved in axonal transport (Mannan et al., 2006; Steiner et al., 2004), and reticulon-1 is also associated with endoplasmic

reticulum which is known to be present in axons (Yamada et al., 1971); RalA regulates neurite branching in rat sympathetic neurons (Lalli and Hall, 2005); Synaptotagmin-13 binds to neurexin-1α, which is required for presynaptic terminals to form (Dean et al., 2003) and which was also identified in the library of thalamic mRNAs presented in Section 1.6.1; and RPS3 is associated with ribosomes which are known to be present in other axonal systems and, as 18S rRNA has also been identified here, are likely to be present in thalamic axons (see Sections 1.6.1 and 4.5.2 for further discussion of the identified mRNAs). It may therefore prove fruitful to investigate these RNAs in other axonal systems as well as further investigate their roles in thalamocortical axons. In particular, while it appears that only a subset of all expressed RNAs are present in axons, it is as yet unclear whether different axonal systems contain different complements of RNAs.

The experiments here have not exhaustively tested the mRNA library presented in Section 1.6.1. The failure to identify the mRNA for the DNA replication and repair protein RPA1 in thalamic axons suggests that some of the remaining untested mRNAs may have come from contaminating cells (for example, DNA polymerase β, although as the sequence identified for this mRNA was intronic it may be that this mRNA is for some other product, not DNA polymerase β). However, there are reasons for believing it would be valuable to test the remaining mRNAs using the qRT-PCR technique presented here; for example, neurexin-1α, which is required for presynaptic terminals to form in axons (Dean et al., 2003), interacts with synaptotagmin-13 (Fukuda and Mikoshiba, 2001), which has been identified in thalamic axons in the results presented here. In addition to the library, there are several axonal mRNAs from the literature such as cofilin (Piper et al., 2006), tau (Aronov et al., 2001) and EphA2 (Brittis et al., 2002) which remain to be tested in thalamic axons, not to mention the large surveys of axonal RNAs reported by Willis et al. (2007) and Hengst and Jaffrey (2007). While these large surveys are informative, the use of qRT-PCRs, following a method similar to that presented in this thesis, will still be important in order to validate these surveys, as there is still a requirement for specific identification of each mRNA to be sure that the mRNA is indeed present in axons.

7.3 Further work

The demonstration of multiple RNAs in thalamic axons raises several issues about the regulation of these RNAs and the behaviour of thalamic axons in general. In this

section, this issue will be discussed and some methods for approaching them proposed.

7.3.1 Analysis of mRNA sequence and structure

It is clear that many mRNAs such as EphA2, tau and β-actin are targeted to the axon or growth cone by regulation of their 3'UTR, most likely through their binding to ribonucleoprotein complexes which transport the mRNAs (see Sections 1.2.1, 1.5.3 and 1.5.5). However, it is not clear how varied this regulation is and exactly what form it takes. It is not known how particular mRNAs but not others become associated with this complex, and exactly which proteins or, perhaps, RNAs are involved in the turning on and off of translation. Also, the region of 3'UTR which targets β-actin to the growth cone in some systems is not present in other axonal mRNAs, but the regions which target those mRNAs have not been clearly identified at present. Therefore there is a need for an analysis of the 3'UTRs of the axonal RNAs identified here and those in the literature to attempt to determine the elements which may cause the mRNAs to be targeted to the growth cone.

The advantage of the present study is that a number of mRNAs have been shown not to be present in axons, at least as far as the methods used here can determine; therefore it might be expected that these mRNAs will not contain elements which would enable them to be targeted to the growth cone and they can be used as a control set to compare with the axonal mRNAs. Both sequence and structure should be compared, as it may be that the targeting element interacts with other transport proteins and so depends on RNA structure, and an mRNA which has changed its sequence may retain its structure. The evolutionary conservation of the mRNAs should also be examined, as axonal RNAs have been shown to be present in several species including mouse, rat and zebrafish and so it might be expected that any targeting elements will have been conserved.

These analyses can be carried out computationally, using alignment algorithms such as BLAST (Altschul et al., 1990) to detect similar elements in the sequences of the 3'UTRs but also more complicated structural algorithms such as those provided by mfold (Zuker, 2003) and RNAforester (Höchsmann et al., 2004), which aligns multiple RNAs according to predicted structural elements. It is recommended that the structural analysis is informed by the sequence analysis; as the number of possible structures increases rapidly as sequence length increases, it is necessary to minimise the length of sequence as much as possible to restrict the number of probable structures

to a manageable size. Therefore the structural analysis should begin with any small regions of sequence which can either be found in multiple mRNAs or which are highly conserved.

Any predictions from these analyses can then be tested by creating 3'UTRs attached to reporters (for example, GFP) which do and do not contain the predicted regulatory regions, and observing whether these reporters can be detected in axons by immunohistochemistry or in situ hybridisation.

It is possible that the small RNA molecules known as microRNAs are involved in axonal RNA regulation. MicroRNAs are known to bind to the 3'UTRs of mRNAs and repress their translation; they are also known to bind to mRNAs contained and transported in protein complexes (Wu and Belasco, 2008). MicroRNAs have also been shown to regulate mRNA translation in dendritic spines, where the gene Limk1 is upregulated when the microRNA miR-134 is repressed, causing the widths of the dendritic spines where Limk1 is expressed to increase (Schratt et al., 2006).

The study of microRNAs is appealing, particularly for bioinformaticians, as microRNA-mRNA bindings can be predicted computationally and the small size of the binding (perhaps as little as 8bp) makes accurate prediction very challenging. However, despite several years of speculation in a number of papers (see, for example, Wu et al. (2005) and Hengst and Jaffrey (2007)), no axonal microRNA has been reported to date. This may be because the technical difficulties of doing so are severe; it took many years longer for mRNAs to be identified in axons compared to their identification in dendrites, and the same may happen with microRNAs. It may also be because microRNAs are not, in fact, present in axons; while the hypothesis that they regulate multiple mRNAs is attractive, there is no reason in principle why a sufficiently complex set of switches in the 3'UTR which bind to various regulatory proteins couldn't account for the regulation of hundreds of mRNAs in axons.

However, there is no doubt that, if hundreds of mRNAs are indeed present in axons of various systems, and if these mRNAs vary from system to system, there is a great deal of work left to be done to unravel the precise regulatory networks controlling the targeting and expression of these mRNAs in axons.

7.3.2 Translation at the growth cone in the thalamocortical system

The results presented here demonstrating the presence of multiple RNAs in thalamic axons raise many questions about the development of the thalamocortical system. How

does the presence or absence of these RNAs affect the response of thalamocortical axons to their environment? Is translation at the growth cone required for thalamocortical axons to respond to guidance cues such as netrin-1, Slits 1 and 2 and ephrin-A5? Is local translation involved in the interaction of thalamocortical axons with the axons of cells from the internal capsule and the lateral ganglionic eminence, and with corticothalamic axons? And does local translation have a role to play in the targeting of thalamocortical axons from particular thalamic nuclei to their appropriate cortical target areas?

These questions can be addressed using combinations of the *in vitro* techniques encountered in Chapter 1; thalamic axons can be grown in culture either with tissue from the hypothalamus, ventral telencephalon or cortex, or with gradients of specific guidance cues, and the axons can be treated with protein synthesis inhibitors such as cycloheximide or anisomycin to see if turning effects are abolished as they are for retinal or commissural axons, for example. Co-cultures will pose more technical challenges than treatment with guidance cues as it will be necessary to shield target tissue sources from the protein synthesis inhibitors; this could be done by the use of Campenot chambers, where membranes which permit the growth of axons but prevent free flow of medium could be used to isolate thalamic tissue from target tissue (Eng et al., 1999; Roche et al., 2009). Alternatively, specific antisense morpholinos could be used against particular mRNAs, as has been done for β-actin (see Section 1.5.5).

It is possible that variants of the qRT-PCR technique presented in this thesis could be developed which would enable quantities of mRNAs in the presence or absence of guidance cues or target tissues to be examined, although once again the co-culture experiments would be complicated by the need to isolate the thalamic axons away from any other tissue. Also, the difficulty in growing sufficient quantities of axons for detection by qRT-PCR may make testing of multiple guidance cues prohibitive.

Indeed, while it is easy to generate many tens of hypotheses about the interactions of mRNAs, guidance cues and other axonal tracts given the large number of each which are involved in thalamocortical development, it may prove very difficult to accurately test these hypotheses. Firstly, the explant cultures used for the qRT-PCR experiments used here only flourished with the addition of fetal calf serum; as it is very likely that this serum contains growth factors and probably guidance cues as well, treating serum-fed axons with guidance cues may not have an effect, as the axons may already be saturated in their response to the cue. Secondly, the sheer number of factors involved in thalamocortical development make it difficult to draw strong conclusions about *in*

vitro results, as it is virtually impossible to simulate the *in vivo* environment of thalamic axons in culture, and factors which have effects that are dependent on several other factors may not influence axons directly *in vitro*.

Nevertheless, the *in vitro* approach should be pursued, particularly as no corresponding *in vivo* approach is available at present for the study of axonal RNAs. While the expression of particular guidance cues and the disruption of axon growth can be examined *in vivo* by generating genetic mutants, it is as yet unclear how to generate mutants which will lack axonal RNA alone without disrupting cellular RNA expression; it is even less clear how this might be done for thalamocortical axons alone, without interfering with the other axonal systems with which the thalamocortical axons must interact. It is hoped that this will become clearer as the structure and function of the 3'UTRs of axonal RNAs is investigated, as it may be possible to identify regions of the 3'UTR which are crucial for axonal targeting but no other function, which could be excised from the gene in mutant animals.

In summary, multiple RNAs have been identified in thalamic axons, using gene-specific qRT-PCR and in situ hybridisation experiments, including the mRNA for the cell adhesion and signalling-related molecule β-catenin. This lays the foundation for a thorough investigation of the role of local translation in thalamic axons, which it is hoped will throw light on the development of the thalamocortical system and axonal systems in general.

Appendix A

Source code for in situ image analysis

Below is the source code for the analysis of axonal in situs presented in Section 5.3.5, written in the statistical programming language R (R Development Core Team (2008)).

```
# Input: traces of axon pixel intensities in separate
# files with the extension plot.txt in the format:
# position1 intensity1
# position2 intensity2
# ...
#
# Output: PDF images comparing specified pairs of probes
# and CSV format list of images, pixels, bin means and
# standard deviations for each probe

# Get maximum pixel intensity for all long/oligo probes for
# conversion of intensities to percentages
get_highest_intensity<-function(probes) {
    highest_intensity<-0
    axon_files <- list.files(path = ".",  pattern = probes)
    for(i in 1:length(axon_files)) {
        axon_filename <- axon_files[i]
        axon_file<-read.table(axon_filename)
        highest_intensity <-
            max(c(highest_intensity , max(axon_file$V2)))
    }
    return(highest_intensity)
}
```

```
# Get all the average pixel intensities in a bin
# for all bins for all the files for single probe
get_av_pixints<-function(probe_id, bins) {
    axon_files <- list.files(path = ".", pattern = probe_id)
    probe_pixints<-array(-1, c(length(bins), 15))

    for(i in 1:length(axon_files)) {
        # Read in trace file for one axon for the probe
        axon_filename <- axon_files[i]
        axon_file<-read.table(axon_filename)
        num_pixels <- length(axon_file$V1)

        # Convert position along axon to percentage
        for (j in 1:num_pixels) {
            axon_file$V1[j] <- (axon_file$V1[j]/num_pixels)*100
        }

        # Get pixels for each bin
        for (j in 1:length(bins)) {
            bin_pixels <- axon_file$V2[   axon_file$V1>=
                                (bins[j]-bins[1]+0.000000001)
                                & axon_file$V1<bins[j]]
            # Convert pixels to percentage of maximum intensity
            # and invert percentage
            # (so increasing staining increases value)
            for(l in 1:length(bin_pixels)) {
                bin_pixels[l] <- 100 -
                    ((bin_pixels[l]/highest_intensity) * 100)
            }
            # Calculate mean pixel intensity for this image
            probe_pixints[j, i] <- mean(bin_pixels)
        }
    }
    return(list(probe_pixints=probe_pixints,
                num_files=length(axon_files)))
}

```

```
# Plot error bars for pixels in each bin for two probes
print_plot<-function
    (probe_1, probe_2, probe_bin_means, probe_bin_stderrs,
     bin_pvalues, bins, colour_1, colour_2) {

    # Open PDF file for plot
    pdf_file<-paste("../axon_trace_figs/", probe_1, "_",
                    probe_2, ".pdf", sep='')
    pdf(pdf_file)

    # Create error bars for second (low expression) probe
    errbar(bins, probe_bin_means[2, ],
        probe_bin_means[2, ] + probe_bin_stderrs[2, ],
        probe_bin_means[2, ] - probe_bin_stderrs[2, ],
        ylim=c(0, 105),  col = colour_2, type="o", pch=22,
        xlab="Distance along axon (%)",
        ylab="Intensity of staining (%)", add = FALSE)

    # Create error bar for first (high expression) probe
    # on top of second probe
    errbar(bins, probe_bin_means[1, ],
        probe_bin_means[1, ] + probe_bin_stderrs[1, ],
        probe_bin_means[1, ] - probe_bin_stderrs[1, ],
        ylim=c(0, 105), col = colour_1,  type="o", pch=20,
        add = TRUE)

    legend(65, 100, c(probe_1, probe_2),
           pch=c(20, 22),  col=c(colour_1, colour_2))

    # Add significance stars with pvalues
    for (k in 1:length(bin_pvalues)) {
        if (bin_pvalues[k] < 0.05) {
            text(k*5, 104, "*")
        }
    }
}

```

```
compare_probes<-function
    (probe_1, probe_2, highest_intensity,
     colour_1, colour_2, bins) {

    probe_list<-c(probe_1, probe_2)
    all_probe_bins <-
        array(-1, c(length(probe_list), length(bins), 15))
    probe_files <- array(0, length(probe_list))
    probe_print_out <- array("", length(probe_list))

    # Get average pixel intensities for each probe
    for(k in 1:length(probe_list)) {
        probe_id <- probe_list[k]
        probe_av_pixints <- get_av_pixints(probe_id, bins)
        all_probe_bins[k, , ] <-
            probe_av_pixints$probe_pixints
        probe_files[k] <- probe_av_pixints$num_files
        probe_print_out[k*2] <-
            paste(probe_id, ',', probe_files[k], sep='')
        probe_print_out[k*2+1] <- ",,S.E.M.,"
    }

    # Initialise mean, standard error and p-value arrays
    probe_bin_means <- array(0,
                        c(length(probe_list), length(bins)))
    probe_bin_stderrs  <- probe_bin_means
    bin_pvalues<-vector()
    # For each bin,
    # calculate means and standard errors for both probes
    # and calculate p-value for comparison of probes
    for (j in 1:length(bins)) {
        for (k in 1:length(probe_list)) {

            # Get pixels for this bin and probe
            bin_pixints <- vector()
            for(i in 1:length(all_probe_bins[k, j, ])) {
                if (all_probe_bins[k, j, i] >= 0) {
```

```
135                     bin_pixints <-
136                         c(bin_pixints,  all_probe_bins[k,j,i])
137                 }
138             }
139             if (j==1) {
140                 probe_print_out[k*2] <-
141                     paste(probe_print_out[k*2],
142                       ',Mean,',  sep='')
143             }
144
145             probe_bin_means[k, j] <-mean(bin_pixints)
146             probe_bin_stderrs[k, j]<-sd(bin_pixints) /
147                                       sqrt(length(bin_pixints))
148
149             probe_print_out[k*2] <-
150                 paste(probe_print_out[k*2],
151                   probe_bin_means[k, j], ",", sep="")
152             probe_print_out[k*2+1] <-
153                 paste(probe_print_out[k*2+1],
154                   probe_bin_stderrs[k, j], ",", sep="")
155             if (k==1) {one_bin_pixints<-bin_pixints}
156             else      {two_bin_pixints<-bin_pixints}
157         }
158         # Calculate one-tailed Wilcoxon rank sum test for bin
159         # and add to list of p-values for probes
160         wilcox_out <- wilcox.test(one_bin_pixints,
161                         two_bin_pixints, paired=FALSE,
162                         alternative="greater",)
163         bin_pvalues <- c(bin_pvalues, wilcox_out$p.value)
164     }
165
166     # Adjust p-values for multiple tests (20 bins)
167     bin_pvalues<-p.adjust(bin_pvalues,  method = "bonferroni")
168
169     print_plot(probe_1, probe_2,
170                probe_bin_means, probe_bin_stderrs,
171                bin_pvalues, bins, colour_1, colour_2)
```

```
172     for(i in 2:5) {
173         cat(probe_print_out[i], "\n", sep="")
174     }
175 }
176 
177 library(Hmisc) # For errbar function
178 system("rm axon_trace_figs/*.pdf")
179 directory<-"axon_plots"
180 setwd(directory)
181 
182 # Initialise 5% bins and create an empty array
183 # to hold pixels for each probe for each bin
184 bins<-c( 5, 10, 15, 20, 25, 30, 35, 40, 45, 50,
185         55, 60, 65, 70, 75, 80, 85, 90, 95, 100)
186 
187 csv_header<-"Probe,Pictures,"
188 for (i in 1:(length(bins))){
189     bin_start <- bins[i]-bins[1]+1
190     if (i==1) {bin_start<-bin_start-1}
191     csv_header<-paste(csv_header, bin_start, '-',
192                       bins[i], '%,', sep="")
193 }
194 cat(csv_header, "\n", sep='')
195 # Compare long probes
196 highest_intensity<-get_highest_intensity("long.plot.txt")
197 compare_probes("BCatL2-Antisense", "BCatL2-Sense",
198                highest_intensity, "red", "green", bins)
199 compare_probes("BActL", "BCatL2-Sense",
200                highest_intensity, "blue", "green", bins)
201 compare_probes("BCatL2-Antisense", "No-Probe",
202                highest_intensity, "red", "yellow", bins)
203 compare_probes("BActL", "No-Probe",
204                highest_intensity, "blue", "yellow", bins)
205 compare_probes("BCatL2-Sense", "No-Probe",
206                highest_intensity, "green", "yellow", bins)
207 compare_probes("BActL", "BCatL2-Antisense",
208                highest_intensity, "blue", "red", bins)
```

```
209 # Compare oligoprobes
210 highest_intensity<-get_highest_intensity("oligo.plot.txt")
211 compare_probes("Beta-Catenin-Oligo", "Scrambled",
212                highest_intensity, "red", "yellow", bins)
213 compare_probes("Beta-Actin-Oligo", "Scrambled",
214                highest_intensity, "blue", "yellow", bins)
215 compare_probes("18S", "Scrambled",
216                highest_intensity, "black", "yellow", bins)
217
218 # END
```

Bibliography

Abdel-Mannan, O., Cheung, A. F., and Molnár, Z. (2008). Evolution of cortical neurogenesis. *Brain Research Bulletin*, 75(2-4):398–404.

Abramoff, M. D., Magelhaes, P. J., and Ram, S. J. (2004). Image processing with ImageJ. *Biophotonics International*, 11(7):36–42.

Adams, N. C., Lozsádi, D. A., and Guillery, R. W. (1997). Complexities in the thalamocortical and corticothalamic pathways. *European Journal of Neuroscience*, 9(2):204–209.

Aikin, R. A., Ayers, K. L., and Thérond, P. P. (2008). The role of kinases in the Hedgehog signalling pathway. *EMBO reports*, 9(4):330–6.

Alberts, B., Johnson, A., Lewis, J., Raff, M., Roberts, K., and Walter, P. (2004). *Molecular Biology of the Cell*. Garland Science, 4th edition.

Allendoerfer, K. L. and Shatz, C. J. (1994). The subplate, a transient neocortical structure: Its role in the development of connections between thalamus and cortex. *Annual Review of Neuroscience*, 17:185–218.

Altschul, S. F., Gish, W., Miller, W., Myers, E. W., and Lipman, D. J. (1990). Basic local alignment search tool. *Journal of Molecular Biology*, 215(3):403–410.

Alvarez, J., Giuditta, A., and Koenig, E. (2000). Protein synthesis in axons and terminals: significance for maintenance, plasticity and regulation of phenotype. With a critique of slow transport theory. *Progress in Neurobiology*, 62(1):1–62.

Andreae, L. C., Peukert, D., Lumsden, A., and Gilthorpe, J. D. (2007). Analysis of Lrrn1 expression and its relationship to neuromeric boundaries during chick neural development. *Neural Development*, 2:22.

Andrews, G. L. and Mastick, G. S. (2003). R-cadherin is a Pax6-regulated, growth-promoting cue for pioneer axons. *Journal of Neuroscience*, 23(30):9873–9880.

Andrews, W., Liapi, A., Plachez, C., Camurri, L., Zhang, J., Mori, S., Murakami, F., Parnavelas, J. G., Sundaresan, V., and Richards, L. J. (2006). Robo1 regulates the development of major axon tracts and interneuron migration in the forebrain. *Development*, 113(11):2243–2252.

Angevine, Jr., J. B. (1970). Time of neuron origin in the diencephalon of the mouse. an autoradiographic study. *Journal of Comparative Neurology*, 139(2):129–187.

Antar, L. N., Li, C., Zhang, H., Carroll, R. C., and Bassell, G. J. (2006). Local functions for FMRP in axon growth cone motility and activity-dependent regulation of filopodia and spine synapses. *Molecular and Cellular Neuroscience*, 32(1-2):37–48.

Arcelli, P., Frassoni, C., Regondi, M. C., Bias, S. D., and Spreafico, R. (1997). GABAergic neurons in mammalian thalamus: A marker of thalamic complexity? *Brain Research Bulletin*, 42(1):27–37.

Arévalo, J. C. and Chao, M. V. (2005). Axonal growth: where neurotrophins meet Wnts. *Current Opinion in Cell Biology*, 17(2):112–115.

Aronov, S., Aranda, G., Behar, L., and Ginzburg, I. (2001). Axonal Tau mRNA localization coincides with Tau protein in living neuronal cells and depends on axonal targeting signal. *Journal of Neuroscience*, 21(17):6577–6587.

Aronov, S., Aranda, G., Behar, L., and Ginzburg, I. (2002). Visualization of translated tau protein in the axons of neuronal P19 cells and characterization of tau RNP granules. *Journal of Cell Science*, 115(19):3817–3827.

Asavaritikrai, P., Lotto, B., Anderson, G., and Price, D. J. (2003). Regulation of cell survival in the developing thalamus: an in vitro analysis. *Experimental Neurology*, 181(1):39–46.

Auladell, C., Pérez-Sust, P., Supèr, H., and Soriano, E. (2000). The early development of thalamocortical and corticothalamic projections in the mouse. *Anatomy and Embryology*, 201:169–179.

Badre, D. (2008). Cognitive control, hierarchy, and the rostro-caudal organization of the frontal lobes. *Trends in Cognitive Sciences*, 12(5):193–200.

Bagnard, D., Lohrum, M., Uziel, D., Püschel, A. W., and Bolz, J. (1998). Semaphorins act as attractive and repulsive guidance signals during the development of cortical projections. *Development*, 125(24):5043–5053.

Bagnard, D., Thomasset, N., Lohrum, M., Püschel, A. W., and Bolz, J. (2000). Spatial distributions of guidance molecules regulate chemorepulsion and chemoattraction of growth cones. *Journal of Neuroscience*, 20(3):1030–1035.

Bagri, A., Marín, O., Plump, A. S., Mak, J., Pleasure, S. J., Rubenstein, J. L. R., and Tessier-Lavigne, M. (2002). Slit proteins prevent midline crossing and determine the dorsoventral position of major axonal pathways in the mammalian forebrain. *Neuron*, 33(2):233–248.

Barallobre, M. J., Pascual, M., Del Rio, J. A., and Soriano, E. (2005). The Netrin family of guidance factors: emphasis on Netrin-1 signalling. *Brain Research Reviews*, 49(1):22–47.

Barbe, M. F. and Levitt, P. (1992). Attraction of specific thalamic input by cerebral grafts depends on the molecular identity of the implant. *Proceedings of the National Academy of Sciences*, 89(9):3706–3710.

Bas, A., Forsberg, G., Hammarström, S., and Hammarstroöm, M.-L. (2004). Utility of the housekeeping genes 18S rRNA, β-actin and glyceraldehyde-3-phosphate-dehydrogenase for normalization in real-time quantitative reverse transcriptase-polymerase chain reaction analysis of gene expression in human T lymphocytes. *Scandinavian Journal of Immunology*, 59(6):566–573.

Bassell, G. J., Zhang, H., Byrd, A. L., Femino, A. M., Singer, R. H., Taneja, K. L., Lifshitz, L. M., Herman, I. M., and Kosik, K. S. (1998). Sorting of β-Actin mRNA and protein to neurites and growth cones in culture. *Journal of Neuroscience*, 18(1):251–265.

Basyuk, E., Bertrand, E., and Journot, L. (2000). Alkaline fixation drastically improves the signal of in situ hybridization. *Nucleic Acids Research*, 28(10):e46–e48.

Bayatti, N., Sarma, S., Shaw, C., Eyre, J. A., Vouyiouklis, D. A., Lindsay, S., and Clowry, G. J. (2008). Progressive loss of PAX6, TBR2, NEUROD and TBR1 mRNA gradients correlates with translocation of EMX2 to the cortical plate during human cortical development. *European Journal of Neuroscience*, 28(8):1449–1456.

Bellion, A. and Métin, C. (2005). Early regionalisation of the neocortex and the medial ganglionic eminence. *Brain Research Bulletin*, 66(4-6):402–409.

Bertrand, N. and Dahmane, N. (2006). Sonic hedgehog signaling in forebrain development and its interactions with pathways that modify its effects. *Trends in Cell Biology*, 16(11):597–605.

Besse, F. and Ephrussi, A. (2008). Translational control of localized mRNAs: restricting protein synthesis in space and time. *Nature Reviews Molecular Cell Biology*, 9(12):971–980.

Bhanot, P., Brink, M., Samos, C. H., Hsieh, J.-C., Wang, Y., Macke, J. P., Andrew, D., Nathans, J., and Nusse, R. (1996). A new member of the frizzled family from Drosophila functions as a Wingless receptor. *Nature*, 382:225–230.

Bienz, M. (2005). β-Catenin: A pivot between cell adhesion and Wnt signalling. *Current Biology*, 15(2):R64–R67.

Binz, S. K., Sheehan, A. M., and Wold, M. S. (2004). Replication protein A phosphorylation and the cellular response to DNA damage. *DNA Repair*, 3:1015–1024.

Birnbacher, D. and Albus, K. (1987). Divergence of single axons in afferent projections to the cat's visual cortical areas 17, 18, and 19: A parametric study. *Journal of Comparative Neurology*, 261(4):543–561.

Bishop, K. M., Goudreau, G., and O'Leary, D. D. M. (2000). Regulation of area identity in the mammalian neocortex by Emx2 and Pax6. *Science*, 288(5464):344–349.

Bolz, J., Uziel, D., Mühlfriedel, S., Güllmar, A., Peuckert, C., Zarbalis, K., Wurst, W., Torii, M., and Levitt, P. (2004). Multiple roles of Ephrins during the formation of thalamocortical projections: maps and more. *Journal of Neurobiology*, 59(1):82–94.

Bonnin, A., Peng, W., Hewlett, W., and Levitt, P. (2006). Expression mapping of 5-HT1 serotonin receptor subtypes during fetal and early postnatal mouse forebrain development. *Neuroscience*, 141(2):781–794.

Bonnin, A., Torii, M., Wang, L., Rakic, P., and Levitt, P. (2007). Serotonin modulates the response of embryonic thalamocortical axons to netrin-1. *Nature Neuroscience*, 10(5):588–97.

Braisted, J. E., Catalano, S. M., Stimac, R., Kennedy, T. E., Tessier-Lavigne, M., Shatz, C. J., and O'Leary, D. D. M. (2000). Netrin-1 promotes thalamic axon growth and is required for proper development of the thalamocortical projection. *Journal of Neuroscience*, 20(15):5792–5801.

Braisted, J. E., Tuttle, R., and O'Leary, D. D. M. (1999). Thalamocortical axons are influenced by chemorepellent and chemoattractant activities localized to decision points along their path. *Developmental Biology*, 208(2):430–440.

Brembeck, F. H., Rosário, M., and Birchmeier, W. (2006). Balancing cell adhesion and Wnt signaling, the key role of β-catenin. *Current Opinion in Genetics & Development*, 16(1):51–59.

Brittis, P. A., Lu, Q., and Flanagan, J. G. (2002). Axonal protein synthesis provides a mechanism for localized regulation at an intermediate target. *Cell*, 110(2):223–235.

Bruckenstein, D. A., Lein, P. J., Higgins, D., and Fremeau, R. T. (1990). Disctinct spatial localization of specific mRNAs in cultured sympathetic neurons. *Neuron*, 5:809–819.

Brunet, I., Weinl, C., Piper, M., Trembleau, A., Volovitch, M., Harris, W., Prochiantz, A., and Holt, C. (2005). The transcription factor Engrailed-2 guides retinal axons. *Nature*, 438(7064):94–98.

Bulchand, S., Grove, E. A., Porter, F. D., and Tole, S. (2001). LIM-homeodomain gene Lhx2 regulates the formation of the cortical hem. *Mechanisms of Development*, 100(2):165–175.

Bult, C. J., Eppig, J. T., Kadin, J. A., Richardson, J. E., and Blake, J. A. (2008). The mouse genome database (MGD): mouse biology and model systems. *Nucleic Acids Res*, 36(Database issue):D724–8.

Bustin, S. A., editor (2006). *A-Z of Quantitative PCR*. IUL Biotechnology Series. International University Line Press.

Bustin, S. A., Benes, V., Nolan, T., and Pfaffl, M. W. (2005). Quantitative real-time RT-PCR - a perspective. *Journal of Molecular Endocrinology*, 34(3):597–601.

Caceres, A., Banker, G., Steward, O., Binder, L., and Payne, M. (1984a). MAP2 is localized to the dendrites of hippocampal neurons which develop in culture. *Developmental Brain Research*, 13(2):314–318.

Caceres, A., Binder, L. I., Payne, M. R., Bender, P., Rebhun, L., and Steward, O. (1984b). Differential subcellular localization of tubulin and the microtubule-associated protein MAP2 in brain tissue as revealed by immunocytochemistry with monoclonal hybridoma antibodies. *Journal of Neuroscience*, 4(2):394–410.

Camilli, P. D., Miller, P. E., Navone, F., Theurkau, W. E., and Vallee, R. B. (1984). Distribution of microtubule-associated protein 2 in the nervous system of the rat studied by immunofluorescence. *Neuroscience*, 11(4):819–846.

Campbell, D. S. and Holt, C. E. (2001). Chemotropic responses of retinal growth cones mediated by rapid local protein synthesis and degradation. *Neuron*, 32(6):1013–1026.

Campbell, D. S., Regan, A. G., Lopez, J. S., Tannahill, D., Harris, W. A., and Holt, C. E. (2001). Semaphorin 3A elicits stage-dependent collapse, turning, and branching in Xenopus retinal growth cones. *Journal of Neuroscience*, 21(21):8538–8547.

Canty, A. J. and Murphy, M. (2008). Molecular mechanisms of axon guidance in the developing corticospinal tract. *Progress in Neurobiology*, 85(2):214–235.

Catalano, S. M. and Shatz, C. J. (1998). Activity-dependent cortical target selection by thalamic axons. *Science*, 281(5376):559–562.

Caviness Jr., V. S. (1975). Architectonic map of neocortex of the normal mouse. *Journal of Comparative Neurology*, 164(2):247–264.

Chada, S. R. and Hollenbeck, P. J. (2003). Mitochondrial movement and positioning in axons: the role of growth factor signaling. *Journal of Experimental Biology*, 206(12):1985–1992.

Chalupa, L. M. (2007). A reassessment of the role of activity in the formation of eye-specific retinogeniculate projections. *Brain Research Reviews*, 55:228–236.

Chambers, D. and Fishell, G. (2006). Functional genomics of early cortex patterning. *Genome Biology*, 7:202.

Chao, M. V. (2003). Neurotrophins and their receptors: A convergence point for many signalling pathways. *Nature Reviews Neuroscience*, 4(4):299–309.

Charron, F. and Tessier-Lavigne, M. (2005). Novel brain wiring functions for classical morphogens: a role as graded positional cues in axon guidance. *Development*, 132(10):2251–2262.

Chen, B., Schaevitz, L. R., and McConnell, S. K. (2005). Fezl regulates the differentiation and axon targeting of layer 5 subcortical projection neurons in cerebral cortex. *PNAS*, 102(47):17184–17189.

Chenn, A. and Walsh, C. A. (2002). Regulation of cerebral cortical size by control of cell cycle exit in neural precursors. *Science*, 297(5580):365–369.

Cholfin, J. A. and Rubenstein, J. L. R. (2008). Frontal cortex subdivision patterning is coordinately regulated by Fgf8, Fgf17, and Emx2. *Journal of Comparative Neurology*, 509(2):144–155.

Chuang, D.-M., Hough, C., and Senatorov, V. V. (2005). Glyceraldehyde-3-phosphate dehydrogenase, apoptosis, and neurodegenerative diseases. *Annual Review of Pharmacology and Toxicology*, 45:269–90.

Ciani, L., Krylova, O., Smalley, M. J., Dale, T. C., and Salinas, P. C. (2004). A divergent canonical WNT-signaling pathway regulates microtubule dynamics: Dishevelled signals locally to stabilize microtubules. *Journal of Cell Biology*, 164(2).

Clevers, H. and Batlle, E. (2006). EphB/EphrinB receptors and Wnt signaling in colorectal cancer. *Cancer Research*, 66(1):2–5.

Cooke, J. E. and Moens, C. B. (2002). Boundary formation in the hindbrain: Eph only it were simple... *Trends in Neurosciences*, 25(5):260–267.

Coolican, H. (2004). *Research Methods and Statistics in Psychology*. Hodder and Stoughton, fourth edition.

Cooper, M. A., Son, A. I., Komlos, D., Sun, Y., Kleiman, N. J., and Zhou, R. (2008). Loss of ephrin-A5 function disrupts lens fiber cell packing and leads to cataract. *Proceedings of the National Academy of Sciences*, 105(43):16620–3.

Cox, L. J., Hengst, U., Gurskaya, N. G., Lukyanov, K. A., and Jaffrey, S. R. (2008). Intra-axonal translation and retrograde trafficking of CREB promotes neuronal survival. *Nature Cell Biology*, 10(2):149–59.

Cudeiro, J. and Sillito, A. M. (2006). Looking back: corticothalamic feedback and early visual processing. *Trends in Neurosciences*, 29(6):298–306.

Daugherty, R. L. and Gottardi, C. J. (2007). Phospho-regulation of β-catenin adhesion and signaling functions. *Physiology*, 22:303–309.

Davidson, E. H. and Erwin, D. H. (2006). Gene regulatory networks and the evolution of animal body plans. *Science*, 311(5762):796–800.

de la Torre, J. R., Höpker, V. H., Ming, G.-L., Poo, M.-M., Tessier-Lavigne, M., Hemmati-Brivanlou, A., and Holt, C. E. (1997). Turning of retinal growth cones in a Netrin-1 gradient mediated by the Netrin receptor DCC. *Neuron*, 19(6):1211–1224.

de Leon, S. B.-T. and Davidson, E. H. (2007). Gene regulation: Gene control network in development. *Annual Review of Biophysics and Biomolecular Structure*, 36:191–212.

Dean, C., Scholl, F. G., Choih, J., DeMaria, S., Berger, J., Isacoff, E., and Scheiffele, P. (2003). Neurexin mediates the assembly of presynaptic terminals. *Nature Neuroscience*, 6(7):708–716.

Dehay, C. and Kennedy, H. (2007). Cell-cycle control and cortical development. *Nature Reviews Neuroscience*, 8(7):438–450.

Dehmelt, L. and Halpain, S. (2004). The MAP2/Tau family of microtubule-associated proteins. *Genome Biology*, 6:204.

Deng, J. and Elberger, A. J. (2003). Corticothalamic and thalamocortical pathfinding in the mouse: dependence on intermediate targets and guidance axis. *Anatomy and Embryology*, 207(3):177–192.

Dent, E. W. and Gertler, F. B. (2003). Cytoskeletal dynamics and transport in growth cone motility and axon guidance. *Neuron*, 40(2):209–227.

Dickson, B. J. (2002). Molecular mechanisms of axon guidance. *Science*, 298(5600):1959–1964.

Ding, C. and Cantor, C. R. (2004). Quantitative analysis of nucleic acids - the last few years of progress. *Journal of Biochemistry and Molecular Biology*, 37(1):1–10.

Doherty, P., Rowett, L. H., Moore, S. E., Mann, D. A., and Walsh, F. S. (1991). Neurite outgrowth in response to transfected N-CAM and N-Cadherin reveals fundamental differences in neuronal responsiveness to CAMs. *Neuron*, 6:247–258.

Donoghue, M. J. and Rakic, P. (1999a). Molecular evidence for the early specification of presumptive functional domains in the embryonic primate cerebral cortex. *Journal of Neuroscience*, 19(14):5967–5979.

Donoghue, M. J. and Rakic, P. (1999b). Molecular gradients and compartments in the embryonic primate cerebral cortex. *Cerebral Cortex*, 9(6):586–600.

Drees, F. and Gertler, F. B. (2008). Ena/VASP: proteins at the tip of the nervous system. *Current Opinion in Neurobiology*, 18(1):53–59.

Droz, B., Rambourg, A., and Koenig, H. L. (1975). The smooth endoplasmic reticulum: Structure and role in the renewal of axonal membrane and synaptic vesicles by fast axonal transport. *Brain Research*, 93(1):1–13.

Dufour, A., Egea, J., Kullander, K., Klein, R., and Vanderhaeghen, P. (2006). Genetic analysis of EphA-dependent signaling mechanisms controlling topographic mapping in vivo. *Development*, 133(22):4415–4420.

Dufour, A., Seibt, J., Passante, L., Depaepe, V., Ciossek, T., Frisén, J., Kullander, K., Flanagan, J. G., Polleux, F., and Vanderhaeghen, P. (2003). Area specificity and topography of thalamocortical projections are controlled by ephrin/eph genes. *Neuron*, 39(3):453–465.

Duguay, D., Foty, R. A., and Steinberg, M. S. (2003). Cadherin-mediated cell adhesion and tissue segregation: qualitative and quantitative determinants. *Developmental Biology*, 253:309–323.

Egea, J., Nissen, U. V., Dufour, A., Sahin, M., Greer, P., Kullander, K., Mrsic-Flogel, T. D., Greenberg, M. E., Kiehn, O., Vanderhaeghen, P., and Klein, R. (2005). Regulation of EphA4 kinase activity is required for a subset of axon guidance decisions suggesting a key role for receptor clustering in eph function. *Neuron*, 47(4):515–528.

Endo, Y. and Rubin, J. S. (2007). Wnt signaling and neurite outgrowth: Insights and questions. *Cancer Science*, 98(9):1311–1317.

Eng, H., Lund, K., and Campenot, R. B. (1999). Synthesis of beta-tubulin, actin, and other proteins in axons of sympathetic neurons in compartmented cultures. *Journal of Neuroscience*, 19(1):1–9.

Espada, J., Pérez-Moreno, M., Braga, V. M., Rodriguez-Viciana, P., and Cano, A. (1999). H-Ras activation promotes cytoplasmic accumulation and phosphoinositide 3-OH kinase associateion of β-catenin in epidermal keratinocytes. *Journal of Cell Biology*, 146(5):967–980.

Essen, D. C. V. (2005). Corticocortical and thalamcortical information flow in the primate visual system. *Progress in Brain Research*, 149:173–185.

Evans, S. J., Watson, S. J., and Akil, H. (2003). Evaluation of sensitivity, performance and reproducibility of microarray technology in neuronal tissue. *Intergrative and Comparative Biology*, 43:780–785.

Even, M. S., Sandusky, C. B., and Barnard, N. D. (2006). Serum-free hybridoma culture: ethical, scientific and safety considerations. *Trends in Biotechnology*, 24(3):105–108.

Faedo, A., Tomassy, G. S., Ruan, Y., Teichmann, H., Krauss, S., Pleasure, S. J., Tsai, S. Y., Tsai, M.-J., Studer, M., and Rubenstein, J. L. R. (2008). COUP-TFI coordinates cortical patterning, neurogenesis, and laminar fate and modulates MAPK/ERK, AKT, and β-catenin signaling. *Cerebral Cortex*, 18(9):2117–2131.

Faix, J. and Rottner, K. (2006). The making of filopodia. *Current Opinion in Cell Biology*, 18(1):18–25.

Fang, W. B., Ireton, R. C., Zhuang, G., Takahashi, T., Reynolds, A., and Chen, J. (2008). Overexpression of EPHA2 receptor destabilizes adherens junctions via a RhoA-dependent mechanism. *Journal of Cell Science*, 121(3):358–368.

Farrar, N. R. and Spencer, G. E. (2008). Pursuing a 'turning point' in growth cone research. *Developmental Biology*, 318(1):102–111.

Fass, J., Gehler, S., Sarmiere, P., Letourneau, P., and Bamburg, J. R. (2004). Regulating filopodial dynamics through actin-depolymerizing factor/cofilin. *Anatomical Science International*, 79(4):173–183.

Feldham, D. A., Vanderhaeghen, P., Hansen, M. J., Frisén, J., Lu, Q., Barbacid, M., and Flanagan, J. G. (1998). Topographic guidance labels in a sensory projection to the forebrain. *Neuron*, 21(6):1303–1313.

Fernald, R. D. (2006). Casting a genetic light on the evolution of eyes. *Science*, 313(5795):1914–1918.

Flanagan, J. G. and Vanderhaeghen, P. (1998). The ephrins and eph receptors in neural development. *Annual Review of Neuroscience*, 21:309–45.

Fleige, S., Walf, V., Huch, S., Prgomet, C., Sehm, J., and Pfaffl, M. W. (2006). Comparison of relative mRNA quantification methods and the impact of RNA integrity in quantitative real-time RT-PCR. *Biotechnology Letters*, 28(19):1601–1613.

Flicek, P., Aken, B. L., Beal, K., Ballester, B., Caccamo, M., Chen, Y., Clarke, L., Coates, G., Cunningham, F., Cutts, T., Down, T., Dyer, S. C., Eyre, T., Fitzgerald, S., Fernandez-Banet, J., Graf, S., Haider, S., Hammond, M., Holland, R., Howe, K. L., Howe, K., Johnson, N., Jenkinson, A., Kahari, A., Keefe, D., Kokocinski, F., Kulesha, E., Lawson, D., Longden, I., Megy, K., Meidl, P., Overduin, B., Parker, A., Pritchard, B., Prlic, A., Rice, S., Rios, D., Schuster, M., Sealy, I., Slater, G., Smedley, D., Spudich, G., Trevanion, S., Vilella, A. J., Vogel, J., White, S., Wood, M., Birney, E., Cox, T., Curwen, V., Durbin, R., Fernandez-Suarez, X. M., Herrero, J., Hubbard, T. J. P., Kasprzyk, A., Proctor, G., Smith, J., Ureta-Vidal, A., and Searle, S. (2008). Ensembl 2008. *Nucleic Acids Res*, 36(Database issue):D707–14.

Fraser, S., Keynes, R., and Lumsden, A. (1990). Segmentation in the chick embryo hindbrain is defined by cell lineage restrictions. *Nature*, 344:431–435.

Fukuchi-Shimogori, T. and Grove, E. A. (2001). Neocortex patterning by the secreted signaling molecule fgf8. *Science*, 294(5544):1071–1074.

Fukuda, M. and Mikoshiba, K. (2001). Characterization of KIAA1427 protein as an atypical synaptotagmin (Syt XIII). *Biochemical Journal*, 354(2):249–257.

Fukuda, T., Kawano, H., Ohyama, K., Li, H.-P., Takeda, Y., Oohira, A., and Kawamura, K. (1997). Immunohistochemical localization of neurocan and L1 in the formation of thalamocortical pathway of developing rats. *Journal of Comparative Neurology*, 382(2):141–152.

Gallo, G. (2006). RhoA-kinase coordinates F-actin organization and myosin II activity during semaphorin-3A-induced axon retraction. *Journal of Cell Science*, 119(16):3413–23.

Gallo, G. and Letourneau, P. C. (2004). Regulation of growth cone actin filaments by guidance cues. *Journal of Neurobiology*, 58(1):92–102.

Gao, P.-P., Yue, Y., Zhang, J.-H., Cerretti, D. P., Levitt, P., and Zhou, R. (1998). Regulation of thalamic neurite outgrowth by the Eph ligand ephrin-A5: Implications in the development of thalamocortical projections. *Proceedings of the National Academy of Sciences*, 95(9):5329–5334.

Gardner, M. K., Hunt, A. J., Goodson, H. V., and Odde, D. J. (2008). Microtubule assembly dynamics: new insights at the nanoscale. *Current Opinion in Cell Biology*, 20:64–70.

Garel, S. and Rubenstein, J. L. R. (2004). Intermediate targets in formation of topographic projections: inputs from the thalamocortical system. *Trends in Neurosciences*, 27(9):533–539.

Garel, S., Yun, K., Grosschedl, R., and Rubenstein, J. L. R. (2002). The early topography of thalamocortical projections is shifted in Ebf1 and Dlx1/2 mutant mice. *Development*, 129(24):5621–5634.

Gavalas, A. (2002). ArRAnging the hindbrain. *Trends in Neurosciences*, 25(2):61–64.

Gavard, J., Lambert, M., Grosheva, I., Marthiens, V., Irinopoulou, T., Riou, J.-F., Bershadsky, A., and Mège, R.-M. (2004). Lamellipodium extension and cadherin adhesion: two cell responses to cadherin activation relying on distinct signalling pathways. *Journal of Cell Science*, 117(2):257–270.

Gebauer, F. and Hentze, M. W. (2004). Molecular mechanisms of translational control. *Nature Reviews Molecular Cell Biology*, 5(10):827–835.

Ghosh, A., Antonini, A., McConnell, S. K., and Shatz, C. J. (1990). Requirement for subplate neurons in the formation of thalamocortical connections. *Nature*, 347:179–181.

Gil, O. D., Needleman, L., and Huntley, G. W. (2002). Developmental patterns of cadherin expression and localization in relation to compartmentalized thalamocortical terminations in rat barrel cortex. *Journal of Comparative Neurology*, 453:372–388.

Gingras, A.-C., Raught, B., and Sonenberg, N. (1999). eIF4 initiation factors: Effectors of mRNA recruitment to ribosomes and regulators of translation. *Annual Review of Biochemistry*, 68:913–963.

Glover, J. C., Renaud, J.-S., and Rijli, F. M. (2006). Retinoic acid and hindbrain patterning. *Journal of Neurobiology*, 66(7):705–725.

Godement, P., Vanselow, J., Thanos, S., and Bonhoeffer, F. (1987). A study in developing visual systems with a new method of staining neurones and their processes in fixed tissue. *Development*, 101(4):697–713.

Goidin, D., Mamessier, A., Staquet, M.-J., Schmitt, D., and Berthier-Vergnes, O. (2001). Ribosomal 18S RNA prevails over glyceraldehyde-3-phosphate dehyrogenase and β-actin genes as internal standard for quantitative comparison of mRNA levels in invasive and noninvasive human melanoma cell subpopulations. *Analytical Biochemistry*, 295:17–21.

Goldberg, D. J. and Burmeister, D. W. (1986). Stages in axon formation: Observations of growth of Aplysia axons in culture using video-enhanced contrast-differential interference contrast microscopy. *Journal of Cell Biology*, 103(5):1921–31.

González, G., Puelles, L., and Medina, L. (2002). Organiation of the mouse dorsal thalamus based on topology, calretinin immunostaining and gene expression. *Brain Research Bulletin*, 57(3/4):439–442.

Goodfellow, I. G. and Roberts, L. O. (2008). Eukaryotic initiation factor 4E. *International Journal of Biochemistry and Cell Biology*, 40:2675–2680.

Goodrich, L. V. (2008). The plane facts of PCP in the CNS. *Neuron*, 60(1):9–16.

Gordon-Weeks, P. R. (1993). Organization of microtubules in axonal growth cones: a role for microtubule-associated protein MAP1B. *Journal of Neurocytology*, 22(9):717–725.

Gordon-Weeks, P. R. (2000). *Neuronal Growth Cones*. Cambridge University Press.

Gordon-Weeks, P. R. (2004). Microtubules and growth cone function. *Journal of Neurobiology*, 58(1):70–83.

Grove, E. A. and Fukuchi-Shimogori, T. (2003). Generating the cerebral cortical area map. *Annual Review of Neuroscience*, 26:355–80.

Guan, C., Xu, H., Jin, M., Yuan, X., and Poo, M. (2007). Long-range Ca^{2+} signaling from growth cone to soma mediates reversal of neuronal migration induced by slit-2. *Cell*, 129(2):385–395.

Guo-li Ming, Hong-jun Song, B. B., Inagaki, N., Tessier-Lavigne, M., and Poo, M.-M. (1999). Phospholipase C-γ and phosphoinositide 3-kinase mediate cytoplasmic signaling in nerve growth cone guidance. *Neuron*, 23(1):139–148.

Hamasaki, T., Leingartner, A., Ringstedt, T., and O'Leary, D. D. M. (2004). Emx2 regulates sizes and positioning of the primary sensory and motor areas in neocortex by direct specification of cortical progenitors. *Neuron*, 43(3):359–372.

Hand, P. J. and Morrison, A. R. (1970). Thalamocortical projections from the ventrobasal complex to somatic sensory areas I and II. *Experimental Neurology*, 26(2):291–308.

Harbott, L. K. and Nobes, C. D. (2005). A key role for Abl family kinases in EphA receptor-mediated growth cone collapse. *Molecular and Cellular Neuroscience*, 30(1):1–11.

Harrell, F. E. (2005). `Hmisc`: A library of miscellaneous S functions. Available from `biostat.mc.vanderbilt.edu/s/Hmisc`.

Hay, N. and Sonenberg, N. (2004). Upstream and downstream of mTOR. *Genes & Development*, 18(16):1926–1945.

Hayano, Y. and Yamamoto, N. (2008). Activity-dependent thalamocortical axon branching. *The Neuroscientist*, 14(4):359–368.

Hengst, U., Cox, L. J., Macosko, E. Z., and Jaffrey, S. R. (2006). Functional and selection RNA interference in developing axons and growth cones. *Journal of Neuroscience*, 26(21):5727–5732.

Hengst, U. and Jaffrey, S. R. (2007). Function and translational regulation of mRNA in developing axons. *Seminars in Cell and Developmental Biology*, 18(2):209–215.

Hevner, R. F., Miyashita-Lin, E., and Rubenstein, J. L. R. (2002). Cortical and thalamic axon pathfinding defects in Tbr1, Gbx2, and Pax6 mutant mice: Evidence that cortical and thalamic axons interact and guide each other. *Journal of Comparative Neurology*, 447(1):8–17.

Hevner, R. F., Shi, L., Justice, N., Hsueh, Y.-P., Sheng, M., Smiga, S., Bulfone, A., Goffinet, A. M., Campagnoni, A. T., and Rubenstein, J. L. R. (2001). Tbr1 regulates differentiation of the preplate and layer 6. *Neuron*, 29(2):353–366.

Higashi, S., Molnár, Z., Kurotani, T., and Toyama, K. (2002). Prenatal development of neural excitation in rat thalamocortical projections studied by optical recording. *Neuroscience*, 115(4):1231–1246.

Higgins, D., Waxman, A., and Banker, G. (1988). The distribution of microtubule-associated protein 2 changes when dendritic growth is induced in rat sympathetic neurons in vitro. *Neuroscience*, 24(2):583–592.

Hiltunen, M., Lu, A., Thomas, A. V., Romano, D. M., Kim, M., Jones, P. B., Xie, Z., Kounnas, M. Z., Wagner, S. L., Berezovska, O., Hyman, B. T., Tesco, G., Bertram, L., and Tanzi, R. E. (2006). Ubiquilin 1 modules amyloid precursor protein trafficking and Aβ secretion. *Journal of Biological Chemistry*, 281(43):32240–32253.

Hirata, T., Nakazawa, M., Muraoka, O., Nakayama, R., Suda, Y., and Hibi, M. (2006). Zinc-finger gene Fez and Fez-like function in the establishment of diencephalon subdivisions. *Development*, 133(20):3993–4004.

Hirata, T., Suda, Y., Nakao, K., Narimatsu, M., Hirano, T., and Hibi, M. (2004). Zinc finger gene fez-like functions in the formation of subplate neurons and thalamocortical axons. *Developmental Dynamics*, 230(3):546–556.

Höchsmann, M., Voss, B., and Giegerich, R. (2004). Pure multiple RNA secondary structure alignments: A progressive profile approach. *IEEE Transactions on Computational Biology and Bioinformatics*, 1(1):53–62.

Hohenester, E. (2008). Structural insight into Slit-Robo signalling. *Biochemical Society Transactions*, 36:251–256.

Huang, H. and He, X. (2008). Wnt/β-catenin signaling: new (and old) players and new insights. *Current Opinion in Cell Biology*, 20:119–125.

Huber, A. H. and Weis, W. I. (2001). The structure of the β-catenin/E-cadherin complex and the molecular basis of diverse ligand recognition by β-catenin. *Cell*, 105:391–402.

Huber, G. and Matus, A. (1984). Differences in the cellular distributions of two microtubule-associated proteins, MAP1 and MAP2, in rat brain. *Journal of Neuroscience*, 4(1):151–160.

Huberman, A. D., Feller, M. B., and Chapman, B. (2008). Mechanisms underlying development of visual maps and receptive fields. *Annual Review of Neuroscience*, 31:479–509.

Hübscher, U., Maga, G., and Spadari, S. (2002). Eukaryotic DNA polymerases. *Annual Review of Biochemistry*, 71:133–63.

Huelsken, J. and Behrens, J. (2002). The Wnt signalling pathway. *Journal of Cell Science*, 115(21):3977–3978.

Hunter, T. (1995). Protein kinases and phosphatases: The yin and yang of protein phosphorylation and signaling. *Cell*, 80:225–236.

Hunter, T. (1998). The Croonian lecture 1997. The phosphorylation of proteins on tyrosine: its role in cell growth and disease. *Philosophical Transactions of the Royal Society of London B*, 353:583–605.

Huntley, G. W. and Benson, D. L. (1999). Neural (N)-Cadherin at developing thalamocortical synapses provides an adhesion mechanism for the formation of somatopically organized connections. *Journal of Comparative Neurology*, 407(4):453–471.

Hüttelmaier, S., Zenklusen, D., Lederer, M., Dictenberg, J., Lorenz, M., Meng, X., Bassell, G. J., Condeelis, J., and Singer, R. H. (2005). Spatial regulation of β-actin translation by Src-dependent phosphorylation of ZBP1. *Nature*, 438(7067):512–515.

Inan, M. and Crair, M. C. (2007). Development of cortical maps: Perspectives from the barrel cortex. *The Neuroscientist*, 13(1):49–61.

Ince-Dunn, G., Hall, B. J., Hu, S.-C., Ripley, B., Huganir, R. L., Olson, J. M., Tapscott, S. J., and Ghosh, A. (2006). Regulation of thalamocortical patterning and synaptic maturation by NeuroD2. *Neuron*, 49(5):683–695.

Ishikawa, R. and Kohama, K. (2007). Actin-binding proteins in nerve cell growth cones. *Journal of Pharmacological Sciences*, 105(1):6–11.

Jeong, J.-Y., Einhorn, Z., Mathur, P., Chen, L., Lee, S., Kawakami, K., and Guo, S. (2007). Patterning the zebrafish diencephalon by the conserved zinc-finger protein Fezl. *Development*, 134(1):127–136.

Jones, E. G. (1998). Viewpoint: The core and matrix of thalamic organization. *Neuroscience*, 85(2):331–345.

Jones, E. G. (2007). *The Thalamus*. Cambridge University Press, second edition.

Jones, L., López-Bendito, G., Gruss, P., Stoykova, A., and Molnár, Z. (2002). Pax6 is required for the normal development of the forebrain axonal connections. *Development*, 129(21):5041–5052.

Kaas, J. H. (2005). From mice to men: the evolution of the large, complex human brain. *Journal of Biosciences*, 30(2):155–165.

Kabayama, H., Takei, K., Fukuda, M., Ibata, K., and Mikoshiba, K. (1999). Functional involvement of Synaptotagmin I/II C2A domain in neurite outgrowh of chick dorsal root ganglion neuron. *Neuroscience*, 88(4):999–1003.

Kadonaga, J. T. (2004). Regulation of RNA polymerase II transcription by sequence-specific DNA binding factors. *Cell*, 116:247–257.

Kalil, K. and Dent, E. W. (2005). Touch and go: guidance cues signal to the growth cone cytoskeleton. *Current Opinion in Neurobiology*, 15(5):521–526.

Kapp, L. D. and Lorsch, J. R. (2004). The molecular mechanics of eukaryotic translation. *Annual Review of Biochemistry*, 73:657–704.

Kataoka, A. and Shimogori, T. (2008). Fgf8 controls regional identity in the developing thalamus. *Development*, 135(17):2873–2881.

Kawano, H., Fukuda, T., Kubo, K., Horie, M., Uyemura, H., Takeuchi, K., Osumi, N., Eto, K., and Kawamura, K. (1999). Pax-6 is required for thalamocortical pathway formation in fetal rats. *Journal of Comparative Neurology*, 408(2):147–160.

Kiecker, C. and Lumsden, A. (2004). Hedgehog signaling from the ZLI regulates diencephalic regional identity. *Nature Neuroscience*, 7(11):1242–1249.

Kiecker, C. and Lumsden, A. (2005). Compartments and their boundaries in vertebrate brain development. *Nature Reviews Neuroscience*, 6(7):553–564.

Killeen, M. T. and Sybingco, S. S. (2008). Netrin, Slit and Wnt receptors allow axons to choose the axis of migration. *Developmental Biology*, 323(2):143–151.

Kim, E., Goren, A., and Ast, G. (2008). Alternative splicing: current perspectives. *Bioessays*, 30(1):38–47.

Kiryushko, D., Berezin, V., and Bock, E. (2004). Regulators of neurite outgrowth: Role of cell adhesion molecules. *Annals of the New York Academy of Sciences*, 1014:140–154.

Komar, A. A. and Hatzoglou, M. (2005). Internal ribosome entry sites in cellular mRNAs: Mystery of their existence. *Journal of Biological Chemistry*, 280(25):23425–23428.

Komuta, Y., Hibi, M., Arai, T., Nakamura, S., and Kawano, H. (2007). Defects in reciprocal projections between the thalamus and cerebral cortex in the early development of Fezl-deficient mice. *Journal of Comparative Neurology*, 503(3):454–465.

Kornberg, R. D. (2007). The molecular basis of eukaryotic transcription. *Proceedings of the National Academy of Sciences*, 104(32):12955–61.

Kornberg, T. B. and Guha, A. (2007). Understanding morphogen gradients: a problem of dispersion and containment. *Current Opinion in Genetics & Development*, 17(4):264–271.

Kriegstein, A. R. and Noctor, S. C. (2004). Patterns of neuronal migration in the embryonic cortex. *Trends in Neurosciences*, 27(7):392–399.

Krubitzer, L. (1995). The organization of neocortex in mammals: are species differences really so different? *Trends in Neurosciences*, 18(9):408–417.

Kruger, R. P., Aurandt, J., and Guan, K.-L. (2005). Semaphorins command cells to move. *Nature Reviews Molecular Cell Biology*, 6(10):789–800.

Kuersten, S. and Goodwin, E. B. (2003). The power of the 3' UTR: Translational control and development. *Nature Reviews Genetics*, 4(8):626–637.

Kühn, U. and Wahle, E. (2004). Structure and function of poly(A) binding proteins. *Biochemica et Biophysica Acta*, 1678:67–84.

Lakhina, V., Falnikar, A., Bhatnagar, L., and Tole, S. (2007). Early thalamocortical tract guidance and topographic sorting of thalamic projections requires LIM-homeodomain gene Lhx2. *Developmental Biology*, 306(2):703–713.

Lalli, G. and Hall, A. (2005). Ral GTPases regulate neurite branching through GAP-43 and the exocyst complex. *Journal of Cell Biology*, 171(5):857–869.

Langkopf, A., Guilleminot, J., and Nunez, J. (1994). Two novel HMW MAP2 variants with four microtubule-binding repeats and different projection domains. *FEBS Letters*, 354(3):259–262.

Larsen, C. W., Zeltser, L. M., and Lumsden, A. (2001). Boundary formation and compartition in the avian diencephalon. *Journal of Neuroscience*, 21(13):4699–4711.

Le Clainche, C. and Carlier, M.-F. (2008). Regulation of actin assembly associated with protrusion and adhesion in cell migration. *Physiological Reviews*, 88(2):489–513.

Lee, S. M., Kim, M., Moon, E. P., Lee, B. J., Choi, J.-Y., and Kim, J. (2006). Genomic structure and transcriptional studies on the mouse ribosomal protein S3 gene: Expression of U15 small nucleolar RNA. *Gene*, 368:12–20.

Leighton, P. A., Mitchell, K. J., Goodrich, L. V., Lu, X., Pinson, K., Scherz, P., Skarnes, W. C., and Tessier-Lavigne, M. (2001). Defining brain wiring patterns and mechanisms through gene trapping in mice. *Nature*, 410:174–179.

Lennon, G., Auffray, C., Polymeropoulos, M., and Soares, M. B. (1996). The I.M.A.G.E. consortium: An integrated molecular analysis of genomes and their expression. *Genomics*, 33(1):151–152.

Leung, K.-M., van Horck, F. P. G., Lin, A. C., Allison, R., Standart, N., and Holt, C. E. (2006). Asymmetrical β-actin mRNA translation in growth cones mediates attractive turning to netrin-1. *Nature Neuroscience*, 9(10):1247–1256.

Levers, T. E., Edgar, J. M., and Price, D. J. (2001). The fates of cells generated at the end of neurogenesis in developing mouse cortex. *Journal of Neurobiology*, 48(4):265–277.

Li, H.-P., Oohira, A., Ogawa, M., Kawamura, K., and Kawano, H. (2005). Aberrant trajectory of thalamocortical axons associated with abnormal localization of neurocan immunoreactivity in the cerebral neocortex of reeler mutant mice. *European Journal of Neuroscience*, 22(11):2689–2696.

Liang, P. and Pardee, A. B. (1992). Differential display of eukaryotic messenger RNA by means of the polymerase chain reaction. *Science*, 257(5072):967–971.

Lim, Y. and Golden, J. A. (2007). Patterning the developing diencephalon. *Brain Research Reviews*, 53(1):17–26.

Lin, A. C. and Holt, C. E. (2008). Function and regulation of local axonal translation. *Current Opinion in Neurobiology*, 18(1):60–68.

Litman, P., Barg, J., and Ginzburg, I. (1994). Microtubules are involved in the localization of tau mRNA in primary neuronal cell cultures. *Neuron*, 13(6):1463–1474.

Liu, C., Wang, Y., Smallwood, P. M., and Nathans, J. (2008). An essential role for Frizzled5 in neuronal survival in the parafascicular nucleus of the thalamus. *Journal of Neuroscience*, 28(22):5641–5653.

López-Bendito, G., Cautinat, A., Sánchez, J. A., Bielle, F., Flames, N., Garratt, A. N., Talmage, D. A., Role, L. W., Charnay, P., Marín, O., and Garel, S. (2006). Tangential neuronal migration controls axon guidance: A role for neuregulin-1 in thalamocortical axon navigation. *Cell*, 125(1):127–142.

López-Bendito, G., Chan, C.-H., Mallamaci, A., Parnavelas, J., and Molnár, Z. (2002). Role of Emx2 in the development of the reciprocal connectivity between cortex and thalamus. *Journal of Comparative Neurology*, 451(2):153–169.

López-Bendito, G., Flames, N., Ma, L., Fouquet, C., Meglio, T. D., Chedotal, A., Tessier-Lavigne, M., and Marín, O. (2007). Robo1 and Robo2 cooperate to control the guidance of major axonal tracts in the mammalian forebrain. *Journal of Neuroscience*, 27(13):3395–3407.

López-Bendito, G. and Molnár, Z. (2003). Thalamocortical development: How are we going to get there? *Nature Reviews Neuroscience*, 4(4):276–289.

Lotto, R. B., Aitkenhead, A., and Price, D. J. (1999). Effects of the thalamus on the development of cerebral cortical efferents in vitro. *Journal of Neurobiology*, 39(2):186–196.

Lübke, J. and Feldmeyer, D. (2007). Excitatory signal flow and connectivity in a cortical column: focus on barrel cortex. *Brain Structure and Function*, 212(1):3–17.

Lumsden, A. (1990). The cellular basis of segmentation in the developing hindbrain. *Trends in Neurosciences*, 13(8):329–335.

Lundquist, E. A. (2006). Small GTPases. *WormBook*, 17:1–18.

Lutz, M. B. and Rössner, S. (2007). Factors influencing the generation of murine dendritic cells from bone marrow: The special role of fetal calf serum. *Immunobiology*, 212(9-10):855–862.

Lyckman, A. W., Jhaveri, S., Feldheim, D. A., Vanderhaeghen, P., Flanagan, J. G., and Sur, M. (2001). Enhanced plasticity of retinothalamic projections in an Ephrin-A2/A5 double mutant. *Journal of Neuroscience*, 21(19):7684–7690.

Lyuksyutova, A. I., Lu, C.-C., Milanesio, N., Leslie A. King, N. G., Wang, Y., Nathans, J., Tessier-Lavigne, M., and Zou, Y. (2003). Anterior-posterior guidance of commissural axons by Wnt-Frizzled signaling. *Science*, 302(5652):1984–1988.

Ma, L., Harada, T., Harada, C., Romero, M., Hebert, J. M., McConnell, S. K., and Parada, L. F. (2002). Neurotrophin-3 is required for appropriate establishment of thalamocortical connections. *Neuron*, 36(4):623–634.

Mallamaci, A., Muzio, L., Chan, C.-H., Parnavelas, J., and Boncinelli, E. (2000). Area identity shifts in the early cerebral cortex of Emx2-/- mutant mice. *Nature Neuroscience*, 3(7):679–686.

Mallamaci, A. and Stoykova, A. (2006). Gene networks controlling early cerebral cortex arealization. *European Journal of Neuroscience*, 23(4):847–856.

Mann, F., Peuckert, C., Dehner, F., Zhou, R., and Bolz, J. (2002). Ephrins regulate the formation of terminal axonal arbors during the development of thalamocortical projections. *Development*, 129(16):3945–3955.

Mann, F., Zhukareva, V., Pimenta, A., Levitt, P., and Bolz, J. (1998). Membrane-associated molecules guide limbic and nonlimbic thalamocortical projections. *Journal of Neuroscience*, 18(22):9409–9419.

Mannan, A. U., Boehm, J., Sauter, S. M., Rauber, A., Byrne, P. C., Neesen, J., and Engel, W. (2006). Spastin, the most commonly mutated protein in hereditary spastic paraplegia interacts with reticulon 1 an endoplasmic reticulum protein. *Neurogenetics*, 7(2):93–103.

Marín, O., Baker, J., Puelles, L., and Rubenstein, J. L. R. (2002). Patterning of the basal telencephalon and hypothalamus is essential for guidance of cortical projections. *Development*, 129(3):761–773.

Marshall, O. J. (2004). PerlPrimer: cross-platform, graphical primer design for standard, bisulphite and real-time PCR. *Bioinformatics*, 20(15):2471–2472.

Martin, J. H. (2005). The corticospinal system: From development to motor control. *The Neuroscientist*, 11(2):161–173.

Martinez-de-la-Torre, M., Garda, A.-L., Puelles, E., and Puelles, L. (2002). Gbx2 expression in the late embryonic chick dorsal thalamus. *Brain Research Bulletin*, 57(314):435–438.

Maruyama, T., Matsuura, M., Suzuki, K., and Yamamoto, N. (2008). Cooperative activity of multiple upper layer proteins for thalamocortical axon growth. *Developmental Neurobiology*, 68(3):317–331.

McAllister, A. K., Katz, L. C., and Lo, D. C. (1997). Opposing roles for endogenous BDNF and NT-3 in regulating cortical dendritic growth. *Neuron*, 18(5):767–778.

McAlonan, K., Cavanaugh, J., and Wurtz, R. H. (2008). Guarding the gateway to cortex with attention in visual thalamus. *Nature*, 456(7220):391–4.

McGlinn, E. and Tabin, C. J. (2006). Mechanistic insight into how Shh patterns the vertebrate limb. *Current Opinion in Genetics & Development*, 16(4):426–432.

McQuillen, P. S., DeFreitas, M. F., Zada, G., and Shatz, C. J. (2002). A novel role for p75NTR in subplate growth cone complexity and visual thalamocortical innervation. *Journal of Neuroscience*, 22(9):3580–3593.

Meichsner, M., Doll, T., Reddy, D., Weisshaar, B., and Matus, A. (1993). The low molecular weight form of microtubule-associated protein 2 is transported into both axons and dendrites. *Neuroscience*, 54(4):873–880.

Merrick, W. C. (2004). Cap-dependent and cap-independent translation in eukaryotic systems. *Gene*, 332:1–11.

Métin, C., Deléglise, D., Serafini, T., Kennedy, T. E., and Tessier-Lavigne, M. (1997). A role for netrin-1 in the guidance of cortical efferents. *Development*, 124(24):5063–5074.

Métin, C. and Godement, P. (1996). The ganglionic eminence may be an intermediate target for corticofugal and thalamocortical axons. *Journal of Neuroscience*, 16(10):3219–3235.

Miele, G., MacRae, L., McBride, D., Manson, J., and Clinton, M. (1998). Elimination of false positives generated through PCR re-amplification of differential display cDNA. *Biotechniques*, 25(1):138–44.

Miele, G., Slee, R., Manson, J., and Clinton, M. (1999). A rapid protocol for the authentication of isolated differential display RT-PCR cDNAs. *Preparative Biochemistry and Biotechnology*, 29(3):245–55.

Miller, K., Kolk, S. M., and Donoghue, M. J. (2006). EphA7-ephrin-A5 signaling in mouse somatosensory cortex: Developmental restriction of molecular domains and postnatal maintenance of functional compartments. *Journal of Comparative Neurology*, 496(5):627–642.

Ming, G.-L., Wong, S. T., Henley, J., Yuan, X.-B., Song, H.-J., Spitzer, N. C., and Poo, M.-M. (2002). Adaptation in the chemotactic guidance of nerve growth cones. *Nature*, 417(6887):411–418.

Mitchell, A. S. and Gaffan, D. (2008). The magnocellular mediodorsal thalamus is necessary for memory acquisition, but not retrieval. *Journal of Neuroscience*, 28(1):258–263.

Miyashita-Lin, E. M., Hevner, R., Wassarman, K. M., Martinez, S., and Rubenstein, J. L. R. (1999). Early neocortical regionalization in the absence of thalamic innervation. *Science*, 285(5429):906–909.

Moccia, R., Chen, D., Lyles, V., Kapuya, E., E, Y., Kalachikov, S., Spahn, C. M. T., Frank, J., Kandel, E. R., Barad, M., and Martin, K. C. (2003). An unbiased cDNA library prepared from isolated Aplysia sensory neuron processes is enriched for cytoskeletal and translational mRNAs. *Journal of Neuroscience*, 23(28):9409–9417.

Molnár, Z., Adams, R., and Blakemore, C. (1998a). Mechanisms underlying the early establishment of thalamocortical connections in the rat. *Journal of Neuroscience*, 18(15):5723–5745.

Molnár, Z., Adams, R., Goffinet, A. M., and Blakemore, C. (1998b). The role of the first postmitotic cortical cells in the development of thalamocortical innervation in the reeler mouse. *Journal of Neuroscience*, 18(15):5746–5765.

Molnár, Z. and Blakemore, C. (1991). Lack of regional specificity for connections formed between thalamus and cortex in coculture. *Nature*, 351:475–477.

Molnár, Z. and Blakemore, C. (1995). How do thalamic axons find their way to the cortex? *Trends in Neurosciences*, 18(9):389–397.

Molnár, Z. and Blakemore, C. (1999). Development of signals influencing the growth and termination of thalamocortical axons in organotypic culture. *Experimental Neurology*, 156(2):363–393.

Molnár, Z. and Butler, A. B. (2002). The corticostriatal junction: a crucial region for forebrain development and evolution. *Bioessays*, 24(6):530–541.

Molnár, Z. and Cordery, P. (1999). Connections between cells of the internal capsule, thalamus, and cerebral cortex in embryonic rat. *The Journal of Comparative Neurology*, 413(1):1–25.

Molnár, Z., Higashi, S., and López-Bendito, G. (2003). Choreography of early thalamocortical development. *Cerebral Cortex*, 13(6):661–669.

Molnár, Z., López-Bendito, G., Small, J., Partridge, L. D., Blakemore, C., and Wilson, M. C. (2002). Normal development of embryonic thalamocortical connectivity in the absence of evoked synaptic activity. *Journal of Neuroscience*, 22(23):10313–10323.

Molnár, Z., Métin, C., Stoykova, A., Tarabykin, V., Price, D. J., Francis, F., Meyer, G., Dehay, C., and Kennedy, H. (2006). Comparative aspects of cerebral cortical development. *European Journal of Neuroscience*, 23(4):921–934.

Molyneaux, B. J., Ariotta, P., Menezes, J. R. L., and Macklis, J. D. (2007). Neuronal subtype specification in the cerebral cortex. *Nature Reviews Neuroscience*, 8(6):427–437.

Moore, S. W., Correia, J. P., Sun, K. L. W., Pool, M., Fournier, A. E., , and Kennedy, T. E. (2008). Rho inhibition recruits DCC to the neuronal plasma membrane and enhances axon chemoattraction to netrin-1. *Development*, 135(17):2855–2864.

Morrison, E. E. (2007). Action and interactions at microtubule ends. *Cellular and Molecular Life Sciences*, 64:307–317.

Nakagawa, Y., Johnson, J. E., and O'Leary, D. D. M. (1999). Graded and areal expression patterns of regulatory genes and cadherins in embryonic neocortex independent of thalamocortical input. *Journal of Neuroscience*, 19(24):10877–10885.

Nakagawa, Y. and O'Leary, D. D. M. (2001). Combinatorial expression patterns of LIM-homeodomain and other regulatory genes parcellate developing thalamus. *Journal of Neuroscience*, 21(8):2711–2725.

Nelson, W. J. and Nusse, R. (2004). Convergence of Wnt, β-Catenin, and Cadherin pathways. *Science*, 303(5663):1483–1487.

Northcutt, R. G. and Kaas, J. H. (1995). The emergence of evolution of mammalian neocortex. *Trends in Neurosciences*, 18(9):373–379.

Nural, H. F. and Mastick, G. S. (2004). Pax6 guides a relay of pioneer longitudinal axons in the embryonic mouse forebrain. *Journal of Comparative Neurology*, 479:399–409.

Obst-Pernberg, K., Medina, L., and Redies, C. (2001). Expression of R-cadherin and N-cadherin by cell groups and fiber tracts in the developing mouse forebrain: relation to the formation of functional circuits. *Neuroscience*, 106(3):505–533.

O'Leary, D. D. M., Chou, S.-J., and Sahara, S. (2007). Area patterning of the mammalian cortex. *Neuron*, 56(2):252–269.

O'Leary, D. D. M. and Nakagawa, Y. (2002). Patterning centers, regulatory genes and extrinsic mechanisms controlling arealization of the neocortex. *Current Opinion in Neurobiology*, 12(1):14–25.

O'Leary, D. D. M. and Sahara, S. (2008). Genetic regulation of arealization of the neocortex. *Current Opinion in Neurobiology*, 18(1):90–100.

Olink-Coux, M. and Hollenbeck, P. J. (1996). Localization and active transport of mRNA in axons of sympathetic neurons in culture. *Journal of Neuroscience*, 16(4):1346–1358.

Olson, E. N. (2006). Gene regulatory networks in the evolution and development of the heart. *Science*, 313(5795):1922–1927.

Op de Beeck, H. P., Haushofer, J., and Kanwisher, N. G. (2008). Interpreting fMRI data: maps, modules and dimensions. *Nature Reviews Neuroscience*, 9(2):123–35.

Orme, M. H., Giannini, A. L., Vivanco, M. D., and Kypta, R. M. (2003). Glycogen synthase kinase-3 and Axin function in a β-catenin-independent pathway that regulates neurite outgrowth in neuroblastoma cells. *Molecular and Cellular Neuroscience*, 24(3):673–686.

Pak, C. W., Flynn, K. C., and Bamburg, J. R. (2008). Actin-binding proteins take the reins in growth cones. *Nature Reviews Neuroscience*, 9(2):136–147.

Pan, F., Hüttelmaier, S., Singer, R. H., and Gu, W. (2007). ZBP2 facilitates binding of ZBP1 to β-actin mRNA during transcription. *Molecular and Cellular Biology*, 27(23):8340–8351.

Paves, H. and Saarma, M. (1997). Neurotrophins as in vitro growth cone guidance molecules for embyronic sensory neurons. *Cell Tissue Research*, 290(2):285–297.

Percheron, G., François, C., Talbi, B., Yelnik, J., and Fénelon, G. (1996). The primate motor thalamus. *Brain Research Reviews*, 22(2):93–181.

Persico, A. M., Pino, G. D., and Levitt, P. (2006). Multiple receptors mediate the trophic effects of serotonin on ventroposterior thalamic neurons in vitro. *Brain Research*, 1095(1):17–25.

Peters, I. R., Helps, C. R., Hall, E. J., and Day, M. J. (2004). Real-time RT-PCR: considerations for efficient and sensitive assay design. *Journal of Immunological Methods*, 286:203–217.

Peuckert, C., Wacker, E., Rapus, J., Levitt, P., and Bolz, J. (2008). Adaptive changes in gene expression patterns in the somatosensory cortex after deletion of ephrinA5. *Molecular and Cellular Neuroscience*, 39(1):21–31.

Pfaffl, M. W. (2001). A new mathematical model for relative quantification in real-time RT-PCR. *Nucleic Acids Research*, 29(9):2002–2007.

Phillips, C. G., Zeki, S., and Barlow, H. B. (1984). Localization of function in the cerebral cortex. *Brain*, 107(1):328–361.

Piao, S., Lee, S.-H., Kim, H., Yum, S., Stamos, J. L., Xu, Y., Lee, S.-J., Lee, J., Oh, S., Han, J.-K., Park, B.-J., Weis, W. I., and Ha, N.-C. (2008). Direct inhibition of GSK3β by the phosphorylated cytoplasmic domain of LRP6 in Wnt/β-Catenin signaling. *PLoS ONE*, 3(12):e4046.

Piedra, J., Miravet, S., Castano, J., Pálmer, H. G., Heisterkamp, N., de Herreros, A. G., and Dunach, M. (2003). p120 catenin-associated fer and fyn tyrosine kinases regulate β-catenin tyr-142 phosphorylation and β-catenin-α-catenin interaction. *Molecular and Cellular Biology*, 23(7):2287–2297.

Pinault, D. (2004). The thalamic reticular nucleus: structure, function and concept. *Brain Research Reviews*, 46(1):1–31.

Piñon, M. C., Tuoc, T. C., Ashery-Padan, R., Molnár, Z., and Stoykova, A. (2008). Altered molecular regionalization and normal thalamocortical connections in cortex-specific Pax6 knock-out mice. *Journal of Neuroscience*, 28(35):8724–8734.

Piper, M., Anderson, R., Dwivedy, A., Weinl, C., van Horck, F., Leung, K. M., Cogill, E., and Holt, C. (2006). Signaling mechanisms underlying Slit-2-induced collapse of Xenopus retinal growth cones. *Neuron*, 49(2):215–228.

Piper, M. and Holt, C. (2004). RNA translation in axons. *Annual Review of Cell and Developmental Biology*, 20:505–23.

Polleux, F., Dehay, C., and Kennedy, H. (1997). The timetable of laminar neurogenesis contributes to the specification of cortical areas in mouse isocortex. *Journal of Comparative Neurology*, 385(1):95–116.

Poskanzer, K., Needleman, L. A., Bozdagi, O., and Huntley, G. W. (2003). N-cadherin regulates ingrowth and laminar targeting of thalamocortical axons. *Journal of Neuroscience*, 23(6):2254–2305.

Powell, A. W., Sassa, T., Wu, Y., Tessier-Lavigne, M., and Polleux, F. (2008). Topography of thalamic projections requires attractive and repulsive functions of netrin-1 in the ventral telencephalon. *PLoS Biology*, 6(5):e116.

Prakash, N., Vanderhaeghen, P., Cohen-Cory, S., Frisén, J., Flanagan, J. G., and Frostig, R. D. (2000). Malformation of the functional organization of somatosensory cortex in adult ephrin-a5 knock-out mice revealed by in vivo functional imaging. *Journal of Neuroscience*, 20(15):5841–5847.

Pratt, T., Quinn, J. C., Simpson, T. I., West, J. D., Mason, J. O., and Price, D. J. (2002). Disruption of early events in thalamocortical tract formation in mice lacking the transcription factors Pax6 or Foxg1. *Journal of Neuroscience*, 22(19):8523–8531.

Pratt, T., Vitalis, T., Warren, N., Edgar, J. M., Mason, J. O., and Price, D. J. (2000). A role for Pax6 in the normal development of dorsal thalamus and its cortical connections. *Development*, 127(23):5167–5178.

Price, D. J., Kennedy, H., Dehay, C., Zhou, L., Mercier, M., Jossin, Y., Goffinet, A. M., Tissir, F., Blakey, D., and Molnár, Z. (2006). The development of cortical connections. *European Journal of Neuroscience*, 23(4):910–920.

Puelles, L., Kuwana, E., Puelles, E., Bulfone, A., Shimamura, K., Keleher, J., Smiga, S., and Rubenstein, J. L. R. (2000). Pallial and subpallial derivatives in the embryonic chick and mouse telencephalon, traced by the expression of the genes Dlx-2, Emx-1, Nkx-2.1, Pax-6, and Tbr-1. *Journal of Comparative Neurology*, 424(3):409–438.

Puelles, L. and Rubenstein, J. L. R. (2003). Forebrain gene expression domains and the evolving prosomeric model. *Trends in Neurosciences*, 26(9):469–476.

Qi, J., Wang, J., Romanyuk, O., and Siu, C.-H. (2006). Involvement of Src family kinases in N-Cadherin phosphorylation and β-catenin dissociation during transendothelial migration of melanoma cells. *Molecular Biology of the Cell*, 17:1261–1272.

R Development Core Team (2008). *R: A Language and Environment for Statistical Computing*. R Foundation for Statistical Computing, Vienna, Austria. ISBN 3-900051-07-0.

Rameckers, J., Hummel, S., and Herrmann, B. (1997). How many cycles does a PCR need? Determinations of cycle numbers depending on the number of targets and the reaction efficiency factor. *Naturwissenschaften*, 84(6):259–262.

Rash, B. G. and Grove, E. A. (2005). Area and layer patterning in the developing cerebral cortex. *Current Opinion in Neurobiology*, 16(1):25–34.

Redies, C. (2000). Cadherins in the central nervous system. *Progress in Neurobiology*, 61(6):611–648.

Reichert, H. (2005). A tripartite organization of the urbilaterian brain: Developmental genetic evidence from *Drosophila*. *Brain Research Bulletin*, 66(4-6):491–494.

Rétaux, S., Rogard, M., Bach, I., Failli, V., and Besson, M.-J. (1999). Lhx9: A novel LIM-homeodomain gene expressed in the developing forebrain. *Journal of Neuroscience*, 19(2):783–793.

Rhee, J., Buchan, T., Zukerberg, L., Lilien, J., and Balsamo, J. (2007). Cables links Robo-bound Abl kinase to N-cadherin-bound β-catenin to mediate Slit-induced modulation of adhesion and transcription. *Nature Cell Biology*, 9(8):883–892.

Rhee, J., Mahfooz, N. S., Arregui, C., Lilien, J., Balsamo, J., and VanBerkum, M. F. A. (2002). Activation of the repulsive receptor Roundabount inhibits N-cadherin-mediated cell adhesion. *Nature Cell Biology*, 4(10):798–805.

Riehl, R., Johnson, K., Bradley, R., Grunwald, G. B., Cornel, E., Lilienbaum, A., and Holt, C. E. (1996). Cadherin function is required for axon outgrowth in retinal ganglion cells in vivo. *Neuron*, 17:979–990.

Roche, F. K., Marsick, B. M., and Letourneau, P. C. (2009). Protein synthesis in distal axons is not required for growth cone responses to guidance cues. *Journal of Neuroscience*, 29(3):638–652.

Ross, A. F., Oleynikov, Y., Kislauskis, E. H., Taneja, K. L., and Singer, R. H. (1997). Characterization of a β-actin mRNA zipcode-binding protein. *Molecular and Cellular Biology*, 17(4):2158–2165.

Roth, L., Koncina, E., Satkauskas, S., Crémel, G., Aunis, D., and Bagnard, D. (2009). The many faces of semaphorins: from development to pathology. *Cellular and Molecular Life Sciences*, 66(4):649–66.

Rouillard, J.-M., Zuker, M., and Gulari, E. (2003). OligoArray 2.0: design of oligonucleotide probes for DNA microarrays using a thermodynamic approach. *Nucleic Acids Research*, 31(12):3057–3062.

Sachs, A. B. (2000). Cell cycle-dependent translation initiation: IRES elements prevail. *Cell*, 101(3):243–245.

Sahin, M., Greer, P. L., Lin, M. Z., Poucher, H., Eberhart, J., Schmidt, S., Wright, T. M., Shamah, S. M., O'Connell, S., Cowan, C. W., Hu, L., Goldberg, J. L., Debant, A., Corfas, G., Krull, C. E., and Greenberg, M. E. (2005). Eph-dependent tyrosine phosphorylation of ephexin1 modulates growth cone collapse. *Neuron*, 46:191–204.

Saiki, R. K., Gelfand, D. H., Stoffel, S., Scharf, S. J., Higuchi, R., Horn, G. T., Mullis, K. B., and Erlich, H. A. (1988). Primer-directed enzymatic amplification of DNA with a thermostable DNA polymerase. *Science*, 239(4839):487–491.

Salinas, P. C. (2007). Modulation of the microtubule cytoskeleton: a role for a divergent canonical Wnt pathway. *Trends in Cell Biology*, 17(7):333–342.

Sánchez-Camacho, C. and Bovolenta, P. (2008). Autonomous and non-autonomous Shh signalling mediate the in vivo growth and guidance of mouse retinal ganglion cell axons. *Development*, 135:3531–3541.

Sánchez-Camacho, C., Rodríguez, J., Ruiz, J. M., Trousse, F., and Bovolenta, P. (2005). Morphogens as growth cone signalling molecules. *Brain Research Reviews*, 49:242–252.

Schaefer, A. W., Schoonderwoert, V. T. G., Ji, L., Mederios, N., Danuser, G., and Forscher, P. (2008). Coordination of actin filament and microtubule dynamics during neurite outgrowth. *Developmental Cell*, 15(1):146–62.

Schiff, N. D. (2008). Central thalamic contributions to arousal regulation and neurological disorders of consciousness. *Annals of the New York Academy of Sciences*, 1129:105–118.

Schlessinger, J. (2000). Cell signaling by receptor tyrosine kinases. *Cell*, 103(2):211–225.

Schmittgen, T. D. and Livak, K. J. (2008). Analyzing real-time PCR data by the comparative ct method. *Nature Protocols*, 3:1101–1108.

Scholpp, S., Foucher, I., Staudt, N., Peukert, D., Lumsden, A., and Houart, C. (2007). Otx1l, Otx2 and Irx1b establish and position the ZLI in the diencephalon. *Development*, 134(17):3167–3176.

Schratt, G. M., Tuebing, F., Nigh, E. A., Kane, C. G., Sabatini, M. E., Kiebler, M., and Greenberg, M. E. (2006). A brain-specific microRNA regulates dendritic spine development. *Nature*, 439(7074):283–289.

Seibt, J., Schuurmans, C., Gradwhol, G., Dehay, C., Vanderhaeghen, P., Guillemot, F., and Polleux, F. (2003). Neurogenin2 specifies the connectivity of thalamic neurons by controlling axon responsiveness to intermediate target cues. *Neuron*, 39(3):439–452.

Shamah, S. M., Lin, M. Z., Goldberg, J. L., Estrach, S., Sahin, M., Hu, L., Bazalakova, M., Neve, R. L., Corfas, G., Debant, A., and Greenberg, M. E. (2001). EphA receptors regulate growth cone dynamics through the novel guanin nucleotide exchange factor ephexin. *Cell*, 105:233–244.

Shapiro, L., Love, J., and Colman, D. R. (2007). Adhesion molecules in the nervous system: Structural insights into function and diversity. *Annual Review of Neuroscience*, 30:451–74.

Shatz, C. J. and Stryker, M. P. (1988). Prenatal tetrodotoxin infusion blocks segregation of retinogeniculate afferents. *Science*, 242(4875):87–89.

Sherman, S. M. and Guillery, R. W. (2006). *Exploring the Thalamus and Its Role in Cortical Function*. MIT Press, second edition.

Shimogori, T. and Grove, E. A. (2005). Fibroblast growth factor 8 regulates neocortical guidance of area-specific thalamic innervation. *Journal of Neuroscience*, 25(28):6550–6560.

Siegel, S. and John, C. N. (1988). *Nonparametric Statistics for the Behavioral Sciences*. McGraw-Hill, second edition.

Skaliora, I., Adams, R., and Blakemore, C. (2000). Morphology and growth patterns of developing thalamocortical axons. *Journal of Neuroscience*, 20(10):3650–3662.

Smith, C. L., Afroz, R., Bassell, G. J., Furneaux, H. M., Perrone-Bizzozero, N. I., and Burry, R. W. (2004). GAP-43 mRNA in growth cones is associated with HuD and ribosomes. *Journal of Neurobiology*, 61(2):222–235.

Song, H., Ming, G., and Poo, M. (1997). cAMP-induced switching in turning direction of nerve growth cones. *Nature*, 388(6639):275–9.

Sotelo-Silveira, J. R., Calliari, A., Kun, A., Benech, J. C., Sanguinetti, C., Chalar, C., and Sotelo, J. R. (2000). Neurofilament mRNAs are present and translated in the normal and severed sciatic nerve. *Journal of Neuroscience Research*, 62(1):65–74.

Steiner, P., Kulangara, K., Sarria, J. C. F., Glauser, L., Regazzi, R., and Hirling, H. (2004). Reticulon 1-c/neuroendocrine-specific protein-c interacts with SNARE proteins. *Journal of Neurochemistry*, 89(3):569–580.

Stemmler, M. P. (2008). Cadherins in development and cancer. *Molecular BioSystems*, 4:835–850.

Stoykova, A., Fritsch, R., Walther, C., and Gruss, P. (1996). Forebrain patterning defects in Small eye mutant mice. *Development*, 122(11):3453–3465.

Stoykova, A., Götz, M., Gruss, P., and Price, J. (1997). Pax6-dependent regulation of adhesive patterning, R-cadherin expression and boundary formation in developing forebrain. *Development*, 124(19):3765–3777.

Stoykova, A., Treichel, D., Hallonet, M., and Gruss, P. (2000). Pax6 modulates the dorsoventral patterning of the mammalian telencephalon. *Journal of Neuroscience*, 20(21):8042–8050.

Sur, M. and Rubenstein, J. L. R. (2005). Patterning and plasticity of the cerebral cortex. *Science*, 310(5749):805–810.

Svingen, T. and Tonissen, K. F. (2006). Hox transcription factors and their elusive mammalian gene targets. *Heredity*, 97:88–96.

Tai, H.-C. and Schuman, E. M. (2008). Ubiquitin, the proteasome and protein degradation in neuronal function and dysfunction. *Nature Reviews Neuroscience*, 9(11):826–38.

Tennyson, V. M. (1970). The fine structure of the axon and growth cone of the dorsal root neuroblast of the rabbit embryo. *Journal of Cell Biology*, 44(1):62–79.

Thompson, H., Barker, D., Camand, O., and Erskine, L. (2006). Slits contribute to the guidance of retinal ganglion cell axons in the mammalian optic tract. *Developmental Biology*, 296:476–484.

Tisdale, E. J. and Artalejo, C. R. (2007). A GAPDH mutant defective in Src-dependent tyrosine phosphorylation impedes Rab2-mediated events. *Traffic*, 8:733–741.

Tissir, F., Bar, I., Jossin, Y., Backer, O. D., and Goffinet, A. M. (2005). Protocadherin Celsr3 is crucial in axonal tract development. *Nature Neuroscience*, 8(4):451–457.

Tissir, F. and Goffinet, A. M. (2006). Expression of planar cell polarity genes during development of the mouse CNS. *European Journal of Neuroscience*, 23(3):597–607.

Torii, M. and Levitt, P. (2005). Dissociation of corticothalamic and thalamocortical axon targeting by an EphA7-mediated mechanism. *Neuron*, 48(4):563–575.

Tucker, R. P., Binder, L. I., and Matus, A. I. (1988). Neuronal microtubule-associated proteins in the embryonic avian spinal cord. *Journal of Comparative Neurology*, 271(1):44–55.

Tuttle, R., Nakagawa, Y., Johnson, J. E., and O'Leary, D. D. M. (1999). Defects in thalamocortical axon pathfinding correlate with altered cell domains in Mash-1-deficient mice. *Development*, 126(9):1903–1916.

Tuttle, R., Schlaggar, B. L., Braisted, J. E., and O'Leary, D. D. M. (1995). Maturation-dependent upregulation of growth-promoting molecules in developing cortical plate controls thalamic and cortical neurite growth. *Journal of Neuroscience*, 15(4):3039–3052.

Uchida, A. and Brown, A. (2004). Arrival, reversal, and departure of neurofilaments at the tips of growing axons. *Molecular Biology of the Cell*, 15(9):4215–4225.

Uemura, M., Nakao, S., Suzuki, S. T., Takeichi, M., and Hirano, S. (2007). OL-protocadherin is essential for growth of striatal axons and thalamocortical projections. *Nature Neuroscience*, 10(9):1151–9.

Uziel, D., Mühlfriedel, S., Zarbalis, K., Wurst, W., Levitt, P., and Bolz, J. (2002). Miswiring of limbic thalamocortical projections in the absence of Ephrin-A5. *Journal of Neuroscience*, 22(21):9352–9357.

Vanderhaeghen, P., Lu, Q., Prakash, N., Frisén, J., Walsh, C. A., Frostig, R. D., and Flanagan, J. G. (2000). A mapping label required for normal scale of body representation in the cortex. *Nature Neuroscience*, 3(4):358–365.

Vanderhaeghen, P. and Polleux, F. (2004). Developmental mechanisms patterning thalamocortical projections: intrinsic, extrinsic and in between. *Trends in Neurosciences*, 27(7):384–391.

Vieira, C. and Martinez, S. (2006). Sonic hedgehog from the basal plate and the zona limitans intrathalamica exhibits differential activity on diencephalic molecular regionalization and nuclear structure. *Neuroscience*, 143(1):129–140.

Vitalis, T., Cases, O., Gillies, K., Hanoun, N., Hamon, M., Seif, I., Gaspar, P., Kind, P., and Price, D. J. (2002). Interactions between TrkB signaling and serotonin excess in the developing murine somatosensory cortex: A role in tangential and radial organization of thalamocortical axons. *Journal of Neuroscience*, 22(12):4987–5000.

Votin, V., Nelson, W. J., and Barth, A. I. M. (2005). Neurite outgrowth involves adenomatous polyposis coli protein and β-catenin. *Journal of Cell Science*, 118(24):5699–5708.

Vue, T. Y., Aaker, J., Taniguchi, A., Kazemzadeh, C., Skidmore, J. M., Martin, D. M., Martin, J. F., Treier, M., and Nakagawa, Y. (2007). Characterization of progenitor domains in the developing mouse thalamus. *Journal of Comparative Neurology*, 505(1):73–91.

Wacker, M. J. and Godard, M. P. (2005). Analysis of one-step and two-step real-time RT-PCR using SuperScript III. *Journal of Biomolecular Techniques*, 16(3):266–271.

Wandell, B. A., Dumoulin, S. O., and Brewer, A. A. (2007). Visual field maps in human cortex. *Neuron*, 56(2):366–383.

Wang, Y., Thekdi, N., Smallwood, P. M., Macke, J. P., and Nathans, J. (2002). Frizzled-3 is required for the development of major fiber tracts in the rostral CNS. *Journal of Neuroscience*, 22(19):8563–8573.

Wang, Y., Zhang, J., Mori, S., and Nathans, J. (2006). Axonal growth and guidance defects in Frizzled3 knock-out mice: A comparion of diffusion tensor magnetic resonance imaging, neurofilament staining, and genetically directed cell labelling. *Journal of Neuroscience*, 26(2):355–364.

Wen, Z. and Zheng, J. Q. (2006). Directional guidance of nerve growth cones. *Current Opinion in Neurobiology*, 16(1):52–58.

Wigle, J. T. and Eisenstat, D. D. (2008). Homeobox genes in vertebrate forebrain development and disease. *Clinical Genetics*, 73(3):212–226.

Wilkie, G. S., Dickson, K. S., and Gray, N. K. (2003). Regulation of mRNA translation by 5'- and 3'UTR-binding factors. *Trends in Biochemical Sciences*, 28(4):182–188.

Wilkinson, D. G. (2001). Multiple roles of Eph receptors and Ephrins in neural development. *Nature Reviews Neuroscience*, 2(3):155–164.

Wilkinson, D. G., Bhatt, S., Cook, M., Boncinelli, E., and Krumlauf, R. (1989). Segmental expression of Hox-2 homeobox-containing genes in the developing mouse hindbrain. *Nature*, 341:405–409.

Willis, D., Li, K. W., Zheng, J.-Q., Chang, J. H., Smit, A., Kelly, T., Merianda, T. T., Sylvester, J., van Minnen, J., and Twiss, J. L. (2005). Differential transport and local translation of cytoskeletal, injury-response, and neurodegeneration protein mRNAs in axons. *Journal of Neuroscience*, 25(4):778–791.

Willis, D. E., van Niekerk, E. A., Sasaki, Y., Mesngon, M., Merianda, T. T., Williams, G. G., Kendall, M., Smith, D. S., Bassell, G. J., and Twiss, J. L. (2007). Extracellular stimuli specifically regulate localized levels of individual neuronal mRNAs. *Journal of Cell Biology*, 178(6):965–980.

Windrem, M. S. and Finlay, B. L. (1991). Thalamic ablations and neocortical development: Alterations of cortical cytoarchitecture and cell number. *Cerebral Cortex*, 1(3):230–240.

Winer, J. A. and Lee, C. C. (2007). The distributed auditory cortex. *Hearing Research*, 229(1-2):3–13.

Winning, R. S., Wyman, T. L., and Walker, G. K. (2001). EphA4 activity causes cell shape change and a loss of cell polarity in xenopus laevis embryos. *Differentiation*, 68(2-3):126–132.

Wolf, L. V., Yeung, J. M., Doucette, J. R., and Nazarali, A. J. (2001). Coordinated expression of Hoxa2, Hoxd1 and Pax6 in the developing diencephalon. *Neuroreport*, 12(2):329–333.

Wong, M. L. and Medrano, J. F. (2005). Real-time PCR for mRNA quantitation. *Biotechniques*, 39(1):75–85.

Woodhead, G. J., Mutch, C. A., Olson, E. C., and Chenn, A. (2006). Cell-autonomous β-catenin signaling regulates cortical precursor proliferation. *Journal of Neuroscience*, 26(48):12620–12630.

Wright, A. G., Demyanenko, G. P., Powell, A., Schachner, M., Enriquez-Barreto, L., Tran, T. S., Polleux, F., and Maness, P. F. (2007). Close homolog of L1 and neuropilin 1 mediate guidance of thalamocortical axons at the ventral telencephalon. *Journal of Neuroscience*, 27(50):13667–13679.

Wu, K. Y., Hengst, U., Cox, L. J., Macosko, E. Z., Jeromin, A., Urquhart, E. R., and Jaffrey, S. R. (2005). Local translation of RhoA regulates growth cone collapse. *Nature*, 438(7053):1020–1024.

Wu, L. and Belasco, J. G. (2008). Let me count the ways: Mechanisms of gene regulation by miRNAs and siRNAs. *Molecular Cell*, 29(1):1–7.

Xing, Y., Takemaru, K.-I., Liu, J., Berndt, J. D., Zheng, J. J., Moon, R. T., and Xu, W. (2008). Crystal structure of a full-length β-catenin. *Structure*, 16:478–487.

Yamada, K. M., Spooner, B. S., and Wessells, N. K. (1971). Ultrastructure and function of growth cones and axons of cultured nerve cells. *Journal of Cell Biology*, 49(3):614–635.

Yang, Y. S. and Strittmatter, S. M. (2007). The reticulons: a family of proteins with diverse functions. *Genome Biology*, 8(12):234.

Yao, J., Sasaki, Y., Wen, Z., Bassell, G. J., and Zheng, J. Q. (2006). An essential role for β-actin mRNA localization and translation in ca2+-dependent growth cone guidance. *Nature Neuroscience*, 9(10):1265–1273.

Young-Pearse, T. L., Chen, A. C., Chang, R., Marquez, C., and Selkoe, D. J. (2008). Secreted APP regulates the function of full-length APP in neurite outgrowth through interaction with integrin beta I. *Neural Development*, 3(15).

Yuan, J. S., Wang, D., and Jr., C. N. S. (2008). Statistical methods for efficiency adjusted real-time PCR quantification. *Biotechnology Journal*, 3(1):112–123.

Yun, M. E., Johnson, R. R., Antic, A., and Donoghue, M. J. (2003). EphA family gene expression in the developing mouse neocortex: Regional patterns reveal intrinsic programs and extrinsic influence. *Journal of Comparative Neurology*, 456(3):203–216.

Zarei, M., Johansen-Berg, H., Jenkinson, M., Ciccarelli, O., Thompson, A. J., and Matthews, P. M. (2007). Two-dimensional population map of cortical connections in the human internal capsule. *Journal of Magnetic Resonance Imaging*, 25(1):48–54.

Zeltser, L. M. (2005). Shh-dependent formation of the ZLI is opposed by signals from the dorsal diencephalon. *Development*, 132(9):2023–2033.

Zhang, G., Fenyo, D., and Neubert, T. A. (2008). Screening for EphB signaling effectors using SILAC with a linear ion trap-orbitrap mass spectrometer. *Journal of Proteome Research*, 7(11):4715–4726.

Zhang, H. L., Eom, T., Oleynikov, Y., Shenoy, S. M., Liebelt, D. A., Dictenberg, J. B., Singer, R. H., and Bassell, G. J. (2001). Neurotrophin-induced transport of a β-actin mRNP complex increases β-actin levels and stimulates growth cone motility. *Neuron*, 31(2):261–275.

Zhang, H. L., Singer, R. H., and Bassell, G. J. (1999). Neurotrophin regulation of β-actin mRNA and protein localization within growth cones. *Journal of Cell Biology*, 147(1):59–70.

Zhou, C., Qiu, Y., Pereira, F. A., Crair, M. C., Tsai, S. Y., and Tsai, M.-J. (1999). The nuclear orphan receptor COUP-TFI is required for differentiation of subplate neurons and guidance of thalamocortical axons. *Neuron*, 24(4):847–859.

Zhou, C.-J., Pinson, K. I., and Pleasure, S. J. (2004a). Severe defects in dorsal thalamic development in low-density Lipoprotein Receptor-Related Protein-6 mutants. *Journal of Neuroscience*, 24(35):7632–7639.

Zhou, F.-Q. and Cohan, C. S. (2004). How actin filaments and microtubules steer growth cones to their targets. *Journal of Neurobiology*, 58(1):84–91.

Zhou, F.-Q., Zhou, J., Dedhar, S., Wu, Y.-H., and Snider, W. D. (2004b). NGF-induced axon growth is mediated by localized inactivation of GSK-3β and functions of the microtubule plus end binding protein APC. *Neuron*, 42(6):897–912.

Zhou, L., Bar, I., Achouri, Y., Campbell, K., Backer, O. D., Hebert, J. M., Jones, K., Kessaris, N., de Rouvroit, C. L., O'Leary, D., Richardson, W. D., Goffinet, A. M., and Tissir, F. (2008). Early forebrain wiring: Genetic dissection using conditional Celsr3 mutant mice. *Science*, 320(5878):946–949.

Zipper, H., Brunner, H., Bernhagen, J., and Vitzthum, F. (2004). Investigations on DNA intercalation and surface binding by SYBR Green I, its structure determination and methodological implications. *Nucleic Acids Research*, 32(12):e103.

Zou, Y. (2004). Wnt signaling in axon guidance. *Trends in Neurosciences*, 27(9):528–532.

Zuker, M. (2003). Mfold web server for nucleic acid folding and hybridization prediction. *Nucleic Acids Research*, 31(13):3406–3415.